Antimicrobial Coatings for Biomedical and Wound Healing Devices

Stefani S. Griesser
Bachelor of Psychology (Biophysical Psychology and Neuropharmacology)
Grad Dip Sec Ed (Science)
Bachelor of Medical (Pathology) and Applied Biotechnology (Medical) Science

A thesis submitted for the degree of
PhD in Applied Science

Mawson Institute
University of South Australia
January 2015

Contents

Contents ..... **ii**

List of Figures ..... **vi**

List of Tables ..... **xx**

List of Abbreviations ..... **xxi**

Abstract ..... Error! Bookmark not defined.

Declaration of Originality ..... **xxvi**

Acknowledgements ..... **xxvii**

List of Publications ..... **xxviii**

List of Conference Presentations ..... **xxix**

Chapter 1: Introduction **1**
1.1 General Introduction 1
1.2 Aim and Motivation 3
1.3 General Introduction to Bacterial Disease Mechanisms 5
1.4 Bacterial Infections in Wounds and on Implants 11
1.5 Fungal and Mixed Infections 14
1.6 Outline of Thesis 15

Chapter 2: Literature Review **18**
2.1 Abstract 18
2.2 Introduction 18
2.3 Silver 20
2.3.1 Antimicrobial Activity 20
2.3.2 Silver in Coatings 23
2.4 Non-fouling or Anti-adhesive Coatings 34
2.4.1. Mechanism of Action 36
2.5 Disinfectants and Quaternary Ammonium Compounds 37
2.6 Antimicrobial Peptides 39
2.6.1 Antimicrobial Activity 40
2.6.2 Antimicrobial Peptides as an Antibiotic 42
2.6.3 Immobilisation of Antimicrobial Peptides 42
2.7 Synthetic Polymer Mimics of Antimicrobial Peptides 46
2.7.1. Immobilisation onto Surfaces 50

Chapter 3: Experimental Approach and Theory **54**
3.1 Materials 54
3.1.1 Chemicals 54
3.1.2 Buffer Salts, Proteins, Consumables 54
3.1.3 Substrates 55
3.2 Methods 55
3.2.1 Substrate and Surface Cleaning 55

3.2.2 Plasma Polymerisation of Substrates 56
3.2.2.1 Surface Attachment of Peptides, Antifungal Compounds, and Pharmaceutical Compounds 58
3.2.3 Silver Nanoparticle Surfaces 58
3.2.4 Bacteria Preparation and Testing 59
3.2.4.1 Plating of Bacteria 61
3.2.4.2 Adding of Bacteria to Samples 61
3.2.4.3 BacLight Fluorescence Microscopy 61
3.2.4.3 Plate Counts of Bacteria 62
3.2.4.4 Staining and Absorbance Reading of Bacteria 62
3.2.5 Fungal Preparation 62
3.2.6 Cell Testing of Surfaces 63
3.2.6.1 Cell Preparation and Addition 63
3.3 Theory and Principles of Analytical Techniques 64
3.3.1 Ellipsometry 64
3.4 Surface Analysis Techniques 65
3.4.1 X-ray Photoelectron Spectroscopy 66
3.4.2 Time-of-Flight Secondary Ion Mass Spectrometry 70
3.5 Theory and Understanding of Major Chemical Approaches 74
3.5.1 Plasma Polymerisation 74
3.5.2 Reductive Amination 75

Chapter 4: Mammalian Cell Responses to Antibacterial Coatings Comprising Silver Nanoparticles in Plasma Polymers 77
Abstract 77
4.1 Introduction 77
4.2 Methods 79
4.2.1 Sample Preparation 79
4.2.2 Bacteria 80
4.2.3 Cell Attachment 80
4.3 Results 81
4.3.1 Cell Testing 88
4.4 Discussion 96
4.5 Conclusion 98

Chapter 5: Naturally Occurring Antimicrobial Peptides Immobilised onto Plasma Polymer Surfaces 99
Abstract 99
5.1 Introduction 99
5.2 Methods 103
5.2.1 Samples 103
5.2.2 Bacteria 104
5.2.3 Cell Attachment 105
5.2.4 Surface Analysis 105
5.3 Results 106
5.3.1 Surface Analysis 106
5.3.2 Bacterial Testing 113
5.3.3 Cell Studies 119

5.4 Discussion and Conclusion 121

Chapter 6: Nylon-3 Antimicrobial Peptide Mimics Attached to Surfaces via Plasma Polymerisation 123

Abstract 123
6.1 Introduction 124
6.2 Methods 131
6.2.1 Samples 131
6.2.2 Surface Analysis 133
6.2.3 Bacteria 134
6.2.4 Cell Attachment 135
6.2.5 Wound Scratch Assay 135
6.3 Results 136
6.3.1 Surface Analysis 136
6.3.2 Click Chemistry 140
6.3.3 Bacterial Testing 148
6.3.4 Cell Studies 156
6.3.5 Testing for Antibacterial Activity in the Presence of Serum (FBS) 164
6.3.6 Testing for Antibacterial Activity after Storage and after Soaking in PBS 167
6.3.7 Wound Scratch Assay 167
6.4 Discussion 171
6.5 Conclusion 172

Chapter 7: Daptomycin Covalently Attached to a Biomedical Surface Using a Plasma Polymer 173

Abstract 173
7.1 Introduction 173
7.2 Method 179
7.2.1 Samples 179
7.2.2 Surface Analysis 180
7.2.3 Bacteria 181
7.2.4 Cell Attachment 182
7.3 Results and Discussion 182
7.3.1 Surface Immobilisation and Characterisation 182
7.3.2 Bacterial Testing 184
7.3.3 Cell Testing 190
7.4 Conclusion 190

Chapter 8: Antifungal Compounds Covalently Immobilised onto Plasma Polymers 191

Abstract 191
8.1 Introduction 192
8.2 Methods 202
8.2.1 Samples 202
8.2.2 Surface Analysis 203
8.2.3 Fungal Testing 204
8.2.4 Cell Attachment 204
8.4 Results 205
8.4.1 Surface Analysis 205

8.4.1.1 XPS Results 205
8.4.1.2 Amphotericin B Surface Analysis 205
8.4.1.2 Caspofungin Surface Analysis 209
8.4.2 Fungal Testing 212
8.4.2.1 Amphotericin B 214
8.4.2.2 Caspofungin 221
8.4.3 Cell Toxicity Studies 225
8.5 Conclusion 226
Chapter 9: Conclusion and Future Outlook 228
9.1 Conclusion 228

List of Figures

Figure 1.1: An example of the nanocrystalline silver dressing, Acticoat (Brett 2013) (From: http://www.smith-nephew.com/australia/healthcare/products/product-types/antimicrobial-dressings/silver-dressings/acticoat--product-range/acticoat-/)..... 3

Figure 1.2: The three major types of surfaces with which bacteria frequently come into contact: (a) moist, shedding mucosal surfaces, (b) the dry, shedding surfaces of the skin and (c) non-shedding surfaces such as teeth and prosthetic devices (Wilson, Henderson & McNab 2002) 7

Figure 1.3: The principal types of molecular interaction involved in bacterial adhesion. Adhesion of a bacterium to a substratum may involve one or more of these. (Wilson, Henderson & McNab 2002) 8

Figure 1.4: Diagram showing the major types of molecule to be found on the surface of a typical mammalian cell. Most of these can function as receptors for bacterial adhesins. (Wilson, Henderson & McNab 2002)..... 10

Figure 1.5: Primary, secondary and complicated wounds (Kumar & Robbins 2007) (From: http://2.bp.blogspot.com/-lbZNQEwSv_0/TqrbpdAGKaI/AAAAAAAAD1U/TmSwcm0MTyg/s640/Healing+by+first+intention+healing+by+second+intention.png) 12

Figure 1.6: Knee implant (From: http://orthoinfo.aaos.org/figures/A00389F09.jpg)..... 13

Figure 2.1: Summary of silver nanoparticles (AgNPs) interaction with bacterial cells. AgNPs release silver ions and (1) they accumulate in the cell membrane affecting membrane permeability, (2) they interact with membrane proteins affecting their correct function, 3) the released silver ions along with the generated ROS could damage the DNA (Marambio-Jones & Hoek 2010). 22

Figure 2.2: A summary of chemical approaches that may be used to control silver ion release from antibacterial biomaterials (Liu et al. 2010) 25

Figure 2.3: Schematic representation of a non-fouling, contact-active silver-releasing polymer matrix. Imine functional groups within the polymer matrix coordinate the silver ions prior to reduction to nanoparticles, which become

trapped in the bulk coating, while polyethylene glycol groups anchored at the surface serve to prevent cells from binding. (Ho et al. 2004) 26
Figure 2.4: Schematic diagram of silver nanoparticles incorporated into amine plasma polymer coatings, and the control of the release kinetics of silver ions via adjustable thickness of an additional plasma polymer overlayer. Also shown are test results of antibacterial effectiveness against *S. epidermidis*: (a) and pp: control heptylamine surface with no silver; (b), (c) and rows SN: silver-loaded coatings with different overlayers. (Poulter et al. 2013) 30
Figure 2.5: Synthetic strategies for the preparation of polymer brushes: (a) physisorption of diblock copolymers via preferential adsorption of the red blocks to the surface (*grafting to* approach), (b) chemisorption via reaction of appropriately end-functionalised polymers with complementary functional groups at the substrate surface (*grafting to* approach), (c) polymer brushes grown via surface-initiated polymerisation techniques (*grafting from* approach) (Barbey et al. 2009). (From: http://pubs.acs.org/doi/pdf/10.1021/cr900045a) 35
Figure 2.6: Layer-by-layer assembly (not drawn to scale or exact structure) of polyionic materials containing antimicrobial peptides (AMPs). The peptide is sandwiched between two layers of oppositely charged polyions, which can be achieved by sequential dipping of the solid support in polyanions, AMP and polycations solutions. (Onaizi & Leong 2011) 43
Figure 2.7: Site-directed attachment of cysteine-modified melamine on maleimide-functionalised glass (Chen et al. 2012) 44
Figure 2.8: Immobilisation of antimicrobial peptides via reductive amination onto ALDpp (the XPS data shows aldehyde and hydroxyl groups on the surface) 45
Figure 2.9: Many antimicrobial peptides act by disrupting bacterial membranes. Those with the α-helical folding pattern fold into conformations that are globally or facially amphiphilic with discrete areas of hydrophobic and hydrophilic side chains that are projected from opposite sides of the helix (a). Gellman et al. proposed that flexible, sequence-random polymers containing cationic and hydrophobic subunits can be induced by a bacterial membrane surface to

adopt irregular conformations that result in global amphiphilicity and are equally effective antimicrobials (b). (Mowery et al. 2007; Mowery et al. 2009; Munoz-Bonilla & Fernandez-Garcia 2012) 48
Figure 2.10:Illustration of immobilisation routes of amine and thiol terminated nylon 3 onto epoxide-functionalised surface 52
Figure 3.1: Schematic diagram of plasma apparatus (Kingshott 1998) 57
Figure 3.2: Basic schematic diagram of an ellipsometer (http://en.wikipedia.org/wiki/File:Ellipsometry_setup.svg) 64
Figure 3.3: Different options to analyse surface chemistry (From Physical Electronics Pty Ltd oral presentation) 66
Figure 3.4: Schematic diagram of XPS apparatus. X-rays are directed onto the sample under vacuum in a chamber and the resulting photoelectrons are then focused onto the entrance slit of a concentric hemispherical analyser. Here a negative and positive potential are applied to the outer and inner cylinders, respectively, such that the central line between the cylinders is a line of zero potential. Scanning the potentials allows control of the energy of electrons that are allowed to pass through the analyser and onto the detector, usually a channel electron multiplier (channeltron). (From: http://www.chm.bris.ac.uk/pt/diamond/jamespthesis/chapter2.htm) 67
Figure 3.5: XPS photons going into the sample and electrons as peaks showing binding energy of each atomic group (from http://wiki.utep.edu/display/~dmarrufo/X-ray+Photoelectron+Spectroscopy)... 68
Figure 3.6: Examples of binding energies for Carbon 1s from common organic groups used regularly in plasma polymerisation, such as amine, alcohol and hydrocarbon (From Physical Electronics Pty Ltd oral presentation) 69
Figure 3.7: Basic principles of ToF-SIMS. The ToF-SIMS uses a focused, pulsed particle beam (Ga or CS) to dislodge chemical species on a materials surface. Particles produced closer to the site of impact tend to be dissociated ions (positive or negative). Secondary particles generated farther from the impact site tend to be molecular compounds, typically fragments of much larger organic macromolecules. The particles are then accelerated into a

flight path on their way towards a detector. Because it is possible to measure the 'time-of-flight' of the particles from the time of impact to the detector on a scale of nanoseconds, it is possible to produce a mass resolution of time as atomic mass units. (From Physical Electronics Pty Ltd oral presentation)..... 71
Figure 3.8: Basic principle of ToF-SIMS: (a) dynamic SIMS, (b) static SIMS (From Physical Electronics Pty Ltd oral presentation) 72
Figure 3.9: Schematic showing reduction amination of aldehyde to amine 75
Figure 3.10: Interfacial reaction between surface epoxide groups and primary amine groups present on a biomolecule ligand. Reactions can be either acid or base catalysed. Amine bonds are irreversibly formed. (Coad et al, 2013) ……..76.
Figure 4.1: Loading silver nanoparticles in HApp films: (a) schematic representation of the experimental strategy for the fabrication of silver nanoparticles within amine plasma polymer films (1) plasma deposition of n-heptylamine, 2) loading with silver ions by immersion in $AgNO_3$ solution, (3) reduction of silver ions by immersion in $NaBH_4$ solution; b) glass samples after deposition of a 100 nm HApp layer, after loading with Ag^+ ions and after reduction with $NaBH_4$; (c) UV-Vis absorption spectra of samples after loading with silver ions (black) and after reduction by $NaBH_4$ (red) 82
Figure 4.2: Control over the amount of loaded silver nanoparticles: (a) influence of the time of immersion in $AgNO_3$ on the amount of Ag nanoparticles in the film, for HApp films 100 nm thick and a time of immersion in $NaBH_4$ of 1 hr; (b) influence of the time of immersion in $NaBH_4$ on the amount of Ag nanoparticles in the film, with HA films 100 nm thick and a time of immersion in $AgNO_3$ of 1 hr; (c) influence of the thickness of the HApp film on the amount of Ag nanoparticles in the film, with a time of immersion in $AgNO_3$ of 1 hr and a reduction time of 30 min. The solid lines are guides for the eye, not fits. 84
Figure 4.3: Control over the release of silver ions, achieved by depositing an additional layer of HApp on top of the silver nanoparticles–loaded film, as shown on the right. The graph on the left shows the kinetics of release of silver ions over 20 d immersion in PBS. Black squares = silver-loaded films as

prepared; red circles = after deposition of a 6 nm thick HApp overlayer; green triangles = after deposition of a 12 nm thick HApp overlayer; blue triangles = after deposition of a 18 nm thick HApp overlayer..... 86
Figure 4.4: Antibacterial efficiency: *S. epidermidis* adhesion and colonisation after 4 hours on (a) HApp only (no silver); (b) HA film loaded with silver nanoparticles; (c) HA film loaded with silver nanoparticles and covered with an additional layer 6 nm thick of HApp; (d)–(f) biofilm formation after 24 hours on samples loaded with silver nanoparticles covered with an additional layer of HApp of thickness (d) 6 nm, (e) 12 and (f) 18 nm; pp = plasma polymer only; SN = films loaded with silver nanoparticles..... 87
Figure 4.5: Images with human cornea epithelium (HCE) after 24 hours incubation: (a) control surface with HA only, (b) surface with HA/SNP, (c) surface with HA/SNP/HA at 10 nm, (d) surface with HA/SNP/HA at 20 nm thickness, (e) surface with HA/SNP/HA at 30 nm thickness 89
Figure 4.6: Human cornea epithelium (HCE) after 48 hours showing (a) control surface with HA only, (b) surface with HA/SNP, (c) surface with HA/SNP/HA at 10 nm, (d) surface with HA/SNP/HA at 20 nm thickness, (e) surface with HA/SNP/HA at 30 nm thickness..... 90
Figure 4.7: Retinal pigmented epithelium (RPE) after 24 hours growth: (a) control surface with HA only, (b) surface with HA/SNP, (c) surface with HA/SNP/HA at 10 nm thickness, (d) surface with HA/SNP/HA at 20 nm thickness, (e) surface with HA/SNP/HA at 30 nm thickness..... 91
Figure 4.8: Retinal pigmented epithelium (RPE) after 24 hours growth: (a) control surface with HA only, (b) surface with HA/SNP, (c) surface with HA/SNP/HA at 10 nm thickness, (d) surface with HA/SNP/HA at 20 nm thickness, (e) surface with HA/SNP/HA at 30 nm thickness..... 92
Figure 4.9: NIH/3T3 mouse fibroblast 24 hours after cell seeding: (a) control surface with HA only, (b) surface with HA/SNP, (c) surface with HA/SNP/HA at 10 nm thickness, (d) surface with HA/SNP/HA at 20 nm thickness, (e) surface with HA/SNP.HA at 30 nm thickness..... 93

Figure 4.10: NIH/3T3 mouse fibroblast 24 hours after cell seeding: a) surface with HA/SNP/HA at 20 nm thickness, b) surface with HA/SNP/HA at 30 nm thickness 94
Figure 4.11: MG-63 human osteoblast sarcoma fibroblast: (a) control surface with HA only, (b) surface with HA/SNP, (c) surface with HA/SNP/HA at 10 nm thickness, (d) surface with HA/SNP/HA at 20 nm thickness, (e) surface with HA/SNP/HA at 30 nm thickness 95
Figure 4.12: MG-63 human osteoblast sarcoma fibroblast after 48 hours of cell growth: (a) control surface with HA only, (b) HA/SNP, (c) and HA/SNP/HA at 10 nm thickness were the same as at 24 hours. Surface with HA/SNP/HA at 20 nm and 30 nm thickness showed all dead cells as in (b) and (c). 96
Figure 5.1: The antimicrobial peptide LL-37 102
Figure 5.2: The antimicrobial peptide magainin 2 103
Figure 5.3: The antimicrobial peptide parasin 1 103
Figure 5.4: Immobilisation of antimicrobial peptides via reductive amination onto ALDpp (the XPS data shows aldehyde and hydroxyl groups on the surface) .. 103
Figure 5.5: XPS spectra of ALDpp and ALDpp-Mg2 surfaces: (a) ALDpp, survey; (b) ALDpp, C 1s; (c) ALDpp-Mg2, survey; (d) ALDpp-Mg2, C 1s 108
Figure 5.6: Positive survey mass spectra of ALDpp and its modifications with antimicrobial peptides: (a) th-ALDpp, (b) th-ALDpp-LL37, (c) th-ALDpp-Mg2, (d) th-ALDpp-Pa1 109
Figure 5.7: Positive mass spectra in range of m/z 42.95–43.15 for ALDpp and its modifications with antimicrobial peptides: (a) th-ALDpp, (b) th-ALDpp-LL37, (c) th-ALDpp-Mg2, (d) th-ALDpp-Pa1 (evidence of arginine residues in LL37 and Pa1 modifications–$CH_3N_2^+$) 110
Figure 5.8: Scores plot on PC1 and PC2 for 3 surfaces with covalently immobilised antimicrobial peptides (190 positive fragment ions were used in calculations) 111
Figure 5.9: Loadings of positive fragments on PC1 and PC2 for 3 surfaces with covalently immobilised antimicrobial peptides 112
Figure 5.10: *S. epidermidis* on a control aldehyde plasma polymer (ALDpp) after 5 hours incubation. 114

Figure 5.11: LL-37 covalently immobilised onto an ALDpp after 5 hours incubation. 114
Figure 5.12: Magainin 2 covalently immobilised onto an ALDpp after 5 hours incubation 115
Figure 5.13: Parasin 1 covalently immobilised onto an ALDpp after 6 hours incubation. 115
Figure 5.14: LL37 with $1x10^7$ CFU *S. epidermidis*: (a) after 4 hours incubation, (b) after 6 hours incubation, (c) after 20 hours incubation 116
Figure 5.15: Magainin 2 with $1x10^7$ cfu *S. epidermidis*: (a) after 4 hours incubation, (b) after 6 hours incubation, (c) 20 hours incubation 117
Figure 5.16: Parasin 1 with $1 x 10^7$ cfu *S. epidermidis*: (a) after 4 hours incubation, (b) after 6 hours incubation, (c) after 20 hours incubation, (d) control. 118
Figure 5.17: Growth of primary human fibroblasts on control samples and on AMP-grafted surfaces, counted per view at 10x magnification..... 121
Figure 6.1: Chemical structure of Nylon 3-1. R = methyl. 127
Figure 6.2: Chemical structure of Nylon 3-2. 128
Figure 6.3: Chemical structure of Nylon 3-3. 128
Figure 6.4: Illustration of intended immobilisation routes of Nylons onto epoxide-functionalised surface via (a) backbone-pendent amines and (b) terminal thiol 129
Figure 6.5: Chemical structures of Nylon 3125 (top) and Nylon 3127 (bottom); n = 30 (Runhui Liu, University of Wisconsin, USA)..... 131
Figure 6.6: Schematic illustration of the covalent immobilisation of alkyne-terminated Nylon-3 copolymers onto AGE plasma polymer via click chemistry. ..... **Error! Bookmark not defined.**
Figure 6.7: Positive static mass spectra of AGEpp (a) and grafted with Nylon 3-1 (b) and Nylon 3-1 with the red end group signifying the circled peak at 161 (c)... 138
Figure 6.8: Scores plot for positive ion spectra recorded on AGEpp and Nylon-3 copolymer grafted surfaces 139
Figure 6.9: Loadings plot on PC1 of positive ions recorded on AGEpp and Nylon-3 copolymer grafted surfaces 140

Figure 6.10: High resolution C 1*s* and N 1*s* XPS spectra of the AGEpp substrate [(a) and (b) respectively] and after grafting of Nylon 3127 [(c) and (d) respectively]. .....**Error! Bookmark not defined.**
Figure 6.11: Positive mass spectra recorded on (a) Th-AGEpp-N_3; (b) th-AGEpp-N_3-Nyl3215; (c) th-AGEpp-N_3-Nyl3217..... 147
Figure 6.12: 146
Figure 6.13: PCA analysis of the positive ion spectra recorded on AGEpp, AGEpp with N_3, and after immobilisation of Nylon 3125 and Nylon 3127 ..**Error! Bookmark not defined.**
Figure 6.14: Scores (a) and loadings (b) plots of spectra from coatings of Nylon 3125 and Nylon 3127 145
Figure 6.15: Control AGEpp with *S. epidermidis* after 6 hours incubation at 37 ºC and stained with the LIVE/DEAD *Bac*Light stain. Green bacteria are alive; red bacteria are dead. (20x image) 149
Figure 6.16: AGEpp with nylon 3-1 immobilised on the surface with *S. epidermidis* after 6 hours incubation at 37 ºC stained with the LIVE/DEAD *Bac*Light stain. There is much less bacterial colonisation of the surface; most are dead as seen by the red staining. There is no biofilm present. 150
Figure 6.17: AGEpp with nylon 3-2 immobilised onto the surface with *S. epidermidis* after 6 hours incubation at 37 ºC stained with the LIVE/DEAD *Bac*Light stain. There are large patches of dead bacteria on the surface with some live bacteria present..... 151
Figure 6.18: AGEpp with nylon 3-3 immobilised onto the surface with *S. epidermidis* after 6 hours incubation at 37 ºC stained with the LIVE/DEAD *Bac*Light stain. This is shown as a 60x image to show the live bacteria growing on the dead bacteria..... 152
Figure 6.19: Graph showing amounts of bacteria colonising the surfaces with *S. epidermidis* after 6 hours incubation at 37 ºC, after removing adherent bacteria, serial diluting and plating for overnight growth. Averaged numbers are recorded above the bars. Taken over nine samples each, repeated three times. 153

Figure 6.20: Numbers of *S. epidermidis* after 24 hours incubation at 37 ^{o}C, after removing adherent bacteria, serial diluting and plating for overnight growth. Averages over nine samples each, repeated three times. 154
Figure 6.21: Control click pp with 1 x 10^5 cfu/ml *S. epidermidis* after 24 hours growth.. 155
Figure 6.22: Nylon 3-6 immobilised using click reaction to a pp surface with 1 x 10^5 cfu/ml *S. epidermidis* after 24 hours growth..... 155
Figure 6.23: O 1s, N 1s and C 1s high-resolution spectra for: (a) AGEpp, (b) AGEpp with nylon 3-1 immobilised, (c) AGEpp with nylon 3-1 immobilised and with medium/serum (cell medium, CM)..... 157
Figure 6.24: Number of human primary fibroblasts on the nylon and control surfaces after 3 days growth, counted per frame..... 159
Figure 6.25: Nylon 3-1 immobilised surface with human primary fibroblasts..... 159
Figure 6.26: Nylon 3-2 immobilised surface with human primary fibroblasts..... 160
Figure 6.27: Nylon 3-3 immobilised surface with human primary fibroblasts..... 160
Figure 6.28: Control polystyrene surface with human primary fibroblasts 160
Figure 6.29: Control AGEpp surface with human primary fibroblasts..... 161
Figure 6.30: Scores on PC1 and PC2 (top) and loadings on PC1 (bottom) of positive mass spectra of nylon 3-1 and nylon 3-1 after contact with medium/serum 162
Figure 6.31: Statistically evaluated intensities of aspartic acid (D), glycine (G) and arginine (R) residues across nylon-3 samples (-1, -2 and -3) before and after contact with medium/serum (cell medium, CM) 163
Figure 6.32: A control AGE surface with serum (above) and without serum (below), showing the difficulty testing any surface with serum added. The serum physiosorbs onto the surface and the bacteria attach to this and are easily removed through rinsing before bacteria assessment..... 165
Figure 6.33: AGEpp with nylon-1 immobilised without serum (above) and with serum (below) after 5 hours incubation. There are virtually no bacteria at all on the top image, and there are more dead bacteria on the image with serum added, possibly physisorbed onto the surface. 165
Figure 6.34: AGEpp with nylon 3 immobilised after 5 hours incubation with serum. There are much more bacteria, both dead and alive. Normally, it is not useful

to look at surfaces after only 5 hours incubation because very few bacteria would be present. Further rinsing may affect this image. 166
Figure 6.35: AGEpp with nylon-1 immobilised after 24 hours incubation with serum. This particular substrate and FBS batch did not show full antibacterial activity with serum added. This may be a result of unusually vigorous bacteria or fresh serum, or it may be a result of a new batch of substrates. The control also showed much heavier biofilm colonisation and adherence, which raises the suspicion that the bacterium may have changed its phenotype. 166
Figure 6.36: Control plasma surface with AGEpp only. LIVE/DEAD *Bac*Light stain shows HFF-1 fibroblasts that are colonised with *S. epidermidis*, the cells have not spread over the wound gap and live bacteria are colonising the wound area and between the cells. Some cells have been affected and are dead. 169
Figure 6.37: The scratch area of the wound scratch assay with HFF-1 cells using the LIVE/DEAD BacLight assay to show green/live cells that have migrated or grown across the wound area, closing it completely. No *S. epidermidis* is visible anywhere on the surface. 170
Figure 7.1: Daptomycin, $C_{72}H_{101}N_{17}O_{25}$ (1619.7086 MW) 175
Figure 7.2: Possible mechanism of action of daptomycin: (a) without calcium, (b) with calcium in a 1:1 ratio, (c) upon contact with the bacterial membrane 176
Figure 7.3: A refined model for the mechanism of action of daptomycin (light-blue 'cups' with yellow circles). Also shown is phosphatidylglycerol (green lipids), cardiolipin (yellow lipids), potassium ions (green circles), and DivIVA (blue ovals). (Pogliano, Pogliano & Silverman 2012) 177
Figure 7.4: A proposed mechanism of antibacterial activity if surface attached via the upper cluster of amine group indicated by the green arrow (Powell, Al Nakeeb et al. 2007; Powell, Borg et al. 2007). There are other amine groups in this area and the opposite side that would also attach..... 178
Figure 7.5: High-resolution C 1s spectrum of AGEpp 183

Figure 7.6: *S. epidermidis* after 24 hours incubation at 37 ºC on an AGEpp control surface, and ALDpp control surface with $NaBH^3CN$. Both surfaces showed full biofilm over the entire surface, which detached with rinsing..... 184
Figure 7.7: The same samples as the ones above shown at 20x magnification. No dead bacteria are visible..... 185
Figure 7.8: The same samples again at 100x and 60x magnification and very few dead bacteria are seen..... 185
Figure 7.9: *S. epidermidis* after 24 hours incubation at 37 ºC on an AGEpp daptomycin surface, and ALDpp daptomycin surface with $NaBH^3CN$. Both surfaces showed full biofilm over the entire surface, which seemed to be more firmly adhered and detached less with rinsing..... 185
Figure 7.10: The same samples as the ones in Figure 7.9 shown at 20x magnification. No dead bacteria are visible..... 186
Figure 7.11: The same samples again at 100x magnification and very few dead bacteria are seen..... 186
Figure 7.12: *S. epidermidis* after 6 hours incubation at 37 ºC on an AGEpp surface, and ALDpp surface with $NaBH^3CN$. Both surfaces show some bacteria colonising the surface with a few dead bacteria towards the centre; this could be a result of damage during staining..... 188
Figure 7.13: *S. epidermidis* after 24 hours incubation at 37 ºC on an AGEpp daptomycin surface, and ALDpp daptomycin surface with $NaBH^3CN$..... 188
Figure 7.14: *S. epidermidis* after 24 hours incubation at 37 ºC on a control pp with 5 mM/l Ca^{2+} added to the bacteria solution, and daptomycin surface with 5 mM/l Ca^{2+}. Both surfaces showed biofilm over the surface, which seemed to be more easily detached with rinsing. The daptomycin surface showed much more loosely attached biofilm..... 189
Figure 8.1: *Candida albicans* ATCC 10231. The yeast cells reproduce from buds on the blastospores. The pseudohyphae are elongated chains of yeast cells. Pseudohyphae grow from a bud that remains attached to the mother cell. Chlamydospores are attached to a blastospore via a suspension cell and may represent a dormant phase of yeast. True hyphae grow at the tip and can have

branches. (Deacon & Deacon 2006) Sourced from http://commons.wikimedia.org/wiki/File:C_albicans_en.jpg. 193
Figure 8.2: Images of *Candida albicans* showing the hyphal form: (a) an image of mature hyphae to give an indication of the invasiveness of the hyphae as it branches and invades tissue (http://en.wikipedia.org/wiki/File:C_albicans_en.jpg); (b) the hyphae forming from the blastospores and the beginning of branching—the growth changes in that it grows from the tips of the hyphae and has a much higher amount of chitin in the cell wall (http://lib.jiangnan.edu.cn/ASM/317-3.jpg; Lee, Campbell & Buckley 1975); c) *Candida albicans* hyphae (Gram stain) in a section of lung confirming *Candidal* pneumonia (http://www.life-worldwide.org/fungal-diseases/histopathology/) 195
Figure 8.3: Structure of the *Candida albicans* cell wall. The two layers are seen in the first photo; the outer layer is highly enriched with *O*- and *N*-linked glycoproteins, whereas the inner layer contains the skeletal polysaccharides chitin and β-1,3 glucan that confer strength and cell shape. The outer cell wall proteins are attached to this framework predominantly by glycosylphosphatidylinositol (GPI) remnants that are linked to the skeleton through a more flexible β-1,6 glucan (Gow et al. 2012). Chitin connects this to the plasma membrane..... 196
Figure 8.4: *Candida albicans* invading the epithelium and its subsequent seeding into the bloodstream (Gow et al. 2012)..... 197
Figure 8.5: Chemical structure of amphotericin B. MW 924.08 $C_{47}H_{73}NO_{17}$ 198
Figure 8.6: Chemical structure of caspofungin MW 1093.31 $C_{52}H_{88}N_{10}O_{15}$..... 200
Figure 8.7: Positive mass spectra for: (a) ALDpp, (b) ALDpp-AmphB..... 206
Figure 8.8: PCS/Scores plot on PC1 and PC2 207
Figure 8.9: Loading comparison of the positive mass spectra across ALDpp and its modification with amphotericin B (ALDpp-AmphB). The red circled groups indicate amphotericin B. 208

Figure 8.10: Structure and molecular weight of caspofungin (red-marked structural components contribute to $C_4H_8NO^+$ fragment ion highlighted in positive mass spectrum for ALDpp-caspofungin) 210
Figure 8.11: ToF-SIMS analysis of surface immobilisation of caspofungin to the surface: (a) the control aldehyde surface, (b) the caspofungin-modified surface with the fragment highlighted from Figure 8.5 211
Figure 8.12: Scores plot on PC1 and PC2: (a) loadings on PC1 (b) positive mass spectra for ALDpp and ALDpp-Casp..... 212
Figure 8.13: *Candida albicans* grown after 48 hours: (b) positive control with green live stained fungi; (b) negative control, fungi treated with Virkon for 10 minutes 213
Figure 8.14: (a) Control *Candida albicans* after 48 hours growth, (b) amphotericin B liquid form at 0.6 mg/ml, which shows good killing 214
Figure 8.15: Images at 100x *Candida albicans* after 48 hours incubation. Amphotericin B liquid form treated surface with larger pseudohypae; membranes seem to be compromised and evidence of leakage is seen. 215
Figure 8.16: Control surface with *Candida albicans* 216
Figure 8.17: Amphotericin B on a polystyrene-treated surface. Few live *Candida albicans* are noted. 217
Figure 8.18: Surfaces with amphotericin B immobilised were soaked for 2 weeks: (a) and b) are the control surfaces showing biofilm and mostly yeast cells; (c) and (d) are the amphotericin-treated surface, showing an increase in hyphae and pseudohyphae formation 218
Figure 8.19: Proposed mechanism of action of amphotericin B (Volmer, Szpilman & Carreira 2010) (From http://www.rsc.org/ej/NP/2010/b820743g/b820743g-f6.gif)..... 220
Figure 8.20: Control ALDpp surfaces after 48–56 hours with *Candida albicans* on the surface: (a) control ALDpp showing full surface, (b) 60x image of control surface, (c) 100x image of control surface, (d) TCPS control. 222
Figure 8.21: Caspofungin-treated plasma polymer surfaces with *Candida albicans* after 48 hours incubation—no intact yeast cells or hyphae were found on the

surface: (a) appears greenish due to background fluorescence; (b) full frame of dead fungi; (c) 60x image of dead fungi—backgroup fluorescence makes them appear greenish, but they are misshapen and leaking; (d) 100x image of dead fungi, showing possible leaking and broken hyphae 223
Figure 8.22: Aldehyde plasma polymer surfaces: (a) control surface with multiple yeast cell colonies and some pseudohypae, (b) caspofungin surface soaked and stored for 2 weeks before testing, with *Candida albicans* after 48 hours incubation, showing some contamination from removal of the mask but no viable cells..... 224
Figure 8.23: Control and Caspofungin-treated surface with primary fibroblasts after 3 days growth: (a) control surface, (b) caspofungin-treated surface..... 225
Figure 8.24: Primary human fibroblast cells per view area. Caspofungin was not toxic to cells. 226

List of Tables

Table 1.1: Surface structures of bacteria involved in adhesion (Wilson, Henderson & McNab 2002) 9
Table 3.1: Composition of silver nanoparticles 59
Table 4.1: Composition of silver nanoparticles 79
Table 4.2: Results of samples with no rinsing, and with one, two and three rinses. Antibacterial activity is compromised if rinsed. 88
Table 5.1: Compositions determined by XPS of plasma polymers on a Thermanox (Th) substrate (ALDpp) and grafted with antimicrobial peptides..... 107
Table 5.2: Quantitative XPS data for ALDpp and its modifications with antimicrobial peptides 107
Table 6.1: Compositions determined by XPS of plasma polymers at 0.1 mg/ml on a Thermanox (Th) substrate, (AGEpp) and grafted with nylon 3 polymers..... 136
Table 6.2: Elemental compositions of samples, with (red) referring to reductive amination. The percentages are calculated from survey spectra..... 158
Table 6.3: XPS results showing percentage of nitrogen on fresh samples and samples soaked for 10 days..... 167
Table 7.1: Surface composition using XPS..... 183
Table 7.2 Results of manual scraping and plating of bacteria from surfaces 187
Table 8.1. Composition of ALDpp and its amphotericin B modification by XPS 205
Table 8.2: Composition of ALDpp and its caspofungin modification by XPS 209

List of Abbreviations

ADXPS	Angle-dependent X-ray photoelectron spectroscopy
Ag^+	Silver ion
AGE	Allyl glycidyl ether
AGEpp	Allyl glycidyl ether plasma polymer
$AgNO_3$	Silver nitrate
AgNP	Silver nanoparticle
ALD	Aldehyde; here specifically Propionaldehyde (aka Propanal)
ALDpp	Aldehyde plasma polymer (bearing aldehyde surface groups; deposited from Propionaldehyde)
AMP	Antimicrobial peptide
ATP	Adenosine triphosphate
ATRP	Atom transfer radical polymerisation
BAI	Biomaterials-associated infections
BSA	Bovine serum albumin
CDMEM	Dulbecco's modified Eagle medium
CH	Cyclohexyl
CO_2	Carbon dioxide
CPP	Cell-penetrating peptide
CW	Constant wave
DC	Duty cycle
DMSO	Dimethyl sulfoxide
DNA	Deoxyribonucleic acid
ECM	Extracellular matrix
EDC	1-Ethyl-3-(3-dimethylaminopropyl) carbodiimide
EtOH	Ethanol
FBS	Foetal ovine serum
FEP	Fluorinated ethylene propylene
FP	Fusion peptide
GPI	Glycosylphosphatidylinositol

H_2O	Water
HA	Heptylamine
HApp	HA plasma polymer
HBA	Horse blood agar
hCAP18/LL37	Human cathelicidin
HCE	Human cornea epithelium
HDP	Host defence peptide
HIV	Human immunodeficiency virus
ICP-MS	Inductively coupled plasma mass spectrometry
ICU	Intensive care unit
IDR	Innate defence regulator
LBL	Layer-by-layer
MBC	Minimal bactericidal concentration
Mg2	Magainin 2
MIC	Minimal inhibitory concentration
MM	Monomethyl
MQ	Milli-Q
MRSA	Methicillin-resistant *Staphylococcus aureus*
MSCRAMM	Microbial surface components recognising adhesive matrix molecules
MSSA	Methicillin-sensitive *Staphylococcus aureus*
N_2	Nitrogen gas
NA	Nutrient agar
$NaBH_4$	Sodium borohydride
NaCl	Sodium chloride
$NaBH_3CN$	Sodium cyanoborohydride
NADH	Nicotinamide adenine dinucleotide
NHS	N-hydroxysuccinimide
NMP	Nitroxide-mediated polymerisation
PA	Propanaldehyde
Pa1	Parasin 1
PBS	Phosphate buffered saline

PCA	Principal component analysis
PCS	Principal component scores
PEG	Polyethylene glycol
PIA	Polysaccharide intercellular adhesion
PLGA	Poly(lactide-co-glyclolide)
pp	Plasma polymer
PTFE	Poly(tetrafluoroethylene)
PVA	Polyvinyl acetate
QAC	Quaternary ammonium compound
RAFT	Reversible addition-fragmentation chain transfer
rf	Radio frequency
rfGD	Radio-frequency glow discharge
RGD	Arginine-glycine-aspartic acid
RNA	Ribonucleic acid
ROS	Reactive oxygen species
RPE	Retinal pigmented epithelium
SAM	Self-assembled monolayer
SMAMP	Synthetic mimic of antimicrobial peptide
SNP	Single nucleotide polymorphism
TCA	Tricarboxylic
TCP	Tricalcium phosphate
ToF-SIMS	Time-of-flight secondary ion mass spectroscopy
TSB	Tryptone soya broth
UHV	Ultra-high vacuum
UV-Vis	Ultraviolet-visible
XPS	X-ray photoelectron spectroscopy
YPD	Yeast extract peptone dextrose

Abstract

This body of work has focused on investigating and producing antimicrobial surface coatings for potential use in biomaterial implants and wound healing products. The main aim was to develop a surface that has excellent antibacterial or antifungal properties, is non-toxic to the surrounding tissue, is cell adhesive, and promotes healing. It needs to have the ability to kill persistent bacterial or fungal adherence to an implant before, during or after surgery, thereby stopping any colonisation of the implant. It also needs to have the ability to support cell growth and encourage integration and healing. The challenge was to find commercially available or experimental substances that would retain antimicrobial activity when bound onto a solid biomaterial surface and remain active over a period of time relevant to clinical applications. The main potential application for the newly developed antimicrobial coatings would be for use on biomaterial implants; however, it could also be applicable to wound healing products or other medical devices, where there is a risk of infection moving into the wound from contaminated hands, surrounding skin, or trauma injuries. Every year, pathology reports on new resistant bacterial infections find that the vast majority of resistant *Staphylococcus aureus* are cultured from wound or implant infections. It is essential to keep bacteria that carry resistance to antibiotics from passing this resistance information on to other bacteria, and an important application for coatings would be to decrease the incidence of resistant infections being produced in wound and implant infections, by preventing bacterial or fungal cells from attaching onto surfaces of biomedical products and forming attached biofilms..

In this study, the approach used was to first coat a surface using plasma polymerisation to create a thin film containing reactive groups that could then be used for a covalent interfacial coupling reaction with an antimicrobial substance, thus creating an antimicrobial surface coating with permanently immobilised antimicrobial substances on plasma polymer interlayers. All coatings were thoroughly analysed by surface analytical techniques at all steps in order to ensure that the coating compositions were in accord with expectations and that biological responses could be interpreted with confidence in terms of specific surface chemistries. The antibacterial coatings studied herein contained silver nanoparticles,

naturally occurring antibacterial peptides, synthetic Nylon-3-class antimicrobial peptides (kindly provided by Prof. Sam Gellman), the antibiotic daptomycin, and the antifungal compounds amphotericin B and caspofungin. The peptides and antibiotics were chosen because they are membrane permeable and thought to kill by forming pores in bacterial membranes, thus causing microbes at all stages—growing, non-growing and persister—to die.

This study combines surface chemistry techniques, surface analysis, pharmacology, microbiology and immunology, and the physiology and pathology of infection and healing within one study to provide understanding of possible solutions to a major problem within the health industry. The most exciting results were obtained with Nylon-3-class synthetic compounds, which when surface-immobilised produced excellent antibacterial activity while showing no cytotoxicity, with human fibroblasts being able to attach and grow on the coated surfaces. In a scratch assay it was shown that such a coating stops bacteria from colonising a gap between fibroblast cell areas and enabling fibroblasts to migrate onto the coated area and close the gap, whereas in the absence of a coating the cells were unable to do so due to the presence of settled bacteria.

Declaration of Originality

This thesis presents work carried out by myself and does not incorporate without acknowledgement any material previously submitted for a degree or diploma in any university; to the best of my knowledge it does not contain any material previously published or written by another person except where due reference is made in the text; and all substantive contributions by others to the work presented, including jointly authored publications, are clearly acknowledged.

Stefani S Griesser

January 2015

Acknowledgements

I would like to thank my husband and support team, Hans. I would also like to thank Krasi for stepping in and saving my PhD.

I am most grateful to Marek Jasieniak for performing XPS and ToF-SIMS analyses of my samples, and for many helpful discussions on the interpretation of data and spectra.

The Wound Management Innovation CRC is gratefully acknowledged for providing funding comprising a scholarship and project consumables. CRC events also provided valuable for information gathering and networking.

List of Publications

Two reviews and two book chapters:

K. Vasilev, S.S. Griesser, H.J. Griesser
Antibacterial Surfaces and Coatings Produced by Plasma Techniques
Plasma Processes and Polymers, 8, 1010-1023 (2011)

H.J. Griesser, H. Hall, A.T.A. Jenkins, S.S. Griesser, K. Vasilev
Antimicrobial and anti-inflammatory intelligent surfaces.
In: *Intelligent Surfaces in Biotechnology*, H.M. Grandin and M. Textor (Eds.), Wiley&Sons, US, p. 183-242 (2012).

N. Poulter, K. Vasilev, S.S. Griesser, H.J. Griesser
Silver containing biomaterials.
In: *Biomaterials Associated Infection* (Eds. Moriarty, Zaat and Busscher), Springer, p. 355-378 (2013).

T.D. Michl, K.E.S. Locock, S.S. Griesser, M. Haeussler, L. Meagher, H.J. Griesser
Bio-inspired antimicrobial polymers.
In: *Biosynthetic polymers for medical applications* (Eds. Poole-Warren, Martens), Woodhead Publishing, p. 87-127 (2016). ISBN: 978-1-78242-105-4.

I contributed to the writing of those outputs, which incorporate some results from my thesis and discuss them in the broader context of infection-resistant biomaterials.

B.R. Coad, M. Jasieniak, S.S. Griesser, H.J. Griesser
Controlled covalent surface immobilisation of proteins and peptides using plasma methods.
Surface and Coatings Technology, **233**, 169-177 (2013)

S.S. Griesser, M. Jasieniak, B.R. Coad, H.J. Griesser
Antifungal coatings by caspofungin immobilization onto biomaterials surfaces via a plasma polymer interlayer.
Biointerphases, **10**, 04A307 (2015)

B.R. Coad, S.J. Lamont-Friedrich, L. Gwynne, M. Jasieniak, S.S. Griesser, A. Traven, A.Y. Peleg, H.J. Griesser
Surface coatings with covalently attached caspofungin are effective in eliminating fungal pathogens
Journal of Materials Chemistry B, **3**, 8469-8476 (2015)

Additional publications are in preparation.

List of Conference Presentations

I presented these contributions containing work described in this thesis:

Stefani S. Griesser, Krasimir Vasilev, Marek Jasieniak and Hans J. Griesser, ‘Antibacterial coatings: antimicrobial peptides grafted onto aldehyde and epoxy plasma polymer interlayers’, 4th International Symposium Interface Biology of Implants, Warnemunde, Germany 9–11 May 2012, poster.

Stefani S. Griesser, Krasimir Vasilev, Marek Jasieniak and Hans J Griesser, ‘Antibacterial coatings: antimicrobial peptides grafted onto aldehyde and epoxy plasma polymer interlayers’, Gordon Research Conference, Biointerface Science, 20–25 May 2012, poster.

Stefani S Griesser, Krasimir Vasilev, Marek Jasieniak and Hans J Griesser, Antibacterial coatings: antimicrobial peptides and synthetic analogues grafted onto aldehyde plasma polymer interlayers’, 22nd Annual Conference of the Australasian Society for Biomaterials and Tissue Engineering, Tanunda, Australia, 2–5 April 2013

Stefani S Griesser, Krasimir Vasilev, Marek Jasieniak and Hans J Griesser**, ‘**Antibacterial coatings: antimicrobial peptides and synthetic analogues grafted onto aldehyde plasma polymer interlayers’, Australian Microbiology Society (2014).

Chapter 1: Introduction

1.1 General Introduction

An ageing population along with an increase in antibiotic resistance and the emergence of disease resulting from mixed pathogens has led to an urgent need for alternative approaches to infection management, particularly for biomedical device–associated infections and chronic wounds. Biomedical devices and biomaterials encompass a massive part of modern medicine and cover a range of materials used to fabricate hip and knee implants, stents, catheters, feeding tubes, wound coverings and sutures, and many other items. Wounds comprise those that are a result of primary intention, which are clean and precise surgical wounds; secondary wounds from injuries; and complicated wounds from a combination of issues, including underlying illness and age. To complicate matters further is the complex issue of hospital pathogens. Hospitals are collections of patients exhibiting many combinations of illnesses, wounds, surgeries and biomaterials, providing an excellent environment for pathogens to hide and grow. An estimated 5% of all hospital admissions are complicated by a hospital-acquired infection, equating to approximately 1.7 million infections per year in the US alone (Klevens et al. 2007). Of these infections in the US alone, approximately 99,000 die each year, making hospital-acquired infections the sixth leading cause of death (Peleg & Hooper 2010). Costs to the health care budget are staggering, with estimates of $5 to $6 billion annually in the US (Stone et al. 2005).

The Australian Group on Antimicrobial Resistance Community Survey for 2012 reported that the six resistant strains of *Staphylococcus aureus* that emerged in that year were all found in chronic wounds, including one from an implant infection. Trends show that antibiotic resistance is increasing significantly (Chua et al. 2011; Coombs et al. 2011; Palavecino 2014). Resistant pathogens remain one of the biggest threats to health care today and new resistant bacteria are easily outpacing our development of new antibiotics (Peleg & Hooper 2010).

There is enormous scope to improve biomedical devices and wound dressings to address the problems associated with infections arising at their surfaces. For example, coating devices with a non-toxic, cell-promoting, infection- and inflammation-reducing peptide can provide a biocompatible surface for integration with the body (Costa et al. 2011). Antimicrobial peptides (AMPs) are found naturally in all plants and animals and are an important part of the innate immune system in humans (Brogden 2005). Many studies have investigated ways to make use of their underexploited antimicrobial activity (Hurdle et al. 2011). AMPs also have many signalling activities, and not only can they reduce infection, but they also control inflammation and signal for a healing response (Zaat & Hiemstra 2013). By coupling these biomolecules onto a material surface, one can integrate them into the wound and assist the body with its own infection control and healing. Avoiding infections can decrease the occurrence of resistance resulting from those infections.

There is a large body of literature on surfaces/surface coatings and on materials releasing silver ions and other antimicrobials, designed for treating infections, but few treatments are in current medical use; one example is the Acticoat™ silver-impregnated barrier dressing from Smith & Nephew (see Figure 1.1). There are still questions and literature controversy about the safety and clinical benefit of the use of silver in wound dressings, yet Acticoat™ is a highly used and popular choice (Burd, Chiu & Huang 2008; Chopra 2007).

The number of types of antibacterial dressing continues to rise, but no biomaterial implants with antibacterial coatings are in use. Biomaterial-associated implant infections continue to have the high infection rate that was estimated to be in the millions in 2004 (Brooks, Brooks & Grainger 2013). Implant infections are a result of bacteria adhering to an implant before, during or after surgery, allowing colonisation and subsequent bacterial growth on the implant and creating a clinical grade infection on and around the device. They are treated through antibiotics and removal or replacement of the implant. This makes implant infections highly costly and very difficult for patients. As the need for implants continues to rise, a solution to implant infections has become highly desirable.

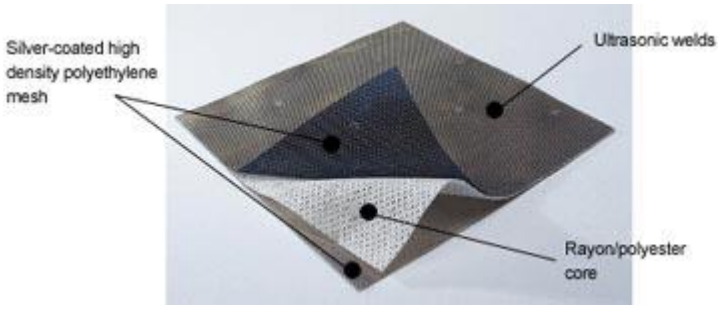


Figure 1.1: An example of the nanocrystalline silver dressing, Acticoat (Brett 2013) (From: http://www.smith-nephew.com/australia/healthcare/products/product-types/antimicrobial-dressings/silver-dressings/acticoat--product-range/acticoat-/)

1.2 Aim and Motivation

The present research is motivated by the question of how best to develop antibacterial coatings for various applications. It seems reasonable to assume that there is no single universal solution because the causative bacteria and the environment differ for the wide range of biomedical devices and implants that become infected. For example, hip and knee implants tend to be colonised by *Staphylococcus*, catheters are colonised most often by *Escherichia coli* or *Candida* species, and contact lenses are colonised by *Pseudomonas aeruginosa*. Therefore, in this thesis, several approaches were investigated. One approach was the local delivery of antibacterial agents; the features of this approach have been reviewed by ter Boo et al. (ter Boo et al, 2015) and Campoccia et al. (Campoccia et al. 2013). First, silver-containing coatings were investigated because this approach is in current use and is quite controversial owing to differences in opinion about the safety of silver (Albers et al. 2013) and some literature reports showing no benefits while others show benefits, as discussed below in the literature review. However, the aim in this study was to examine a more controlled silver release system that may address some of the safety issues by limiting the amount of silver introduced into the wound (Griesser et al. 2012) and, specifically, the question of differential toxicity to bacteria versus mammalian cells.

Other chapters of this thesis will detail the development of coatings with surface-immobilised antibiotics, utilising both naturally occurring antimicrobial peptides (AMPs) and synthetic analogues. AMPs immobilised onto a synthetic surface can be tethered in a way to maintain an

active conformation (Chen et al. 2012), and minimal adverse effects on mammalian cells will be shown. The biological tests are accompanied by detailed surface analyses to ensure that we can draw reliable interpretations about observed bio-interfacial interactions.

Infections associated with biomaterials are an ever-increasing problem in the medical world. As one pathogen is controlled, another takes its place, and fungal infections are following on from bacteria and taking advantage of conditions in immune-compromised patients (Peleg, Hogan & Mylonakis 2010). There is a clear need for a broad-spectrum antimicrobial that prevents colonisation of biomaterials without damaging mammalian cells, minimises the potential for bacteria resistance and is stable over time. AMPs and their synthetic analogues have enormous potential for satisfying these criteria because of their membrane-permeabilising abilities and stability. Although many studies have examined using them as an antimicrobial surface, most are lacking in investigation of solid surface characterisation and specific investigations that would define tethering parameters such as surface concentrations and peptide orientation, as well as thorough investigations into actual killing on the surface (Chen et al. 2012; Costa et al. 2011). It is essential to follow up visual evidence such as *Bac*Light stains with cell counts to assure results are reliable.

AMPs are an abundant and diverse group of molecules that are found in many tissues and different cells in a large variety of plant and animal species. LL37 (active sequence 134-170) is a well-known antimicrobial protein from human cathelicidin (hCAP18/LL37) (Hell et al. 2010; Ramos et al. 2011). It is an effector of the innate immune system and expressed in leukocytes and epithelial cells, and in neutrophils and keratinocytes of inflamed skin (Zaat & Hiemstra, 2013). Magainin 2 (Mg2) is found in amphibians (e.g. African clawed frog) and is also a well-known AMP (Ludtke et al. 1996; Woo & Wallqvist 2011). Both LL37 and magainin 2 are linear cationic alpha-helical peptides, and activity is through transmembrane pore formation. Parasin 1 (Pa1), isolated from the catfish skin mucosa, is a histone H2A-derived AMP (Koo et al. 2008). As an amphipathic alpha-helical peptide, it has pore-forming ability but has also been found to induce intracellular killing by binding to nucleic acids (Brogden 2005).

One possible drawback of all these AMPs is their possible removal from biomaterials surfaces by proteolytic enzymes. An interesting alternative approach is the use of synthetic non-proteolysable AMP mimics. Gellman and co-workers have developed a series of such synthetic polymers, of the nylon-3 family (Mowery et al. 2009), and kindly supplied us with them for covalent surface attachment. Their polymers showed excellent antibacterial performance in solution; here, we extend this to surface grafting.

This study begins by investigating the antimicrobial activity of silver ions released from nanoparticles in coatings and the toxicity associated with them. It continues by investigating the three AMPs mentioned above, and the nylon-3 synthetic nylon peptide mimics covalently attached to surfaces. This study will also report briefly on the antibiotic daptomycin covalently attached to surfaces, which is also thought to have a pore-forming mechanism of action. Finally, this study investigates antifungal surfaces and the covalent attachment of amphotericin B and caspofungin, because recent studies have shown that not only are the long-recognised bacterial infections clinically important but so are fungal and polymicrobial infections (Peleg, Hogan & Mylonakis 2010).

1.3 General Introduction to Bacterial Disease Mechanisms

The human body is host to many millions of bacteria, an amount estimated to be around 10^{14} or around 10 times more than human cells (Wilson, Henderson & McNab 2002). Most of these bacteria can be classified as non-pathogenic, often symbiotic, and are referred to as indigenous biota or ‘good bacteria’. This balance is maintained through the natural barrier of our skin, natural oils and acidic secretions along with natural AMPs, which are found in secreted fluids throughout the body. The internal body is sterile except for the digestive and reproductive systems, which harbour very important biota that aid the immune system in reducing attack by pathogens. Many bacteria are necessary in the digestion of food and the production of vitamins. Among these ‘good’ bacteria are many that can become pathogens. Opportunistic pathogens must wait for an injury or a breach in the natural barrier, or a change in the natural balance of indigenous biota before the body is open to colonisation by pathogens. Successful pathogens have been described as ‘expert cell biologists’, because they demonstrate a sophisticated

understanding of our body's complex cellular system. Bacteria excel at exploiting pre-existing regulatory pathways, inducing the eukaryotic cell host to perform energetically demanding and, ultimately, self-destructive feats (Cossart, 2005; Wilson, Henderson & McNab 2002).

With the exception of bacteria that are found in the faeces and saliva, all of the bacteria present in the body maintain themselves by adhering to a surface. This is one of the most important ways in which the indigenous biota help protect our body from pathogens in that they dock on exposed cells and create an environment around them that suits themselves and the host, and deters other, pathogenic bacteria. The body normally has three main surface sites for bacterial adhesion: mucosae, skin and teeth (see Figure 1.2). Each of these provides a number of environments and variations of site for bacterial attachment. The mucosal surfaces include the gastrointestinal tract from mouth to anus, the reproductive tract and the respiratory tract. The skin is open to the environment yet has dryer and moister areas. Both of these systems have a number of protective mechanisms to prevent the attachment of opportunistic bacteria or limit the numbers, the most important of which would be the continually shedding of layers along with any adherent organisms. In contrast to these, the teeth are non-shedding and available to huge numbers of bacteria collecting on their surfaces. The glycoproteins in saliva coat the teeth and help to control bacterial adhesion, along with manual brushing to help remove the biofilms; however, large colonies of bacteria still form, and if allowed to accumulate, can cause decay and disease of the gums.

It is interesting and illustrative to consider biomaterial implants in comparison with teeth; they are also non-shedding surfaces, which can be sites that are completely defenceless and open to colonisation by bacterial and fungal biofilms. Biomaterial implants will always be covered with a layer of absorbed molecules, a 'conditioning film', whose composition will depend on where it is located; however, the implant will not come into direct contact with bacteria unless colonised before implantation. The 'conditioning film' consists of serum proteins that promote cell recruitment and tissue repair; unfortunately, these same serum proteins are used by pathogens for adhesion and virulence. This conditioning film also sets the scene for the immune response: C3 is an activator of the complement system, which is a part of the non-specific immune system; even very small amounts of C3 adsorbed with serum and blood proteins are

sufficient to assemble C3 convertase complexes, which can trigger the formation of ligands for receptors on leukocytes that then trigger inflammation (Andersson et al. 2002, 2005).

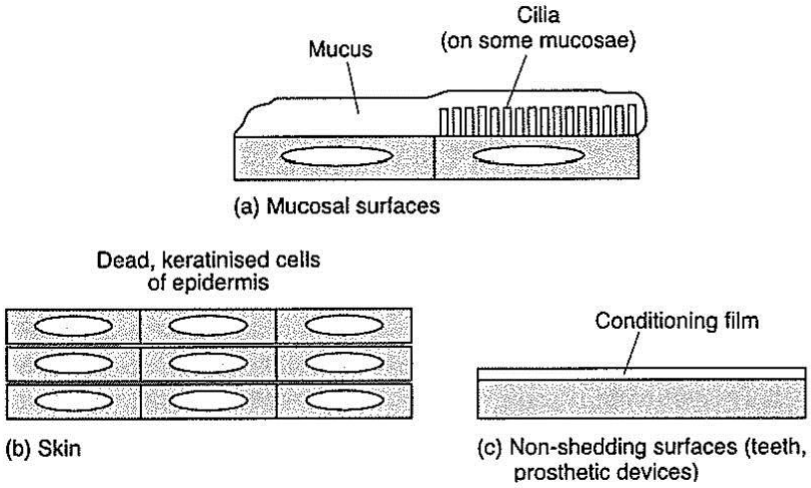


Figure 1.2: The three major types of surfaces with which bacteria frequently come into contact: (a) moist, shedding mucosal surfaces; (b) the dry, shedding surfaces of the skin; (c) non-shedding surfaces such as teeth and prosthetic devices (Wilson, Henderson & McNab 2002)

The mechanisms involved in bacterial adhesion are still not fully understood. It is assumed that physical forces such as van der Waals forces and electrostatic forces apply as the bacteria approach a surface (Daghighi et al. 2012; van der Mei & Busscher 2012), followed by biochemical enhancement with adhesin proteins for example. However, bacteria are living entities that may have other, active attraction or adhesion mechanisms that have not yet been fully understood. Adhesive interactions between host cells and bacteria are thought to be mediated primarily by hydrophobic, ion-bridging and receptor-ligand interactions (see Figure 1.3). Understanding the mechanism by which bacteria colonise surfaces with various chemistries and then enhance that adhesion would provide valuable insights into the rational design of antibacterial surfaces.

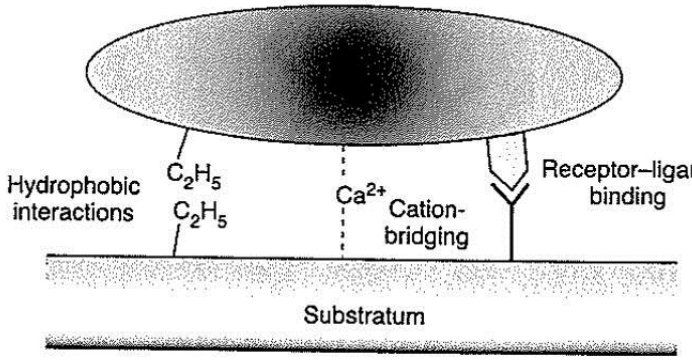


Figure 7.8 The principal types of molecular interaction involved in bacterial adhesion. Adhesion of a bacterium to a substratum may involve one or more of these.

Figure 1.3: The principal types of molecular interaction involved in bacterial adhesion. Adhesion of a bacterium to a substratum may involve one or more of these. (Wilson, Henderson & McNab 2002)

The bacterial surface also has many structures, some of which are associated solely with adhesion and others that are multifunctional. Some examples of these are the lipopolysaccharide S layer in *Aeromonas*, which adheres to cell surface proteins; the capsule with polysaccharide adhesins surrounding *Staphylococcus epidermidis*, which helps it to adhere to biomaterials surfaces; fimbriae found on many Gram-negative bacteria; flagella found on *Pseudomonas*; and the lipoteichoic acids, proteins and enzymes in the cell wall, which give *Streptococcus pyogenes* and *S. aureus* exceptional ability to adhere to epithelial cells, bone and other tissue.

Bacteria can adhere to host cells in three main ways: by adhering directly to the lipid bilayer, by binding directly to cell surface receptors on the host molecule or, indirectly, by binding to the extracellular matrix (ECM) and other molecules already bound to the host cell surface (see Table 1.1; Wilson, Henderson & McNab 2002). The ECM contains a number of adhesion molecules such as collagens, fibronectin and other matrix proteins, or adhesion receptors such as integrins, associated with the host cell. Bacteria can form permanent bonds with these proteins and activate cellular mechanisms that can influence the cell to support the pathogen, and promote their invasion and entry into tissues (Cossart 2005). These proteins are also found in serum throughout the body, and form the 'conditioning film' on implants, thus forming convenient attachment sites for bacteria (see Figure 1.4). They are also in abundance in wounds. Some bacteria can also carry \ their own receptor that they inject into the host cell membrane and then adhere.

Table 1.1: Surface structures of bacteria involved in adhesion (Wilson, Henderson & McNab 2002)

Structure	Bacterium	Surface/molecule to which the structure adheres
S layer	*Aeromonas salmonicida*	Fibronectin, laminin, vitronectin
	Lactobacillus acidophilus	Intestinal epithelial cells
Capsule	*Klebsiella pneumoniae*	Mucus
	Staphylococcus epidermidis	Various biomaterials
	Streptococcus pyogenes	Keratinocytes
	Bacteroides fragilis	Intestinal epithelial cells
Fimbriae	*Escherichia coli*	Intestinal and urinary epithelial cells
	Salmonella typhimurium	Intestinal epithelial cells
	Vibrio cholerae	Intestinal epithelial cells
	Bordetella pertussis	Laryngeal epithelial cells
	Actinomyces spp.	Bacteria (e.g. *Streptococcus* spp.)
	Pseudomonas aeruginosa	Epithelial cells of respiratory tract
Flagella	*Pseudomonas aeruginosa*	Epithelial cells
Cell wall	*Streptococcus pyogenes*	Epithelial cells
	Staphylococcus aureus	Epithelial cells
Fibrils	*Haemophilus influenzae*	Epithelial cells
	Streptococcus sanguis	Blood platelets, salivary proteins
Curli	*Escherichia coli*	Fibronectin, laminin, plasminogen, intestinal epithelial cells
	Salmonella spp.	Fibronectin, laminin, plasminogen, intestinal epithelial cells

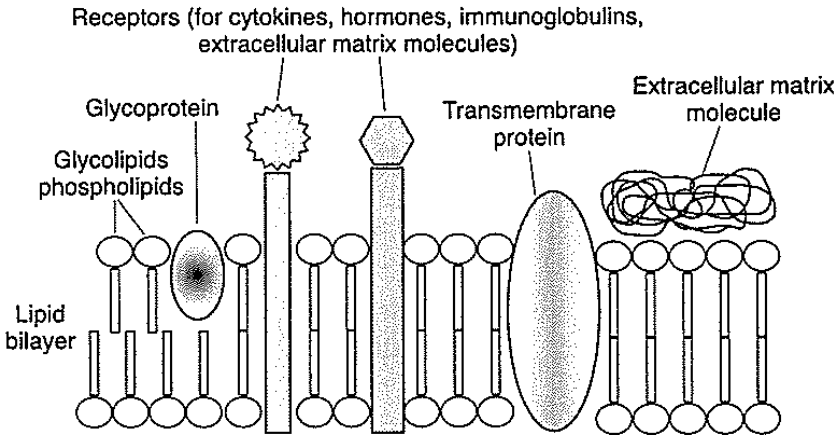


Figure 1.4: Diagram showing the major types of molecule to be found on the surface of a typical mammalian cell. Most of these can function as receptors for bacterial adhesins. (Wilson, Henderson & McNab 2002)

Once adhesion is obtained, bacteria can adjust to their environment by altering their phenotype to suit, and the cell and bacteria can begin their relationship. Successful adhesion will stimulate growth in some bacteria and inhibit growth in others; some bacteria will express proteins, and some will secrete proteins. The cell to which it is anchored will also be affected: the proteins and secretions from the bacteria will cause the cell to respond by induction of cytokines, or upregulation of proteins; the cell morphology can be altered, cells can be killed outright or apoptosis induced; bacteria can invade the cell; or the cell may have no response at all. Once bacteria are established on a surface, they will move from their sessile state to a community state in the form of a biofilm. Biofilms are typically characterised by dense clusters of bacterial cells held together by a highly hydrated extracellular polymeric substance secreted by the bacteria. This matrix protects them from the host immune response and makes them highly resistant to antibiotics. As bacteria adapt to this community, they continue to adapt their phenotype and state (Franklin & Stewart 2008). Persister states of bacteria are thought to be responsible for many chronic infections and may be responsible for infections of biomaterials years after implantation. Persister bacteria are dormant variants of regular cells that can survive long term and are highly resistant to antibiotics (Cossart 2005; Lewis 2010). Biofilms are often highly colonised with persister bacteria.

Bacteria can survive both extracellularly and intracellularly, with evidence showing them to invade cells far more often than was earlier believed (Cossart 2005). *Staphylococcus* can survive near implants by invading cells around them and survive in an intracellular state (Fraunholz & Sinha 2012). This makes them extremely hard to kill using the available treatments.

1.4 Bacterial Infections in Wounds and on Implants

There are many antibacterial defences in the human body, such as hairs in the nose, saliva flow, low pH in the stomach, salt and lipids produced by the skin, shedding, normal micro flora or indigenous biota, immunity, and AMPs and proteins. However, the most important defence is the epithelial layers and, in particular, the skin. Once the skin is breached, bacteria can quickly enter and access cell surfaces, adhere and colonise. The repair of wounds is one of the most complex biological processes that the body has to perform. Immediately after injury, multiple biological pathways become activated and are synchronised to respond to the needs of the wounded area. This requires complex coordination of various intracellular and intercellular pathways, which are simultaneously activated and organised to control blood loss, stabilise the wound and restore homeostasis. Cutaneous wound healing of the skin is a process that involves both epithelial regeneration and the formation of a connective tissue scar. Cutaneous wound healing has three main steps: (1) inflammation, (2) formation of granulation tissue and (3) ECM deposition and remodelling (Gurtner et al. 2008). Wounds are classified as primary, secondary or complicated.

A comparison of primary or first intention surgical wounds and secondary or second intention wounds gives a good indication of how infection can develop (see Figure 1.5). Although primary wounds generally have few issues with healing, secondary wounds have cell or tissue loss as a result of trauma, or can be an abscess, or can show ulceration. They can quickly become complicated wounds because of colonisation from surrounding tissue, the trauma, which also contaminates them and introduces foreign material and bacteria, or through underlying factors such as illness or age that affect healing. The presence of a biomaterial in host tissue strongly predisposes it for infection, mainly by commensal bacteria. Primary wounds with implanted biomaterials represent a large number of infections caused by bacteria infecting the wound or the biomaterial, or the wound not healing in good time, possibly because of some underlying issue, leaving the wound and implant open for bacteria colonisation. However, pathogenesis can also occur through colonisation of peri-implant tissue by bacteria (Broekhuizen et al. 2008; Daghighi et al. 2012). Secondary and complicated wounds present a greater challenge because they can require a very large clot, inflammation is more intense and wound contraction will be

affected (Kumar & Robbins 2007). Complicated wounds often have an unknown aetiology and may be related to other factors such as poor nutrition, obesity or underlying disease, which makes them a very difficult target (Carville 2005). These underlying factors also contribute to implant infections.

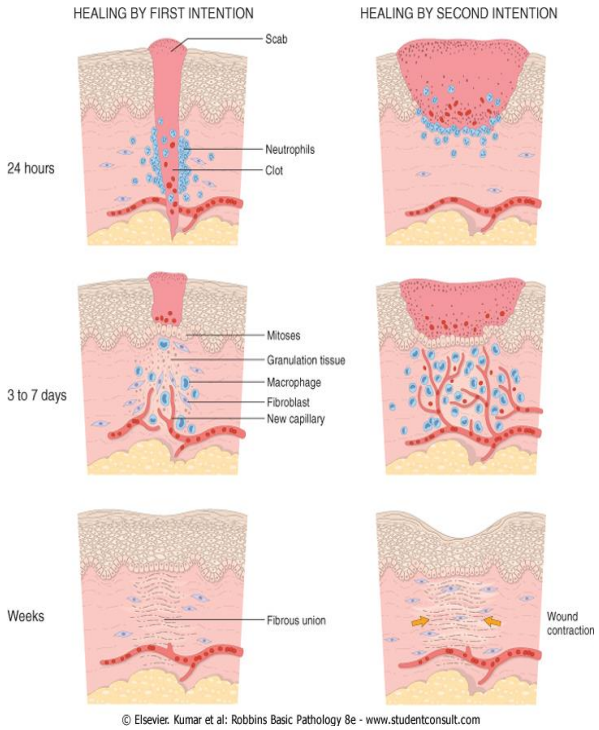


Figure 1.5: Primary, secondary and complicated wounds (Kumar & Robbins 2007) (From: http://2.bp.blogspot.com/-lbZNQEwSv_0/TqrbpdAGKaI/AAAAAAAAD1U/TmSwcm0MTyg/s640/Healing+by+first+intention+healing+by+second+intention.png)

Recent figures show that in the US alone, over four million knee replacements are undertaken per year (Weinstein et al. 2013). As Figure 1.6 shows, the knee implant is a complicated metal form and can easily become contaminated without very careful handling. Sterile surgical techniques and other practices that have contributed to reducing the numbers of implant infections are (1) antibiotics before and after surgery; (2) short operating time and minimal operating room traffic; (3) use of strict sterile technique and sterilisation of instruments; (4) antibiotic prophylaxis, that is, antibiotic spacer, antibiotic-impregnated bone cement; (5) preoperative nasal screening for bacterial colonisation; and (6) preoperative chlorhexidine

wash. Many biomaterial replacement operations are for osteoarthritic joints; osteoarthritis also predisposes the individual to other infections and chronic wounds (Losina et al. 2011).



Figure 1.6: Knee implant (From: http://orthoinfo.aaos.org/figures/A00389F09.jpg)

Certain wounds, such as leg ulcers, pressure ulcers and cancerous wounds, are generally problematic and progress to chronic wounds. Chronic wounds do not go through the normal expected reparative processes of haemostasis, inflammation, reconstruction (angiogenesis, granulation, contraction and epithelialisation) and maturation (remodelling) that dictate acute wound healing (Carville 2005; Gurtner et al. 2008). They are generally described as 'recalcitrant', 'stunned' and 'non-progressive', or 'stuck'. Infection in an acute wound is a major predisposing factor for the lack of healing, resulting in lengthy hospital stays and increasing wound management costs.

Infected wounds are classed into four types:

1. wound contamination—the presence of bacteria in a wound without a host reaction,
2. wound colonisation—the presence of bacteria in a wound that do not multiply or initiate a host reaction,
3. critical colonisation—a relatively new term to describe the multiplication of bacteria causing a delay in wound healing usually associated with an exacerbation of previously unreported pain but still no overt host reaction,
4. wound infection—the invasion and multiplication of bacteria in tissue with an associated host reaction (Benbow 2010).

Infected wounds have many causes, including neuropathy, venous hypertension, burns, pressure sores and tearing of aged skin, vasculitis and arterial disease, and often have underlying contributing factors, such as anaemia, cardiovascular disease, diabetes and ageing. Any wound that has not progressed towards a normal phase of healing within 3 months is considered chronic (Benbow 2010).

1.5 Fungal and Mixed Infections

In the past 10 years, medical advances have meant that there are now many practices and interventions involving severely immune-compromised patients who need regular medical care. These severely immune-compromised patients have brought out a whole new repertoire of infectious pathogens that have not been encountered extensively before. The human immunodeficiency virus (HIV) was the first indication that there were far more pathogens of a completely different nature inhabiting the human body, which nature keeps under control with a normal functioning immune system. Once the immune system is damaged or artificially dampened, viral, bacterial and fungal infections show themselves to be formidable foes. Organ transplants require the body's immune system to be controlled, while cancer treatments for myeloid and leukocyte leukemias require its complete destruction. Neonates have undeveloped immune systems and the elderly have an immune system that is waning. Fungal infections target these groups and have emerged as a new and even greater threat to health care than bacteria. *Candida albicans* is the most common fungal human pathogen and forms robust biofilms that are very difficult to eradicate. It commonly colonises cutaneous and mucosal surfaces, but in the hospital environment, where invasive medical biomaterial–based devices are used in many applications in an immune-compromised patient, it can invade and cause life-threatening disease (Brown et al. 2012). In a multicentre study of 10,038 patients from 1,417 intensive care units (ICUs), invasive candidiasis accounted for 17% of hospital-acquired infections and ranked third in aetiology of central (neck, chest or groin) line–associated bloodstream infection (Vincent et al. 1995). Mortality rates reach 45% and cost approximately $2.6 billion per year to treat in the US (Gudlaugsson et al. 2003; Leroy et al. 2009; Miller, Hajjeh & Edwards 2001). *Candida* species readily form biofilms on almost all invasive medical devices, and commonly co-inhabit with other microbes, particularly hospital-acquired bacteria such as *Acinetobacter*

baumannii and *S. aureus* (Chim, Tan & Song 2007; Kojic & Darouiche 2004; Peleg, Hogan & Mylonakis 2010; Rosenthal et al. 2006). Polymicrobial biofilms may protect one or more organisms from antimicrobial treatment or immune inactivation, and microbial virulence or invasive properties may be enhanced (Peleg, Hogan & Mylonakis 2010). In fact, for *S. aureus*, *Candida* biofilms provide a scaffold for adherence and increased resistance to vancomycin (Harriott & Noverr 2009). Furthermore, mixed infections often have different and more serious consequences for the patient than those associated with single species infections. It is estimated that 27% to 56% of hospital-acquired candidaemia are polymicrobial and the resultant bacteraemia is associated with a poorer prognosis compared with *Candida* infection alone (Guerraromero et al. 1989; Klotz et al. 2007; Pulimood et al. 2002). These sobering statistics are a reminder that we must do better in our development of biomaterials. The pace of medical intervention has outdistanced the development of better biomaterials and one consequence is in the patient infection rates.

1.6 Outline of Thesis

The first chapter of this thesis gives, above, an outline of the problems with wound and biomaterials-associated infections (BAI), the aims of this thesis and the motivations. It gives a general introduction to bacterial disease mechanisms and infections in wounds and implanted biomaterials. There is also a brief introduction to mixed microbial and fungal infections.

Chapter 2 comprises a literature review of the multi-disciplinary aspects of research on antimicrobial surfaces. Condensed exerpts from this chapter have been used in a co-authored book chapter in *Intelligent Surfaces in Biotechnology* (Griesser et al, 2012) and in a literature review published in *Plasma Polymers and Processes* (Vasilev, Griesser and Griesser, 2011) and recently reprinted in *The Best of Plasma Polymers and Processes*. The section on AMPs below was edited and condensed to form part of a book chapter that is in print (Michl et al, 2015).

The first section is a general introduction to biomaterials, BAIs and wound infections. The next section explores silver, its mechanism of killing and silver nanoparticles as an antibacterial surface. The next surface is coatings produced with non-fouling/anti-adhesive activity, the

mechanism of killing and on biomaterials. Quaternary ammonium compounds are also covered briefly. A large section is presented on AMPs because they are behind the hypothesis in much of my work, including a general background, the mechanism of killing, and immobilisation on surfaces. Synthetic AMPs are covered in the next section, considering the same aspects. Discussions on the positives and shortcomings of each surface are given.

Chapter 3 outlines the experimental materials and methods as well as some theoretical principles and the limitations of the techniques. This is an important chapter because the bacterial and cell-testing methods were developed or adapted specifically for this research project and could be important to future continuing work in the field.

Chapter 4 is the beginning of the experimental work. The only antibacterial wound healing product in use is the Acticoat so it made sense to spend some time examining the activities of silver in an attempt to possibly control and improve the release. This study also uses different cell lines to examine the effects of silver nanoparticles in the hope of answering some questions about the differing results concerning the toxicity of silver to cells.

Chapter 5 reports experiments using a number of well-known AMPs to create antimicrobial surfaces. These experiments are less sophisticated than later experiments because techniques for testing activity on the surfaces were still in the development phase of research. Given the much more exciting results in later chapters and time constraints, however, it was decided not to go back and repeat the work with AMPs using better-developed tests.

Chapter 6 describes the experiments using synthetic AMP mimics. It includes extensive surface analysis, done with the help of Marek Jasieniak, an expert in the field. The antibacterial testing has also been further developed, and results are of higher quality and precision. Further analysis is done in an attempt to discover more about what the mechanism of action is with these extremely interesting and well-thought-out peptides.

Chapter 7 comprises experiments using daptomycin, a new antibiotic that is thought to have similar activities to AMPs because it has been shown to be membrane permeabilising with

bacteria. It is an exceptionally beneficial antibiotic in use today as it has this particular ability whereas all the other antibiotics that target the bacterial membrane tend to have toxicity issues that have impeded development.

Chapter 8 summarises an initial screening project in which antifungal surfaces were developed, and interesting results were collected to support a future project that would develop surfaces targeting polymicrobial biomedical device-associated infections. The results are brief yet exciting.

The thesis is summarised in Chapter 9 with a discussion of the collective results and knowledge gained during this study. Finally, some future directions as well as potential for growth and understanding of the field are discussed.

All references are collated at the end of the thesis, to avoid duplication since many of them are cited in more than one chapter.

Chapter 2: Literature Review

2.1 Abstract

Bacterial adhesion to biomaterials is a major problem in the medical devices field. It also contributes to serious problems in wounds and results in debilitating infections and amputation. Much research is focused on adding antibiotics to biomaterials, in particular, antibacterial coatings for biomaterial and antibacterial wound dressings. Non-fouling surfaces resist bacterial adhesion and also resist cell adhesion. However, non-fouling surfaces are rarely active over a long period, do not enable tight cell and tissue apposition by definition, and may cause healing abnormalities, which makes them unsuitable for implants. Bactericidal surfaces with chemicals such as chlorhexidine and povidine iodine incorporation into materials and on surfaces are another option. Unfortunately, these chemicals can cause cytotoxicity and serious immune responses and have not become popular. Silver is an ancient antibacterial and has been used since the ancient Greek era; however, it affects cell growth, which hinders normal healing. Most traditional antibiotics act on intracellular targets such as enzymes and thus require in-diffusion into the bacteria to exert their effect on the reproducing, growing bacteria, thus making them unsuitable for surface attachment. AMPs and AMP mimics, in contrast, would seem suitable antibiotics for surface attachment because they target membrane function. While specificity of activity of AMPs remains a hotly debated topic, much hope is placed on these important new antimicrobials.

This review will examine antimicrobial surfaces and, in particular, plasma polymerisation as a surface-tethering technique.

2.2 Introduction

The use of biomaterials in modern medicine is essential in virtually all applications. Biomaterials are introduced into the body in almost every health care application, including taking samples of blood, long-term replacement of hips and knees, and improving blood flow with stents. Although every precaution is made to prevent infection from transferring to the

body through biomaterials, infections are common. The body has a huge arsenal of means to protect itself from attacking bacteria, including innate responses such as shedding, saliva and mucous, except in the area of implants, the only part the body that has no protection whatsoever. The only analogous body part is the teeth; even after brushing and other mechanical means, teeth are still compromised by biofilms (Wilson, Henderson & McNab 2002). As our population ages and people demand a better lifestyle, the use of biomaterials will only increase and the number of infections will grow. Resistance is the serious consequence of wound and biomaterial implant infections, and resistant bacteria are being discovered regularly and specifically in this area of infection. Most of the antibiotics in use today are based on the initial antibiotic developments of the 1940s and 1950s, the golden age of drug discovery (Hurdle et al. 2011). They also generally tend to target the five main biosynthetic processes found in actively growing bacteria: the biosynthesis of protein, ribonucleic acid (RNA), deoxyribonucleic acid (DNA), peptidoglycan and folic acid. Because these are all internal processes in the reproducing of bacteria, they are under threat from the constantly developing resistance by the bacteria and they do not affect slow-growing or dormant bacteria (Hurdle et al. 2011). Wound infections in particular are at greatest risk of producing resistant bacteria. Wounds are open to the environment, allowing colonised pathogenic bacteria to interact with other bacteria present and exchange resistant genes through transfer of mobile genetic elements.

Until recently, biomaterial engineering has focused on using inert biomaterials to avoid or reduce immune responses. It was assumed that an inert biomaterial would minimise the host response by avoiding cell–material interactions. Inert biomaterials are recognised as foreign by the body but remain essentially unchanged and are encapsulated in fibrous tissue and simply ‘tolerated’ (Ratner 2013). However, it has been realised that fibrous encapsulation may not be the best solution and that allowing specific host responses may in fact be beneficial for biomaterial integration and improve implant performance (Ratner 1996). It is difficult to assess what the interplay is among integration of the implant, healing of the wound site and bacterial infection: if the wound does not heal in a timely manner then bacterial infection is more likely; if the wound is infected then healing will be delayed. Integration may mean more rapid healing and less likely infection, leading to a better outcome. Considering the number of implants and

biomaterials used in medical care, any improvements that result in better performance would be welcome.

In this thesis two types of antimicrobial coatings were investigated: diffusive release and covalent tethering. The focus of the delivery strategy was on silver ions; accordingly the less voluminous literaute on releasing organic antibiotics will not be reviewed although there are some notable recent clinical studies (Nast et al., 2016).

2.3 Silver

Silver has been used as an antibacterial agent for thousands of years; documented records report its use as early as 750 AD (Maillard & Hartemann 2013). With the increased awareness of the limitations of antibiotics, it has re-emerged as a popular antibacterial agent. Early uses were in the form of silver vessels and coins. Late nineteenth century uses include as a medicinal for cholera and eye drops for eye infections (Maillard & Hartemann 2013). Recent developments have described silver as the 'super antibacterial' and have incorporated it into a wide range of domiciliary applications, textiles, including underwear and socks, surfaces and health care products, with the intention of making them more hygienic (Marambio-Jones & Hoek 2010). The broad-spectrum properties of silver have made it an obvious choice for incorporation into biomaterials and wound dressings; however, serious questions concerning its safety, toxicity, environmental relationship and risks associated with microbial resistance have not been addressed. Silver is most often used in the form of nanoparticles because of the improved microbicidal activity. Silver nanoparticles are defined as having a dimension measuring less than 100 nm (Maillard & Hartemann 2013).

Antimicrobial activity is only due to free Ag+ ions, not Ag (solid) metal. In this thesis, when using silver or Ag, I refer to Ag ions.

2.3.1 Antimicrobial Activity

Silver differs greatly from other antibiotic substances in that it is not an antibiotic but a metal ion toxin that enters all cells and bacteria and exerts a toxic event with more or less serious consequences. Bacteria are able to use enormously diverse energy sources. Some bacteria

derive their energy from sources similar to those of animal cells in that they are aerobic and synthesise adenosine triphosphate (ATP) from sugars that they oxidise to carbon dioxide (CO_2) and water (H_2O) by glycolysis and the citric acid cycle through a respiratory chain in their plasma membrane, similar to mitochondria in animal cells. Other bacteria are strict anaerobes, deriving their energy from glycolysis through fermentation and/or from an electron transport chain that employs a molecule other than oxygen as the final electron acceptor, a nitrogen, sulphur or carbon compound. The electrons are transferred to these acceptors by a series of electron carriers in the plasma membrane, similar to those in the mitochondrial respiratory chains. The vast majority of bacteria use ATP synthase and a proton-motive force that drives the ATP synthase to make ATP. The proton-motive force is essential for the survival of bacteria; it not only provides electrons for ATP production but it also provides electrons to drive the flagellar motor, pump ions across the membrane and transport nutrients (Alberts 2008).

Silver nanoparticles are thought to kill bacteria through a number of target sites. Once enough ionic silver has penetrated the bacteria, it can combine with and alter microbial proteins. It can disrupt structural integrity causing leakage, possibly due to reactive oxygen species (ROS), and disrupt metabolic functions such as the proton-motive force and the respiratory electron transport chain (responsible for oxidative phosphorylation, which takes nicotinamide adenine dinucleotide [NADH] from the tricarboxylic [TCA] cycle and gives ATP) (Alberts 2008; Gordon et al. 2010; Marambio-Jones & Hoek 2010). Silver ions may react with electron donor groups such as N, O or S atoms, notably thiol groups (Gordon et al. 2010), and possibly DNA (Marambio-Jones & Hoek 2010), and inactivates the proteins. It is believed that this causes an uncoupling of the respiratory chain from oxidative phosphorylation and the collapse of the proton-motive force (Gordon et al. 2010). In addition, the respiratory chain contains iron in the form of iron-sulphur clusters, which are also damaged by silver ions; the clusters are inactivated and the iron is liberated (Gordon et al. 2010).

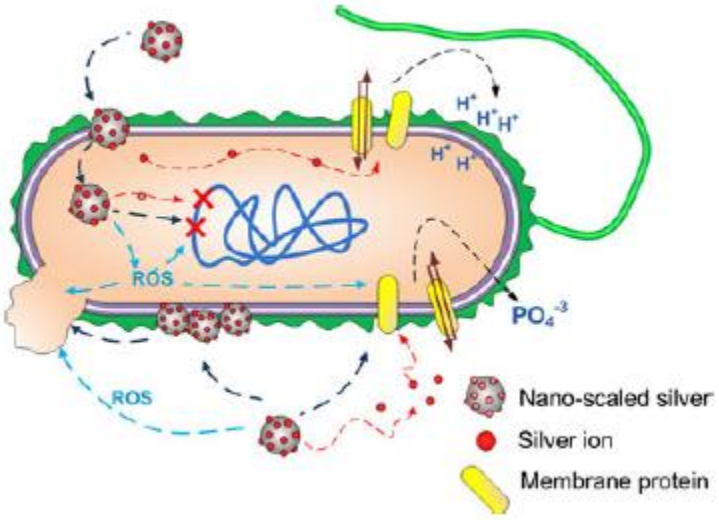


Figure 2.1: Summary of silver nanoparticles (AgNPs) interaction with bacterial cells. AgNPs release silver ions and (1) they accumulate in the cell membrane affecting membrane permeability, (2) they interact with membrane proteins affecting their correct function, 3) the released silver ions along with the generated ROS could damage the DNA (Marambio-Jones & Hoek 2010).

The respiratory chain is the major source of ROS, so blockage of this chain would result in the immediate inaction of respiratory enzymes, and the build-up of electrons trapped in the chain could result in high levels of ROS (Gordon et al. 2010). Antioxidant enzymes rely on thiol groups for production, so would not be available for de-toxication of excess ROS.

The evidence that silver is an excellent antimicrobial is overwhelming. In solution, antimicrobial nanoparticles can show activity in ranges from 7 to 33 nM (Kim et al. 2007) and on surfaces the activity is dose dependent but ranges from 1 mM for 3 hours of activity on Au (III) and 2 mM for 72 hours on titanium (Gordon et al. 2010). These results are selected from two of the distinguished groups undertaking research in this area; however, there are thousands of publications with results from many different variations of antibacterial treatments and analysis, and they all give very good results, proving unquestionable effectiveness of silver (ions) as an antimicrobial compound.

However, the toxicity of silver in bacteria raises questions about its usefulness as an antimicrobial product because mitochondria in human cells use a similar mechanism of energy production; therefore, silver is potentially toxic to human cells too. In order to use silver as an antimicrobial, one must carefully consider how to balance the release so that minimal bactericidal concentrations (MBCs) are reached while causing minimal host damage. This may not be feasible with the variation between ages and pathologies in patients and the inability to define the toxicity of silver. Reviews consistently question the effectiveness of silver in dressings, and as a topical treatment, because of a lack of evidence (Aziz, Abu & Chong 2012; Maillard & Hartemann 2013; Marambio-Jones & Hoek 2010; Percival, Bowler & Russell 2005; Poon & Burd 2004). There is also disagreement as to whether it is at all useful considering the toxicity to human cells, which may be very close to the toxicity levels applicable to bacteria.

Furthermore, there is evidence that resistance of bacteria to silver is emerging (Mijnendonckx et al. 2013; Percival, Bowler & Russell 2005). Bacteria can respond to the bactericidal activity from silver nanoparticles using a genome-wide adaptive response of altered gene expression (Gordon et al. 2010). Studies presented in this thesis found that silver is not fully bactericidal and selected for the hardiest bacteria, which, once the silver was gone, was an extremely vigorous form of bacteria that was very difficult to kill. Other studies have also noted this effect and raised concerns, along with reports that silver is toxic to fish, fruit fly and cell lines derived from mice, rats and humans (Kim et al. 2008; Mijnendonckx et al. 2013; Percival, Bowler & Russell 2005; Powers et al. 2011).

Perhaps relative cell size matters; bacteria are generally 10–100 times smaller than eukaryotic cells, and therefore contain a much smaller surface but a higher surface area to volume ratio, which would enhance silver uptake per cell volume. This might mean that bacteria are more easily affected by the toxic effects of silver per unit concentration. However, a larger number of bacterial cells per unit volume would reduce this effect.

2.3.2 Silver in Coatings

There is considerable interest in developing coatings for biomaterials that would release silver ions and make surfaces of biomedical devices and implants resistant to bacterial attachment.

Compared with systemic delivery, a key advantage of local delivery at a specific site is that high local doses could be administered without exceeding the systemic toxicity levels. Many polymers suitable for biomedical devices, such as polystyrenes and silicones, can be blended or loaded by in-diffusion with silver nanoparticles or silver salts and then release silver ions when in contact with a fluid environment. A number of commercial products containing silver have emerged, including wound dressings for burns and chronic wounds, silver-coated catheters and other medical devices. Silver has been added to a number of wound dressings on the market, including Acticoat™ (Smith & Nephew) and Melgisorb Ag™ (Molnlycke). There is, however, considerable concern about their effectiveness, particularly in burn wounds (Aziz, Abu & Chong 2012).

Liu et al. (2010) investigated various methods of controlling silver diffusion from biomaterials, ranging from accelerated release through to slowed release (see Figure 2.2). The approaches of pre-oxidation or particle size reduction (i.e. increased nanoparticle surface area) provide routes to enhanced silver release in slow-leaching systems; whereas complexing silver with sulphides, amines or citrates may be used to slow down silver release in the case of biomaterial surfaces where the silver release is too rapid for the intended application. As silver ions are released from the surface of silver nanoparticles following oxidation of surface atoms, the extent of oxidation of silver nanoparticles and the surface-to-volume ratio are important operational parameters. The sterilisation techniques of ethylene oxide and steam autoclaving both lead to enhanced surface oxidation of silver nanoparticles and, hence, usually faster release of silver ions compared with non-sterilised analogous samples, a factor that has been overlooked in some studies. It is thus essential to characterise silver ion release rates and antibacterial activity with samples sterilised by a method appropriate to the intended biomedical device application.

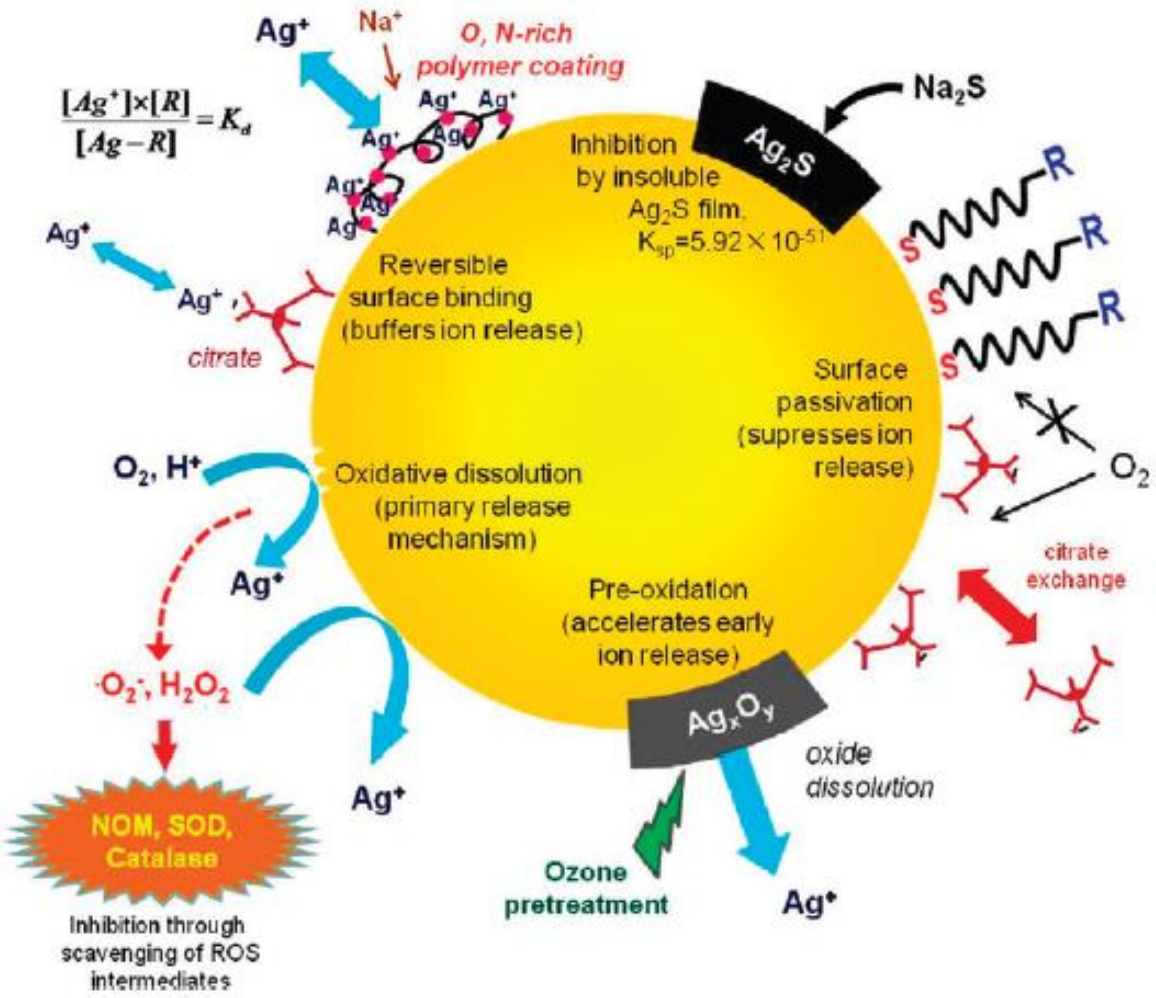


Figure 2.2: A schematic diagram of chemical approaches that may be used to control silver ion release from antibacterial biomaterials (Liu et al. 2010)

There have been substantial research efforts towards engineering thin polymer films loaded with silver and silver nanoparticles to achieve more prolonged release through both chemical and physical means. Many studies show effectiveness *in vitro*, but these newer approaches are yet to be verified *in vivo*. While some studies have applied contiguous silver film coatings onto substrates such as fibres (Amberg et al. 2008), most studies focus on silver (nano)particles incorporated within polymeric matrices. For biomedical devices, it may be advantageous to use thin polymer films containing silver nanoparticles fully encapsulated within the polymer matrix, as opposed to the situation in which larger silver particles partly protrude from the polymer film layer, in which case it has been alleged that protruding asperities can 'puncture'

both bacterial and eukaryotic cells. Ho et al. (2004) presented an interesting approach (see Figure 2.3), first forming silver nanoparticles within a thin film of polyethylene imine. The polymer was copolymerised with 2-hydroxyethyl acrylate, which allowed further surface grafting of polyethylene glycol (PEG). In this manner, coatings with two functions were generated, with the PEG layer preventing bacterial adhesion and the silver ions released from the coating providing biocidal activity against *S. aureus*.

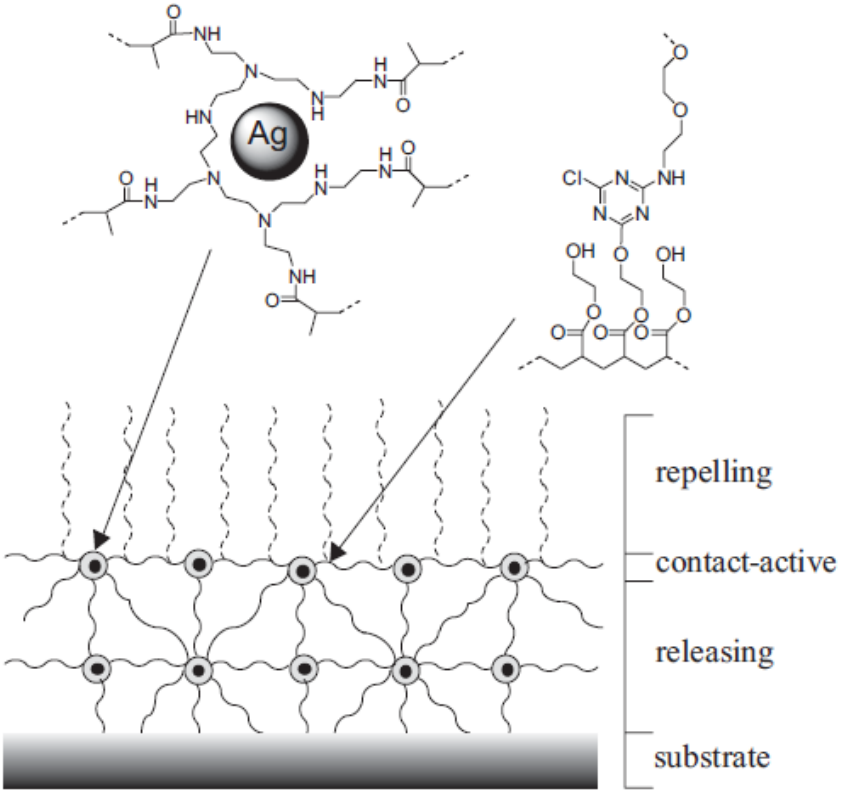


Figure 2.3: Schematic representation of a non-fouling, contact-active silver-releasing polymer matrix. Imine functional groups within the polymer matrix coordinate the silver ions prior to reduction to nanoparticles, which become trapped in the bulk coating, while polyethylene glycol groups anchored at the surface serve to prevent cells from binding. (Ho et al. 2004)

Vimala et al. (2009) prepared hydrogel networks based on cross-linked poly(acrylamide) and three different carbohydrate polymers—gum acacia, carboxymethylcellulose and starch. Silver nanoparticles were loaded into the hydrogel networks via *in situ* reduction of silver nitrate using

sodium borohydride as reducing agent. Lee at al. (2008) generated multilayer films, through layer-by-layer assembly, rich in catechol groups, and used these groups to reduce silver ions to metallic silver when immersed in an aqueous metal salt solution. This resulted in the generation of silver nanoparticles within the films. Another study (de Santa Maria et al. 2008) synthesised silver nanoparticles in commercial cross-linked Amberlite resins. Sulfhydryl and −N $(CH_2COOH)_2$ groups present on these resins were used for Ag+ chelation. Reductants were used to reduce the Ag+ ions under alkaline pH. The coatings were bactericidal against *E. coli* within a few minutes (de Santa Maria et al. 2008). An approach by Ramstedt et al. (2007) utilised the properties of polyanionic electrolyte brushes to trap ionic silver within a film of atom transfer radical polymerised poly(3-sulfopropylmethacrylate). This method allows silver release by ion exchange with cations present in physiological media (e.g. Na^+ K^+), causing *in vitro* bactericidal action against *S. aureus*. The brushes were 'rechargeable' upon soaking in aqueous silver nitrate after depletion of the loaded silver, which could be advantageous for multiple use applications such as contact lenses. However, the highly soluble nature of ionic silver in these films creates problems with excessive out-diffusion of silver and potential cyctotoxicity in a mammalian environment due to an elevated local silver concentration (Ramstedt et al. 2009).

An interesting approach comprises the simultaneous deposition of silver and the polymer matrix coating, thus embedding silver atoms, atomic clusters, and silver nanoparticles within a coating during its application rather than in a separate step. Thin layers of poly(tetrafluoroethylene) (PTFE) can be sputter-deposited with concurrent incorporation of nanosilver (Zaporojtchenko et al. 2006), or plasma polymerisation can be used to form a polymeric thin film while simultaneously adding silver by sputtering (Despax & Raynaud 2007). The advantages of vapour deposition of polymeric matrices for nanosilver are that vacuum deposition often creates better interfacial adhesion and better coating uniformity at lower, controllable thicknesses, compared with solvent coating processes. However, the issue of even more limited loading and particle size, and thus limited duration of antibacterial action, needs to be considered. The issue of silver loading into co-sputtered plasma polymer films has been addressed by Koerner et al. (2010), who demonstrated that the input power may be used to facilitate loading, but silver release from such systems is still under investigation.

An alternative approach comprises the creation of a polymeric coating by plasma polymerisation, which is a convenient vacuum coating method for depositing thin polymeric films onto various substrates, followed by loading with silver nanoparticles. Such coated articles can be stored dry, and when brought into contact with aqueous solutions or body fluids, oxidation of silver atoms at the surface of the nanoparticles occurs, which leads to silver ion release and gradual erosion of the nanoparticles. Moreover, by vacuum depositing a second, ultrathin layer, the release rate can be controlled.

In most reported studies, neither the amount of silver nor the release rate can readily be tailored to specific requirements. For a technology to be applicable to a range of biomedical devices, a smarter approach is needed that enables control over those parameters with minor process variation when using one basic technology. In particular, it is desirable to adjust the release rate of silver ions to comply with the different requirements of different biomedical devices, so that effective therapeutic dosage can be delivered over periods as short as a few days or as long as a month or more. In most systems, the loading and the release kinetics cannot be tailored independently.

The design of a system that enables independent control over both loaded amounts and delivery kinetics (Vasilev et al. 2010), while retaining the advantage of good coating adhesion inherent in the plasma deposition of polymeric coatings, is shown in Figure 2.4. Silver nanoparticles are loaded into an amine plasma polymer matrix by in-diffusion from a silver salt solution followed by reduction of the silver ions, which leads to their spontaneous agglomeration to nanoparticles within the polymeric matrix. A subsequently applied ultrathin barrier overlayer of adjustable thickness was used to control the rate of out-diffusion of silver ions. Plasma polymerisation is a uniquely suitable approach for this because it enables the creation of ultrathin polymeric coatings with nanometre precision for the film thickness and excellent coating uniformity. The silver loading can be controlled either via the solution concentration of silver ions during loading or via the time of immersion for loading, leading to an approach with considerable flexibility and a wide range of controllable properties (Vasilev et al. 2010). Plasma polymerisation of n-heptylamine or allylamine was used to create amine-rich uniform

polymeric coatings into which silver ions were diffused by placing samples in a solution of $AgNO_3$. The coalescence of silver ions into nanoparticles upon reaction with a reducing agent such as $NaBH_3CN$ was detected by a characteristic plasmon band in the ultraviolet-visible (UV-Vis) absorption spectrum (Figure 2.4). When placed in an aqueous solution, oxidation causes release of silver ions. The rate of release was shown to be adjustable by the application of a second plasma polymer layer (not containing silver ions and applied after loading the first coated layer with silver nanoparticles), with the thickness of this overlayer providing a convenient means of tailoring the release rate (Figure 2.4). In this way, the loading and the release kinetics were adjustable independently over a considerable range. Even when slowing the rate of release such as to achieve sustained release over several weeks, antibacterial effectiveness was still obtained *in vitro* (Figure 2.4).

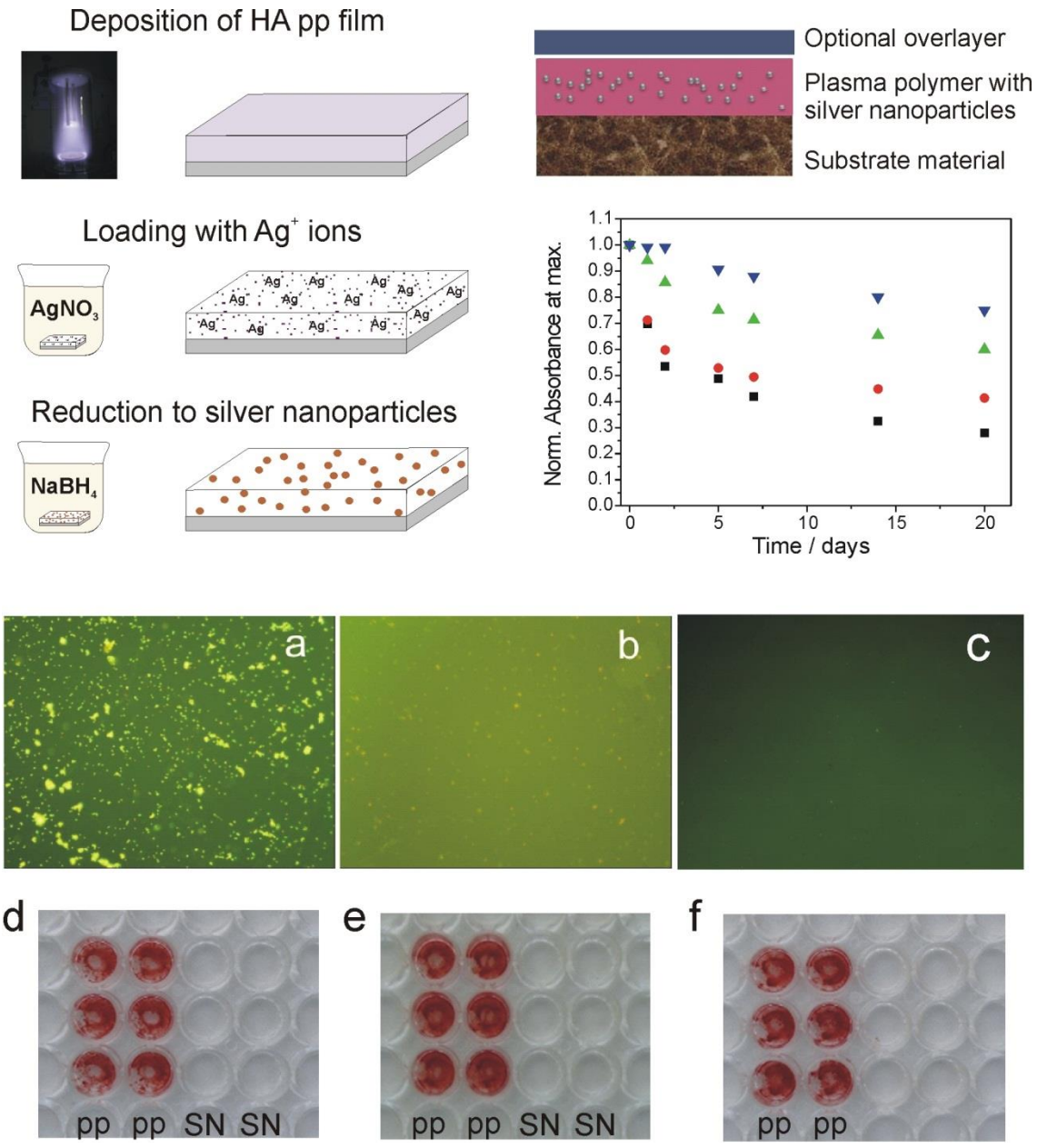


Figure 2.4: Schematic diagram of silver nanoparticles incorporated into amine plasma polymer coatings, and the control of the release kinetics of silver ions via adjustable thickness of an additional plasma polymer overlayer. Also shown are test results of antibacterial effectiveness against *S. epidermidis*: (a) and pp: control heptylamine surface with no silver; (b), (c) and rows SN: silver-loaded coatings with different overlayers. (from Poulter et al. 2013)

An antibacterial coating can also be produced by the plasma polymerisation of a phosphine-stabilised silver maleimide complex (Poulter et al. 2009). This method is attractive in terms of comprising a single step but requires synthesis of the precursor molecule used for the plasma deposition of the antibacterial coating. Also, it is largely contact active because of the limited amount of silver within the film.

More commonly, conventional polymers and fabrication methods have been used. Eksik, Erciyes and Yagci (2008) used electron transfer reaction and free-radical polymerisation processes to prepare triglyceride oil–based polymer-silver nanocomposites. The antibacterial effect of the polymer nanocomposite was examined against Gram-positive, Gram-negative and spore-forming bacteria. Furno et al. (2004) impregnated silicone with nanoparticulate silver metal using supercritical carbon dioxide and examined bacterial adherence and the rate of killing of planktonic bacteria by chemiluminescence and viable counts. The release rate of silver ions from the polymers in the presence and absence of blood was measured using inductively coupled plasma mass spectrometry (ICP-MS). It was found that the antibacterial efficiency of the coatings was dependent on the rate of release of silver ions. Kelly et al. (2007) prepared polypyrrole and polyaniline conducting polymer composites with individual fibres of cellulose by direct polymerisation of the respective monomers and used the redox active surface of the polymers to reduce silver ions to silver metal, thus producing cellulose/conducting polymer/silver composites. Kong and Jang (2008a) synthesised poly(methyl methacrylate) nanofibers containing silver nanoparticles by radical-mediated dispersion polymerisation and tested antibacterial properties against Gram-negative (*E. coli*) and Gram-positive (*S. aureus*) bacteria; minimal inhibitory concentration (MIC) results showed that the silver-loaded nanofibers had superior antimicrobial efficacy compared with that of silver sulfadiazine and silver nitrate at the same silver concentration. Liu et al. (2009) developed a procedure for the synthesis of Ag nanoparticles in transparent polyvinyl acetate (PVA) films via a two-step procedure consisting of ion incorporation in the matrix followed by thermal reduction. These composite films containing silver nanoparticles showed excellent antimicrobial performance towards bacteria such as *E. coli*. Silver nanoparticles were synthesised also in covalently linked layer-by-layer polymeric assemblies from methoxysilane polymers (Sambhy, Peterson & Sen 2008), in methoxy PEG (Mallick, Witcomb & Scurrell 2006), an epoxy polymer matrix (Lu,

Moon & Wong 2008), poly(ether urethanes) (Gray, Norton & Griffiths 2005), polyethylene (Sanchez-Valdes et al. 2009), poly(vinyl alcohol) (Galya et al. 2008), diamond-like carbon (Schwarz et al. 2008), polyacrylate film (Voccia et al. 2006), polytetrafluorethylene (Zaporojtchenko et al. 2006) and polyrhodanine nanofibers (Kong & Jang 2008b). Vachon and Yager (2006) loaded silver ions into sulphonated polymer hydrogels. Kumar et al. (2008) reported an approach to synthesise silver nanoparticle–embedded paint in a single step from common household paint, taking advantage of the naturally occurring oxidative drying process in oils, involving free-radical exchange, as a mechanism for reducing silver salts and dispersing silver nanoparticles in the oil media without the use of external reducing or stabilising agents. Surfaces coated with silver-nanoparticle paint showed antimicrobial activity against Gram-positive human pathogens (*S. aureus*) and Gram-negative *E. coli*. A system devised by Sambhy et al. (2006) uses a dual-action approach in which a cationic polymer is infused with silver bromide. Silver is released from the film while the polymer, from the quarternised ammonium compound family, itself acts to disrupt bacteria cell membranes on the surface. Antibacterial properties were recorded both before and after exposure to mammalian fluids and the release rate of silver ions may be modulated by tailoring the nanoparticle size. Gordon et al. (2010) prepared coordination polymers of ethanediyl bis(isonicotinate) and silver nitrate, which can be grafted onto medical implants. Silver release was moderated by tuning the solubility of the compound. This method showed *in vitro* antimicrobial activity against *S. epidermidis* over several days without significantly reducing the viability of eukaryotic cells.

Silver can be incorporated not only into polymeric carrier matrices or thin films, but also into some ceramics. Schneider et al. (2008) described the use of silver on amorphous tricalcium phosphate (TCP) nanoparticles for electrospun, highly porous poly(lactide-co-glyclolide) (PLGA) fibrous composites. *In vitro* bioactivity tests of PLGA/Ag-TCP composite containing 0.5 wt% silver showed hydroxyapatite deposition on the nanocomposite within 2 days. Antibacterial tests using *E. coli* demonstrated a prolonged antibacterial effect of the scaffolds containing finely dispersed silver on TCP compared with current clinically used methods based on soaking the scaffolds with a tetracycline solution prior to implantation.

Even though only a small (but representative) part of the very extensive literature has been discussed above in detail, it is evident that many approaches exist towards the same goal: elemental silver, nanoparticulate silver, ionic silver, complexed silver and nanocomposite silver. Each of these forms of silver have advantages and disadvantages according to (1) the desired release rate of silver, (2) the total required loading dose of silver, (3) the substrate to which the coating is to be applied and (4) the considerations of the ultimate application of the material. It is also apparent that although much research is being carried out in the field of silver-containing biomaterials, there is little in the way of standardised testing to allow comparison of antibacterial properties, silver release and potentially adverse cytotoxic effects of the coatings.

Increasingly, because of the large array of antibacterial coatings that utilise silver, differentiation will be governed by the ability of a synthetic surface to resist the proliferation of bacteria while simultaneously providing a suitable environment for eukaryotic cells in the desired application. Thus, silver-containing coatings must be optimised for the specific requirements of a specific application, rather than the trend to date of claiming generic utility; clearly, the doses and rates of release, as well as the sensitivity of the host environment, might differ markedly for the wide range of biomedical devices that require antibacterial protection.

In addition, ease of upscaling, manufacturing costs and feasibility need to be taken into consideration when designing antimicrobial biomaterials. It is likely that future antimicrobial coatings will be derived from current iterations with advantages pertaining to speed and cost of manufacture, alongside application relevancy (e.g. release rate) and ability to combat the evolutionary ability of bacteria to resist the effects of silver.

In summary, clearly, silver ions are effective against various bacteria *in vitro*. However, the questions of clinical effectiveness and damage to human cells and tissue are subjects of continuing controversy. With improved understanding and better control of dosage and release rates, silver-releasing coatings may find a wider range of applications, but given the concern of potential side effects from silver complexing with proteins and altering their functions, the application of silver release from coatings for biomedical devices must be approached with due

caution except where much of the silver is likely to be removed rapidly from the body, such as with urinary catheters. The elimination of bacterial infections via the local release of silver has the potential to bring considerable benefits, but too little is known about downstream consequences such as a spike in silver ion concentration in blood and the excretion or accumulation in organs of silver ions.

2.4 Non-fouling or Anti-adhesive Coatings

The use of materials made by humans such as catheters, cardiac pacemakers, in-line direct and intravenous tubes and other medical devices used in the human body to restore functions or deliver or remove substances has grown substantially and will continue to grow. These materials present surfaces for opportunistic bacteria to attach, colonise and form biofilms. Some devices such as catheters allow only a limited time of use due to the bacterial colonisation and some have an infection rate approaching 100% within a few days (Klatte, Newland & Jackson 2013; Safdar, O'Horo & Maki 2013). These devices require regular replacement to keep the bacterial load to a minimum, and even with regular replacement, they are still a serious source of infections for the many patients that require them. Because they do not require integration into the body, one option is to create a surface that is non-fouling or will repel initial bacterial adhesion and further colonisation. Non-fouling surfaces that are placed in the body tend to attract a strong immune response with heavy scar tissue forming around the implant. In biomaterials that do not require integration, a non-fouling surface that could avoid contamination would be highly desirable. Moreover, a non-fouling coating added to a catheter, along with the body's natural cleaning mechanisms, could be used to refresh itself.

Non-fouling surfaces are generally made from polymer chains tethered to a solid substrate either end on to form brushes, or via side groups to form loops and tails (Minko et al. 2002). When tethered at sufficiently high density, tethered polymer chains are forced to stretch away from the surface. The tethering of polymer chains to a surface is usually carried out via physisorption or chemical bonding.

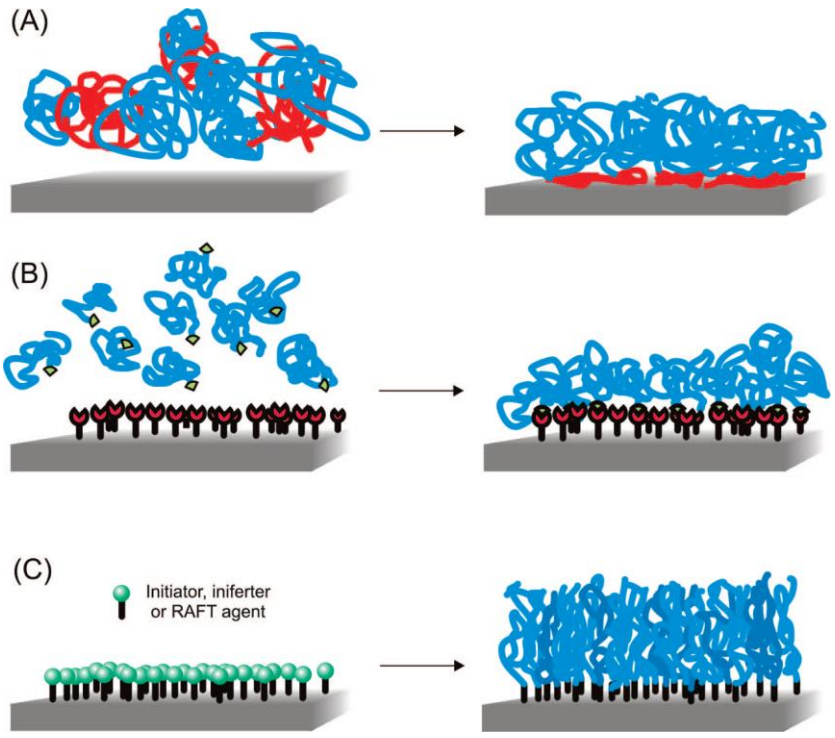


Figure 2.5: Synthetic strategies for the preparation of polymer brushes: (a) physisorption of diblock copolymers via preferential adsorption of the red blocks to the surface (*grafting to* approach), (b) chemisorption via reaction of appropriately end-functionalised polymers with complementary functional groups at the substrate surface (*grafting to* approach), (c) polymer brushes grown via surface-initiated polymerisation techniques (*grafting from* approach) (Barbey et al. 2009). (From: http://pubs.acs.org/doi/pdf/10.1021/cr900045a)

Polymer brushes synthesised using the physisorbed method generally are made using a two-component polymer chain, such as a diblock copolymer; one component strongly adheres to the surface and the other is tethered on to the end of this and extends away from the surface (Boyes et al. 2004). Physisorbed surfaces lack the stability of covalently bonded surfaces because of the inherently weaker bond. Covalent bonding of polymer chains can be carried out using either the 'grafting to' or the 'grafting from' method. In the 'grafting to' technique, preformed polymer molecules with reactive end groups react with complementary reactive groups on the surface to form tethered polymer chains. This is an easy method to form surfaces; however, it is difficult to achieve a high grafting density because of steric hindrance from already attached chains, unless using cloud-point grafting (Kingshott et al, 2002). Because

antibacterial properties are related to grafting density, the 'grafting from' method can be used. In this method, initiating groups are first attached to the substrate surface, a monomer solution is introduced that initiates polymerisation with the chains propagating outwards from the substrate surface (Edmondson, Osborne & Huck 2004). The 'grafting from' method is also referred to as surface-initiated polymerisation. This polymerisation can be carried out through conventional free-radical polymerisation or controlled/'living' polymerisation techniques such as reversible addition-fragmentation chain transfer (RAFT) polymerisation, nitroxide-mediated polymerisation (NMP), and atom transfer radical polymerisation (ATRP). The 'living' polymerisation techniques allow better control over brush thickness, composition and architecture.

2.4.1. Mechanism of Action

The bacteria-killing action of non-fouling surfaces varies depending on the type of polymer chain attached and whether it has additional groups such as alkyl pyridinium or quaternary ammonium added (Tiller et al. 2002; Waschinski et al. 2004). They can be conjugated with antibiotics (Wu & Grainger 2006) and antibacterial peptides (Glinel et al. 2009), and complexed with silver (Ho et al. 2004; Ramstedt et al. 2009). Non-fouling coatings on their own are often termed as immobilised biopassive polymers, and they provide passive protections of surfaces only, with no killing of the bacteria. They provide passive protection of the surface in that they prevent attractive interfacial forces, and thereby protein adsorption and bacterial colonisation on the surface. Some examples of polymers that have been studied for the reduction of protein adsorption and bacterial adhesion include poly(oligo(ethylene glycol) methyl ether methacrylate), a zwitterionic polymer with sulfoctaine side chain and poly(2methyl-2-oxazoline) (Charnley, Textor & Acikgoz 2011). These polymers reduce bacterial adhesion but do not kill bacteria.

Kingshott et al. (2003) compared physisorbtive grafting with covalent grafting using PEG (MW 5000) and created identical surfaces as assessed through high-sensitive surface analysis. Both surfaces were tested against a *Pseudomonas* sp.; the physisorbed surface showed no antibacterial activity whereas the covalent PEG graft showed a fourfold decrease in attachment.

The reasons for the lack of antimicrobial activity in the physisorbed surface are not fullt establsihed; perhaps bacteria have some mechanism that can de-sorb the adsorbed surfactant or perhaps the extracellular polymeric matrix that bacteria secrete can push the PEG layer aside.

While much effort has been given to this area of research, there are still a number of issues that keep them from advancing into medical use. The non-fouling properties tend to be quite limited, with studies showing 5 hours or less of antibacterial integrity (Kingshott et al. 2003). The long-term stability of the coatings in the presence of body fluids and natural abrasion through insertion and contact/wear is also a concern. Sterilisation is difficult and cytotoxic effects from degraded surfaces need to be addressed. These challenges indicate that there is more work to be done before a non-fouling surface can be brought into clinical use.

2.5 Disinfectants and Quaternary Ammonium Compounds

Disinfectants including quaternary ammonium compounds (QACs) are very potent biocides. They are common in household products and in water treatment. They cover a wide range of compounds with many different structural features. They interfere with the cytoplasmic membrane by causing leakage through destabilisation (Tiller et al. 2012; Waschinski et al. 2004). While many disinfectants are cytotoxic, it is believed that bacterial membranes are more susceptible to QACs than mammalian cells and that toxic effects can be controlled through covalent surface tethering. Many biocides are used against skin bacteria but the amount is highly controlled; in addition, shedding of the skin is part of the natural innate immune response to keep it from becoming colonised by pathogens. In-depth studies of show, however, a different picture: mitochondrial dysfunction has been found to be an early event in induced cytotoxicity starting at sublethal concentrations and characterised by mitochondrial fragmentation accompanied by decreased cellular energy production (Inácio et al. 2013). Furthermore, they acted by a common mechanism that involved the inhibition of the NADH ubiquinoneoxidoreductase (complex I) and slowing down of the mitochondrial phosphorylative system (Inácio et al. 2013). The end response is, of course, apoptosis or cell death. Toxic responses were also found in a study that looked at inhaled compounds: they produced rapid shallow breathing and inflammation (Larsen, Verder & Nielsen 2012).

In clinical, domestic and industrial applications, low-molecular-weight disinfectants are widely used. While there are many different structures, they generally comprise a positively-charged species and a hydrophobic moiety. A common example is chlorhexidine, a strong basic compound that becomes a cationic species after protonation in an aqueous environment.

Surfaces modified with QAC layers have attracted considerable interest since the pioneering work of Tiller et al. (2001). Various reactions have been used to immobilise them on various biomaterials. Many studies have demonstrated the antimicrobial effectiveness of QAC-grafted surfaces, yet the mechanism of antibacterial action of QACs specifically on surfaces is still not fully resolved. The first and most cited hypothesis is that sufficiently long cationic polymer chains penetrate cell membranes (Tiller et al. 2001). A second hypothesis suggests that a highly charged surface can induce ion exchange between the positive charges on the surface and structurally essential mobile cations within the bacterial membrane. Being in close contact with a cationic surface, vital divalent cations cannot perform their normal role in charge neutralisation and bridging of the head groups of membrane lipids, which results in a loss of membrane function, fluidity and finally integrity (Kügler, Bouloussa & Rondelez 2005). QACs are highly active antiseptics that act very efficiently against all bacteria, so it is likely that more than one mechanism occurs, as has been found in their highly toxic behaviour towards mammalian cells. It is believed that if these compounds are covalently attached, they will not contaminate the body. However, this would render them less accessible towards the bacteria because they would not be available to enter the membrane. In addition, the studies mentioned above show that they have far broader activities than simply membrane destabilisation alone. There is no evidence that QACs are bactericidal when restricted to only bacterial membranes; it seems quite likely that they would have other killing mechanisms, considering their toxicity to mitochondria. This leads to questions about their safety when used in other modes such as tethered to the ends of non-fouling brushes.

2.6 Antimicrobial Peptides

Antimicrobial strategies that target the bacterial membrane by disrupting it or the proteins that are integral to membrane function are an alternative approach and one that has only recently gained much attention. Membrane-active agents provide a new means of eradicating recalcitrant non-growing bacteria and bacteria that are attracted to the unprotected biomaterial surface (Hurdle et al. 2011).

AMPs are an abundant group of biomolecules that are part of the innate immune system and part of the first line of defence against bacterial invasion for all multicellular organisms. They are highly diverse and have been isolated from a wide variety of animals, plants, bacteria, fungi and viruses (Brogden 2005). AMPs are unique in that they function as both antimicrobial agents and modulators of the immune system (Barns & Weisshaar 2013). Many bodily secretions and fluids have been known to have antibacterial properties, and in the 1950s, the antimicrobial substances in normal tissues and fluids of the body were first identified and proposed as an allied mechanism of natural and adaptive immunity (Skarnes & Watson 1957). Lysozyme is a common antibacterial protein found throughout the body; it was isolated from oral mucosa and reported on by Fleming in 1922 (Aoki, Kuroda & Ueda 2012).

While AMPs are highly diverse, they have three characteristics that are shared by almost all known AMPs. The three characteristics are a small size (10–20 amino acids), a highly cationic character, and an amphipathic nature (Costa et al. 2011). Antibacterial peptides are of intense interest because of the extremely concerning increase in bacterial multidrug resistance that is raising the spectre of inability to control some infections. AMPs offer many significant potential advantages in that they have broad-spectrum activity across a broad range of Gram-positive and Gram-negative bacteria, including drug-resistant strains and are also active against fungi (Wimley & Hristova 2011). Many AMPs target bacterial membrane function rather than specific protein binding sites (Brogden 2005; Wimley & Hristova 2011). This makes them highly advantageous because they can kill the bacteria in growing and non-growing states as well as in dormancy, and do not induce resistance. Bioavailability of AMPs is reduced because

they cannot be taken orally. However, they are excellent candidates for topical and surface-attached applications.

2.6.1 Antimicrobial Activity

Although AMPs have both membrane and intracellular modes of killing, it is the membrane activity that most interests developers of new antibiotics (Brogden 2005). While this membrane-permeabilising mechanism is still not well understood, the advantages make them an important class of antimicrobial agents. They act without high specificity towards a protein target, which reduces the likelihood of induced resistance (Wimley & Hristova 2011). Linear amphipathic peptides have a distribution of polar and hydrophobic residues that cause interaction of the peptide with the phospholipid membrane; this disturbs the bilayer integrity through defects, disruption or pore formation. Various models have been proposed to explain the action of AMPs; however, they can generally be placed into two categories: the *transmembrane pore models* and the *non-pore models*. Within the transmembrane pore category, there are two main models of membrane permeation by peptides involved in the formation of membrane-spanning pores: the barrel-stave pore model and the toroidal pore model. The barrel-stave model is the simplest model and is also known as the helical-bundle model; peptides interact with one another to form a pore enclosing a channel, much like a protein ion channel (Bechinger 1999; Pieta, Mirza & Lipkowski 2012; Rapaport & Shai 1991). In the toroidal pore model, the peptides affect the curvature of the membrane, causing an opening in which the peptides can insert themselves and partially line the opening (Henzler Wildman, Lee & Ramamoorthy 2003; Mihajlovic & Lazaridis 2012). The non-pore models involve destabilisation of the bacterial membrane. In the carpet model, peptides accumulate on the membrane surface until they reach a critical mass and permeabilisation occurs via global destabilisation (Gazit et al. 1996). The detergent model is used to describe the destabilisation seen with many AMPs and describes a direct peptide–lipid interaction causing collapse of the membrane (Bechinger & Lohner 2006). Many other models have been described that also explain the various observations made in AMP membrane disruption; however, the exact lipid bilayer effects remain under question. The recent investigations into these functions have brought many interesting observations to the surface. Other peptides have also been found to

affect biological membranes, and they are now discussed as a group referred to as *membrane-active peptides*, which, according to their distinct biological functions, are generally classified as antimicrobial (AMPs), cell-penetrating peptides (CPPs) or fusion peptides (FPs) (Moiset et al. 2013; Wadhwani et al. 2012). AMPs and CPPs are known to have some structural and physicochemical similarities; however, fusogenic peptides tend to have different features and sequences (Wadhwani et al. 2012). Yet many AMPs and CPPs exhibit pronounced fusogenic activity. Magainin, a potent AMP isolated from the African clawed frog, has been found to accumulate on the bacterial surface and produce toroidal-type pores. It has also been found to be mildly fusogenic; however, it does not translocate across the membrane so is not cell penetrating (Almeida & Pokorny, 2009; Wadhwani et al. 2012). Other AMPs such as melittin are highly pore forming yet also translocate across membranes (Almeida & Pokorny 2009; Krauson, He & Wimley 2012). LL37 is a very important and widely researched AMP found in human macrophages and polymorphonuclear leukocytes, and it is found throughout the human body. It has been thought to be pore forming, yet has recently been shown to permeabilise membranes through destabilisation and it does not form pores. Despite the many contributions being made towards our understanding of membrane-active peptides, we still do not know how many fundamentally different mechanisms of activity exist, what the molecular membrane binding activity is, and how the vesicle leakage and killing are correlated. To complicate matters further, it is now known that some chemokines can also have antimicrobial activity (Yang et al. 2004). Chemokines are a small group of chemotactic cytokines that play an important role in the innate and adaptive immune system. Their main function is related to the recruitment of white blood cells to the site of infection, where they bind to chemokine receptors, which subsequently triggers signalling pathways in the leukocytes. Some AMPs have been shown to be involved in the regulation of the immune response as well by binding to these same receptors (Zaat & Hiemstra 2013). It is interesting to consider what the interplay might be between naturally occurring AMPs and chemokines, particularly in the area of wound repair, where it has long been hypothesised that they both have a role in healing. A new group of synthetic variants, termed innate defence regulators (IDRs), have been developed that are synthetic immunomodulatory versions of AMPs based on the immunomodulatory activities of such natural peptides and are specifically aimed at wound healing (Steinstraesser et al. 2012).

2.6.2 Antimicrobial Peptides as Antibiotics

While AMPs have enormous potential as antimicrobials, their development has been hampered because of this lack of understanding of mode of action, as well as production costs. There have been issues with bioavailability, which has been hampered because of toxicity when administered; however, this can likely be overcome with further research, and they have enormous potential for topical and surface applications (Fox 2013; Wimley & Hristova 2011; Zaat & Hiemstra 2013). Proteolytic degradation is possible, particularly in the wound healing environment, yet AMPs are expressed at the wound edge and studies on LL-37, an endogenous human peptide that is known to be found in wounds, has been shown to be relatively resistant to degradation in chronic wound fluid, possibly because of endogenous proteinase inhibitors (Grönberg, Zettergren & Agren 2011). A number of products are being developed for topical application using AMPs including a magainin-based product for diabetic foot ulcers and OP-145 based on LL-37 for chronic inner ear infections (Fox 2013).

2.6.3 Immobilisation of Antimicrobial Peptides

The membrane-permeabilising activity of membrane-active AMPs makes them promising candidates in the pursuit of an antimicrobial surface coating for biomaterials. An antimicrobial coating on a biomaterial would kill bacteria that attempt to colonise them. The coating must be non-toxic and must not initiate an immune response. Implantable biomaterials also require a surface that could encourage tissue growth and integration. AMPs have been immobilised onto solid substrates using two main strategies: physically, via absorption into layer-by-layer (LBL) thin films and gels, and chemically, where AMPs are covalently tethered using self-assembled monolayers (SAMs), or plasma polymerisation (Glinel et al. 2012; Onaizi & Leong 2011). Other techniques use PEGs and linkers. Many researchers have used AMPs in surface applications; however, recent reviews have highlighted the lack of rigour in these studies and the importance of essential surface analysis for tethering parameters such as peptide orientation, surface concentration and proof of covalent attachment (Costa et al. 2011; Onaizi & Leong 2011).

LBL is a layer-by-layer assembly method of polymeric films, which can be used with AMPs embedded in the layers, thus allowing for high and controllable amounts of AMPs within the film. The release is through diffusion, which may be affected by the electrostatic interactions of peptides and the polyelectrolyte matrix, making control of the diffusion process difficult; moreover, long-term stability of these films has not been tested (Onaizi & Leong 2011).

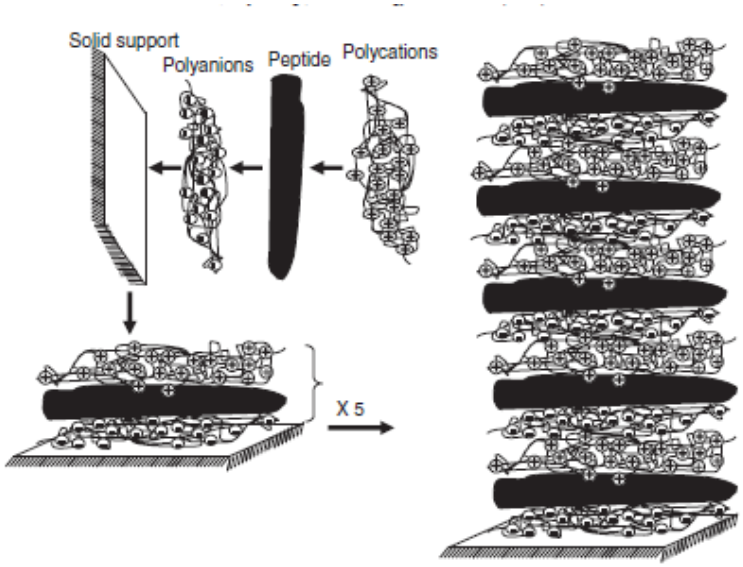


Figure 2.6: Layer-by-layer assembly (not drawn to scale or exact structure) of polyionic materials containing antimicrobial peptides (AMPs). The peptide is sandwiched between two layers of oppositely charged polyions, which can be achieved by sequential dipping of the solid support in polyanions, AMP and polycations solutions. (Onaizi & Leong 2011)

Covalently based techniques require a surface with a reactive group that can bind to the AMP, allowing it movement so that function is maintained. These surfaces are advantageous in that the density of surface-attached AMPs can be controlled and confirmed through the use of surface analysis techniques, and AMPs can interact directly with bacteria. SAMs of reactive compounds on a suitable substrate provide an easy and effective method to produce an antimicrobial surface (Onaizi & Leong 2011). Peptides can be modified with a group such as cysteine and reacted with a maleimide-functionalised glass, which produces a highly effective antimicrobial surface (Chen et al. 2012).

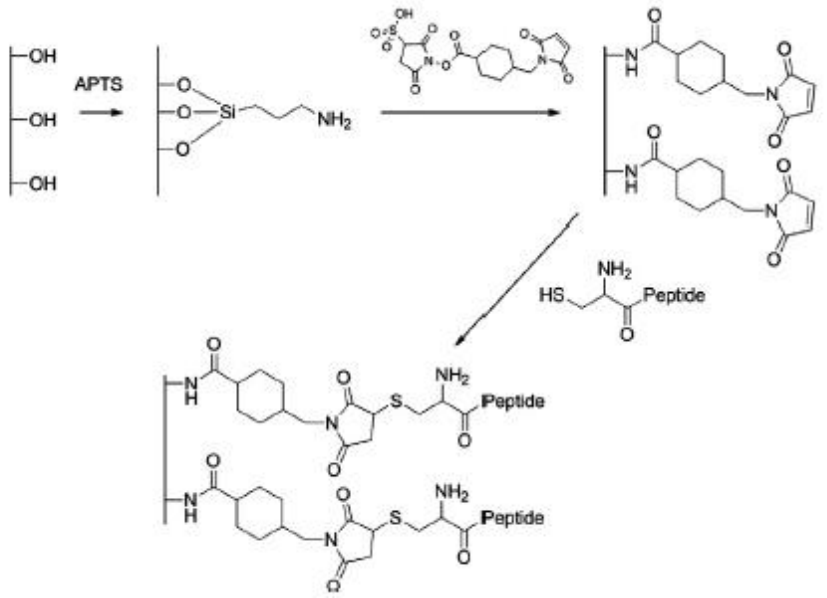


Figure 2.7: Site-directed attachment of cysteine-modified melamine on maleimide-functionalised glass (Chen et al. 2012)

SAM surfaces also allow for the use of spacers and functionalised PEG or other 'brushes' (Onaizi & Leong 2011). PEG is commonly used because of its non-fouling, anti-adhesive properties; however, there is confusion between antibacterial and non-fouling surfaces. If PEG is added to a surface, one must question as to whether any antibacterial effect is actually a result of the non-fouling PEG rather than the antibacterial peptides added. A lack of cell attachment or lack of dead bacteria on the surface would be an indication that the surface is non-fouling rather than antibacterial. The non-fouling features of PEG have been studied quite extensively, and the surfaces have been shown to be resistant to bacteria for only a short time. Observations seem to indicate that the bacteria push physisorbed PEG aside and adapt to the PEG quite easily (Kingshott et al. 2003), and with an antibacterial peptide added, they may kill bacteria on the ends while bacteria populate the PEG.

Plasma polymerisation is a method widely used in industry to coat solid materials and is also in use for coating a number of biomedical products; a case in point is Ciba Vision's extended wear contact lenses. Using a suitable plasma polymer to attach biomolecules provides long-term stable attachment of peptides, adaptable to any device and highly reproducible. It has been

used to covalently attach nisin onto biomaterials surfaces using amine groups (Duday et al. 2013). Immobilisation of AMPs onto various solid biomaterial surfaces functionalised with aldehyde groups can be used to bind AMPs covalently via the formation of imine bond between the functionalised surfaces and the peptide molecules (Vreuls et al, 2010). The imine bond is then reduced using sodium cyanoborohydride ($NaBH_3CN$) to convert the imine into amine bond and thus stabilise the attachment of the peptide to the surface. AMPs bearing accessible NH of the lysine or S of the cysteine amino acid residue can be easily immobilised on epoxide-functionalised surfaces in a reagent-free coupling process. The peptide binding to the surface is through nucleophilic ring opening of the epoxide by thiol or primary amino group of the peptide. The immobilisation of AMPs onto amine-functionalised surfaces can be achieved using 1-Ethyl-3-(3-dimethylaminopropyl) carbodiimide (EDC) and N-hydroxysuccinimide (NHS), analogously to the peptide coupling to carboxylic-functionalised surfaces.

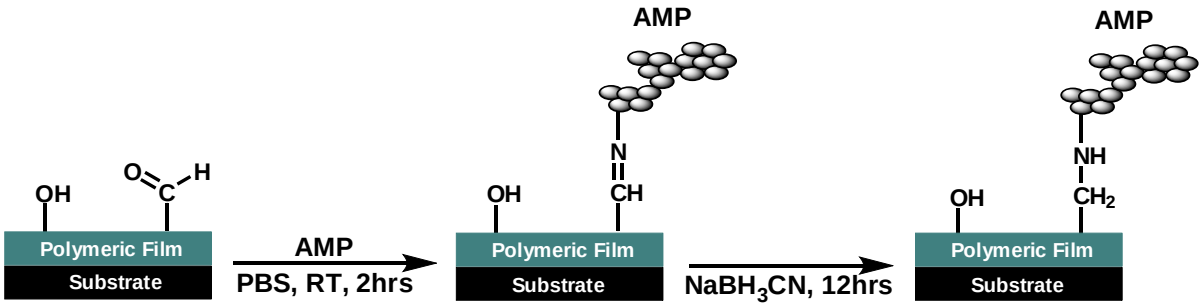


Figure 2.8: Immobilisation of antimicrobial peptides via reductive amination onto ALDpp (the XPS data shows aldehyde and hydroxyl groups on the surface)

While a number of studies have also shown that AMPs are still antibacterial when attached to surfaces (Costa et al. 2011; Glinel et al. 2012; Onaizi & Leong 2011), there is a distinct lack of knowledge about how long they can be stored and how long they are effective in the body, and how deep they penetrate or signal into the tissue or wound. Many publications have mentioned that they can be highly stable and can be stored, but no published data have been found to verify this. Some studies report that AMPs can be degraded and inactivated by bacteria (Schmidtchen et al. 2002), while others report that they are stable and active in the non-healing wound environment (Grönberg, Zettergren & Agren 2011). There is also evidence of resistance to AMPs (Zaat & Hiemstra 2013); Peschel and Sahl (2006) have deliberated the possible co-

evolutionary development of resistance within bacteria to AMPs because of their ancient and highly conserved nature. As they point out, it is surprising that resistance has not evolved further in light of their mutual survival over millions of years. An understanding of how this has happened may assist in the devising of methods to control pathogens. Further findings that may raise questions about the use of AMPs have emerged with studies implicating AMPs and, in particular, LL37 with the pathogenesis of a number of autoimmune disorders, such as systemic lupus erythematosus, rheumatoid arthritis and atherosclerosis (Craft, 2011; Kahlenberg & Kaplan 2013). It will be interesting to see where this research leads in regard to the importance of AMPs in the overall picture of immune response and healing.

In summary, while AMPs show excellent promise as surface antimicrobials, their application has been hindered by their high manufacturing cost, questions concerning their susceptibility to proteolysis and poorly understood pharmacokinetics (Marr, Gooderham & Hancock 2006). In addition, it is difficult to elucidate their biological activity and understand the structure–property relationship because of the complexity of their native structures and differences between the many different AMPs. Because of this, there has been considerable interest in developing synthetic AMPs.

2.7 Synthetic Polymer Mimics of Antimicrobial Peptides

Considerable research has been devoted to the development of synthetic mimics of antimicrobial peptides (SMAMPs) to take advantage of their unique ability to target the membrane and kill microbial pathogens at all stages of infection. Natural AMPs have provided the knowledge on how to control microbes using mechanisms that have survived millions of years of evolutionary change yet continue to be an essential part of the innate immune system in all living organisms (Peschel & Sahl 2006). Their complexity makes the study of their pharmacokinetics and structure–property relationship difficult. Synthetic peptides are extremely interesting because specific sections can be produced and studied in order to define activity, known functions can be enhanced and unwanted toxicity such as haemolysis of red blood cells can be controlled or removed. This in-depth knowledge can be applied downstream to produce the most efficient product in both activity and cost.

The field of synthetic AMPs is massive and increasing rapidly. Many are based on the natural peptide skeleton of repeating oligomers of α-amino acids or peptides, and with pendant functional groups to mimic the amino acid side chains found in AMPs. The amino acid sequences of α-helical AMPs leads to a global segregation of cationic and lipophilic side chains in the folded state, with cationic groups arrayed along one side of the helix and lipophilic groups arrayed along the other, forming a regular amphiphilic conformation (Mowery et al. 2009). The antimicrobial activity is thought to be a multistep process, with the peptides, which are cationic under physiological conditions, and Coulombic forces apparently causing the initial attraction to the anionic surface of bacterial cells, which then allows insertion of lipophilic groups resulting in cell lysis. Eukaryotic cells generally have a lesser negative charge density relative to prokaryotic cell surfaces, which is thought to underlie the selectivity for prokaryotic cells displayed by AMPs in the body. The level of prokaryote selectivity compared with eukaryotic toxicity is generally assessed by comparing the ability of a given peptide to induce haemoglobin release from red blood cells, or haemolysis.

The killing activity resides specifically with the ability of the peptide mimic to form a globally amphiphilic conformation. It was thought that a regular helix forming backbone structure was required; however, the work done by Gellman's group challenges this view. His work, which investigates altering this natural skeleton and assessing function, is a fascinating probe into structure–activity relationships (Horne & Gellman 2008) and has shown that many conformationally irregular structures or random structures are also active (Mowery et al. 2009). It was postulated that the amphiphilic nature of AMPs is the dominant reason behind their selective antimicrobial effects and could be replicated within a polymeric, random coil structure. This has allowed them to reproduce a series of random copolymers that are easier to prepare in quantity and are more cost effective.

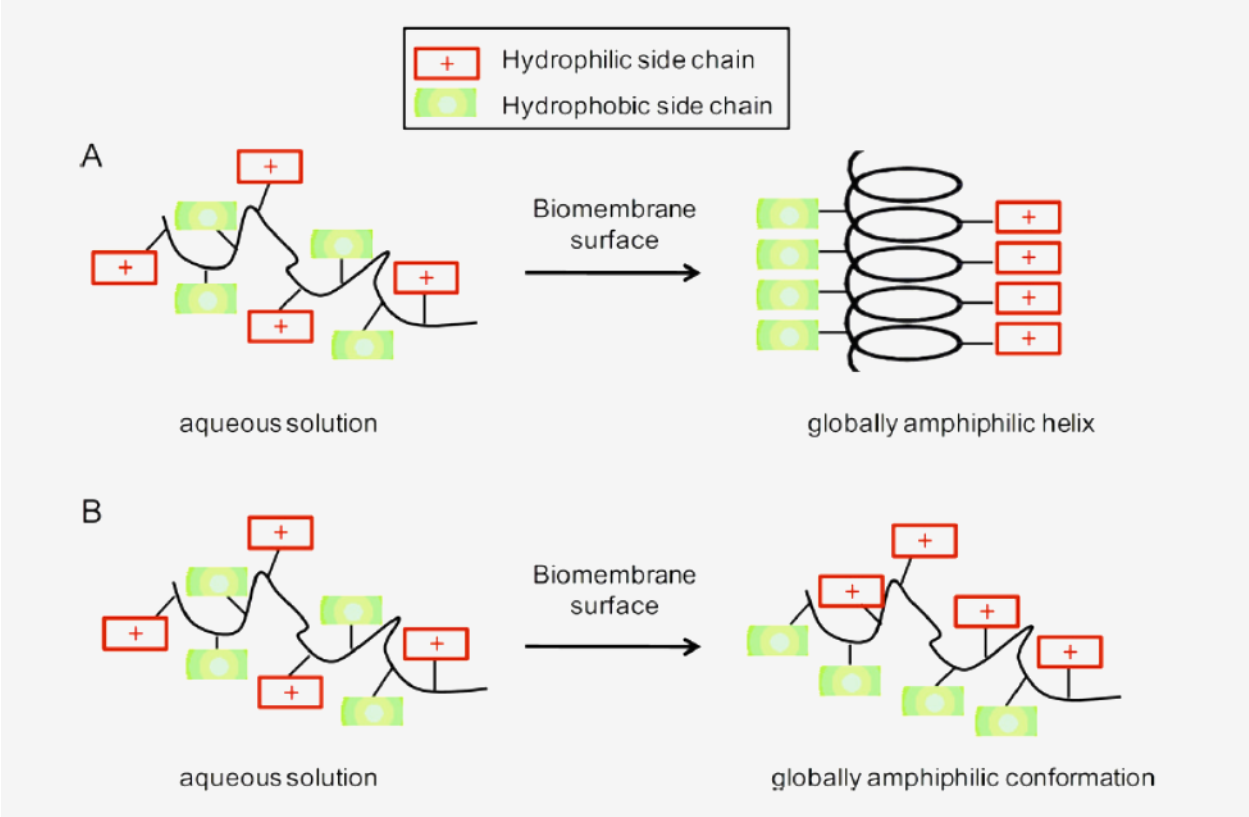


Figure 2.9: Many antimicrobial peptides act by disrupting bacterial membranes. Those with the α-helical folding pattern fold into conformations that are globally or facially amphiphilic with discrete areas of hydrophobic and hydrophilic side chains that are projected from opposite sides of the helix (a). Gellman et al. proposed that flexible, sequence-random polymers containing cationic and hydrophobic subunits can be induced by a bacterial membrane surface to adopt irregular conformations that result in global amphiphilicity and are equally effective antimicrobials (b). (from Mowery et al. 2007; Mowery et al. 2009; Munoz-Bonilla & Fernandez-Garcia 2012)

The ability of these peptides to provide highly potent antimicrobial activity with minimal human cell toxicity seems to be through identifying the correct balance between the cationic charge and the hydrophobic character. Higher degrees of hydrophobic character were found to lead to increased haemolytic behaviour (Mowery et al. 2007), while highly cationic polymers display agglutination of human red blood cells (Oda et al. 2011). This is similarly illustrated with quaternary ammonium cationic compounds, which also show little lytic selectivity between bacterial and mammalian cells, resulting in indiscriminate killing of both.

Synthetic peptides based on maintaining the natural peptide skeleton as well as non-natural skeletons have been studied extensively by Hancock et al. He has consistently maintained a very high optimism in the usefulness of AMPs and has furthered this through his work with analogues of a number of natural AMPs. One example is his work with indolidcin, a naturally occurring peptide isolated from bovine neutrophils, which was chemically altered to obtain less toxic polymers that would retain high antimicrobial activity (Halevy et al. 2003; Steinstraesser et al. 2012). Other groups have done similar work with grasitin, bactenecin and melittin (Pandey et al. 2010; Shestakov et al. 2013; Spindler et al. 2011; Tamaki et al. 2011). β-peptides are polyamides designed to mimic AMPs that can adopt the numerous helical conformations while resisting the proteolysis that often degrades the α-amino acid backbone found in conventional peptides. These peptides showed reasonable antibacterial activity and low toxicity; however, length and hydrophobicity control was essential because high toxicities developed if peptides were too long or too hydrophobic (Liu & DeGrado 2001).

The enzymatic susceptibility of α-peptides prompted Gellman's group towards β-peptides, and with the knowledge gained from these, on to the development of "nylon-3" polymers. Nylon-3 polymers are readily produced by the ring-opening polymerisation of β-lactams. Random copolymers are synthesised using a mixture of hydrophobic monomers bearing cyclic alkane structures (cyclopentane to cyclooctane) with another monomer bearing a primary amine group. Additional variations were also investigated by introducing a variation in hydrophobic character to the polymer by incorporating an additional one or two methyl groups adjacent to the amine (Liu et al. 2013; Mowery et al. 2007; Mowery et al. 2009). Gellman et al. have found, using their random nylon-3 copolymers, that a content of approximately 60% of the cationic monomer led to the optimum balance between haemolytic behaviour and antibacterial activity. Increasing the cationic monomer by only 10% to an overall content of 70% led to reduction of activity against *E. coli* by an order of magnitude. Conversely, decreasing the cationic monomer percentage by 10% to a total of 50% led to an increase of haemolysis by an order of magnitude (Mowery et al. 2007).

Tew and his group have designed and synthesised many interesting AMP mimics, with most recent work concentrating on aryl-based SMAMPs (Thaker, Sgloastra et al. 2012). These peptides have been created after a concerted effort in defining systematically chemical structure-activity relationships needed for a specific response. Tew et al systematically adjusted charge and aromatic groups in order to fine-tune peptides to give the best mimicking response. The surprising result is that these new compounds mimic the range of responses that are often found in natural human AMPs, specifically the antimicrobial effects and the immunomodulatory responses (Som et al. 2012). The term host defence peptide (HDP) is often used because it encompasses this range of abilities. Tew et al have also worked extensively with polynorbornene derivatives and looked specifically at primary amine groups in order to improve hydrophilicity and selectivity (Al-Badri et al. 2008; Som, Choi & Tew 2009). His fascinating work has also replaced the amines with guanidine analogues, which further improved his polymers, creating a highly potent and specific mimic (Gabriel et al. 2008).

Other important contributors to the field of AMP mimics are Kuroda et al., who investigated amine groups and hydrophobicity (Oda et al. 2011) and spatial separation between charge and polymer backbone (Palermo, Vemparala & Kuroda 2012), which may have an effect on the ability of the polymer to adopt the facially amphiphilic conformation and deeper insertion into the membrane.

2.7.1. Immobilisation onto Surfaces

While the vast majority of work conducted with AMP mimics has been based on activity in solution, there is great potential for the immobilisation of these polymers to create antimicrobial surfaces. Such polymer coating technologies could be produced cheaply and easily for integration into medical implants, leading to an effective method to combat device-related infections. Such approaches may lead to more targeted antimicrobial applications than systemic antibiotics, thus increasing effectiveness, and reducing potential toxicity and the propensity for bacterial resistance. The major problem with this approach is that the translation from a three-dimensional environment in solution to that of the two dimensions on the surface is associated with a very different picture of the relationship between polymer structure and activity. Very

little research has been conducted in this area, and what has been done has achieved little success. Gellman and co-workers immobilised their nylon-3 polymers onto surface-borne carboxylic acid groups. The primary amines of the synthetic AMPs were believed to have been covalently bonded via amide bonds in a 'side-on' manner to the surface. The surfaces showed protein adsorption and NIH 3T3 cell proliferation superior to controls, even under serum-free conditions. These observations could be explained by the peptide-like backbone of nylon-3 polymers used, favouring interactions with natural proteins and peptides (Lee et al. 2009). In a follow-up study, it was found that longer polymer chains of a less hydrophobic nature provided the best conditions for cell adhesion (Liu et al. 2012). There was no examination of the antibacterial activity of the surfaces reported; however, discussions with this group revealed that experiments with bacteria were unsuccessful after surface immobilisation. The studies lacked the essential surface analysis data needed to indicate the amounts of peptide bound to the surface, or the orientation of the binding, or prove that the peptides were indeed covalently bound, which might explain the lack of activity. It is often the case that groups lack the techniques in surface analysis that can enhance understanding of results. It is possible that they were not bound in sufficient numbers to have an effect, or were too firmly tethered to respond to bacteria.

In contrast, as discussed in Chapter 6, my studies using Gellman's nylon-3 mimics tethered to biomaterial surfaces using plasma polymerisation (Figure 2.16) to immobilise them covalently via amine and thiol groups produced different results, in that excellent antimicrobial activity was found. Surface analysis data showed that the intended covalent immobilisation was successful, by X-ray photoelectron spectroscopy (XPS) and time-of-flight secondary ion mass spectroscopy (ToF-SIMS) data. Samples remained antibacterial in the presence of serum and after weeks of storage. They were also found to enhance cell growth, giving better coverage of the treated area than TCPS, and close a wound gap, in a scratch wound assay, as opposed to the control scratch wound, which was colonised by bacteria, and cells did not close the wound gap. Perhaps the differing attachment routes are the cause of the differences in activity between Gellman's immobilisation and mine. This example is useful here in illustrating that conclusions in studies in the literature may be affected by absence of critical data or by the immobilisation approach; care is needed to dismiss or select reported strategies.

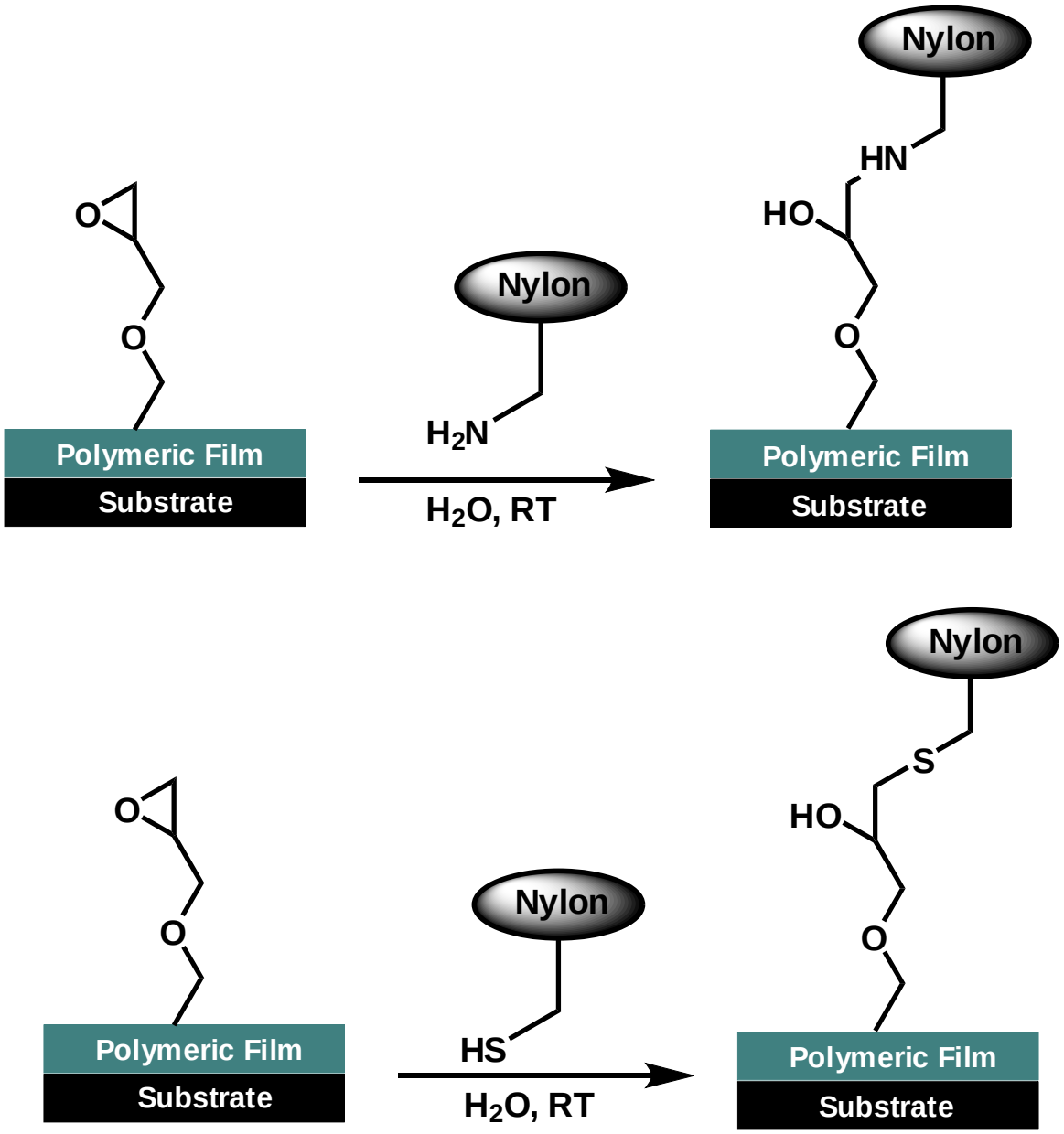


Figure 2.10: Illustration of immobilisation routes of amine and thiol terminated nylon 3 onto epoxide-functionalised surface

Tew et al. used a dip-coating method to coat surgical sutures with polymethacrylate antimicrobial polymers. The resulting sutures showed superior kill efficacy at lower loading than those coated commercially with Tricosan. Unfortunately, no mention of biocompatibility or human cell proliferation was made (Li et al. 2012).

A surface-based antibacterial study was also conducted by Hammond and co-workers involving spin cast solutions onto surfaces of their peptide polymers bearing quaternary ammonium groups with alkyl chains of various lengths. In the case of *E. coli*, the most potent polymer in solution with a medium length alkyl chain also showed best efficacy on surfaces. Interestingly, for *S. aureus*, polymers with long alkyl chains were most efficient in solution whereas on surfaces a medium length was found to be optimal (Engler et al. 2011).

While data are limited in the area of surface immobilisation of AMP-mimicking polymers, there is a growing body of evidence to suggest that such work could lead to the development of robust and safe antimicrobial surfaces for integration into medical devices. To achieve this, the same careful and systematic investigation of the relationships between polymer structure and antimicrobial potency and selectivity that were performed in solution will need to be replicated with surface coatings.

Chapter 3: Experimental Approach and Theory

This thesis chapter describes the materials and methods used throughout the various chapters of this project. Because antibacterial testing on surfaces is a field without an accepted standard method, most techniques have had to be adapted or created from existing traditional techniques for surface assessment.

3.1 Materials

3.1.1 Chemicals

AGE, allyl glycidyl ether, 99% Aldrich, USA
$AgNO_3$, silver nitrate, Aldrich, USA
DMSO, dimethyl sulfoxide
EtOH, ethanol, 100% undenatured AR grade, Aldrich, USA
HA, heptylamine, 99% Aldrich, USA
$NaBH_4$, sodium borohydride, 99% Sigma Life Science, USA
$NaBH_3CN$, sodium cyanoborohydride, 95% Aldrich, USA
PA, propionaldehyde

3.1.2 Buffer Salts, Proteins, Consumables

Amphotericin B, injectable liquid, research only, complimentary from SA Pathology
Amphotericin B, Sigma-Aldrich, USA
Antimicrobial peptides, parasin 1, magainin 2 & LL37 custom peptide, American Peptide Co., USA
BSA, bovine serum albumin, > 99% BSA, Aldrich, USA
Caspofungin, research only, complimentary from SA Pathology,
Caspofungin, Sigma-Aldrich, USA
Culture dishes, with inserts u-dish, DKSH, Australia

Culture slide, 18-well uncoated, u-chamber 12-well cell culture slides & coverslips, DKSH, Australia

Daptomycin, Sigma-Aldrich, USA

DMEM, Dulbecco's modified Eagle medium, Sigma, USA

Bovine serum, 10% Bovogen Biological Pty Ltd, Australia

FlexiPERM 12-well reusable masks, Sarstedt, Australia

Gram Staining Kit, Sigma, USA

HBA, horse blood agar, Thermo Fisher, Australia

LIVE/DEAD *Bac*Light Bacterial Viability Kit for microscopy and quantitative assays, Invitrogen, USA

Loops, spreaders, and sterile Petri dishes, Southern Cross Scientific, Australia

NaCl, sodium chloride, >99%, Southern Cross Scientific, Australia

Nunc Cell-Culture Multidish 96-well, 48-well, 24-well, and 4-well polystyrene plates, Invitro, Australia

NA, nutrient agar, Thermo Fisher, Australia

PBS, phosphate buffered saline, 137 mM NaCl, 27 mM KCl, 6.64 mM $Na_2HPO_4.H_2O$, 1.76 mM KH_2PO_4, Sigma, USA

TSB, tryptone soya broth plus 10% glucose, Thermo Fisher, Australia

3.1.3 Substrates

Thermanox plastic coverslips, ProSciTech, Australia

FEP; fluorinated ethylene propylene; DuPont

Polystyrene dishes, various suppliers

Si, Silicon wafers, <100>, p-type boron doped, Micro Materials and Research Consumables, Australia

3.2 Methods

3.2.1 Substrate and Surface Cleaning

Silicon wafers (Si, p-type, <100> were cut into pieces (size between 15 x 15 and 5 x 5 mm) and washed in acetone, ethanol and rinsed 10 times in Milli-Q (MQ) water (18.2 MΩ·cm at 25 °C) They were stored in MQ and rinsed a minimum of two times before use and dried under a stream of nitrogen gas (N_2) before immediate use. Thermanox plastic coverslips were rinsed under a stream of acetone and ethanol, then rinsed a minimum of 10 times in MQ water and dried under a stream of N_2 gas before immediate use.

3.2.2 Plasma Polymerisation of Substrates

Plasma polymerisation of the monomer allyl glycidyl ether (AGE) or propionaldehyde (PA) was used for depositing a functionalised layer onto fluorinated ethylene propylene (FEP) polymer, Thermanox, polystyrene substrates, or Si wafers (the last mainly for surface analyses). This technology is based on radio-frequency glow discharge (rfGD) and the basic design of the apparatus used was first described in 1989 (Griesser 1989). Fresh monomer liquid was placed in a clean round-bottom flask and connected to the plasma chamber by a stainless steel line, glass tap and two manual control valves. Any volatile impurities that may have been present in the monomer line or the chamber were removed by pumping the monomer liquid through the chamber until the appropriate pressure could be adjusted and left for stabilisation again before ignition of the plasma.

Plasma polymerisation was carried out in a custom-built reactor, as illustrated in Figure 3.1.

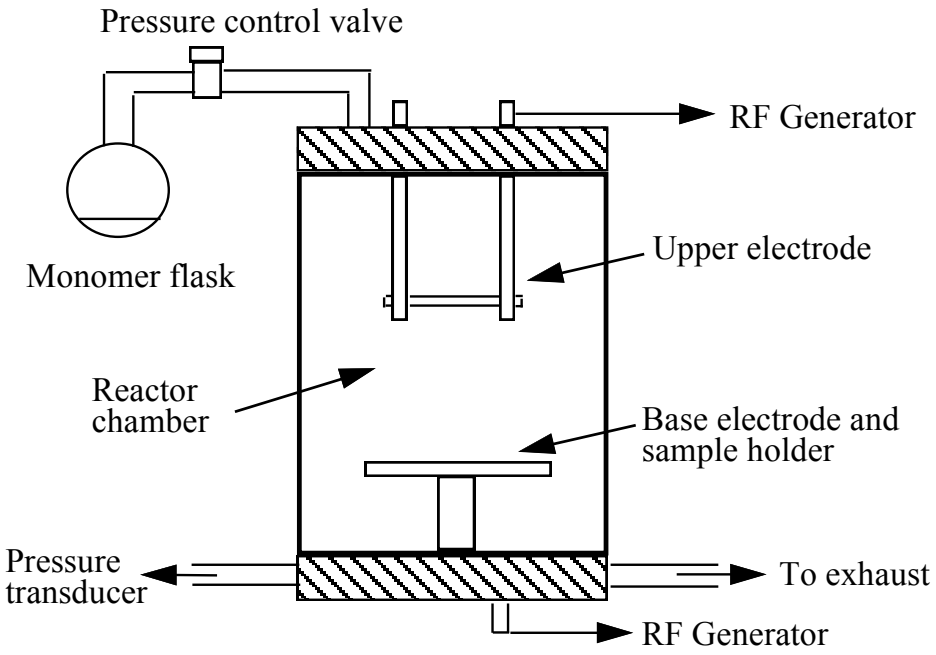


Figure 3.1: Schematic diagram of plasma apparatus (Kingshott 1998)

The glass cylinder was 17 x 36 cm; the other components were the upper lid electrode, which had two brass rods (18 cm long) with a cross strut, and the lower electrode, which was a 10 cm or 15 cm diameter copper disc with a brass centre post. The oscillator used in these studies was a commercial plasma generator (Advanced Energy) with a matching network, operating at 13.56 MHz. A rotary high vacuum pump was used to evacuate the system. A pressure transducer (MKS Baratron) was used to measure the pressure in the chamber. With the samples placed on the base electrode for the plasma treatment, the chamber was outgassed to 0.025–0.02 mbar. The exit valve was opened slightly to introduce air into the plasma chamber at a pressure of approximately 0.35 mbar. An 'air' plasma was ignited, which further cleaned the surfaces of samples from residual adventitious hydrocarbons, and adjusted the applied rf power to the desired power of 25 or 40 watts. The generator was turned off at this setting so it could be started at the exact position and ensured reproducible rf power settings for the ensuing plasma polymerisation. The monomer vapour stream was then introduced to fill the chamber and ten adjusted to a specific pressure (usually 0.21 mbar). After the pressure was stabilised at the desired level, the glow discharge was generated by applying a radio-frequency electric field at a power of 25 watts for 1 minute 30 seconds and 2 minutes of pulsing for AGE or 40 watts

for 90 seconds using PA. To reduce the reaction of active free radicals left over after plasma treatment with atmospheric oxygen, the monomer was left to flow into the chamber for another 10 minutes to assist in quenching free radicals. The pressure in the reactor chamber was brought back to atmospheric pressure by introducing air via a separate inlet valve.

3.2.2.1 Surface Attachment of Peptides, Antifungal Compounds, and Pharmaceutical Compounds

Immediately following plasma polymerisation, samples were removed with sterile forceps and placed into a sterile container. Samples were moved to a clean fume cupboard or biohazard cupboard and AMPs, SMAMPs or pharmaceutical compounds were added at 0.1 mg/ml unless otherwise stated. Most were tested initially at 1 mg/ml also, but due to cost, this was reduced to 0.1 mg/ml. Other compounds were added at stated amounts. In the group's research experience, 0.1 mg/ml has always provided an excess of molecules for attachment, giving dense coverage as suggested by surface analysis data close to when using 1 mg/ml solutions. Higher amounts sometimes provided somewhat better results but not enough to warrant regular use because of the high cost of the compounds and extra time required for rinsing to ensure unattached and physisorbed compounds were not affecting results

3.2.3 Silver Nanoparticle Surfaces

The silver nanoparticle samples were prepared on Thermanox coverslips, and placed into a sterile 24-well plate after plasma treatment. An oxygen plasma at 0.22 Torr and 20 watts for 90 seconds was used and plasma parameters were set for the heptylamine plasma polymer to produce appropriate thickness as verified using ellipsometry (without silver) for a thickness of 10, 15, 20 and 25 nm for cell culture and bacterial assays. The silver nanoparticles were made up in the concentrations shown in Table 3.1.

Table 3.1: Composition of silver nanoparticles

	Concentration	*Amount*	*Needed Amount*	*Weight in Amount*
$AgNO_3$	*0.02M*	*50ml*	*169.87mg*	*170.5mg*
$NaBH_4$	*0.01M*	*50ml*	*18.92mg*	*18.6mg*

The amount required was weighed into a flask, 50 ml of MQ water was added and the mixture was sonicated for 5 minutes on high. Silver nanoparticles were loaded using a time of immersion in $AgNO_3$ of 1 hour and a time of reduction in $NaBH_4$ of 30 minutes.

The surfaces were assessed using ellipsometry after treatment to determine surface thickness of the final assembly of multilayer structures, with a heptylamine plasma polymer layer including silver nanoparticles, which was approximately a further 60 nm.

3.2.4 Bacteria Preparation and Testing

Common methods of assessing bacteria include MIC, MBC, the disk diffusion method, the broth dilution test and other tests such as E tests. These are all used for testing antibacterial activity of drugs in solution using log growth bacteria in growth medium. Testing for antibacterial activity on solid material surfaces is a newer and less defined area, and to date, there is no standard or widely accepted reliable test. These tests needed to be revised and researched along with the topic in this thesis. There are also many questions about when to use the bacteria because antibiotics generally target bacteria in the actively growing phase. Therefore, bacteria have always been grown to the log phase in a planktonic or liquid solution overnight, diluted and grown again for 2 hours, when the pharmaceuticals developed to date would be most effective. Because all the surface-coupled antimicrobials used in this thesis target bacteria when they are actively adhering to and colonising a surface and not just actively growing in a planktonic phase, the bacteria were not grown to a third of the time to log phase, but harvested from planktonic dilutions at approximately 1 million or 0.1 million (10^6 or 10^5) CFU ml^{-1}. Most studies test surfaces by simply adding bacteria diluted in PBS, rinsing it off after a desired time, then staining with safranin and reading the absorbance. This was found to be problematic in my initial work, because active antimicrobial surfaces have dead bacteria

attached, or a loosely adherent surface that rinses off after testing, or surface absorbance of the stain, and the absorbance readings can be erroneous. In addition, while absorbance readings are often used in surface chemistry labs, they are not used in microbiology and are considered by microbiologists to be meaningless in giving information on specific numbers of bacteria. The other concern is that the bacteria are diluted in PBS rather than TSB or another broth to maintain the growth of the bacteria. This alone will give a major reduction in bacteria and a better result because studies comparing bacterial adhesion to plastic surfaces in TSB versus PBS have shown clearly that bacteria in PBS showed virtually no adherence (less than 5×10^4 CFU/mm^2, which was less than the seeded amount) as compared with over 10^6 CFU/mm^2 (in less than 10 hours for both groups) accumulated on the surface with bacteria in TSB (Herrera et al. 2007).

The gold standard in microbiology practice today is still to dilute the bacteria serially and plate out each dilution, incubate the plates overnight and count by hand, every colony on each plate. This meant that experiments on a set of surfaces may require more than 500 plates to count. Although most pathology labs have automated counters, our research lab is not equipped thus, and hand counting is still required, making it impractical to assess each coating by such extensive plating. There are concerns about other approaches that other labs have invented, such as sandwiching surfaces with the biomaterial surface and coating on the bottom, then bacteria, then another layer of some sort (Teflon, or polystyrene) on this, because 'surfaces will never be in a sea of bacteria but with other *things* around them'. A biomaterial surface will never be sandwiched either because the first encounter any surface will have is with proteins forming a conditioning film from blood, tissues, mucous or saliva contacting it. Other options are to add a bacteria solution, leave it a few hours, then remove it and replace it with fresh broth, PBS or something else. In this study, that was not found to be accurate either because fresh broth encourages extra strong growth, PBS limits bacterial life span. In this study, it was consistently found that the best test method was simply to add a solution of bacteria at 1×10^5 CFU ml^{-1} or less, leave it, rinse it, and check with LIVE/DEAD *BacLight* staining for half the samples. To supplement the *Bac*Light results, the other half of the samples had the bacteria manually removed from the surface using a microscope either by hand or with sonication, quickly serially diluted, plated and incubated, then hand counted the following day. This testing approach was adopted after extensive investigation into the various methodologies.

Fungi were only investigated with *Bac*Light staining because they are so much bigger and it is much easier to define the mechanism of killing by observing membrane disintegration.

3.2.4.1 Plating of Bacteria

Bacteria (*S. epidermidis* ATCC 35984, *S. aureus* MRSA ATCC 43300 and *E. coli* ATCC 35922) were plated from frozen stock and incubated overnight at 37 ^{o}C. One colony was picked from the plate and grown in 10 ml TSB with glucose (Oxoid) overnight at 37 ^{o}C. Bacteria were diluted 1/100 and grown to log phase and then diluted in the above broth to 1 x 10^{6} CFU ml^{-1} using predetermined spectroscopy measurements as a guide.

3.2.4.2 Adding of Bacteria to Samples

Depending on the substrate, bacteria solutions were added at 100 µl or 300 µl (actual amounts at approximately 1 x 10^{5} or 3 x 10^{5} CFU ml^{-1}; note that growth occurs between diluting and adding to samples, and with some bacteria, even 30 minutes can result in a doubling or more of bacteria) and grown for 5, 6 and 24 hours at 37 ^{o}C. As a control, the same amounts were serial diluted and plated on nutrient agar (Oxoid) and counted to ascertain exact bacteria added to surface.

Polystyrene slides or ibidi µ-Slide wells were plasma treated. A FlexiPERM 12-well removable mask was placed on the slide and ibidi µ-Slides were used as is; antimicrobial polymers were added to the wells for grafting overnight. After rinsing, bacteria were added for incubation for various periods, followed by rinsing twice to remove loosely attached bacteria.

3.2.4.3 BacLight Fluorescence Microscopy

Surfaces were analysed using LIVE/DEAD *Bac*Light Bacterial Viability assay kits (Invitrogen), and viable bacteria count plating. LIVE/DEAD *Bac*Light stain comes in two solutions, labelled A and B; 30 µl of A and 30 µl of B were added to 10 ml of MQ water,

aloquated into 1 ml tubes and stored in the freezer. These are light sensitive so this is done in a darkened room and they are stored away from light. Before use, a 1ml tube must be thawed away from light.

The wells were treated with enough of the LIVE/DEAD *Bac*Light stain to cover the sample, generally 50 µl, and left for approximately 10 minutes in the dark. The stain was removed and a drop of *Bac*Light oil was dropped onto the sample. Any excess was removed and the mask carefully removed. A coverslip was added before microscopy examination.

3.2.4.3 Plate Counts of Bacteria

Viability counts were done by rinsing samples twice to remove non-adherent bacteria and then scraping/sonicating and rinsing the wells carefully with 1 ml of TSB. The wells were visually examined to ascertain whether all adherent bacteria were harvested. The 1 ml of TSB with bacteria was then serial diluted and 100 µl was plated onto nutrient agar plates. Plates were incubated for 24 hours and colonies were counted. Up to 20 plates for each dilution were needed for each sample.

3.2.4.4 Staining and Absorbance Reading of Bacteria

Samples were rinsed twice to remove non-adherent bacteria; 1 ml safranin stain was added and left for 3 minutes. The stain was rinsed until all excess was removed and samples were assessed using a plate reader.

3.2.5 Fungal Preparation

Candida albicans ATCC 90028 stored at –80 ^{o}C at the Royal Women's and Children's Hospital, North Adelaide, was streaked onto an SAB+ANTI (Oxoid) plate and grown at 37 ^{o}C. One colony was streaked onto a fresh SAB+ANTI plate and incubated again at 35 ^{o}C overnight. This plate was placed into a plastic bag and stored at 2 ^{o}C to 5 ^{o}C and was used to supply yeast colonies for all the experiments. The rest of the colonies were collected in 50/50 glycerol TSB

and frozen at –80 ^{o}C as stock. Before use, one colony was picked off the plate and placed in a vial with 10 ml of yeast extract peptone dextrose (YPD) growth medium for overnight incubation at 35 ^{o}C, diluted to 0.5 McFarland standard using a VITEK colorimeter, then diluted 1/100, giving approximately 1–3 x 10^{6} CFU ml^{-1}. One hundred millilitres is used per sample. Samples need a minimum of 3 days for growth and psydohyphae/hyphae development.

3.2.6 Cell Testing of Surfaces

As with bacteria, the methods to test the surfaces with immobilised antimicrobial compounds needed to be investigated and defined. Because the morphology of mammalian cells is often affected upon contact with a biomaterial surface, cells were often left unstained and counted by eye. The DAPI stain is used to stain the nucleus of cells and is used for counting using automatic counting software on most microscopes. It is often used to prove that cells can grow on a surface without reference to cells that are not growing well, because altered morphology and toxic effects and may even have possible mutations. It is not a good assessment method and should be used in conjunction with images. In this study, it was only used for ease of counting cell numbers *after* the morphology was checked and found to be unaffected and morphology was recorded if possible. If the morphology was affected in any way, the cells were not stained, but the image was recorded in the actual state. Counting by eye is not as reliable; therefore, most cell counts were treated as an estimate rather than a specific, accurate count.

3.2.6.1 Cell Preparation and Addition

Two fibroblast cell lines were used—HFF-1 (HFF-1 human fibroblast, ATCC SCRC-1041) and 3T3 (NIH-3T3 mouse fibroblast, ATCC CRL-1658)—primary human fibroblasts were harvested from fresh skin (MacNeil, Shepherd & Smith 2011). All cell cultures were maintained according to ATCC instructions or published protocols (MacNeil, Shepherd & Smith 2011). Thermanox coverslips were plasma treated and coated with the agents to be tested as outlined above and in the chapters, rinsed with sterile PBS and placed in sterile 24-well culture plates (Nunc, Invitrogen) and prewarmed in a cell culture oven. Primary cells were tested using plasma treatment and attachment of polymers in ibidi micro-chamber 12-well glass slides (ibidi 81201,

Germany). Cells were made up to 50,000 transformed cells per ml in medium/serum or 5,000–10,000 primary cells per ml in medium/serum and added at 1 ml to each well or 100 µl to ibidi wells. (Primary cells are more difficult to provide, which means that for some experiments there were simply not enough available to provide the same amounts for each experiment.) Well plates were placed into the culture oven and left for 2–3 days. The coverslips were rinsed to remove non-adherent cells and placed on a glass slide and coverslip for immediate microscopic analysis. ibidi wells were stained using DAPI nucleus stain (Invitrogen) and used as per instructions.

3.3 Theory and Principles of Analytical Techniques

3.3.1 Ellipsometry

Ellipsometry was used to measure the thickness of plasma polymer coatings. The general principle of ellipsometry is to use polarised light to probe the optical properties of a material. The sample under investigation will change the polarisation of the incident light, which can then be monitored by the instrument.

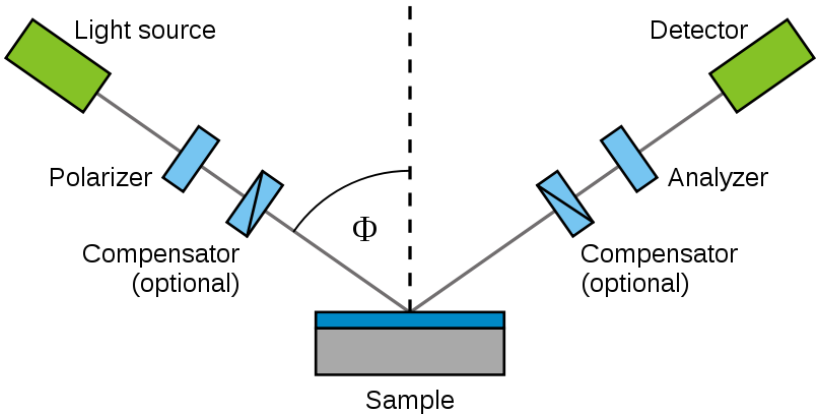


Figure 3.2: Basic schematic diagram of an ellipsometer (http://en.wikipedia.org/wiki/File:Ellipsometry_setup.svg)

The incident light is passed through a polarising element to produce light of known polarisation. This light interacts with the system under investigation and a change in polarisation occurs. Subsequently, the modified light (reflected from the surface) is analysed by a variable

polarisation analyser and a detector. The measurement of the initial and final states of polarisation are used to determine the level of transformation of polarisation by the system and using one wavelength either the thickness or the refractive index of a given material can be mathematically determined based on the explicit knowledge of one or the other (Aspnes 2013), but modern instruments using multiple wavelengths allow fitting for both simultaneously. In materials science and, in particular, polymeric coatings research, a common technique is to deposit a coating onto a well-known reflective substrate such as a silicon wafer and perform ellipsometry to determine coating thickness. Through use of modelling and analysis of controls, multiple layers can also be analysed (Azzam 1976). This method was used in this project for quality control of reproducibility of plasma polymerisation.

3.4 Surface Analysis Techniques

There is no single surface analysis technique that will give all the answers necessary to understand the surface chemistry details relevant to understanding bio-interfacial interactions; therefore, a number of techniques are combined to give the most information possible. The technique chosen depends on a number of factors about the surface:

- the bonding geometry of the molecules to the surface
- physical topography
- chemical composition
- chemical structure
- atomic structure
- electronic state.

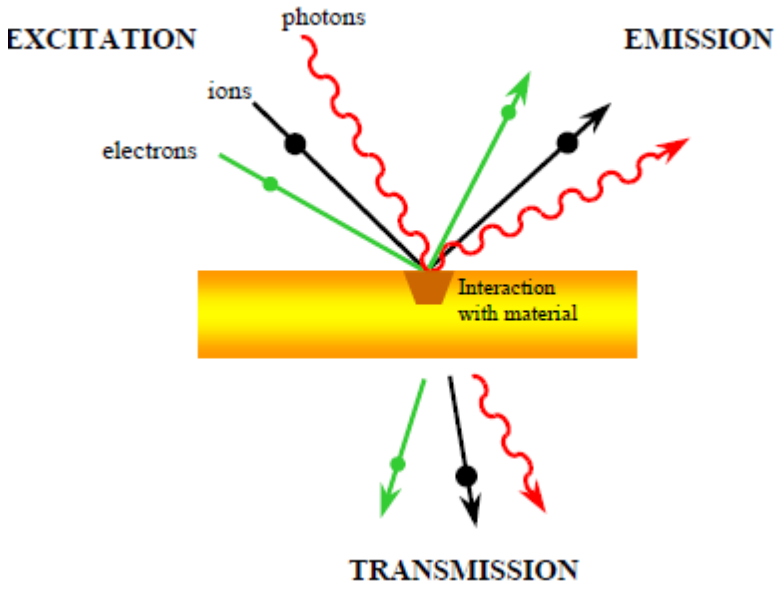


Figure 3.3: Different options to analyse surface chemistry (From Physical Electronics Pty Ltd oral presentation)

3.4.1 X-ray Photoelectron Spectroscopy

XPS has been used widely for the surface characterisation of polymeric biomaterials used for biomedical applications. It has the ability to determine the elemental and chemical structure of the surface, making it useful for determining the elements present and functional groups on the surface (the terminology used is surface analysis though it is noted that the depth of XPS analysis is ~ 8-10 nm with polymers, with sensitivity decreasing with distance into the material).

Collecting information about the surface chemistry of the first few layers of a polymer is considered very important because it determines the biological responses and it can differ greatly from the chemistry of the polymer bulk. Therefore, XPS becomes very useful because it can give information about the chemical composition of the polymer surface, the oxidation state, and reorientation of polymer segments. It also can give information about the presence of additives and contaminants such as organic siloxane (Andrade & Chen 1986; Chatelier et al. 1995a; StJohn et al. 2000; Tyler 1997), which, if unrecognised, can lead to erroneous conclusions about biological responses.

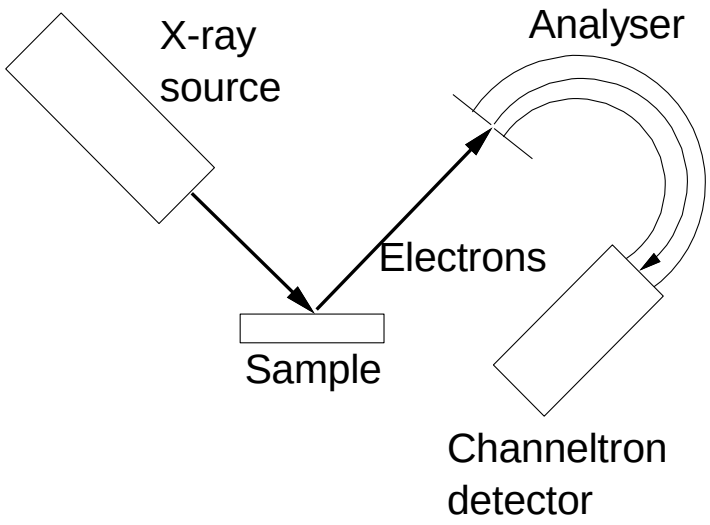


Figure 3.4: Schematic diagram of XPS apparatus. X-rays are directed onto the sample under vacuum in a chamber and the resulting photoelectrons are then focused onto the entrance slit of a concentric hemispherical analyser. Here a negative and positive potential are applied to the outer and inner cylinders, respectively, such that the central line between the cylinders is a line of zero potential. Scanning the potentials allows control of the energy of electrons that are allowed to pass through the analyser and onto the detector, usually a channel electron multiplier (channeltron). (From: http://www.chm.bris.ac.uk/pt/diamond/jamespthesis/chapter2.htm)

XPS is principally used to obtain elemental data of surfaces based on ejected electrons. For polymeric materials, the escape depth or inelastic mean free path of electrons normal to the surface is approximately 8–10 nm. Therefore, the spectra collected represent only the uppermost 10 nm of the material. Angle-dependent XPS (ADXPS) involves collection of ejected electrons at set angles defined as degrees from normal. This can allow the sampling depth to be reduced and can provide a depth profile if such a gradient exists in the upper 1–10 nm of the material.

For thin layers and absorbed macromolecules, XPS can give information on thickness based on the attenuation of specific substrate elements, for example, Si in silicon wafer substrates or F in fluorinated polymer substrates (Siow et al. 2006). Monitoring of substrate elements can also

provide an indication of delamination of coatings. However, caution must be used in the interpretation of the presence of substrate elements because a thin coating may give the same spectra as a patchy coating considering that information is collected over a relatively large area (a few hundred µm) depending on the aperture being used.

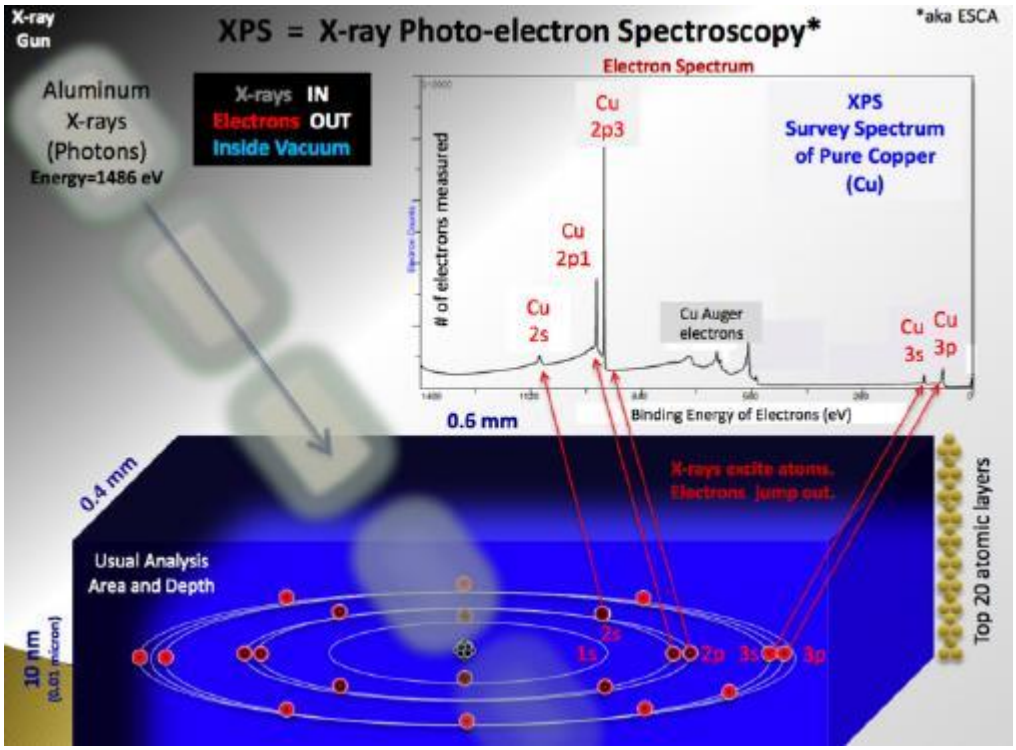


Figure 3.5: XPS photons going into the sample and electrons as peaks showing binding energy of each atomic group (from http://wiki.utep.edu/display/~dmarrufo/X-ray+Photoelectron+Spectroscopy)

Understanding the surface chemistry of thin polymer films created by plasma techniques is essential because these coatings can undergo time-dependent oxidation as well as reorientation due to reptation of polymer chains. Because these surfaces are designed to have functional groups available for subsequent reactions, XPS can be useful to monitor the type of the functional groups introduced and the subsequent oxidation processes (Gengenbach, Chatelier & Grisser 1996; Gengenbach, Vasic et al. 1994), the changes of the chemical composition during ageing of these surfaces (Gengenbach & Griesser 1998, 1999), the surface restructuring (Chatelier et al. 1995b; Gengenbach & Griesser 1998; Griesser et al. 1991) and changes in the elemental composition versus depth by ADXPS (Gengenbach, Xie et al. 1994). Analysis of the

high-resolution XPS spectra of each element recorded on the surface by constrained component fitting can give information about the type of functional groups and their binding energies. One limitation is that sometimes the differences in binding energies for some functional groups are too small to be separated by XPS (Gengenbach, Chatelier & Griesser 1996).

Typical binding energies for C 1s photoemission peaks from organic materials

functional group		Binding energy (eV)
hydrocarbon	C-H, C-C	285.0
amine	C-N	286.0
alcohol, ether	C-O-H, C-O-C	286.5
fluorocarbon	C-F	287.8
carbonyl	C=O	288.0
2F bound to a carbon	$-CH_2CF_2-$	290.6
3F bound to a carbon	$-CF_3$	293-294

Figure 3.6: Examples of binding energies for Carbon 1s from common organic groups used regularly in plasma polymerisation, such as amine, alcohol and hydrocarbon (From Physical Electronics Pty Ltd oral presentation)

XPS can also be utilised to assess polymer grafting on various polymer substrates using both the changes in the atomic concentration and the high-resolution spectra, particularly C 1s. For example, XPS was used for assessing grafting of poly(acrylic acid) on heptylamine plasma polymer modified silicon wafer and FEP substrates via EDC/NHS chemistry (Read et al. 2003; Vermette & Meagher 2002). In addition, it was utilised to assess grafting of different poly(ethylene glycol) derivatives onto different types of amine plasma polymer via reductive amination (Kingshott, Thissen & Griesser 2002). In that study, XPS data could differentiate between low and high grafting density simply by monitoring the evolution of the oxygen from the grafted polymer and the attenuation of the nitrogen signal. Furthermore, XPS was utilised to assess grafting of other polymers and organic molecules to various surfaces (Dai et al. 2000; Gong et al. 2000; Hartley et al. 2002; Mao, Castner & Grainger 1997; Medard et al. 2001; Sabbatini & Zambonin 1996).

Irreversible protein adsorption to biomaterial surfaces from biological media *in vitro* or *in vivo* is a well-known phenomenon. This layer of adsorbed proteins known as a 'conditioning film' plays an important role, because it can trigger an immune response that may cleave tethered peptides from the surface or degrade them. Protein adsorption can be assessed via XPS by monitoring the changes in the elemental compositions, particularly for nitrogen and/or a unique element from a substrate (e.g. fluorine) or an underlying grafted layer (e.g. bromine in the case of this project) before and after protein adsorption. Amide incorporation in the high-resolution C 1s (amide; 288.2 eV) or N 1s (amide; 400 eV) spectra can be used as an alternative way to assess protein adsorption (Browne et al. 2004; Griesser et al. 2003; Ratner et al. 1981; Wagner, Horbett & Castner 2003).

One limitation of the XPS technique is that all analyses must be carried out in the dry state and under ultra-high vacuum (UHV) conditions. This affects the thickness of an overlayer (grafted polymer or adsorbed protein) in a way that film thickness will be lower than in the hydrated state. In addition, assessment of protein adsorption in the dry state may induce conformational changes. This problem might be overcome by using freeze hydration XPS, a method initially developed by Lewis and Ratner (1993). Another limitation of the XPS technique is that XPS cannot differentiate between proteins in a mixture or biological media such as plasma or tears. This again supports the view that no single technique can describe fully the properties of a surface.

3.4.2 Time-of-Flight Secondary Ion Mass Spectrometry

ToF-SIMS provides a spectrum of surface fragments (secondary ions) that are ionised following impact by a primary beam that is composed of energetic ions (Wagner & Castner 2001). Both positively and negatively charged fragments can be detected from a ToF-SIMS experiment. From these spectra, detailed molecular information about the chemical structure and composition, from the first 1–2 nm, of the surface can be obtained. The high surface sensitivity of static ToF-SIMS makes it very attractive to be used for surface characterisation of biomaterials used for biomedical applications (Belu, Graham & Castner 2003; Castner & Ratner 2002; Ratner 1995).

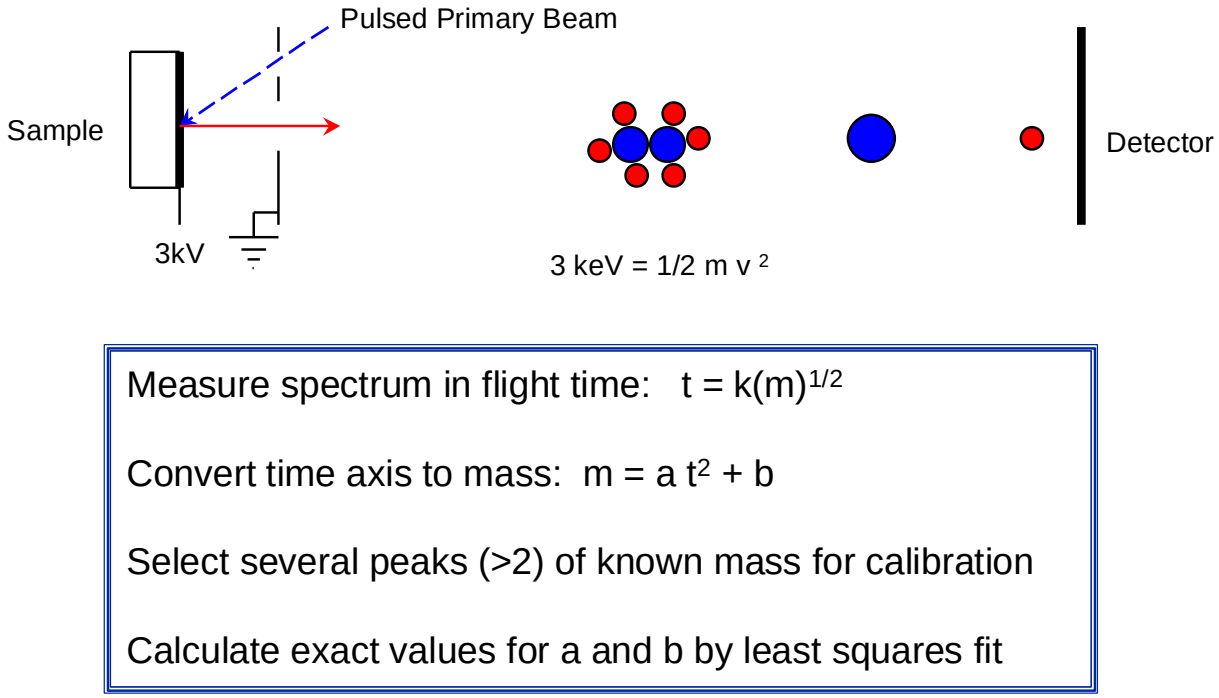
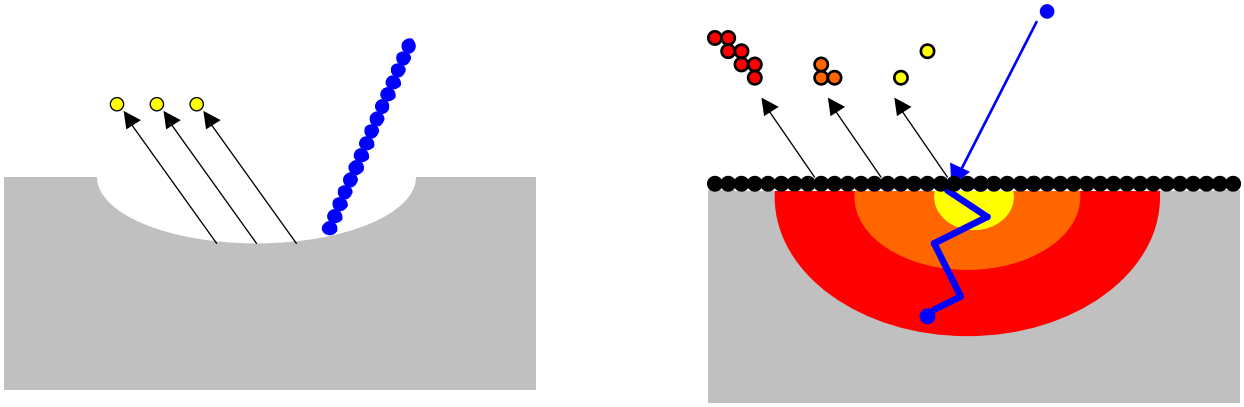


Figure 3.7: Basic principles of ToF-SIMS. The ToF-SIMS uses a focused, pulsed particle beam (Ga or CS) to dislodge chemical species on a materials surface. Particles produced closer to the site of impact tend to be dissociated ions (positive or negative). Secondary particles generated farther from the impact site tend to be molecular compounds, typically fragments of much larger organic macromolecules. The particles are then accelerated into a flight path on their way towards a detector. Because it is possible to measure the 'time-of-flight' of the particles from the time of impact to the detector on a scale of nanoseconds, it is possible to produce a mass resolution of time as atomic mass units. (From Physical Electronics Pty Ltd oral presentation)

There are two main modes employed for ToF-SIMS analysis: first, dynamic SIMS, which is generally used for inorganic substrates, and, second, static SIMS, which is commonly used for substrates with organic coatings. Static SIMS uses a low primary ion current to 'tickle' the sample surface in order to liberate ions, molecules and molecular clusters for analysis. In contrast, 'dynamic' SIMS is the method of choice for quantitative analysis of metals and ceramics because a higher primary ion current results in a faster sputtering rate and produces a much higher ion yield. Thus, dynamic SIMS creates a better statistical counting ratio for trace

elements. Organic compounds are broken up excessively by ‘dynamic’ SIMS, producing only small molecular fragments from polymers and organic molecules, and thus much less diagnostic information is obtained.



(a) (b)

Figure 3.8: Basic principle of ToF-SIMS: (a) dynamic SIMS, (b) static SIMS (From Physical Electronics Pty Ltd oral presentation)

Accordingly, static ToF-SIMS is used for analysing polymeric layers, surface-grafted chemicals and biological materials such as absorbed proteins, and was used exclusively in this research.

The emitted secondary ions within the low mass region (0–500 Da) are usually characteristic of the backbone and the side chains of a specific polymer and they can give information about the repeat units. In addition, the collected fragment ions, especially of low mass, can give information about the functional groups at the polymer chain ends. The collected fragment ions can be considered the ‘fingerprint spectrum’ characteristic for that specific polymer (Belu, Graham & Castner 2003). Numerous studies have been documented in the literature in which ToF-SIMS was utilised for surface characterisation of various polymeric materials (Biesinger, Corcoran & Walzak 2011; Briggs 1986; Briggs, Fletcher & Goncalves 2002; Leeson et al. 1997; Li et al. 2000; Leonard & Mathieu 1999; Lopez-Donaire et al. 2012; Sabbatini & Zambonin 1996; Vanden Eynde & Bertrand 1999).

The surface chemistry and chemical structure of thin films generated by plasma polymerisation from volatile organic precursors can be characterised by static ToF-SIMS. Ward and Short (1995) have investigated the retention of functional groups and structure from several monomers as a function of the power applied for the plasma deposition and the precursor monomer flow rate. The oxygen uptake by plasma-deposited films from styrene and ethylene was also investigated with the aid of static ToF-SIMS (Oran et al. 2005). Other studies were also documented in the literature (Cheng et al. 2005; Kinmond et al. 2005; von Gradowski et al. 2005).

Modification of functionalised surfaces with sequentially grafted polymer layers for biomedical applications has grown widely. Static ToF-SIMS can be utilised to investigate grafted thin polymeric layers on functionalised surfaces. Kingshott et al. (2003) investigated the covalent attachment of poly(ethylene glycol) onto functionalised surfaces using static ToF-SIMS and static ToF-SIMS in the imaging mode for the aim of creating surfaces that have the capability to reduce bacterial adhesion. Other grafted polymers such as polysaccharides (McArthur et al. 2002), a polycataionic copolymer (poly(L-lysine)-grafted-poly(ethylene glycol) (Pasche et al. 2003), polyelectrolyte thin films (Delcorte et al. 1996) and many others have also been characterised by static ToF-SIMS.

Static ToF-SIMS with its high surface sensitivity and chemical specificity is able to identify adsorbed proteins on solid surfaces (Mantus et al. 1993). However, since most proteins have similar fragment ions, further processing of the data, such as analysing the relative intensities of these fragments, should be done in order to be able to identify particular proteins (Lhoest et al. 2001). In addition, static ToF-SIMS can be utilised to determine the relative surface concentrations in binary or ternary adsorbed protein films (Wagner, Horbett & Castner 2003) and the conformation and orientation of proteins adsorbed on solid surfaces (Lhoest, Detrait & van den Bosch de Aguilar 1998; Tidwell et al. 2001). Static ToF-SIMS in the imaging mode can provide information about the spatial distribution of protein films on solid surfaces (Belu, Graham & Castner 2003; Griesser et al. 2003).

The large number of peaks present in static ToF-SIMS spectra is one of the primary difficulties associated with ToF-SIMS data analysis. There are two options to deal with this challenge: one option is to select a number of peaks and monitor their intensities during subsequent modifications (Delcorte et al. 1996); another option is to select the entire set of peaks and process them with the aid of principal component analysis (PCA), a multivariate analysis technique (Belu, Graham & Castner 2003). The latter option has been used in combination with static ToF-SIMS in many studies involving adsorbed proteins and grafted thin films (Graham & Ratner 2002; Lhoest et al. 2001; McArthur et al. 2002; Vanden Eynde & Bertrand 1997; Wagner & Castner 2003).

Although static ToF-SIMS has been applied widely in the characterisation of biomaterial samples, it has some limitations. It can only operate under UHV conditions and samples have to be in the dry state; this may cause denaturation especially for biological samples such as proteins. However, a cold-stage method has been developed to overcome this challenging problem. Since ToF-SIMS is a technique with high sensitivity, the presence of contaminants on the surface can compromise the static ToF-SIMS spectra and multivariate analysis results (Belu, Graham & Castner 2003; Griesser et al. 2003), although experienced analysts are well versed in identifying such artefacts.

3.5 Theory and Understanding of Major Chemical Approaches

3.5.1 Plasma Polymerisation

Plasma excitation occurs when a current is passed through a gas or, in the case of plasma polymerisation, an organic molecule (“monomer”) vapour at reduced pressure. A plasma consists of high energy electrons, ions, and molecular fragments, which, upon encountering a substrate surface, can either etch away the surface or deposit onto that surface depending on the conditions and gas/monomer employed. It is possible to have both etching and deposition occurring concurrently. The position of equilibrium will decide which process dominates. Plasma polymerisation is the generation of a polymeric coating using a monomer and plasma. The process involves activation of organic molecules to reactive forms such as radicals and ions, followed by their transport to the substrate surface where they condense into a polymeric

film. A number of non-thermal as well as conventional chemical processes are expected to occur, leading to a cross-linked polymer network with regions of conventional linear polymer. Plasma polymerisation and fragmentation behaviour of various small organic molecules have been studied, which often include a vinyl moiety (Siow et al. 2006). The carbon double bond (C=C), depending on the power used, is found to undergo fragmentation or radical activation in preference to saturated amine, aldehyde and epoxy groups; plasma polymers can be obtained that display these functional species on the surface of the coating. These functional groups can then be used for subsequent chemical surface modification (Siow et al. 2006; Thierry et al. 2008). Substrate surfaces such as Teflon and glass can be plasma treated with air to etch the surface and then coated with a monomer species to improve polymer adhesion with the substrate. Plasma polymerisation is highly reproducible and stable, and widely used in industrial situations in a number of applications. Further details of plasma polymerisation can be found in the following references: Biederman 1987; Siow et al. 2006.

3.5.2 Reductive Amination

The peptides and antimicrobial agents were covalently immobilised onto intermediate thin coatings prepared by plasma polymerisation using propionaldehyde, with the intermediate Schiff base (imine) stabilised by reductive animation using sodium cyanoborohydride (see Figure 3.9). Reductive amination is a simple reaction that can be performed in aqueous media and gives a well-defined covalent bond with no side products to interfere with the desired outcome. The sodium cyanoborohydride is used at 1 mg/ml and left for approximately 20 hours to achieve full reaction. Reductive amination has been a common strategy for covalent attachment of molecules to plasma polymers with many years of successful use and research (Blättler et al. 2006; Coad et al. 2013; Dai et al. 2000; Griesser et al. 2001).

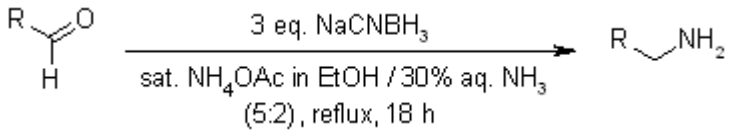


Figure 3.9: Schematic showing reduction amination of aldehyde to amine

Alternatively, molecules bearing amine groups can be immobilised onto surface epoxy groups under mild aqueous reaction conditions, which makes this approach equally suitable for the surface immobilisation of biomolecules. A plasma polymer with surface epoxy groups was developed by Thierry et al (Thierry et al, 2008) by the plasma polymerisation of allyl glycidyl ether (AGE) and was used in this project, as discussed in Chapter 6. The reaction schematic is as follows.

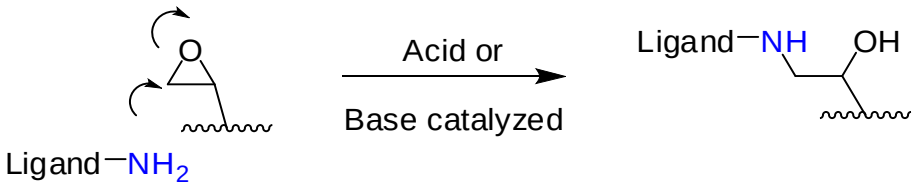


Figure 3.10: Interfacial reaction between surface epoxide groups and primary amine groups present on a biomolecule ligand. Reactions can be either acid or base catalysed. Amine bonds are irreversibly formed. (Coad et al, 2013).

Chapter 4: Mammalian Cell Responses to Antibacterial Coatings Comprising Silver Nanoparticles in Plasma Polymers

Abstract

Antibacterial coatings with silver and silver nanoparticles have received significant attention in recent years; however, reported data vary enormously regarding benefits and toxicity. The research jn this chapter is an attempt to address some of these issues using silver nanoparticles in a diffusible layer. We have found that the type of cell affects the toxicity of single nucleotide polymorphism (SNP) to the cell. Surfaces that contained silver nanoparticle in a heptylamine layer of varying thickness that were found to be antibacterial were tested against the 3T3 fibroblast, the Mg63 fibroblast precursor osteoblast, and two epithelial cell lines: human corneal epithelium and retinal epithelium. The fibroblast showed higher susceptibility to silver than the epithelial cell lines, which accords with published research in which silver was found to be toxic to fibroblasts yet not toxic to epithelium and useful in wound healing.

The key results from this chapter have been included in a published book chapter:
N. Poulter, K. Vasilev, S.S. Griesser, H.J. Griesser, Silver containing biomaterials. In: *Biomaterials Associated Infection* (Eds. Moriarty, Zaat and Busscher), Springer, p. 355-378 (2013). Here a more comprehensive data set and background information is provided.

4.1 Introduction

Bacterial colonisation and biofilm formation have been recognised as serious issues in many areas, including medicine, food processing, marine vessels and heat exchangers. Synthetic antibiotics are a common means to combat microbes; however, several generic problems are associated with their use (Albrich et al. 1999; Costerton, Stewart & Greenberg 1999; Hoffman et al. 2005; Loeffler et al. 2003; Mah et al. 2003; Stewart & Costerton 2001; Yoneyama & Katsumata 2006). A synthetic antibiotic is often specific to certain bacteria or a family of

bacteria; in addition, not all bacteria can be killed by antibiotics. Many bacteria, such as *S. aureus* and *E. coli*, have resistant forms. Most importantly, bacteria are living organisms and can mutate and develop antibiotic resistance or gain resistance-providing genetic material from other resistant bacteria (Wilson, Henderson & McNab 2002). All these issues have led to a renaissance of silver as an antiseptic agent in recent years.

Silver has been known from the time of the ancient Greeks to have antimicrobial properties, but its use was much reduced after the discovery of penicillin. Silver is a widely used non-specific biocidal agent that acts against a broad spectrum of bacterial and fungal species, including several antibiotic-resistant strains (Wright, Hansen & Burrell 1998). Silver is widely used in ointments and wound dressings; however, they contain a high excess of silver and this has been associated with cell toxicity and impaired healing (Atiyeh et al. 2007; Klasen 2000a; Trop et al. 2006). Silver ions have been reported to accumulate in epithelial cells, macrophages and fibroblasts, and connective tissue, and they have been shown to cause tissue toxicity and impaired would healing (Klasen 2000a, 2000b; Trop et al. 2006).

Vasilev et al developed a novel thin polymer film system loaded with silver nanoparticles in which it is possible to control the amount of silver nanoparticles loaded in the films as well as the rate of release of silver ions (Vasilev et al, 2010). The approach uses plasma polymerisation to create anime-rich thin film coatings, in which amine groups enable binding, by complexation, of in-diffusing silver ions. The process of preparation is fast, simple and convenient, and it enables control the amount of silver nanoparticles loaded in the films as well as the rate of release of silver ions. Plasma polymerisation to create amine-rich thin film coatings has the advantage, compared with alternative approaches, to enable deposition of well-adhering polymer films on practically any type of substrate without the need for surface pre-modification. Plasma polymerisation has been used in a number of applications ranging from corrosion protection (Lin, Chang & Huang 2006) to functional layers for biomaterials and medical application (Siow et al. 2006; Vasilev, Griesser & Griesser 2011). The plasma polymerisation of n-heptylamine (HA) has been studied previously; it provides stable, cohesive, adherent films, for which considerable analytical data are available (Gengenbach et al 1996; Kingshott, Thissen & Griesser 2002; Vasilev et al. 2008; Vasilev et al. 2009). The appearance of nanoporous

morphology in HA plasma polymer (HApp) films upon immersion in aqueous solution (Vasilev et al. 2008) led to the hypothesis that HApp coatings might provide a suitable matrix for the diffusive release of silver ions from embedded silver nanoparticles. It was shown (Vasilev et al 2010) that such coatings provided excellent antibacterial performance.

The same publication also reported no measurable cytotoxicity to mammalian cells and thus claimed selectivity of silver ions. In the work reported in this chapter, plasma polymer films containing silver nanoparticles have been evaluated for cytotoxicity, because based on the many publications reporting cytotoxic effects from silver I hypothesised that the different media used for testing antibacterial activity and cytotoxicity might have induced an artefactual appearance of selectivity. Also, different cell lines might exhibit different susceptibilities to silver.

4.2 Methods

4.2.1 Sample Preparation

Samples containing silver nanoparticles in HA plasma polymer films were prepared on glass or Thermanox coverslips (ProSciTech, Thuringowa, Qld, Australia) following the procedures established by Vasilev et al (Vasilev et al 2010). An oxygen plasma at 0.22 Torr and 20 watts for 90 seconds was used to clean and prepare surfaces, and plasma parameters were set for the HApp to produce appropriate thickness as verified using ellipsometry (before addition of Ag NPs as this allowed use of the previously established refractive index) for a thickness of 50–80 nm for cell culture and bacterial assays. The samples were placed into a sterile 24-well plate (Nunc, Invitrogen, Noble Park, Australia) after plasma treatment. The silver nanoparticles were made up in the concentrations shown in Table 4.1.

Table 4.1: Composition of silver nanoparticles

	Concentration	*Amount*	*Needed Amount*	*Weight in Amount*
$AgNO_3$	*0.02M*	*50ml*	*169.87mg*	*170.5mg*
$NaBH_4$	*0.01M*	*50ml*	*18.92mg*	*18.6mg*

The amount required was weighed into a flask, 50 ml of MQ water was added and the mixture was sonicated for 5 minutes on high. Silver nanoparticles were loaded using a time of immersion in $AgNO_3$ of 1 hour and a time of reduction in $NaBH_4$ of 30 minutes.

The surfaces were assessed using ellipsometry after treatment to determine surface thickness of the plasma film before and after incorporation of AgNPs, and an additional overlayer of HApp, with a thickness of 10, 20 and 30 nm for the various sample sets. Samples were dried under a stream of N_2.

4.2.2 Bacteria

Bacteria (*S. epidermidis* ATCC 35984, *S. aureus* MRSA ATCC 43300 and *E. coli* ATCC 35922) were plated from frozen stock and incubated overnight at 37 ^oC, two colonies were picked from plates and grown in 10 ml TSB (Oxoid) overnight at 37^o, bacteria was diluted 1/100 and grown to log phase then diluted to 1 x 10^6 bacteria/ml using predetermined spectroscopy measurements as a guide. (Note that *E. coli* and *S. aureus* are very fast growing and viability plating after seeding of samples shows that they can vary greatly in actual amounts.) Bacteria solutions were added at 100 ul and grown for five and 24 hours at 37^o C. Surfaces were analysed using LIVE/DEAD *Bac*Light Bacterial Viability assays kits (Invitrogen), viable bacteria count plating, disk diffusion assay, safranin staining of biofilm and spectroscopy readings.

4.2.3 Cell Attachment

Four different mammalian cell lines were used—the mouse fibroblast cell line NIH-3T3, human fibroblast–forming osteosarcoma MG63, human cornea epithelium HCE-2 and human retinal pigmented epithelium ARPE-19—all obtained from ATCC (Manassas, VA, USA).

All cell cultures were maintained according to ATCC instructions. Treated Thermanox coverslips (ProSciTech, Thuringowa, Qld, Australia) were placed in sterile 24-well culture plates (Nunc, Invitrogen) and pre-warmed in a cell culture oven. Cells were made up to 50,000

cells per ml in medium/serum and added at 1 ml to each well. Well plates were placed into the culture oven and left for 48 hours. The coverslips were rinsed to remove non-adherent cells and placed on a glass slide and coverslip for immediate microscopic analysis.

Treated coverslips were placed in Nunc 24-well culture plates (Invitrogen) and prewarmed in the cell culture oven. Cells were made up to 100,000 cells per ml and added at 1 ml to each well. Well plates were placed into the culture oven and left for 24 and 48 hours, plus up to 5 days to assess long-term growth. For assessment, the coverslips were moved to a fresh well plate to make sure that the cells were attached to the coverslips and not the well plate.

4.3 Results

The experimental strategy for the generation of silver nanoparticles within HApp films employed in this work is shown schematically in Figure 4.1a. First, a HApp film was deposited on substrates. Loading with silver ions was implemented by placing samples in a solution of $AgNO_3$ for a predetermined time. In this loading step, we took advantage of the well-known fact that amine groups can complex silver ions, according to:

$$Ag^+ + 2\ RNH_2 = [Ag(RNH_2)_2]^+$$

Reduction of silver ions (Ag^+) to metallic silver was subsequently achieved by immersion of samples in a solution of $NaBH_4$, which acts as a reducing agent for the synthesis of silver nanoparticles from silver ions.

Examples of the appearance of coated samples are shown in Figure 4.1b. After the deposition of a 100 nm thick HApp layer, the glass substrate was still transparent, maintaining its optical properties. After immersion in $AgNO_3$, no visible change of the optical properties of the sample was observed. After reduction of the complexed Ag^+ ions to Ag^0 by immersion in $NaBH_4$, the colour of the sample changed to yellowish-brownish due to the presence of Ag NPs. In Figure 4.1c, UV-Vis spectra of a sample loaded with Ag^+ (black) and the same sample after reduction in $NaBH_4$ (red) are shown. The new peak at a wavelength of ~ 420 nm that appears after reduction is assignable to the plasmon resonance of silver nanoparticles embedded in the film.

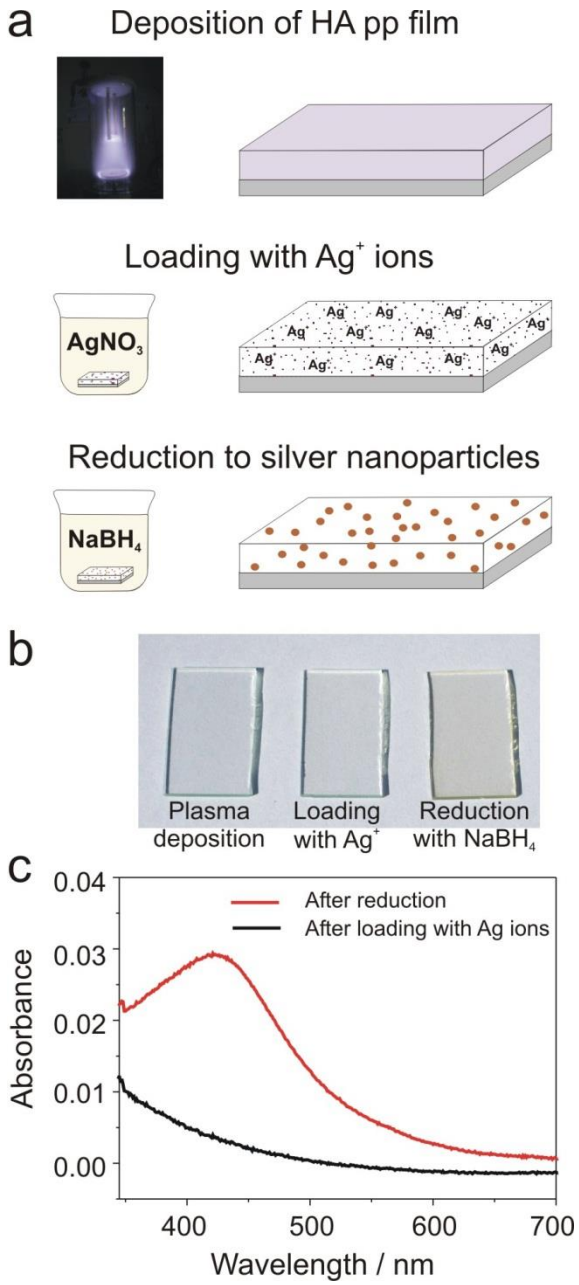


Figure 4.1: Loading silver nanoparticles in HApp films: (a) schematic representation of the experimental strategy for the fabrication of silver nanoparticles within amine plasma polymer films (1) plasma deposition of n-heptylamine, 2) loading with silver ions by immersion in $AgNO_3$ solution, (3) reduction of silver ions by immersion in $NaBH_4$ solution; b) glass samples after deposition of a 100 nm HApp layer, after loading with Ag^+ ions and after reduction with $NaBH_4$; (c) UV-Vis absorption spectra of samples after loading with silver ions (black) and after reduction by $NaBH_4$ (red)

Next, we aimed to control the amount of loaded silver nanoparticles, conducting a series of studies to document the influence of the Ag^+ loading time, time of reduction and thickness of the HApp film on the amount of embedded silver nanoparticles. The intensity of the plasmon resonance peak serves as a quantitative measure for the amount and size of silver nanoparticles within the film. All studies were conducted with HApp films deposited at a radio-frequency (rf) power of 40 W.

The influence of the time of immersion in $AgNO_3$ on the final amount of silver nanoparticles within the film was evaluated based on the intensity of the absorption maxima and is shown in Figure 4.2a. All samples were prepared using identical plasma polymerisation conditions and were exposed to $NaBH_4$ for the same time. In the time frame of 120 minutes, the absorption intensity of the plasmon resonance of silver nanoparticles increased with the time of immersion in $AgNO_3$. The increase was steeper in the first 40 minutes. After 1 hour of immersion, the absorption maximum still increased, but at a slower rate. These data show that by increasing the time of immersion in $AgNO_3$ solution up to 2 hours, more silver ions can be complexed within the HApp film, and as a consequence, more silver nanoparticles are formed after reduction in $NaBH_4$. Notably, increasing the Ag^+ loading time did not lead to significant changes in the wavelength of the plasmon resonance, which was 420 (+/– 2) nm, which indicates that particles of the same size were produced irrespective of the loading.

In addition, we examined the effect of the reduction time on the amount of embedded silver nanoparticles (see Figure 4.2b). Identical conditions of plasma polymerisation and immersion in $AgNO_3$ were used for all samples. The reduction proceeded with a high rate in the first 10 minutes. The amount of silver nanoparticles almost doubled after 30 minutes. Between 30 minutes and 60 minutes, the rate of reduction decreased. The wavelength of the adsorption maxima did not change in the first 30 minutes, remaining at about 420 nm, but longer times of immersion in $NaBH_4$ led to a slight shift to a longer wavelength, of ~424 nm.

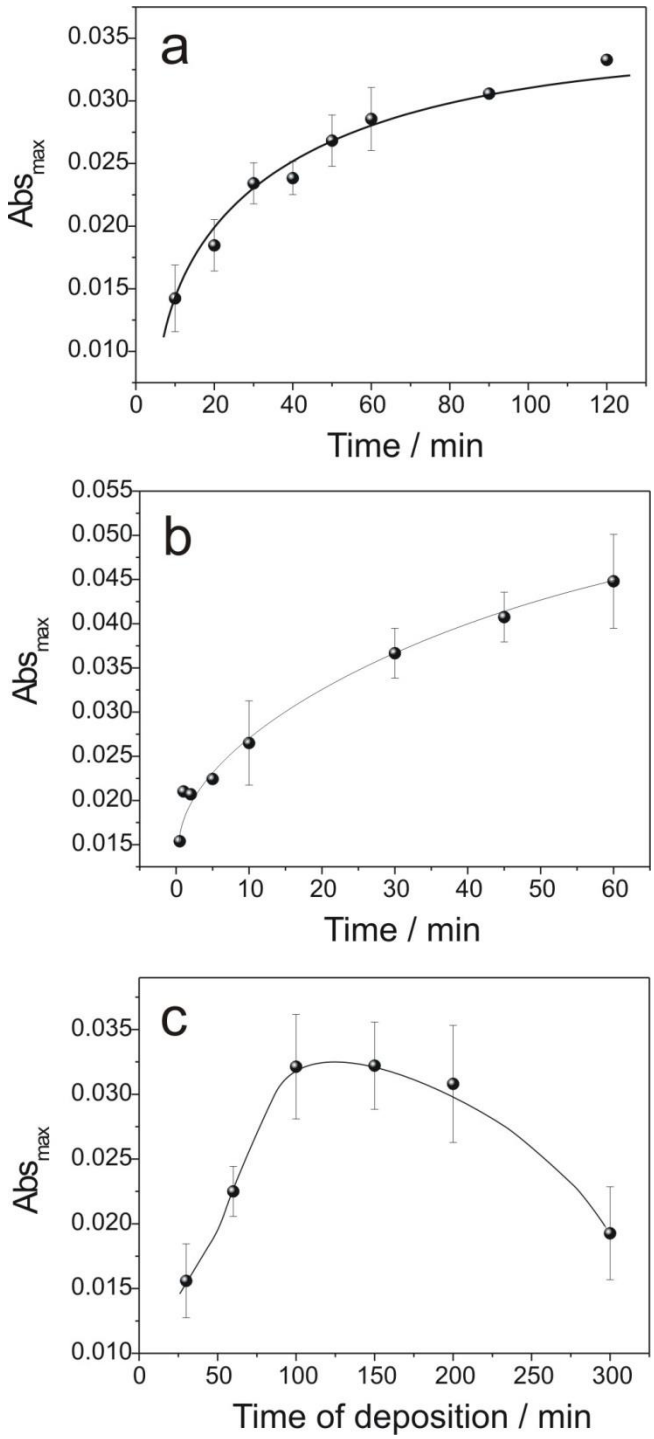


Figure 4.2: Control over the amount of loaded silver nanoparticles: (a) influence of the time of immersion in $AgNO_3$ on the amount of Ag nanoparticles in the film, for HApp films 100 nm thick and a time of immersion in $NaBH_4$ of 1 hr; (b) influence of the time of immersion in $NaBH_4$ on the amount of Ag nanoparticles in the film, with HA films 100 nm thick and a time of immersion in $AgNO_3$ of 1 hr; (c) influence of the thickness of

the HApp film on the amount of Ag nanoparticles in the film, with a time of immersion in $AgNO_3$ of 1 hr and a reduction time of 30 min. The solid lines are guides for the eye, not fits.

Our interpretation of this trend is in terms of the mechanism of nucleation and growth of silver nanoparticles. In the first 30 minutes, nucleation occurs and particles grow to a size similar for all particles. The shift in the plasmon resonance peak to longer wavelengths upon longer reduction times can be explained in terms of consuming remaining silver ions within the HApp film for additional growth of existing nanoparticles and perhaps some Ostwald ripening.

We also explored the effect of the film thickness on the amount of embedded AgNPs, expecting an increase in the loading with increasing thickness. However, as Figure 4.2c shows, while increasing the thickness in the range 0–100 nm leads to an increase in the amount of AgNPs, above 100 nm the amount remained constant to a film thickness of ~200 nm and then gradually decreased. The synthesis of Ag NPs within HApp films is based on earlier findings (Vasilev et al. 2008) that showed that immersion in aqueous solution leads to extraction of low-molecular-weight water-soluble fractions of the films, thus creating a porous structure, which allows the loading of Ag^+ ions and the subsequent formation of silver nanoparticles within the films. The data presented in Figure 4.2c suggest that increasing the plasma polymerisation time leads to a gradual change of the chemistry and properties of the HApp films, probably an increase in the crosslink density and thus smaller numbers of pores accessible for loading.

Release studies were carried out by immersion in PBS solution for 20 days and measuring the reduction in the content of silver nanoparticles within the films by the change in the intensity of the plasmon resonance peak. Figure 4.3 shows that deposition of an additional HApp film of thickness of 6 nm (circles) achieves a reduction of the rate of release of silver ions compared with films without such an additional pp film (squares). Increasing the thickness of the overlayer to 12 nm (triangles) and 18 nm (blue triangles) led to further reductions of the rate of release of silver ions, and within 20 days only 35% and 20%, respectively, of the silver content was released. Thus, a HApp overlayer of predetermined thickness can serve to adjust the release rate to a value intended for a specific application, over a time frame of several weeks.

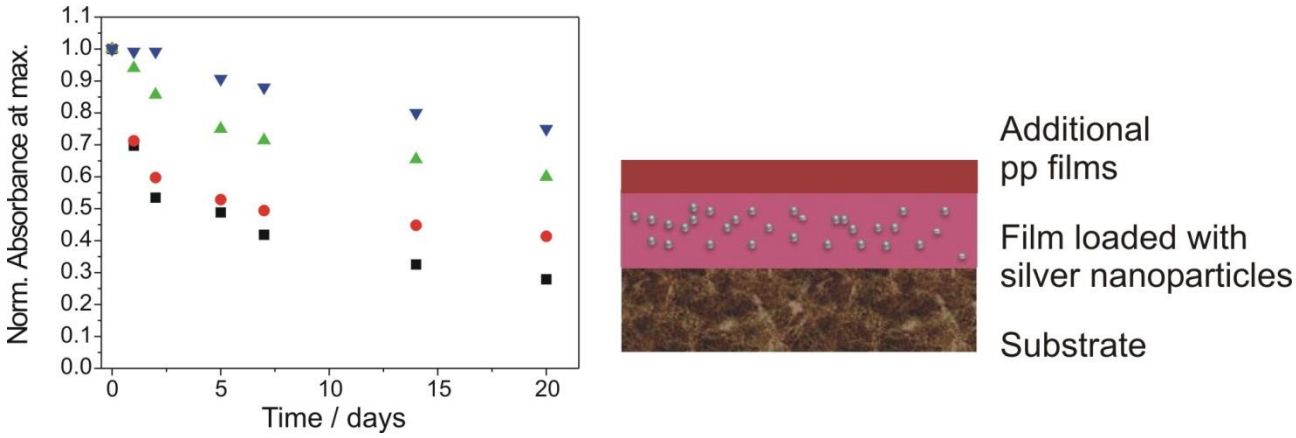


Figure 4.3: Control over the release of silver ions, achieved by depositing an additional layer of HApp on top of the silver nanoparticles–loaded film, as shown on the right. The graph on the left shows the kinetics of release of silver ions over 20 d immersion in PBS. Black squares = silver-loaded films as prepared; red circles = after deposition of a 6 nm thick HApp overlayer; green triangles = after deposition of a 12 nm thick HApp overlayer; blue triangles = after deposition of a 18 nm thick HApp overlayer.

The antibacterial properties of Ag NP–loaded HApp films were assessed with cultures of *S. epidermidis*, a bacterium prevalent in serious implant infections (Campoccia, Montanaro & Arciola 2006). For all samples, the HApp film thickness was 100 nm and the rf power for polymerisation was 40 W. Ag NPs were loaded using a time of immersion in $AgNO_3$ of 1 hour and a time of reduction in $NaBH_4$ of 30 minutes. Figure 4.4a shows representative images after exposure to bacteria. The HApp film without Ag NPs allows bacteria to readily adsorb and start colonising the surface within 4 hours. The situation is very different when bacteria are exposed to silver nanoparticle–loaded films for the same time (Figure 4.4b). Very few bacterial cells are evident and they appear to have a rounded shape indicative of poor attachment. The diffuse staining across the entire sample results from dye uptake into the plasma polymer film and the automatic camera setting amplifying its apparent intensity; visual observation showed a much lower intensity of this diffuse staining compared with the brightly stained bacteria. Figure 4.4c shows the same effectiveness in preventing bacterial attachment when the silver nanoparticle–loaded HApp layer was covered with an additional thin pp film to reduce the rate of release of

silver ions. Few bacteria are able to attach to the surface and the silver ions prevent them from dividing and colonising the surface.

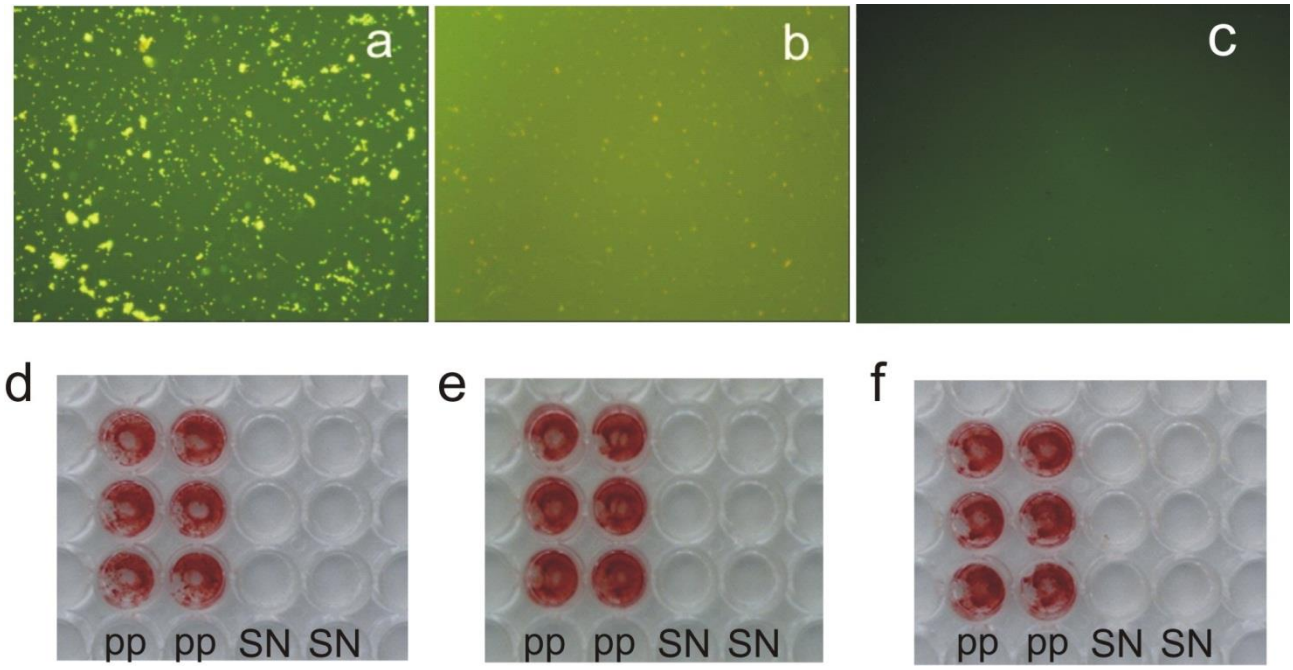


Figure 4.4: Antibacterial efficiency: *S. epidermidis* adhesion and colonisation after 4 hours on (a) HApp only (no silver); (b) HA film loaded with silver nanoparticles; (c) HA film loaded with silver nanoparticles and covered with an additional layer 6 nm thick of HApp; (d)–(f) biofilm formation after 24 hours on samples loaded with silver nanoparticles covered with an additional layer of HApp of thickness (d) 6 nm, (e) 12 and (f) 18 nm; pp = plasma polymer only; SN = films loaded with silver nanoparticles.

Results of tests performed over 24 hours with films loaded with Ag NPs and subsequently coated with HApp overlayers of thicknesses 6 nm, 12 nm and 18 nm are shown in Figures 4.4d, e and f. In each test, six wells were coated with HApp film only and another six wells with HApp loaded with silver nanoparticles. Safranin staining was used to detect bacterial biofilms. The photographs show rapid colonisation of the samples without silver nanoparticles. In contrast, all films containing silver nanoparticles, regardless of the rate of silver release, show complete (100%) inhibition of bacterial growth.

These observations confirm the earlier results reported in Vasilev eat al (Vasilev et al 2010) on the antibacterial effectiveness of the coatings.

However, if the surfaces were rinsed before adding bacteria, antibacterial ability was seriously compromised and no activity was seen after two rinses.

Table 4.2: Results of samples with no rinsing, and with one, two and three rinses. Antibacterial activity is compromised if rinsed.

Batch 1											
Properties	Thickness	Thickness Additional layer	Test method	Sample Set 1 No rinse		SampleSet 2 One rinse		Sample Set 3 Two rinses		SampleSet 4 Three rinses	
				S.epidermidis	*E. coli*	S.epidermidis	E. coli	S.epidermidis	E. coli	S.epidermidis	E. coli
HA	67.29nm	n/a	Disk Diffusion	100%	100%	100%	100%	100%	100%	100%	100%
			Stain/plate reader	1.03abs	1.5abs	1.5	1.72				
HA+SNP	67.29nm	n/a	Disk Diffusion	3-4mm diffusion	2 mm	UTE> 20%	U.T.E> 30%	100%	100%	100%	100%
			Stain/plate reader	0.012abs	0.021	1.2	1.34				
HA+SNP+HA 20 sec	67.29nm	10.95nm	Disk Diffusion	3-4mm diffusion	2 mm	UTE>70%	100%	100%	100%	100%	100%
			Stain/plate reader	0.016	0.027	1.4	1.54				
HA+SNP+HA 40 sec	67.29nm	20.23nm	Disk Diffusion	3-4mm diffusion	2 mm	100%	100%	100%	100%	100%	100%
			Stain/plate reader	0.029	0.04	1.4	1.8				
HA+SNP+HA 60 sec	67.29nm	27.58nm	Disk Diffusion	3-4mm diffusion	2 mm	100%	100%	100%	100%	100%	100%
			Stain/plate reader	0.04	0.09	1.5	1.7				
Batch 2											
HA	54.97nm	n/a	Disk Diffusion	100%	100%	100%	100%	100%	100%	100%	100%
			Stain/plate reader								
HA+SNP	54.97nm	n/a	Disk Diffusion	3-4mm diffusion	2mm	All 100% and absorbance readings showed no to very little activity.					
			Stain/plate reader								
HA+SNP+HA 20sec	54.97nm	10.95nm	Disk Diffusion	3-4mm diffusion	2mm						
			Stain/plate reader								
HA+SNP+HA 40sec	54.97nm	20.23nm	Disk Diffusion	3 mmdiffusion	1mm						
			Stain/plate reader								
HA+SNP+HA 60sec	54.97nm	27.58nm	Disk Diffusion	1-2mm diffusion	UTE						
			Stain/plate reader								

Staining and reading using a spectrophotometer also presented problems because the biofilm rinses off very easily and the samples look as though they are all antibacterial, even the controls.

4.3.1 Cell Testing

We assessed the cytotoxicity of samples with embedded Ag NPs using four different mammalian cell lines: the mouse fibroblast cell line NIH-3T3, the human fibroblast–forming osteosarcoma MG63, human cornea epithelium HCE-2 and human retinal pigmented epithelium ARPE-19. All these cells showed very good attachment and growth on the HApp coated control slides with 70% to 100% confluent monolayers achieved with the 3T3 and MG63 cell lines after 48 hours. The retinal pigmented epithelium cells (RPEs) and human cornea epithelium cells (HCEs) showed healthy confluent cell layers covering 50% to 100% of the surface. Figures 4.5 to 4.9 show optical microscopy images of the growth of the various cell lines on control HApp surfaces and on HApps with embedded AgNPs.

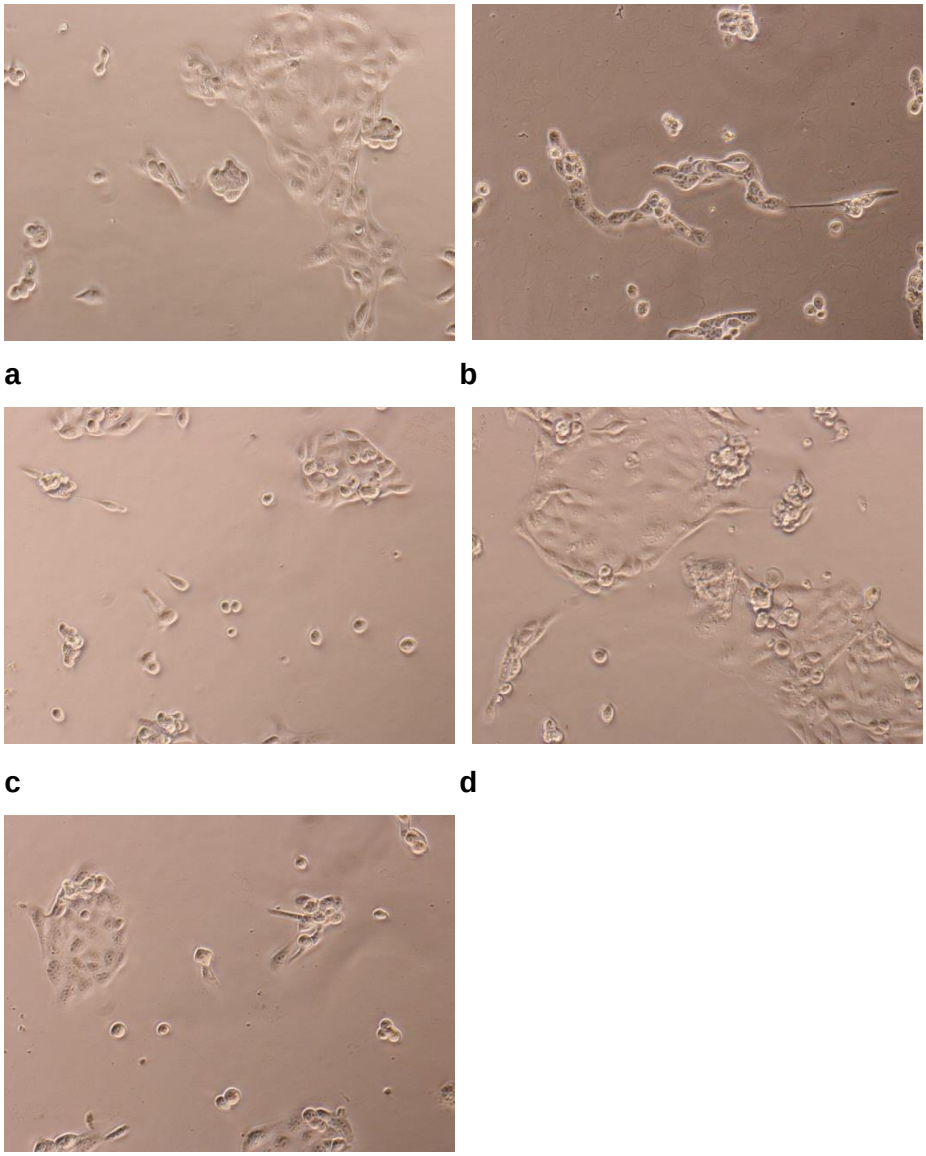


Figure 4.5: Images of human cornea epithelium (HCE) after 24 hours incubation: (a) control surface with HA only, (b) surface with HA/SNP, (c) surface with HA/SNP/HA at 10 nm, (d) surface with HA/SNP/HA at 20 nm thickness, (e) surface with HA/SNP/HA at 30 nm thickness

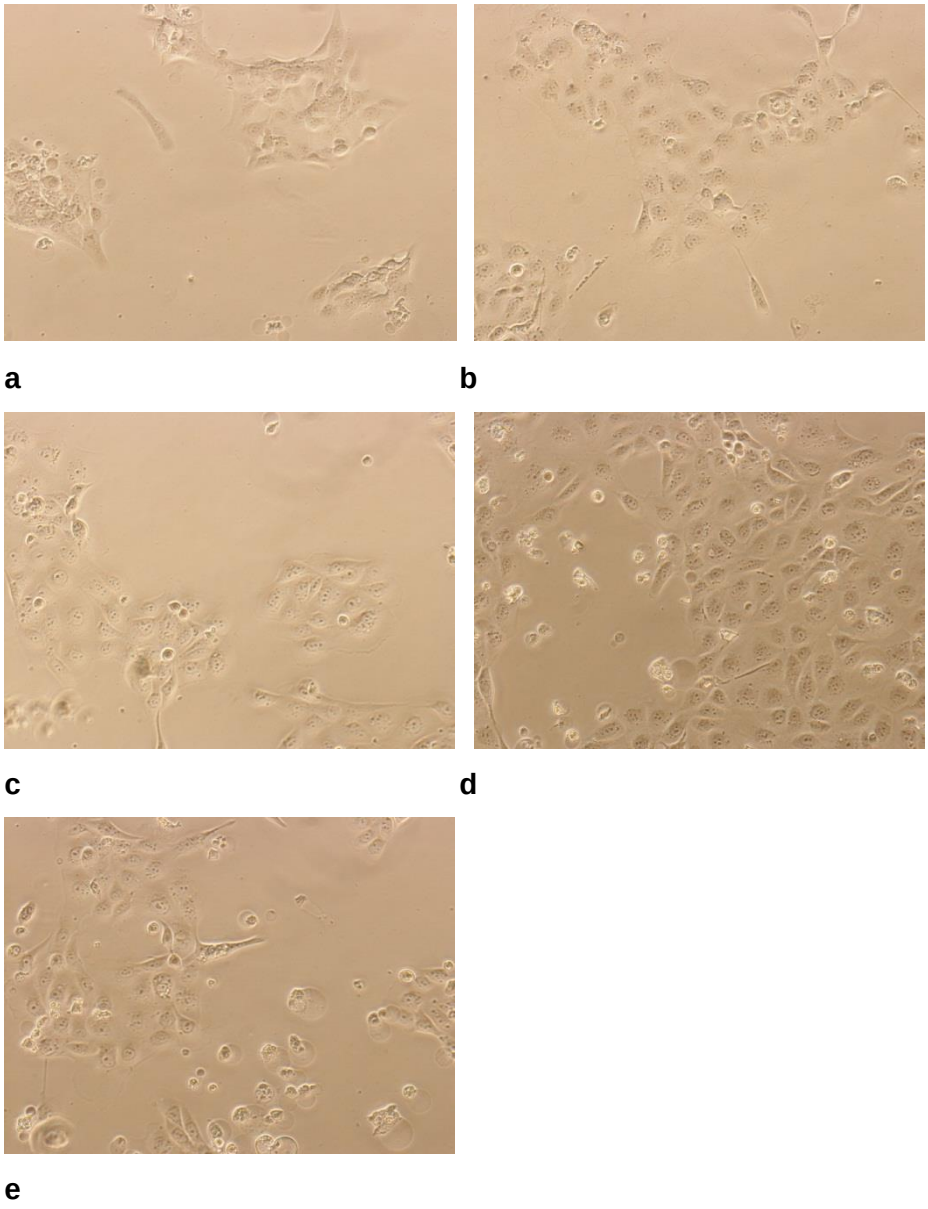


Figure 4.6: Human cornea epithelium (HCE) after 48 hours showing (a) control surface with HA only, (b) surface with HA/SNP, (c) surface with HA/SNP/HA at 10 nm, (d) surface with HA/SNP/HA at 20 nm thickness, (e) surface with HA/SNP/HA at 30 nm thickness

The growth is healthy and forming good confluent cell layers covering 50% of the surface. The SNP does not seem to have affected cell growth after 48 hours culture and growth that was affected after 24 hours has recovered.

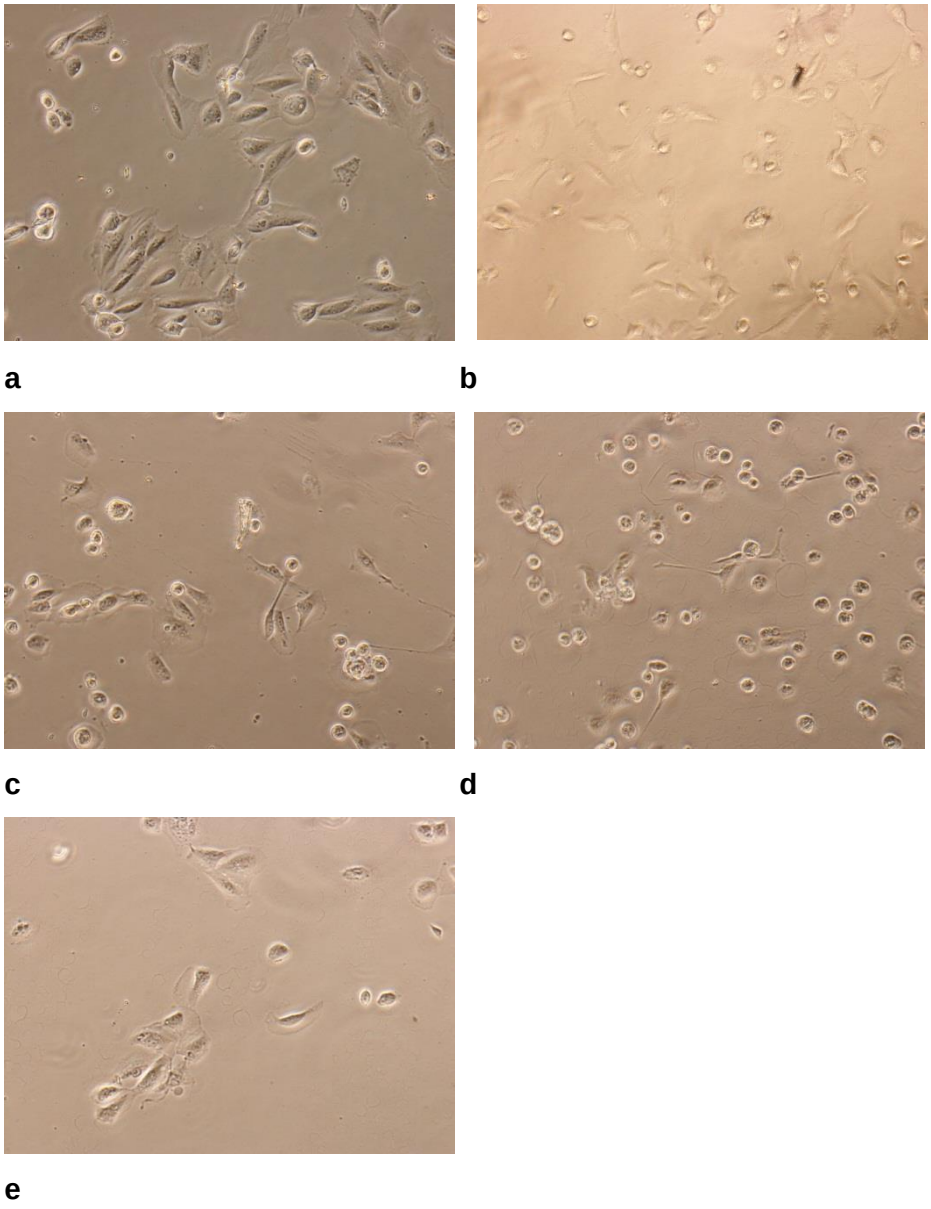


Figure 4.7: Retinal pigmented epithelium (RPE) after 24 hours growth: (a) control surface with HA only, (b) surface with HA/SNP, (c) surface with HA/SNP/HA at 10 nm thickness, (d) surface with HA/SNP/HA at 20 nm thickness, (e) surface with HA/SNP/HA at 30 nm thickness

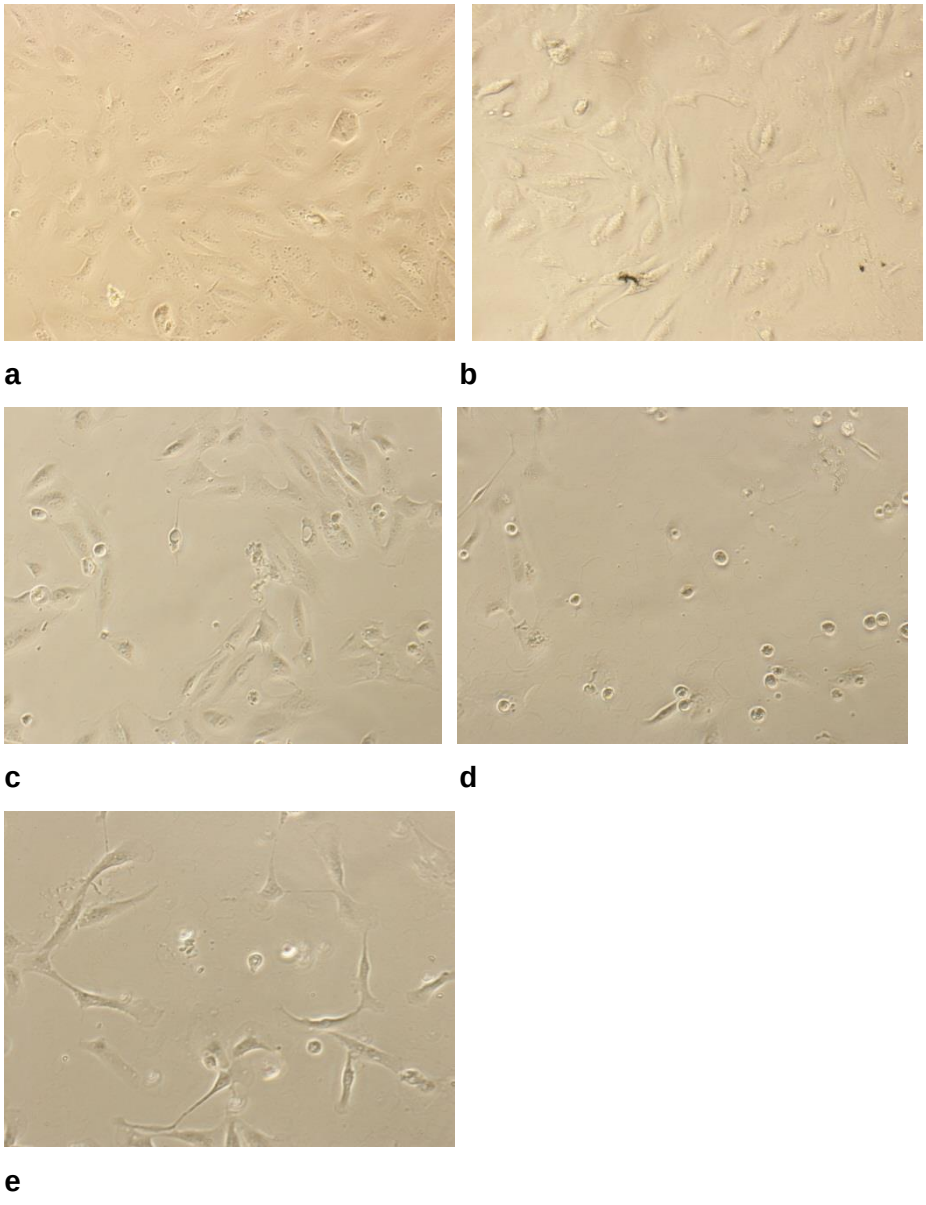


Figure 4.8: Retinal pigmented epithelium (RPE) after 24 hours growth: (a) control surface with HA only, (b) surface with HA/SNP, (c) surface with HA/SNP/HA at 10 nm thickness, (d) surface with HA/SNP/HA at 20 nm thickness, (e) surface with HA/SNP/HA at 30 nm thickness.

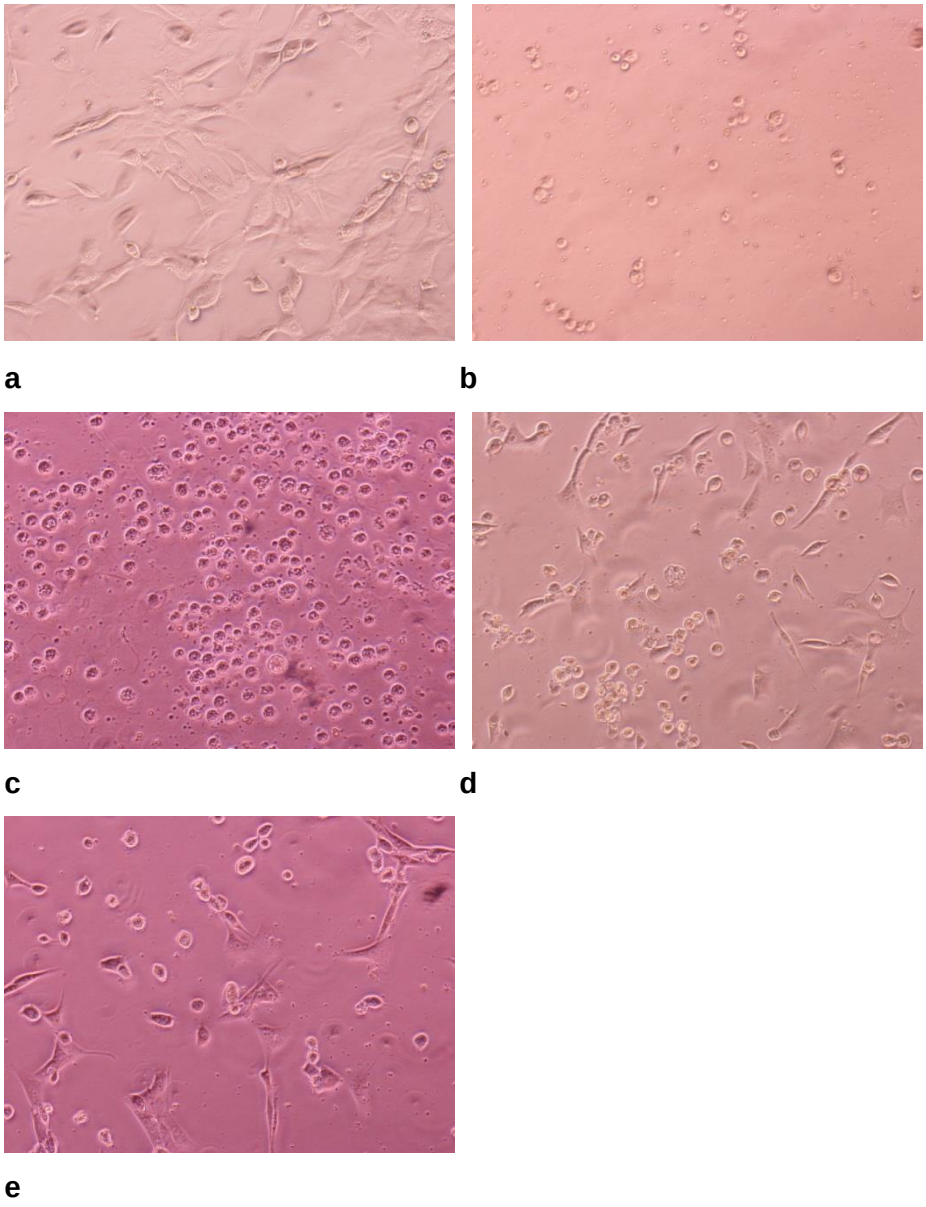
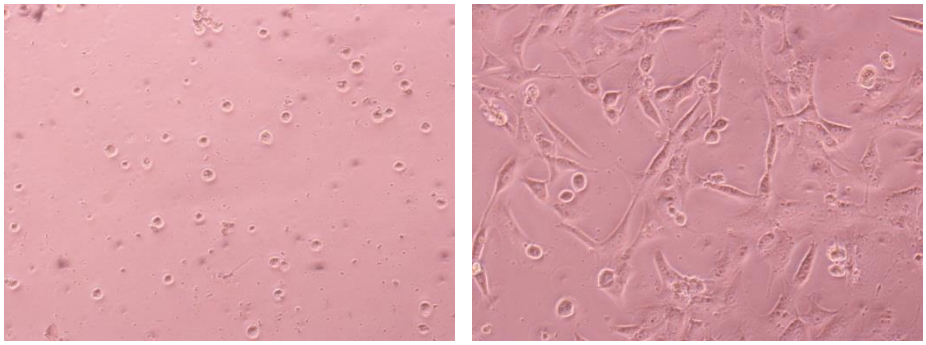


Figure 4.9: NIH/3T3 mouse fibroblast 24 hours after cell seeding: (a) control surface with HA only, (b) surface with HA/SNP, (c) surface with HA/SNP/HA at 10 nm thickness, (d) surface with HA/SNP/HA at 20 nm thickness, (e) surface with HA/SNP.HA at 30 nm thickness

The control surfaces, HA/SNP, and HA/SNP/HA at 10 nm thickness showed the same results at 48 hours as at 24 hours after seeding surfaces.



a b

Figure 4.10: NIH/3T3 mouse fibroblast 24 hours after cell seeding: a) surface with HA/SNP/HA at 20 nm thickness, b) surface with HA/SNP/HA at 30 nm thickness

Figure 4.10 shows the effect of overlayer thickness and hence release rates. With a 20 nm overlayer the cells are highly affected, while with a 30 nm thick overlayer there exists a combination of rounded cells, some apparently dead judged from dark nuclei, and some alive and spreading. It appears that a 30 nm thick overlayer resulted in a release rate that was insufficient for complete cytotoxicity, but some cytotoxicity is still evident.

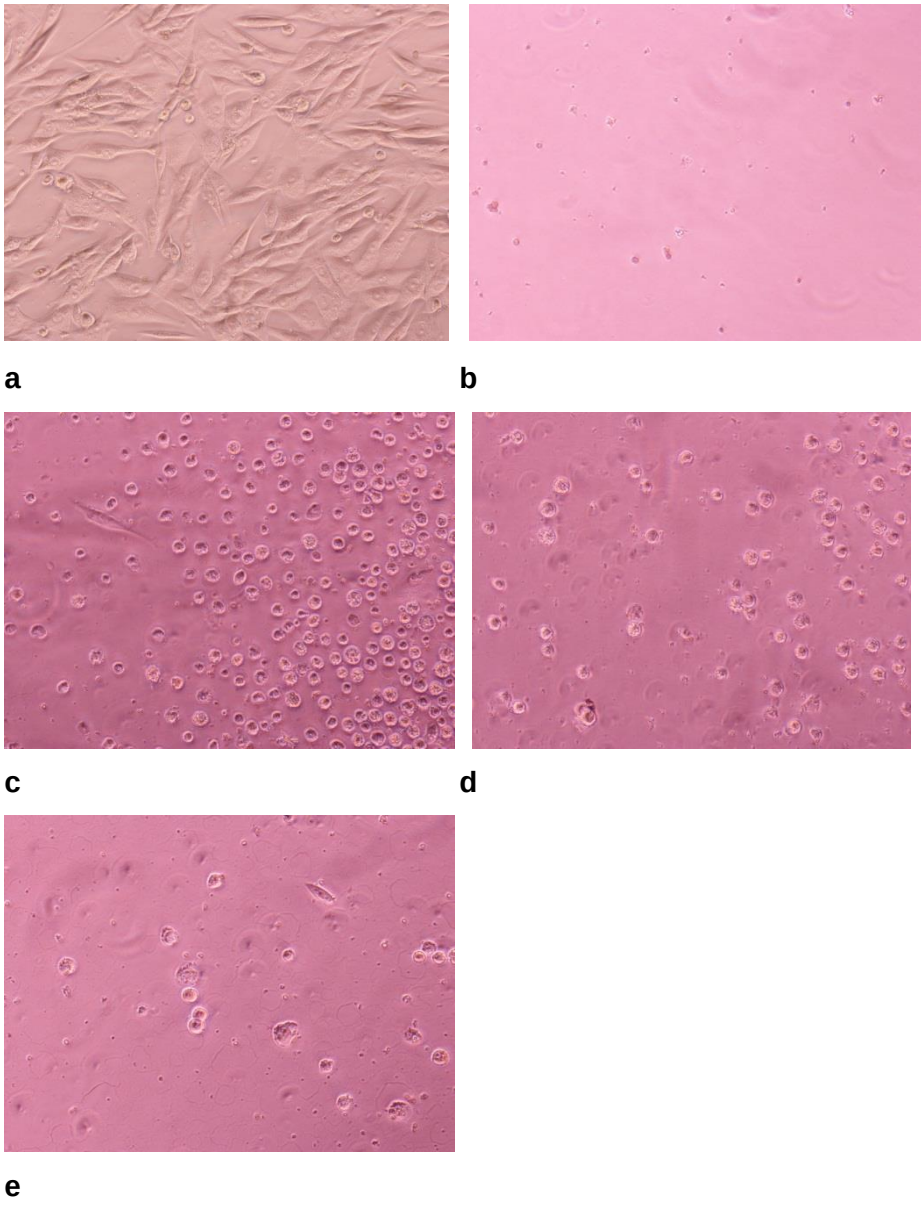


Figure 4.11: MG-63 human osteoblast sarcoma fibroblast: (a) control surface with HA only, (b) surface with HA/SNP, (c) surface with HA/SNP/HA at 10 nm thickness, (d) surface with HA/SNP/HA at 20 nm thickness, (e) surface with HA/SNP/HA at 30 nm thickness

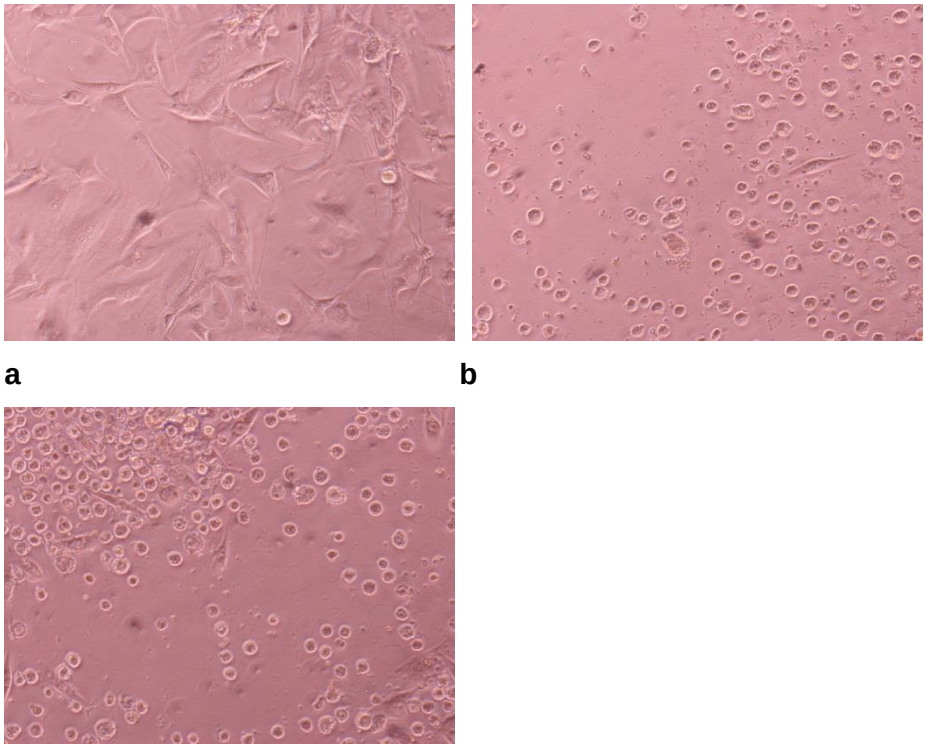


Figure 4.12: MG-63 human osteoblast sarcoma fibroblast after 48 hours of cell growth: (a) control surface with HA only, (b) HA/SNP, (c) and HA/SNP/HA at 10 nm thickness were the same as at 24 hours. Samples with HA/SNP/HA at 20 nm and 30 nm thickness showed all dead cells as in (b) and (c).

4.4 Discussion

This study was undertaken to clarify the variations and differences between results in studies using silver nanoparticles. Two specific issues were identified: the use of different cell lines to give different results, and the bacterial and cell-testing methods. A simple step undertaken by different researchers, namely, rinsing of the samples, gave completely different results. The step of rinsing before adding bacteria or cells is so common that many researchers do not even mention this step or lack of this step in their methods; therefore, it is unclear whether this single step is responsible for the many variations. Most researchers will pre-warm their samples in TSB or media/serum before adding bacteria or cells; this can be considered a rinse and would therefore give different results. Whereas soaking in medium will give better toxicity results, not

rinsing gives excellent killing; however, rinsing the samples, as we have shown in the bacteria work, before adding bacteria greatly compromises the antibacterial integrity. This has been shown in products containing silver; a single wash removes much of the silver, which leads to questions about the amount of silver collecting in the environment (Lorenz et al. 2012).

The application for this particular type of nanoparticle release is in biomaterials, as a wound dressing or with medical devices such as catheters, lines or implantable biomaterials. The standard cell line for biomaterial toxicity testing is the primary fibroblast and the fibroblast cell line because they are easy to grow in cell culture, are dispersed through the body in the connective tissue, and are the least specialised cells in the connective tissue family. They migrate to injured tissue and proliferate, and produce large amounts of collagenous matrix, which helps to isolate and repair the damaged tissue. They are also the most versatile and display a remarkable capacity to differentiate into other members of the family. How they undergo this differentiation is still unclear, yet when injected into animals they can induce formation of cartilage, bone or fibrous matrix depending on the site and circumstances of the area. Osteoblasts are also often used for toxicity testing on biomaterials. Bone is continually remodelled by cells within it, and is in contact with many implanted biomaterials. For wounds, the cell line of choice is an epithelial cell line. These are known to be hardier because of their function as a protective barrier, but are sometimes more difficult to culture.

HCE cells were not affected significantly by HApp-embedded SNPs, growing to a confluent cell layer composed of healthy, normal cells; the thicker HA layer may have even improved cell growth. ARPE-19 cells also grew well and are not noticeably affected by SNPs. They seem to grow less well on the HApp surface than on TCPS. 3T3/NIH cells grow very well on HA but SNPs give rise to cytotoxicity unless covered by at least 20–30 nm of an additional HApp overlayer, which causes much slower release. This does not support long-term growth with survival rate of 3T3s at less than 3 days in most cases. MG-63 cells grow extremely well on HApp surfaces, which seem to be very suitable for this interesting cell line. While MG-63 does not form osteoblasts, it is representative of early undifferentiated osteoblast-like cells. This cell line seems to be particularly sensitive to the SNPs, with no viable cell growth proceeding on any sample containing SNPs.

4.5 Conclusion

This study shows that it is not possible to generalise the cytotoxic response of mammalian cell lines to AgNPs. All cells grew well on HApp samples without AgNPs. Two of the four cell lines tested showed little cytotoxicity arising from the AgNPs, but two other cell lines suffered considerable extents of cytotoxicity. The MG-63 cell line proved particularly sensitive; even when adding a 30 nm thick HApp overlayer to reduce the release rate of silver ions, cells were unable to achieve viable growth on Ag NP-loaded samples. To some extent, it is possible to control the cytotoxic effects of Ag NPs by adjusting the release rate, and still maintain its antibacterial properties. This process is quick and highly reproducible.

Chapter 5: Naturally Occurring Antimicrobial Peptides Immobilised onto Plasma Polymer Surfaces

Abstract

AMPs are found throughout the body and are part of the innate immune system. Their membrane-permeabilising activity makes them excellent candidates for antibacterial surface coatings that could be added to biomaterials. Plasma polymerisation is a technique used to modify surfaces in a number of industries, and in this study, it is used to immobilise three different AMPs to surfaces via covalent interfacial bonds. All three peptides were found to retain activity when covalently bound to surfaces, and two were found to be non-toxic to primary fibroblasts. AMPs can be used to make a suitable antibacterial surface coating for biomaterials.

Although I performed all the coating and bio-testing experiments in the thesis, I did not perform the acquisition of the surface analysis data myself, other than sample loading and data interpretation, because the university's XPS and ToF-SIMS instruments are only accessible to trained, experienced operators. The surface analyses were performed by Marek Jasieniak because of the extensive training required to become proficient in running the XPS and ToF-SIMS instrumentation. Marek also trained me in data interpretation. The extra training and time required to become proficient with surface analysis instrumentation would have substantially reduced the time available for other experimental work.

5.1 Introduction

As discussed in the literature review (Chapter 2), AMPs are an abundant group of molecules that are part of the innate immune system and part of the first line of defence against bacterial invasion for all multicellular organisms (Brown et al. 2011). They are highly diverse and have been isolated from a wide variety of animals, plants, bacteria, fungi and virus (Brogden 2005).

AMPs are unique in that they function as both antimicrobial agents and modulators of the immune system (Barns & Weisshaar 2013). Although they are highly diverse, they have three characteristics that are shared by almost all known AMPs: a small size (10–20 amino acids), a highly cationic character and an amphipathic nature (Costa et al. 2011). Antibacterial peptides are of intense interest because of the extremely concerning increase in bacterial multidrug resistance that is severely compromising our ability to control infection in our world. AMPs offer many significant potential advantages in that they have broad-spectrum activity across a broad range of Gram-positive and Gram-negative bacteria, including drug-resistant strains, and are also active against fungi (Wimley & Hristova 2011). Many AMPs target bacterial membrane function rather than specific protein binding sites (Brogden 2005; Wimley & Hristova 2011). This makes them highly advantageous because they can kill the bacteria in growing and non-growing states and in dormancy and do not induce resistance. Bioavailability of AMPs is reduced; therefore, at present, they cannot be taken orally. However, they are excellent candidates for topical and surface-attached applications.

Because of their bacterial surface–perturbing nature, AMPs make interesting candidates for surface immobilisation. Analogous to silver-releasing coatings, however, it is essential to probe for possible cytotoxic effects.

For this work, three representative AMPs were selected. AMPs are an abundant and diverse group of molecules that are found in many tissues and different cells in a large variety of plant and animal species. In mammals and humans, there are only two distinct groups of AMPs: defensins and cathelicidins. Cathelicidins share a highly conserved N-terminal cathelin domain, flanked by a variable AMP on the C-terminus (Ramanathan et al. 2002). LL-37 (active sequence 134-170) is a well-known antimicrobial protein from hCAP18/LL37; when hCAP-18 is stimulated, it is cleaved extracellularly by proteinase 3 to generate the peptide LL37 (Sorensen et al. 2001). It is referred to as LL37 because it has 37 amino acids starting with two leucines (Ramos et al. 2011). It is a 4,5 kDa, cationic (+6), amphipathic α-helical peptide, with broad-spectrum antimicrobial activity (Durr, Sudheendra & Ramamoorthy 2006). It is an effector of the innate immune system and expressed in leukocytes and epithelial cells, and in neutrophils and keratinocytes of inflamed skin (Ramos et al. 2011).

Magainin 2 (Mg2) is found in amphibians (for example the African clawed frog) and is also a well-known AMP. Both LL37 and magainin 2 are linear cationic alpha-helical peptides and the mechanism of activity is thought to be similar, through transmembrane pore formation.

There is considerable variation in the reports of toxicity of magainin, in that it is generally considered toxic to human cells. This has been found to be related to hydrophobicity; many magainin type peptides have a highly hydrophobic nature. Magainin 2 has a lower hydrophobicity and was found to be non-haemolytic and non-toxic to human cells (Tachi et al. 2002). Magainin 2 was found to produce pores of a similar size to magainin itself; however, they were shorter, quicker to form and more in numbers, which makes up for the lack of depth (Tachi et al. 2002). Although interesting work has been done on developing mimics for magainin 2 peptides (Fox et al. 2012), no detailed work has considered the healing and immune properties of this peptide. It may be that most researchers believe it will lack these properties because it is non-human and the frog immune system is dissimilar; however, the innate immune system in the frog is actually similar and magainin may have healing properties similar to LL-37 (Fites et al. 2013).

Parasin 1 (Pa1), isolated from catfish skin mucosa, is a histone H2A-derived AMP. As an amphipathic α-helical peptide, it has pore-forming ability; the N-terminal binds to the membrane, the α-helical structure inserts either in a barrel-stave or snorkel manner, causing permeabilisation. A single lysine residue near the N-terminal in the random coil region is essential to the mechanism of action, and one possible explanation is that this anchors the peptide into the membrane, causing destabilisation of the membrane and allowing the peptide to become embedded into the bacterial membrane. However, because of its similarity to the histone H2A-derived peptide buforin II, it is also believed to induce intracellular killing by binding to nucleic acids (Koo et al. 2008; Uyterhoeven et al. 2008). Parasin 1 is upregulated via matrix metalloproteinase 2, possibly in response to injury (Cho et al. 2002), which indicates it may have some qualities that enhance wound healing.

The research described in this chapter was motivated by the question of whether AMPs immobilised onto a synthetic surface can be tethered in a way to maintain an active conformation and what the effects are on mammalian cells. The biological tests are accompanied by detailed surface analyses to ensure that we can draw reliable interpretations about observed bio-interfacial interactions.

For these three selected AMPs, key properties and their amino acid sequences are shown in Figures 5.1 to 5.3.

All these AMPs possess amine groups by way of their lysine residues. Thus, they can be immobilised conveniently from aqueous solutions onto surface aldehyde or surface expoxy groups, as discussed in Chapter 3. Their covalent immobilisation onto a propionaldehyde plasma polymer bearing surface aldehyde groups (ALDpp) via reductive amination is shown schematically in Figure 5.4.

LL37 (134-170)

From human cathelicidin antimicrobial protein hCAP18/LL37. Effector of the innate immune system. Expressed in leukocytes and epithelial cells. Toroidal pore (wormhole, disk) model of killing and lysis.

- LL37 Custom peptide C-terminal sequence (134-170)
- Extracellularly released and unregulated in response to inflammation and injury
- M.W. 4493.37

H-Leu-Leu-Gly-Asp-Phe-Phe-Arg-Lys-Ser-Lys-Glu-Lys-Ile-Gly-Lys-Glu-Phe-Lys-Arg-Ile-Val-Gln-Arg-Ile-Lys-Asp-Phe-Leu-Arg-Asn-Leu-Val-Pro-Arg-Thr-Glu-Ser-OH

Figure 5.1: The antimicrobial peptide LL-37

Magainin 2

Cationic, amphiphilic. Toroidal pore (wormhole, disk) model of killing and lysis.

- M.W. 2466.95
- From African clawed frog

H-Gly-Ile-gly-Lys-Phe-Leu-His-Ser-Ala-Lys-Lys-Phe-Gly-Lys-Ala-Phe-Val-Gly-Glu-Ile-Met-Asn-Ser-OH

Figure 5.2: The antimicrobial peptide magainin 2

Parasin 1

From catfish skin mucosa.

- N-terminal essential for membrane binding
- Mode of killing similar as to buforin II and intracellular, binds to nucleic acids. Also thought to kill using barrel-stave model to permeabilise cell membrane.
- M.W. 2000.3

H-Lys-Gly-Arg-Gly-Lys-Gln-Gly-Gly-Lys-Val-Arg-Ala-Lys-Ala-Lys-Thr-Arg-Ser-Ser-OH

Figure 5.3: The antimicrobial peptide parasin 1

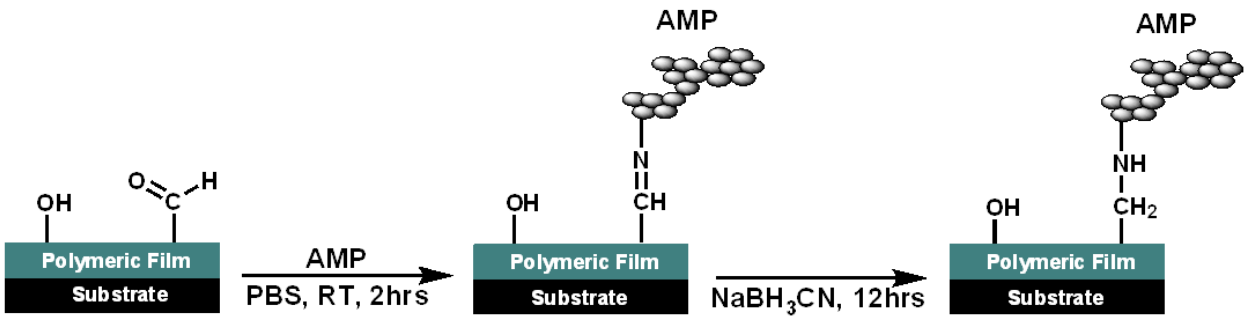


Figure 5.4: Immobilisation of antimicrobial peptides via reductive amination onto ALDpp (the XPS data shows aldehyde and hydroxyl groups on the surface)

5.2 Methods

5.2.1 Samples

LL37(134-170), magainin 2 and parasin 1 (first set from the American Peptide Company, USA, and the second set from GL Biochem, Shanghai, China, >97% purity) were made up into sterile solutions of 0.1 mg/ml in PBS (Sigma, Australia), and were covalently immobilised onto intermediate thin coatings (approximately 21–24 nm thick, as determined by ellipsometry) prepared by the plasma polymerisation (pp) of ALD. The intermediate Schiff base (imine) was stabilised by reductive animation (sodium cyanoborohydride, 1 mg/m; 4 ^{o}C, ~20 hours). Substrates used were silicon wafers (MMRC, Malvern, Australia), Thermanox coverslips (GL083, ProSciTech, Brisbane, Australia), ibidi well plates (81201 and 81821, DKSH, Hallam, Australia), and polystyrene slides (ProSciTech, Brisbane, Australia). FlexiPERM 12 reusable masks (Sarstedt, Mawson Lakes, Australia) were used to define areas for coatings. Peptides were added in a biohazard or clean cupboard at 0.1 mg/ml and left for 2 hours at 18 ^{o}C; then 1 mg/ml sodium cyanoborohydride was added in equal volume, giving 0.05 mg/ml of peptide and 0.5 mg/ml sodium cyanoborohydride solution in total. Samples were left overnight at 18 ^{o}C. Samples were soaked and rinsed six times over 2 hours with sterile PBS (Sigma, Australia). The final rinse after covalent attachment was collected and tested against bacteria to check that no peptide detached into solution and results were indeed from covalently attached peptides only.

5.2.2 Bacteria

Bacteria (*S. epidermidis* ATCC 35984, *S. aureus* MRSA ATCC 43300 and *E. coli* ATCC 35922) was plated from frozen stock and incubated overnight at 37 ^{o}C, two colonies were picked from plates and grown in 10 ml TSB (Oxoid) overnight at 37 ^{o}C, and bacteria were diluted 1/100 and grown to log phase then diluted to 1 x 10^{6} bacteria/ml using predetermined spectroscopy measurements as a guide. (Note that *E. coli* and *S. aureus* are very fast growing and viability plating after seeding of samples show that they can vary greatly in actual amounts.) Depending on the substrate, bacteria solutions were added at 100 ul or 300 ul and grown for 5 and 24 hours at 37 ^{o}C. Surfaces were analysed using LIVE/DEAD *Bac*Light Bacterial Viability assays kits (Invitrogen), viable bacteria count plating, surface stamping onto agar plates, safranin staining of biofilm and spectroscopy readings.

5.2.3 Cell Attachment

Two fibroblast cell lines were used—HFF-1 and 3T3 (HFF-1 human fibroblast, ATCC SCRC-1041 & NIH-3T3 mouse fibroblast, ATCC CRL-1658)—as well as freshly harvested primary fibroblasts from human explant skin, using a reported protocol (MacNeil, Shepherd & Smith 2011). All cell cultures were maintained according to ATCC instructions; primary cells were harvested and maintained according to MacNeil, Shepherd and Smith (2011). Treated Thermanox coverslips were placed in sterile 24-well culture plates (Nunc, Invitrogen) and prewarmed in a cell culture oven. Cells were made up to 50,000 cells per ml in medium/serum and added at 1 ml to each well; primary cells were made up to 10,000 cells per ml. Well plates were placed into a culture oven and left for 48 hours. The coverslips were rinsed to remove non-adherent cells and placed on a glass slide and coverslip for immediate microscopic analysis.

5.2.4 Surface Analysis

Surface analysis was done using XPS and ToF-SIMS, using experimental procedures optimised previously by Marek Jasieniak.

XPS was performed with a Kratos AXIS Ultra DLD spectrometer, using monochromatic AlK_{α} radiation (hv = 1486.7 eV). The system is equipped with a magnetically confined charge compensation system (low-energy electrons are confined and transported to the sample surface by magnetic field). Spectra were recorded using an acceleration voltage of 15 keV at a power of 225 W. Survey spectra were collected with a pass energy of 160 eV and an analysis area of 300 × 700 μm. High-resolution spectra were obtained using a 20 eV pass energy and an analysis area of $\sim$300 × 700 μm. Data analysis was performed with CasaXPS software (Casa Software Ltd). All binding energies were referenced to the low-energy C 1s peak at 285.0 eV. Core level envelopes were curve fitted with the minimum number of mixed Gaussian–Lorentzian component profiles. The Gaussian–Lorentzian mixing ratio (typically 30% Lorentzian and 70% Gaussian functions); the full width at half maximum, and the positions and intensities of peaks were left unconstrained to result in a best fit.

ToF-SIMS measurements were performed with a PHI TRIFT V nanoTOF instrument (PHI Electronics Ltd, USA). A 30 keV, pulsed primary $^{197}Au^{+}$ ion beam was used to sputter and ionise species from each sample surface. PHI's patented dual beam charge neutralisation system using a combination of low-energy argon ions (up to 10 eV) and electrons (up to 25 eV) was employed to provide an excellent charge neutralisation performance. Positive mass axis calibration was done with CH_3^+, $C_2H_5^+$ and $C_3H_7^+$. Spectra were acquired in the bunched mode for 60 seconds from an area of 100 μm x 100 μm. The corresponding total primary ion dose was less than 1 x 10^{12} ions cm^{-2}, and thus met the static SIMS regime (Briggs 1998). A mass resolution m/Δm of >7000 at nominal m/z = 27 amu ($C_2H_3^+$) was typically achieved.

Some samples were characterised by multiple positive ion mass spectra, which were collected from sample areas that did not overlap. All recognisable, clear (i.e. unobscured by overlaps) fragment ions from 2 up to 175 amu range were used in calculations. The peaks were normalised to the total intensity of all selected peaks. Multiple mass spectra were processed with the aid of PCA (Jasieniak et al. 2009). PCA was performed using PLS_Toolbox version 3.0 (Eigenvector Research, Inc, Manson, WA) along with MATLAB software v. 6.5 (MathWorks Inc, Natick, MA, USA).

5.3 Results

5.3.1 Surface Analysis

XPS analysis of samples with surface-attached AMPs showed substantial changes, relative to the substrate and the substrate with an ALDpp coating, in accord with expectations based on an immobilised protein layer (Table 5.1). The data show high surface coverage, particularly for LL37. LL37 has multiple amine groups available for attachment, so would naturally have greater capacity for attachment than those with a smaller number of amine groups. This is not necessarily a problem because these peptides may need conformational flexibility to maintain activity. Angle-dependent XPS showed an increase by ~33% in the N signal when the take-off angle was varied between 0^o and 75^o (relative to the surface normal). This indicates, as expected, that there is minimal in-diffusion of the protein into the aldehyde plasma layer; it appears reasonable to picture them as attached onto the surface of the ALDpp.

Table 5.1: Compositions determined by XPS of plasma polymers (ALDpp) on a Thermanox (Th) substrate, and after grafting with antimicrobial peptides

Sample	Concentration, at%		
	O	N	C
Th-ALDpp	10.6	0	89.4
Th-ALDpp-LL37	12.5	5.5	82.0
Th-ALDpp-Mg2	11.7	3.4	84.9
Th-ALDpp-Pa1	11.3	1.5	87.1

Table 5.2: Component fitting for the XPS C 1s signals recorded with ALDpp and after grafting with antimicrobial peptides

Sample	Fitted omponents in C 1s, [% of total C]				
	C-C/H	C-N	C-O	C=O	N-C=O
Th-ALDpp	87.2	–	8.7	4.08	–
-ALDpp-LL37	67.0	11.9	11.5	–	9.6
-ALDpp-Mg2	76.8	9.5	8.0	–	6.4
-ALDpp-Pa1	81.5	7.8	7.0	–	3.8

Representative spectra are shown in Figure 5.5. The fitted components are in excellent agreement with expectations based on a surface-attached protein layer. In particular the presence of a component assignable to amide C confirms that the elemental changes (Table 5.1) are due to an attached protein layer, as opposed to possible surface contaminants such as adventitious hydrocarbons or fatty acids. The amide C component is often used to quantify protein adsorption, but in this case it was decided not to use a monolayer overlayer calculation approach but simply to conclude that there appears to be quite high coverage by the AMPs. The %N in survey spectra is also often used to quantify amounts of adsorbed proteins; from previous experience in the research group, the amounts recorded her combined with consideration of the relatively small size of these proteins suggest coverage close to monolayer.

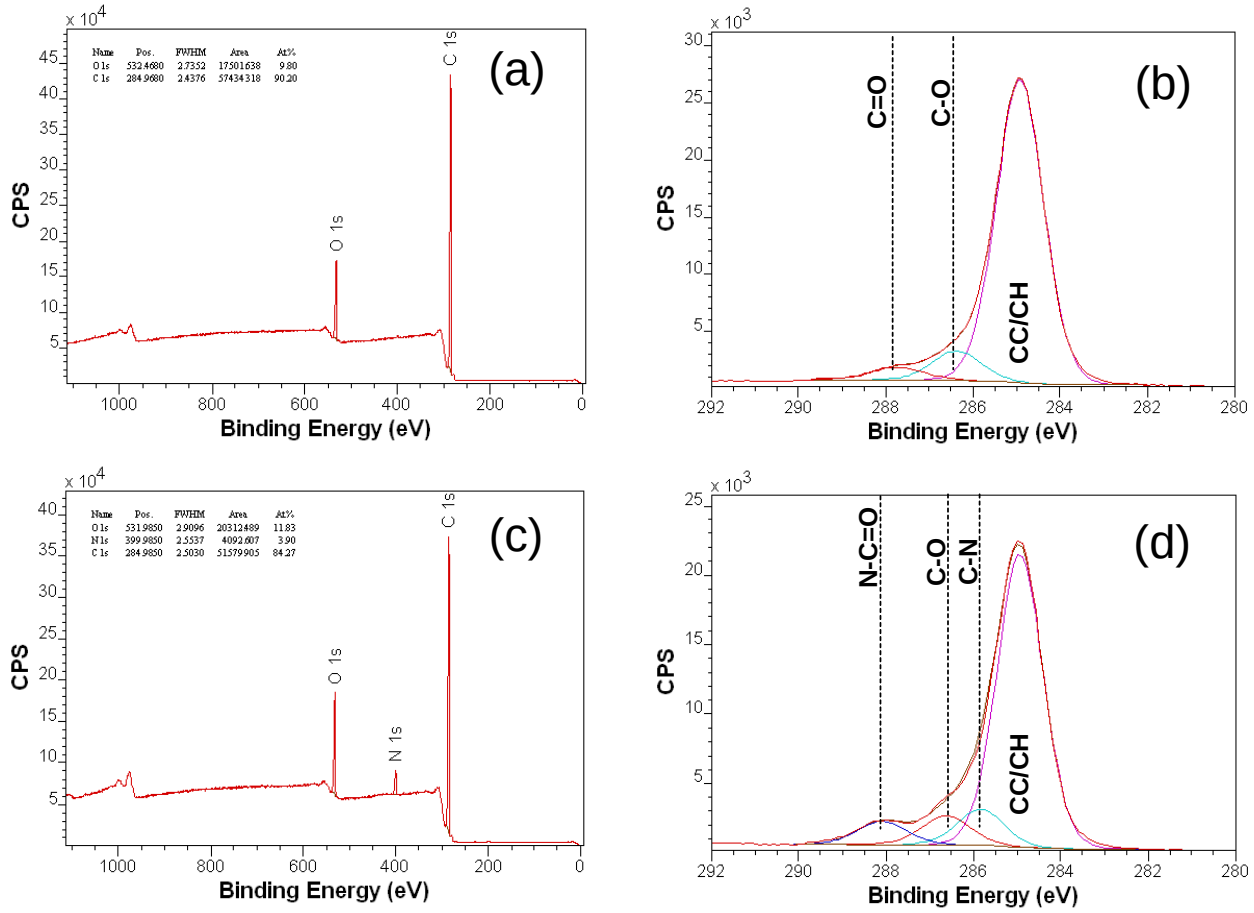


Figure 5.5: XPS spectra of ALDpp and ALDpp-Mg2 surfaces: (a) ALDpp, survey; (b) ALDpp, C 1s; (c) ALDpp-Mg2, survey; (d) ALDpp-Mg2, C 1s

ToF-SIMS spectra (Figures 5.6 and 5.7) also showed the presence of proteins, via characteristic peaks that were in accord with published immonium ion signals. No such signals appeared in spectra recorded with ALDpp samples. No contamination, particularly of silicones, was detected. Recording spectra on duplicate samples and on several separate areas of a sample also showed excellent reproducibility and uniformity of the coatings. The samples were washed and soaked extensively to probe whether the AMPs were indeed covalently attached. Unfortunately, there was no molecular ion detected in these mass spectra that would directly show the interfacial covalent bond via an unambiguous assignment. Nevertheless, considering the high water solubilities of LL-37, Mg2 and Pa1, they should only be present on surfaces after thorough washing if covalently immobilised. This is important because many antimicrobial coatings reported in the literature were not supported with appropriate surface analysis and

washing experiments, raising the question whether they were indeed fully covalently immobilised, or whether dissolving antibiotics might have affected biological testing.

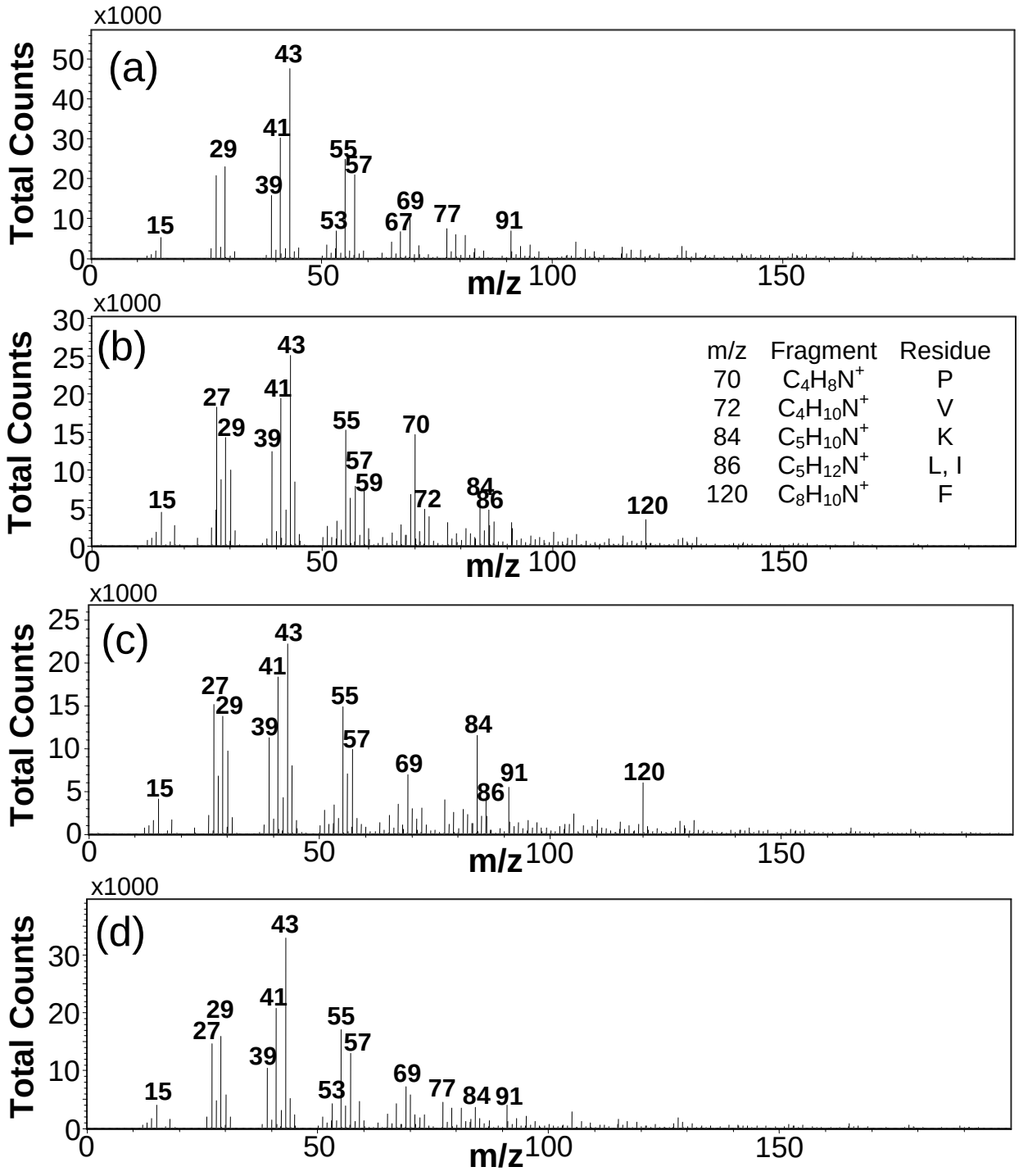


Figure 5.6: Positive mass spectra of ALDpp and its modifications with antimicrobial peptides: (a) th-ALDpp, (b) th-ALDpp-LL37, (c) th-ALDpp-Mg2, (d) th-ALDpp-Pa1

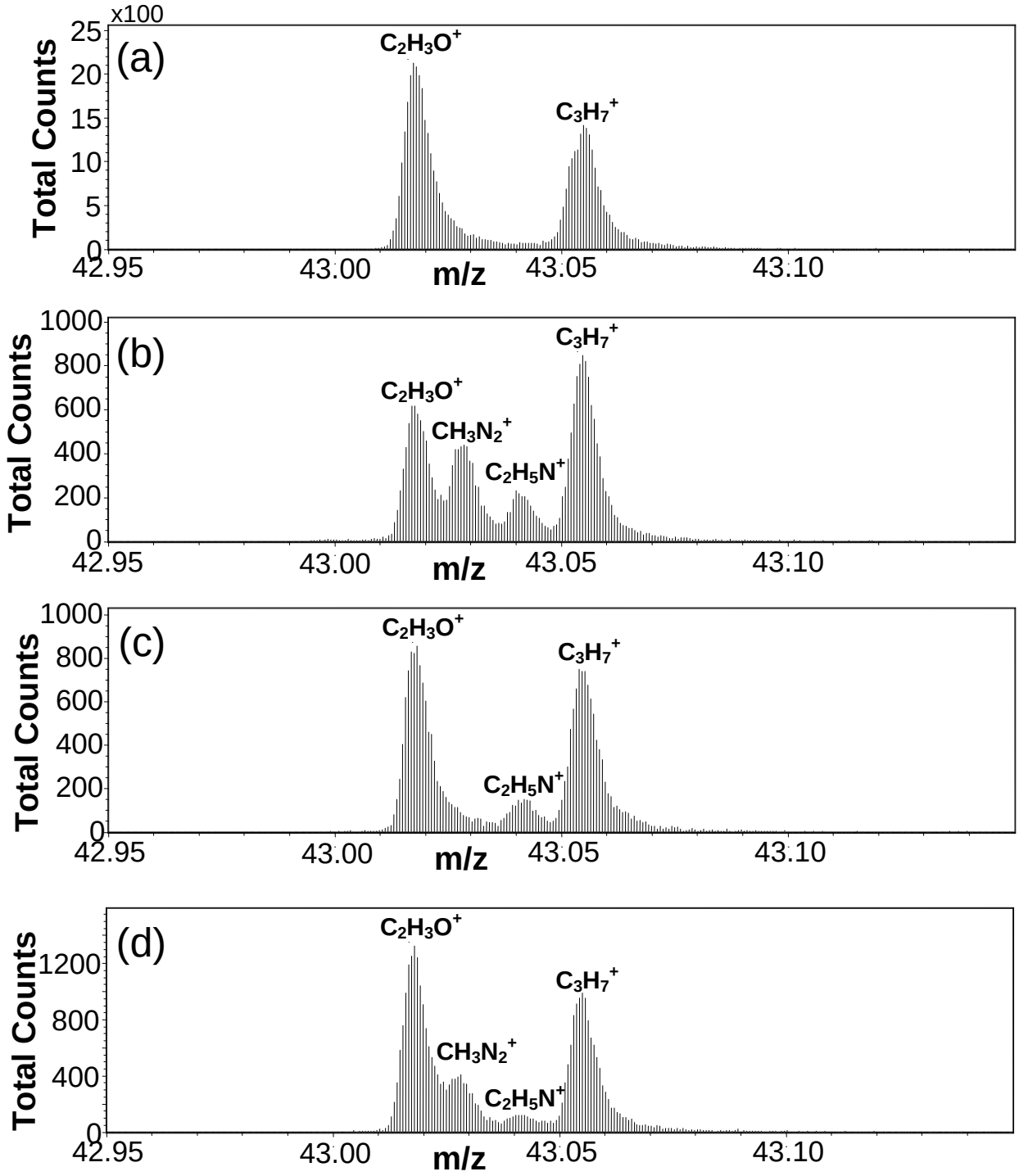


Figure 5.7: Positive mass spectra in range of m/z 42.95–43.15 for ALDpp and its modifications with antimicrobial peptides: (a) th-ALDpp, (b) th-ALDpp-LL37, (c) th-ALDpp-Mg2, (d) th-ALDpp-Pa1 (evidence of arginine residues in LL37 and Pa1 modifications–$CH_3N_2^+$)

The spectra were processed by PCA. The scores plot on the first two principal components, which together contained 97% of the information, is shown in Figure 5.8. The tight clustering of data recorded on separate sample areas again shows high uniformity of the surfaces. In agreement with the XPS data showing the lowest %N for parasin, the PCA analysis shows the parasin coating to be less distant from the ALDpp than the other two AMP graft coatings.

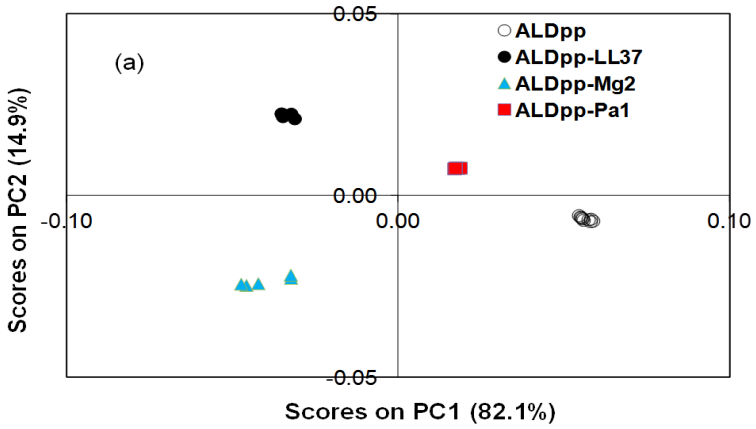


Figure 5.8: Scores plot on PC1 and PC2 for 3 surfaces with covalently immobilised antimicrobial peptides (190 positive fragment ions were used in calculations)

Loadings plots, two examples of which are reproduced in Figure 5.9, reveal the individual peaks that contribute most strongly to the differences in surface composition. Not surprisingly, the peaks that load negatively on PC1 (i.e., increase in relative intensity upon grafting of AMPs onto ALDpp) can be assigned to molecular ions that contain N. The loadings plot on PC1 in Figure 5.9a illustrates that along the PC1 axis the main differences arise in signals assignable to amino acids (loading negatively) and signals assignable to the underlying ALDpp, which load positively and hence are of reduced relative intensity after grafting, as expected. Interestingly, peaks assignable to the amino acid arginine also are of reduced relative intensity. Its guanidine side chain should, based on chemical principles, be highly reactive with aldehyde surface groups, more so than the amino side group of lysine. The data suggest that interfacial immobilisation via reaction between arginines and surface aldehydes is an important aspect in the covalent anchoring of these AMPs.

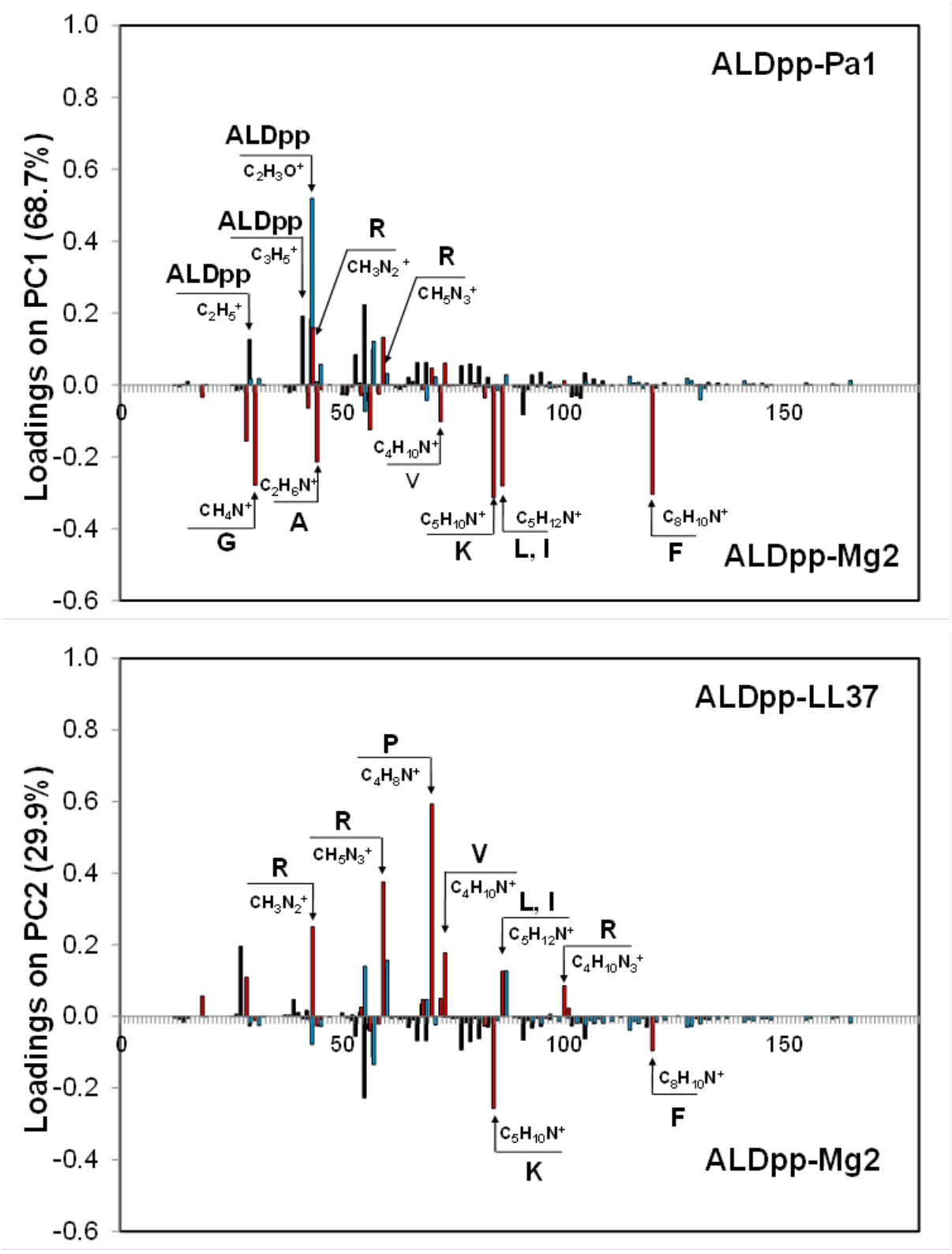


Figure 5.9: Loadings of positive fragments on PC1 and PC2 for 3 surfaces with covalently immobilised antimicrobial peptides

5.3.2 Bacterial Testing

After rinsing, bacteria were visualised using the commercial kit LIVE/DEAD *Bac*Light stain. *Bac*Light contains a pair of nucleic acid stains: a green fluorescent stain, SYTO 9, which is membrane permeable and expected to stain all cells, and a red fluorescent stain, propidium iodide, which is membrane impermeant and should only stain cells that have compromised membranes. In principle, live bacteria are stained green and dead bacteria are stained red. It is important, however, that the *Bac*Light kit be tested in each system before use to ensure accurate scoring of live and dead cells. This was done in our system by growing bacteria on our surfaces with and without plasma treatment and additional peptides; negative controls (dead bacteria) were created by treating bacteria in the wells with Virkon for 30 seconds to 2 minutes. The controls showed good reproducibility. In contrast, biofilm staining by safranin was not reliable because of the combination of dead and live bacteria present.

Polystyrene slides were plasma treated and then a FlexiPERM 12-well removable mask was placed on the slide; AMPs were added to the wells for grafting overnight. After rinsing, bacteria were added for incubation for various periods, followed by rinsing to remove loosely attached bacteria. The wells were treated with the LIVE/DEAD *Bac*Light stain and the mask carefully removed before microscopy examination. Other surfaces were also used, including the ibidi wells and glass slides. Significant differences between coatings on different substrates were found, which were related to the substrate material and batches, and consistent between experimental runs. The plasma lab is a silicone-free lab and none of the surface analyses showed silicone contamination; however, the ibidi based samples could not be tested for possible silicone contamination because of their shape and difficulty in cutting a piece for XPS analysis. It is possible that the ibidi wells and ibidi glass 12-well slides had silicone contamination. This would result in two problems: first, poor adherence of the plasma polymer, and, second, the silicone may affect the bacteria by enhancing growth, because bacteria grow well on silicone. Thus, tests with this convenient substrate were abandoned.

Representative optical microscopy images of bacterial growth on samples are shown in Figures 5.10 to 5.13. On the ALDpp bacteria attached and grew well but not on the AMP surfaces.

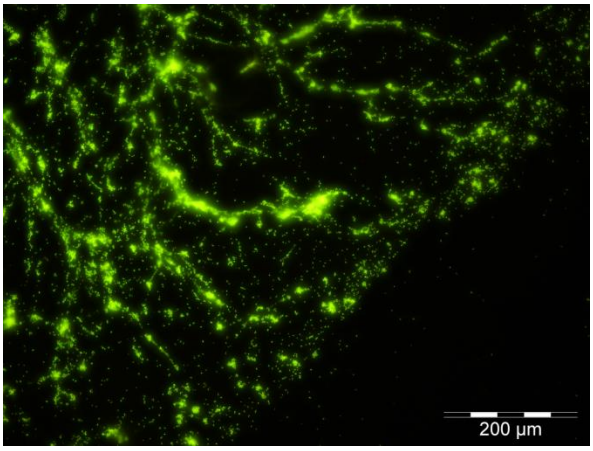


Figure 5.10: *S. epidermidis* on a control aldehyde plasma polymer (ALDpp) after 5 hours incubation.

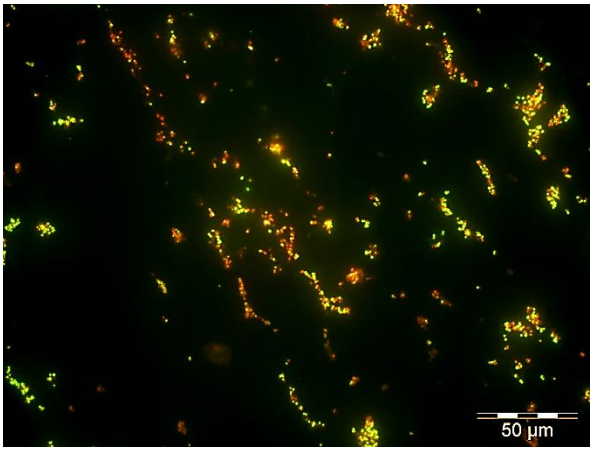


Figure 5.11: LL-37 covalently immobilised onto an ALDpp after 5 hours incubation.

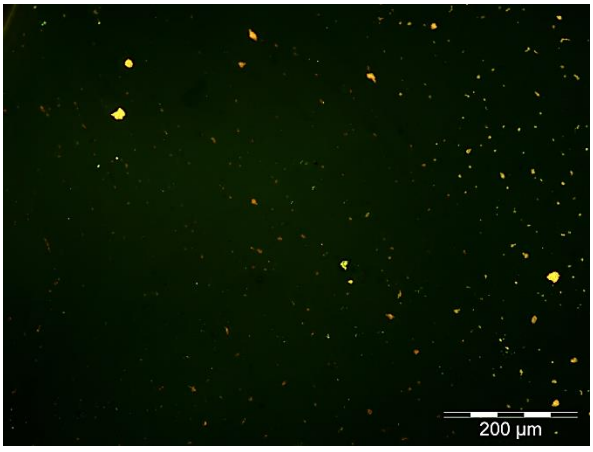


Figure 5.12: Magainin 2 covalently immobilised onto an ALDpp after 5 hours incubation

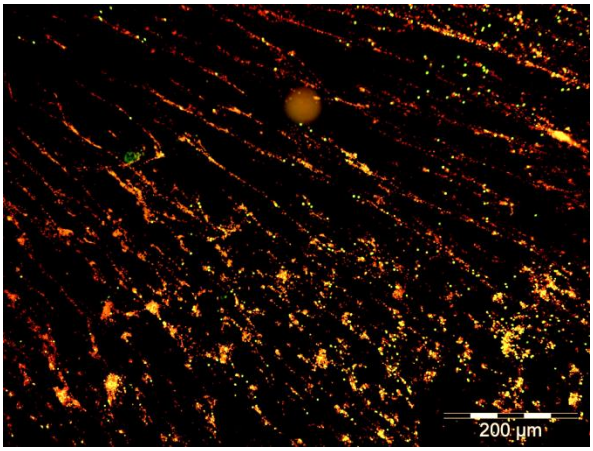


Figure 5.13: Parasin 1 covalently immobilised onto an ALDpp after 6 hours incubation

These images suggest that the grafted magainin 2 coating performs best, in that it shows very few bacteria either dead or alive. On the other two AMP-grafted surfaces there is clear evidence of adhering dead bacteria, as well as a significant number of live bacteria on the LL37 coating. One possible interpretation is that on the magainin coating, surface-contacting bacteria are killed rapidly, before they can establish binding to the surface, whereas on the other two surfaces bacteria manage to attach with sufficient strength before they are killed and thus their dead bodies then do not detach.

Next, bacterial attachment and growth was studied over longer time frames; images are shown in Figures 5.14 to 5.16. Although the AMPs were all quite good at showing antibacterial activity in the first 6–8 hours, increasing numbers of bacteria managed to attach and stay alive, until eventually they were completely overburdened. Once sufficient numbers of bacteria managed to survive, the surface was quickly overgrown with biofilm. This is perhaps not surprising given the continuing onslaught by increasing numbers of bacteria (multiplying in solution). It seems quite possible that the bacterial load after ~ 8 hours significantly exceeds the bacterial load that would apply in a clinical situation. There is, however, no standard specifying what numbers of bacteria should be used for testing surface coatings and how long a surface coating should resist biofilm formation.

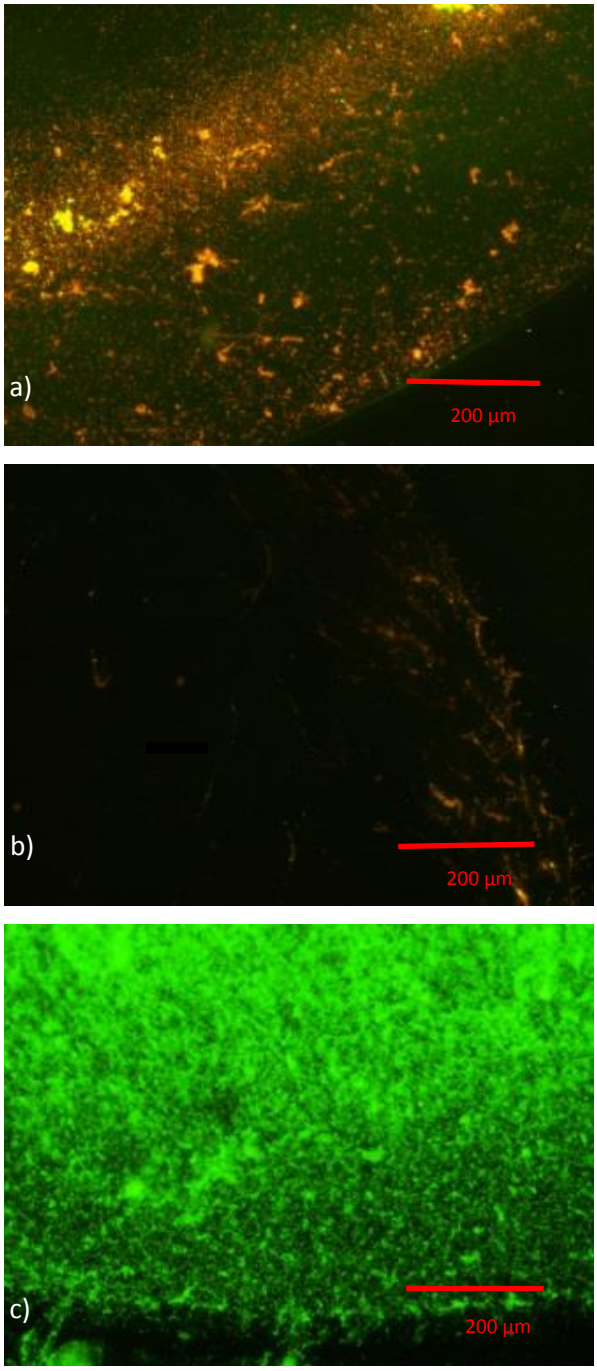


Figure 5.14: LL37 with 1x10^7 CFU *S. epidermidis*: (a) after 4 hours incubation, (b) after 6 hours incubation, (c) after 20 hours incubation

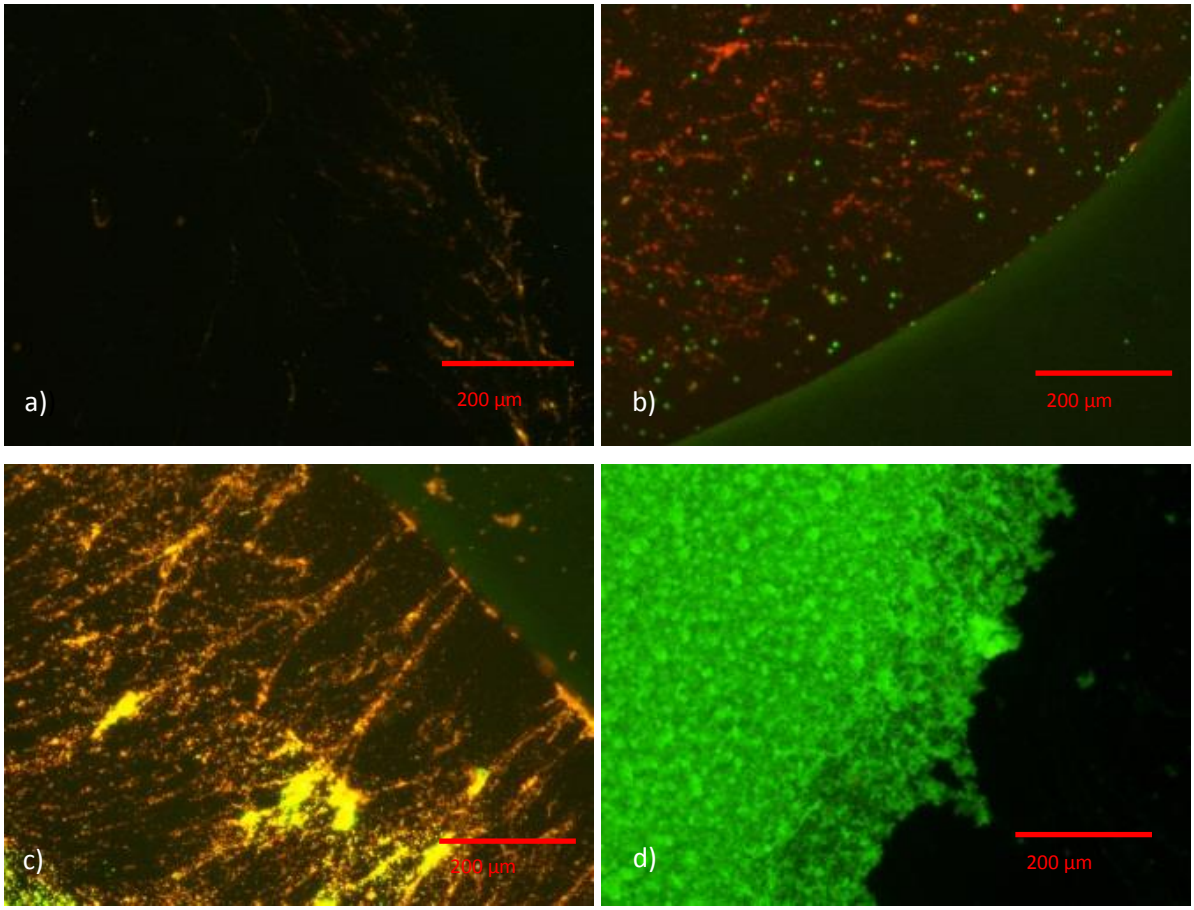


Figure 5.15: Magainin 2 with 1x10^7 cfu *S. epidermidis*: (a) after 4 hours incubation, (b) after 6 hours incubation, (c) 20 hours incubation, (d) control plasma polymer surface.

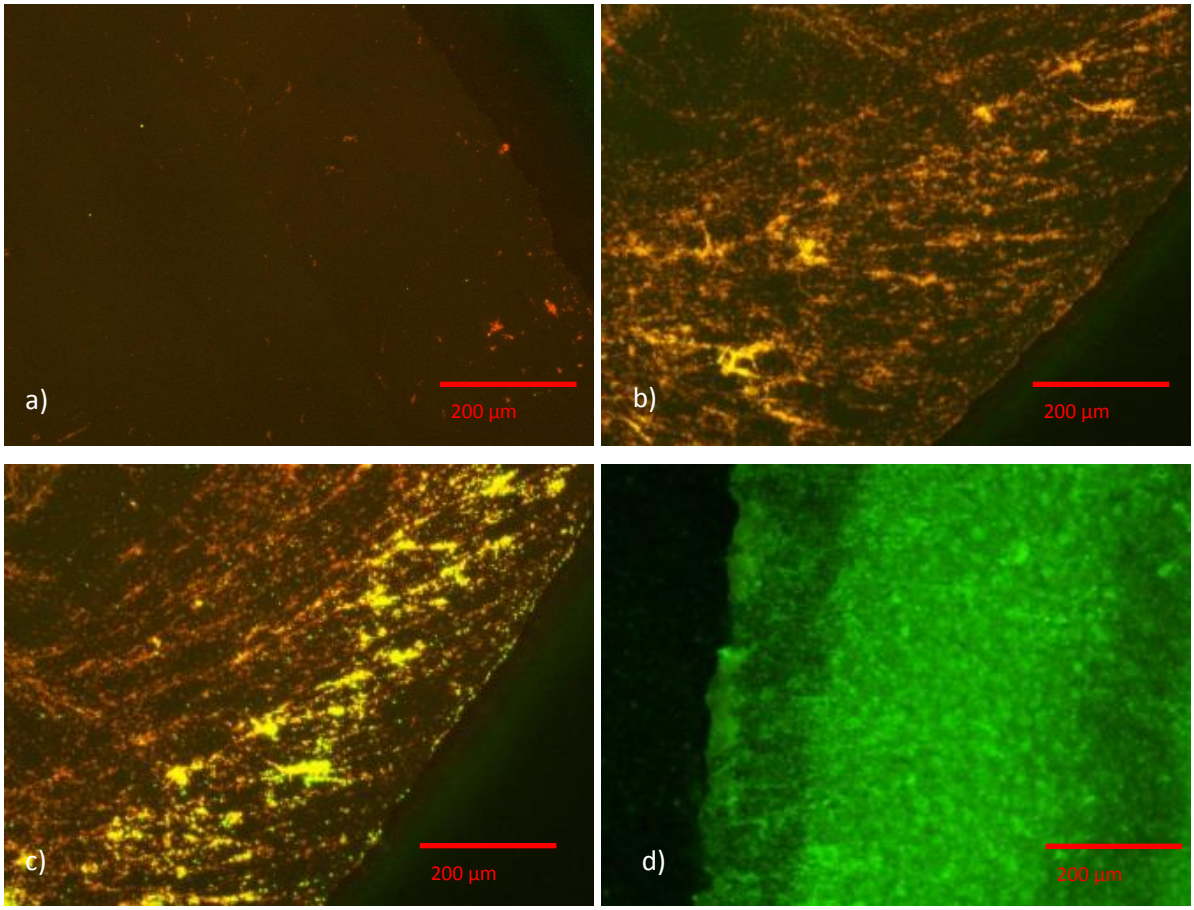


Figure 5.16: Parasin 1 with 1 x 10^7 cfu *S. epidermidis*: (a) after 4 hours incubation, (b) after 6 hours incubation, (c) after 20 hours incubation, (d) control.

Why do the AMP coatings become overgrown eventually? Many publications mention proteolytic degradation of AMPs (Costa et al. 2011; Mowery et al. 2007), but while this may apply to a wound environment for example, it is not clear that proteolytic enzymes are at work in the test system used. A more likely explanation seems to be that dead bacteria eventually cover the grafted AMP layer and bacteria attaching on top of this layer of bacteria are not exposed to the action of surface-immobilised AMPs (as a corollary, good long-term results might be caused by antibiotics diffusing off the surface and it may well be that some reported studies on surface-immobilised antibiotics achieved promising results because of unrecognised diffusion; testing thus should be done until overgrowth is well under way). The images in Figures 5.11 and 5.16 show how live bacteria are growing on top of dead bacteria. Thus, while particularly the magainin 2 grafted coating looks promising, longer-term performance evaluation would require a different testing method or, preferably, an in vivo model.

These coatings were also tested in the presence of serum to determine whether serum proteins might affect or block the antibacterial activity, for example by adsorbing in a layer thick enough to "bury" the AMPs underneath them. For all coatings, however, the activity was not affected within the first 5 hours; after 6 hours, there were indications again that the surfaces were increasingly becoming colonised. It is difficult to separate any effect due to proteins from the increasing colonisation that also occurs in the absence of proteins, as shown above. All that can be concluded is that serum proteins do not immediately block the activity of the grafted AMPs and thus the coatings would be suitable for blood-contacting applications.

Samples were also soaked for 12 days and tested for activity. No reduction of activity was found and results were similar to those above.

Removal of the bacteria and serial dilutions and plating were also done with AMP-grafted samples.

Plate counts of AMPs

LL-37 approximately 150 colonies

Mg 2 approximately 70 colonies

Pa 1 approximately 300 colonies

Control >3,000

The control showed too many colonies to count and was estimated at more than 3,000. The reduction was significant with the AMPs; however, the lack of sustained activity over time is an issue.

5.3.3 Cell Studies

Many studies have claimed that AMPs can be cytotoxic. With AMPs such as melittin, which is isolated from bee venom, it is an obvious concern. Studies with magainin and parasin have found them to be cytotoxic (Jang et al. 2012; Nascimento et al. 2012; Tachi et al. 2002; Vila-Farres et al. 2012). Magainin 2 was developed to limit the toxicity relative to its parent

compound (Tachi et al. 2002). It is often debated whether toxicity would still be relevant when peptides are covalently tethered, because most toxicity issues are manifested in renal and hepatic sites through the processes of breaking down the compounds and excreting the products. However, these AMPs all show surface-permeabilising activity against mammalian cells and it is therefore essential to study whether this would still be the case when the AMPs are tethered.

Cell attachment and growth was assessed on AMP-grafted surfaces and on two control surfaces (TCPS and ALDpp), using primary human fibroblasts and the fibroblast cell line. Figure 5.17 shows data collected with primary human fibroblasts; with the fibroblast cell line the data were closely analogous and are not shown. The ALDpp surface gave results identical within experimental uncertainty to the attachment and growth observed on the standard tissue culture surface TCPS. After grafting the three AMPs onto the ALDpp layer, there was no difference in cell attachment and growth for LL37 and magainin 2, whereas for parasin 1 there were fewer cells on the surface and they showed some morphological abnormalities. However, these tests were done with a parasin 1 sample that was of only 76% purity and it was impossible to decide what the cause of the toxicity might be. Subsequent tests using a parasin 1 sample of 98.2% purity (grafted again on ALDpp) showed little to no toxicity and the cells were perhaps somewhat smaller, yet almost as numerous as on the ALDpp control and the other AMP-grafted samples. Accordingly, the AMP-grafted coatings look promising in that there appears to be no substantial cytotoxicity, though with parasin 1 there should be further work before moving to an animal model.

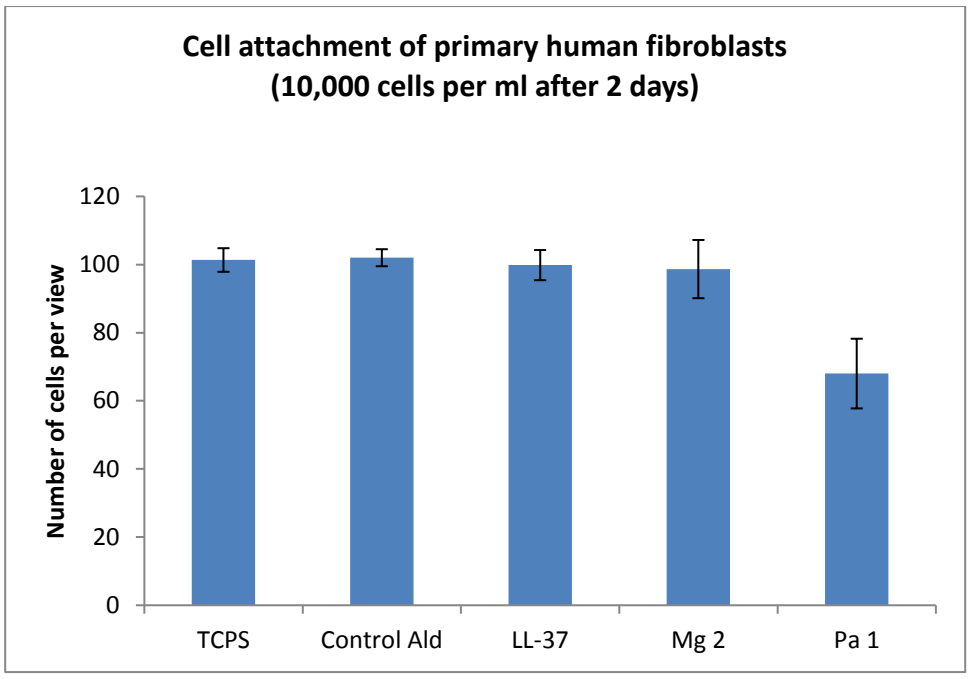


Figure 5.17: Growth of primary human fibroblasts on control samples and on AMP-grafted surfaces, counted per view at 10x magnification.

5.4 Discussion and Conclusion

LL37 and magainin 2 retained good antimicrobial activity when covalently attached onto ALDpp interlayers and showed no cytotoxicity, whereas parasin 1 is less well suited for an implant coating because of its lesser activity over time and some apparent cytotoxicity (though the latter may relate to sample purity). Clear results were obtained with S. epidermidis, whereas bacterial testing with *S. aureus* and *E. coli* was more difficult because the bacteria are far less inclined to colonise surfaces, the result being very little colonisation of the coated surfaces over the first 5 to 6 hours (data not shown). After 24 hours, however, colonisation was evident on all samples, as for *S. epidermidis*. There was a noticeable improvement when the samples were exposed to lower amounts of bacteria; it seemed to give the surfaces time to deter the bacteria because there was far less colonisation after 6 hours, which lasted up to 10 hours. This resulted in fewer dead bacteria to colonise, which possibly enhanced antibacterial effects.

One key observation is that, after some time, the coatings become overwhelmed and bacteria form live biofilm-anchored colonies on top of dead bacteria. Because bacteria continue to

multiply in the broth solution above the sample, it is not surprising that, after a period, the surface becomes covered by dead bacteria. This leads to the question of what is a typical bacterial load in a real-life implant situation, and can cell/tissue attachment take place within the time that the coating remains effective against bacterial biofilm formation (Gristina et al, 1989)? What do we really want: a deterrent or a treatment solution? And what would the immunological implications be for dead bacteria on an implanted surface with strong bacterial killing?

Chapter 6: Nylon-3 Antimicrobial Peptide Mimics Attached to Surfaces via Plasma Polymerisation

Abstract

In addition to naturally occurring antimicrobial compunds, synthetic derivatives or analogues could also offer promise for the design and development of antibacterial coatings. AMPs have been used in a number of trials; however, their stability and possible removal by naturally occurring enzymes in the body has limited their usefulness in implantable and wound healing devices. Synthetic mimics of AMPs (SMAMPs) have been produced to create polymers that have properties similar to peptides but would resist proteolytic degradation, resolve toxicity issues, and perhaps also increase bactericidal properties. One class of synthetic SMAMPs, Nylon-3 copolymers, developed by the group of Prof. S. Gellman, are the result of years of structure-activity studies undertaken to target the concerns listed above. They show excellent antibiotic properties in solution and no cytotoxicity at bactericidal concentrations. The purpose of the investigations presented in this chapter was to investigate whether nylon-3 copolymers would be functional and remain antibacterial when attached to a biomaterial surface. The copolymers were covalently attached onto a functional plasma polymer interlayer. Surface analysis verified attachment, high surface coverage, and reproducibility. Testing with bacteria showed full elimination of bacterial attachment on the coated surface, which was maintained also when serum was added, and over time. It was also found that nylon-3 coatings showed no measurable cytotoxicity to primary human fibroblasts. An *in vitro* wound scratch mimic assay was used to explore the ability of fibroblasts to migrate along sample surfaces into a gap (mimicking a wound) when the gap area of the sample was coated with surface-grafted nylon-3 copolymer. The assay showed that bacteria did not colonise the surface in the gap, which allowed fibroblast cells to close the gap, whereas, in control samples, bacteria colonised the gap area quickly, which prevented fibroblasts from closing the gap. Nylon-3 copolymer antimicrobial mimics thus show promise as potent antimicrobial coatings for biomaterial implants.

This chapter is an expanded version of a publication intended for submission to the *Journal of the American Chemical Society*: Stefani S. Griesser, Runhui Liu, Marek Jasieniak, Krasimir Vasilev, Kristyn S. Masters, Samuel H. Gellman, Hans J. Griesser, 'Nylon-3 Antimicrobial Peptide Mimics Attached to Surface via Plasma Polymerisation'.

Although I performed all the other experiments reported in this chapter, as for the previous chapter I did not perform the surface analysis experiments myself, other than sample loading and XPS component fitting. The surface analyses were performed by Marek Jasieniak because of the extensive training required to become proficient in running the XPS and ToF-SIMS instrumentation. Marek also trained and assisted me in interpretation of ToF-SIMS data. I also acknowledge Prof. Gellman for supplying nylon-3 copolymers.

6.1 Introduction

An ageing population along with an increase in antibiotic resistance and the emergence of new pathogens has led to an urgent need for alternative approaches to infection management, particularly for biomedical device–associated infections. Quality of life and maintenance of activity are an important expectation of the patient population; however, biomaterial implant infections remain a serious complication leading to patient morbidity and mortality. Wound and implant infections account for the vast majority of new resistant bacteria in Australia and the US. The Australian Group on Antimicrobial Resistance Community Survey for 2012 reported that the six resistant strains of *S. aureus* that emerged in that year were all found in chronic wounds and one new resistant form was found in an implant infection, along with trends that show antibiotic resistance is increasing significantly (Chua et al. 2011; Coombs et al. 2011; Palavecino 2014). Resistant pathogens remain one of the biggest threats to health care today; new resistant bacteria are easily outpacing the development of new antibiotics (Peleg & Hooper 2010). There is enormous scope to improve biomaterials and wound dressings to address the problems associated with infections arising at their surfaces. For example, coating biomedical devices with a non-toxic, cell-promoting, and infection-and-inflammation-reducing drug could improve integration with the host body and deter the development of bacterial biofilms that could serve as incubators for resistance.

As discussed in the previous chapter, AMPs represent one approach; they are an important part of the innate immune system in humans. Many studies have investigated ways to make use of their antimicrobial activity (Hurdle et al. 2011). Generally used antimicrobial therapies target actively growing pathogens, but antibiotics that compromise the bacterial membrane can kill persister or non-growing bacteria as well. AMPs also have many signalling activities and not only can they reduce infection but they also control inflammation and signal for a healing response (Zaat & Hiemstra 2013). However, natural AMPs have a number of significant issues that hinder their progress into clinically useful drugs. There is lack of consensus on mechanisms of action and on structure–activity relationships (Wimley & Hristova 2011). They are also complex and expensive to produce, they have stability and toxicity issues, and they can lack potency, particularly against Gram-negative organisms (Fox 2013).

Synthetic mimics offer an excellent opportunity to address these shortcomings. An expanding number of research groups are designing and producing synthetic mimics of AMPs, usually via polymer synthetic chemistry approaches rather than biochemistry, due to the well-established, simpler, and less expensive synthetic pathways required. Many research groups are focussed on a single structural class of AMP mimics specifically for exploring function upon structural variations. Several groups have been successful in creating classes of potent AMP mimics (for example, Aoki, Kuroda & Ueda 2012; Porter, Weisblum & Gellman 2002; Som et al. 2008; Thaker et al. 2013). Yet, there is still debate over specific mechanisms of action, with questions often concerning the exact mechanism of membrane disruption or pore formation. It is generally accepted that the amphiphilic nature of AMPs is essential to function and AMP mimics are based on this principle.

Many groups started work on β-peptides to mimic the behaviour of a natural AMP, such as magainin, by reproducing the α-helical structure found naturally. This resulted in a number of interesting peptides; however, they showed limited antibacterial activity (Arvidsson et al. 2001; Hamuro, Schneider & Degrado 1999; Liu & DeGrado 2001; Porter, Weisblum & Gellman 2002). This led to structure-activity studies on synthetic non-peptide polymers, in many groups. For a long time it was considered that a regular amphipathic structure was necessary; for example it was observed that non-amphiphilic scrambled peptides were inactive, suggesting

that a facially amphiphilic helix was necessary for antibacterial activity (Porter, Weisblum & Gellman 2002). However, the Gellman group achieved success with random nylon-3 copolymers (Mowery et al. 2009), which led to the insight that a conformationally irregular structure is also antibacterial if sufficiently flexible, presumably to adapt to the bacterial membrane surface. Other studies found that disrupted amphiphilicity is important; SMAMPs needed imperfect segregation of polar and hydrophobic groups with the hydrophobic region broken up by the presence of at least one polar residue, lysine or arginine (Wimley 2010). However, research concentrating on peptides composed mainly of arginine residues and short tryptophan sequences found them to cause less disruption of the membrane (Nguyen et al. 2010). They still showed high antimicrobial activity and low haemolytic activity; therefore, they must act via another mechanism of killing. Although little detail on the exact structure of these arginine/tryptophan peptides was given, they seem to lack an amphiphilic backbone structure; therefore, it is likely that without the backbone, the membrane-disrupting mechanism is lacking; cell penetration might occur.

Tew et al. concentrated on a new series of aryl-based SMAMPs, incorporating a facially amphiphilic backbone, rigidifying the conformation with hydrogen bonds that improved the antimicrobial activity. Further additions of various pendent aromatic groups gave a range of antimicrobial and haemolytic activities (Thaker et al. 2013). Other variations of aryl-based SMAMPS also showed interesting anti-inflammatory activities (Thaker, Som et al. 2012).

Because of their activity against bacterial membranes, SMAMPs are excellent candidates for surface attachment to produce an effective antibacterial coating for wound care products, implants, biomedical devices, and the many articles used in medicine today. Although many antibacterial surfaces/coatings have been reported, few are in current medical use. The number of types of antibacterial dressings continues to expand, yet there are no biomaterial implants with antibacterial coatings in use. Implant infections continue to have an infection rate of between 3% and 20% (Grainger et al. 2013). They are treated through antibiotics and removal or replacement of the implant. This causes implant infections to be costly and difficult for patients. Because the need for implants continues to rise, a solution to implant infections is highly desirable.

Gellman et al. continued the refinement of SMAMPs over several iterations and produced, among others, nylon-3 type copolymers that proved to be highly effective not only antibacterially but also were supportive of cell growth and antifungal. It was shown that those SMAMPs were antimicrobial in solution while not interfering with mammalian cell growth (Lee et al. 2009). While their use was reported not only in solution but also as surface-anchored cell attachment coatings, interestingly no publication appeared in which antibacterial activity of surface-attached nylon-3 copolymers was reported. When we enquired, we learnt that they had tried this but had found no activity. However, their surface analysis capabilities were limited, and it was thus not clear what the reason was for the negative result. We proposed that it could be worth immobilising these compounds onto hydrophilic plasma polymers and investigating biological activity of copolymers attached onto a plasma polymer interlayer, in the regard to both prevention of bacterial attachment and support of mammalian cell attachment. This led to the collaborative work described in this chapter. Using compounds supplied by Gellman et al, surface tethering was done using well-controlled bioconjugation reactions. After verifying attachment by surface analysis, biological testing was done. The nylon-3 copolymers that were investigated are shown in Figures 6.1, 6.2 and 6.3. Their synthesis has been described by Mowery et al (2009).

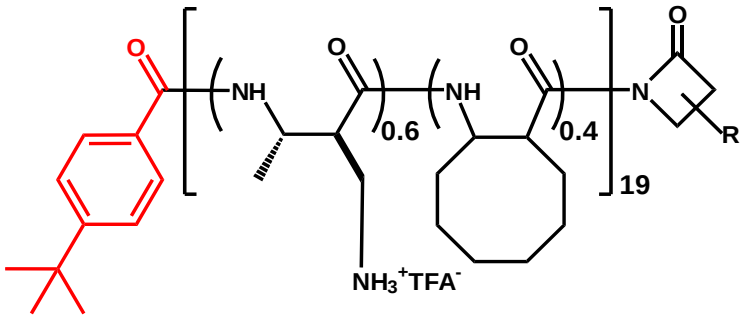


Figure 6.1: Chemical structure of Nylon 3-1. R = methyl.

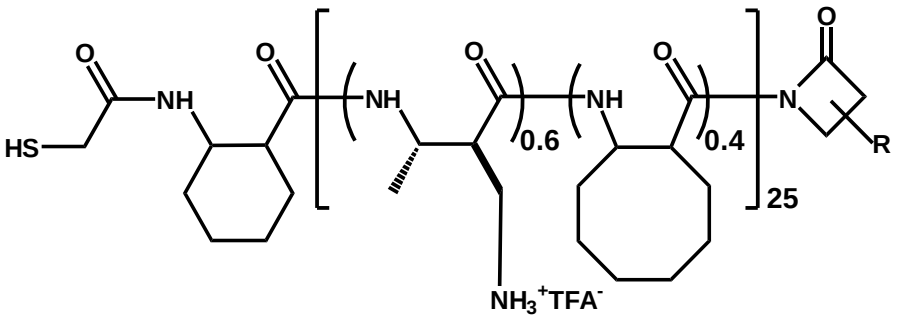


Figure 6.2: Chemical structure of Nylon 3-2.

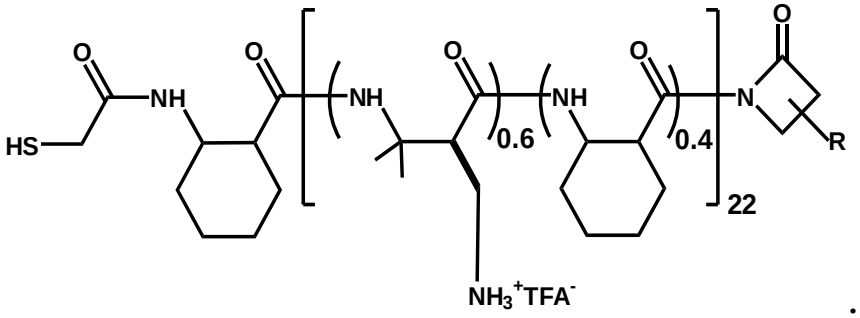


Figure 6.3: Chemical structure of Nylon 3-3.

The MIC values were determined in Gellman's group and given to us as follows:

E. coli 70 μg/ml

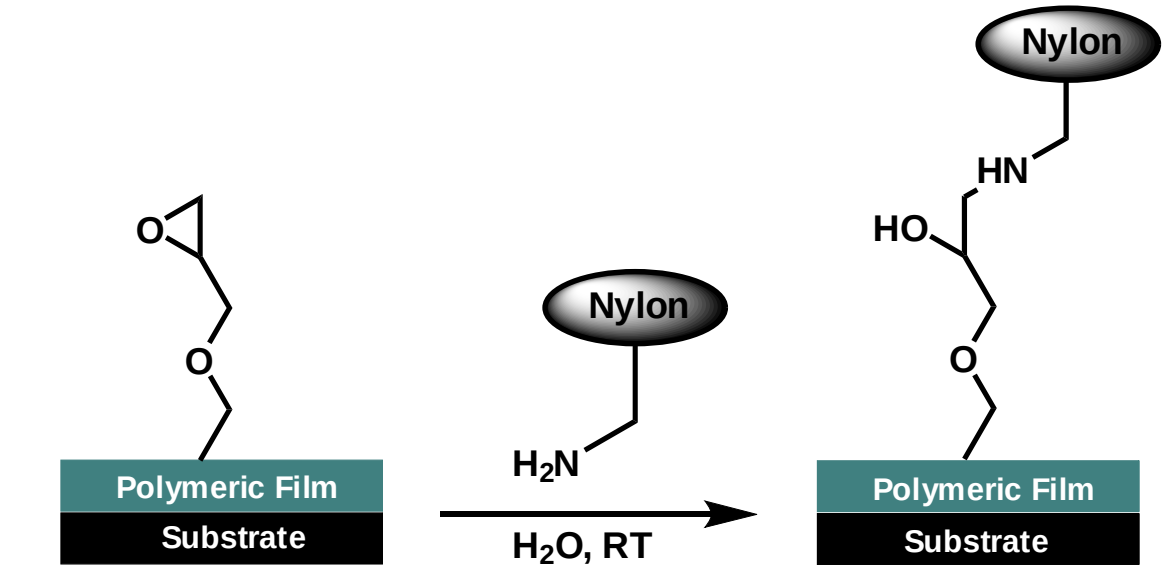
Bacillus subtilis 9 μg/ml

S. aureus 40 μg/ml

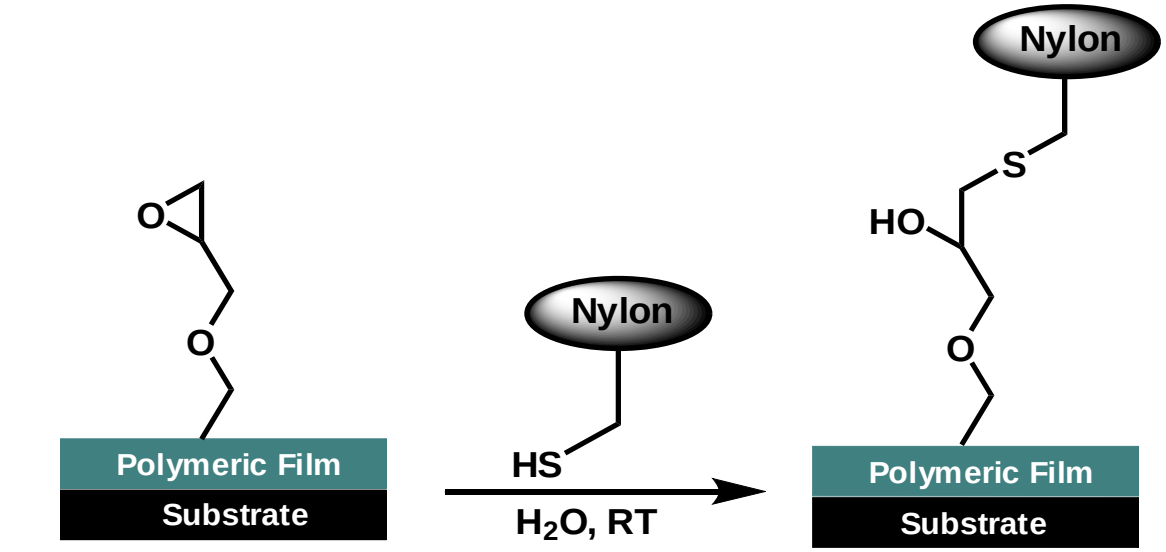
Enterococcus faecium 20 μg/ml.

(Zhang et al. 2011)

These compounds could in principle be immobilised onto ALDpp interlayers in the same way as for the AMPs in the previous chapter, but for this work a plasma polymer with surface epoxide groups (AGEpp) was selected, because this immobilisation scheme does not require a reducing agent and also allows reaction with thiol groups. A suitable plasma polymer with reactive epoxide surface groups was developed earlier in our group (Thierry et al 2008); it is deposited from the "monomer" vapour allyl glycidyl ether (AGE). Nylon 3-1 was expected immobilise covalently "side-on" via its multiple amine groups, while Nylon 3-2 and Nylon 3-3 could also attach "end-on" via their terminal sulfide groups (Figure 6.4).



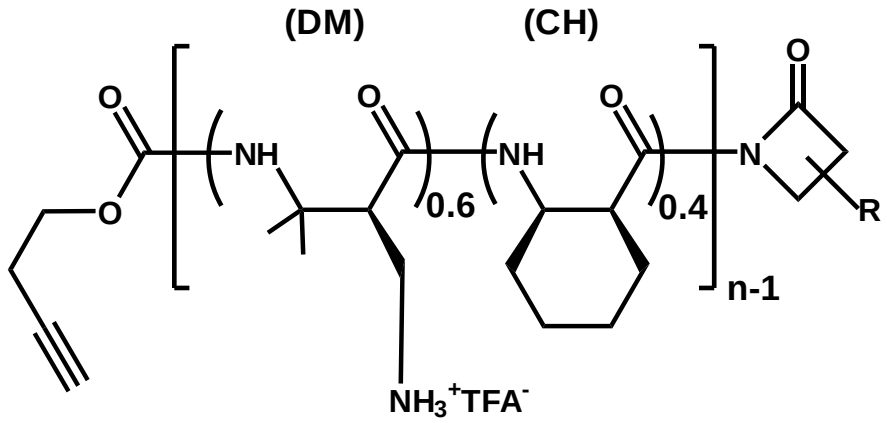
a



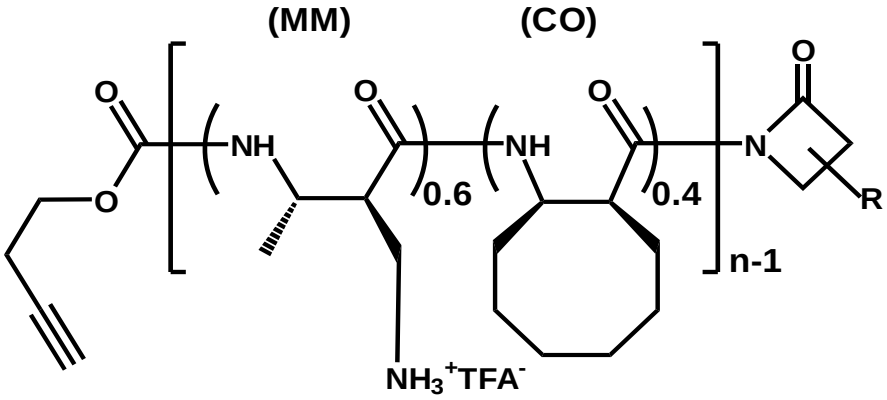
b

Figure 6.4: Illustration of intended immobilisation routes of Nylons onto epoxide-functionalised surface via (a) backbone-pendent amines and (b) terminal thiol

Two additional Nylon copolymers were received later; they bear terminal alkyne groups (Figure 6.5), which enables their surface immobilisation via interfacial "click" chemistry (Figure 6.6).



a Lrh3125



b Lrh3127

Figure 6.5: Chemical structures of Nylon 3125 (top) and Nylon 3127 (bottom); n = 30 (Runhui Liu, University of Wisconsin, USA)

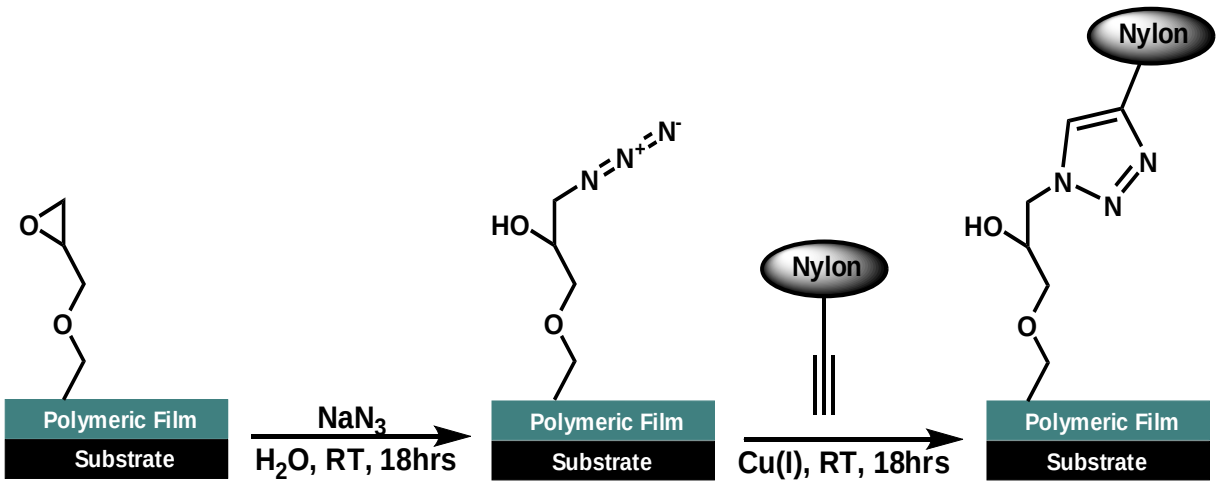


Figure 6.6: Schematic illustration of the covalent immobilisation of alkyne-terminated Nylon-3 copolymers onto AGE plasma polymer via click chemistry

Coatings were tested against bacteria and with primary fibroblast cells. The biological tests were accompanied by detailed surface analyses to ensure that we could draw reliable interpretations about observed bio-interfacial interactions.

6.2 Methods

6.2.1 Samples

The nylon-3 peptides were covalently immobilised onto intermediate thin coatings, (approximately 20 nm thick as determined by ellipsometry) prepared by the plasma polymerisation of allyl glycidyl ether (AGEpp).

Plasma deposition of AGEpp is a two-step process: using a monomer pressure of 0.2 Torr and a plasma power of 25 W, first a constant wave (CW) plasma is applied for 2 minutes, followed by a pulsed plasma using a duty cycle = 1 ms/20 ms for 1 minute.

In contrast to bio-conjugation via reductive amination, immobilisation onto AGEpp requires no further stabilisation of the covalent interfacial bond (Thierry et al. 2008). As substrates, silicon wafers, Thermanox coverslips, polystyrene slides (ProSciTech) with FlexiPERM removable

12-well masks (Sarstedt), ibidi 1 µ-Slide 18-well uncoated microscopy chambers (no. 81821), and ibidi µ-well 12 chamber masks (no. 81201) were used. Surface characterisation was performed with XPS and ToF-SIMS to verify the intended coatings, and was also used to check that coatings were identical on the different substrates used for different tests.

The Nylon-3 compounds were received in powder form and 1 mg was dissolved in 10 µl of methanol with 990 µl of sterile PBS added to give 1 mg/ml solutions, which were again diluted 1/10, giving 0.1 mg/ml solutions that were stored at –15 ^{o}C. The Nylon-3 peptides were added at 100 µl per sample immediately after AGE plasma deposition and left overnight at 15-18 ^{o}C for attachment. Samples were soaked and rinsed seven to 10 times over 2 hours. The final rinse after covalent attachment was collected and tested against bacteria to prove that no peptide remained in solution and results were indeed from covalently attached peptides only. Note that the µ-well 12-chamber masks have some silicone contamination, which might affect results. Washing thoroughly with acetone, ethanol, MQ and nitrogen drying was done for each sample. This seemed to have removed the silicone, but there is always a risk that some contamination may remain.

Immobilisation of Nylons 3-5 and 3-6 via Click chemistry comprised a two-step process (see Figure 6.6):

a. azidolysis of surface epoxide groups using 2.5 M NaN_3 solution in MQ water. The reaction is carried out at room temperature for 16 hours. Following reaction, samples are washed thoroughly in water (10x) and finally blown dry with nitrogen.
b. ‘click’ attachment using as catalyst copper (I) ions generated in situ by reduction of copper (II) ions with ascorbic acid.

Composition of the activating system by molar ratio was: peptide:ascorbic acid:copper (II) = 1:37.5:22.5 (for ~5 kDa Nylon-3 molecules).

The concentration of peptides—1 mg/ml—then 1 ml of the activating solution contains:
Lrh3125—Mw = 5959 (1.0 mg peptide + 1.2 mg of asc.acid + 1.0 mg of $CuSO_4.5H_2O$)
Lrh3127—Mw = 4655 (1.0 mg peptide + 1.4 mg of asc.acid + 1.2 mg of $CuSO_4.5H_2O$)

The process was carried out for 16 hours followed by thorough washing with MQ water (after 10x wash, it is advisable to leave the samples soaking in water overnight to remove copper ions, which would interfere in bacterial testing) and finally dried in nitrogen.

6.2.2 Surface Analysis

Surface analysis was done using XPS and ToF-SIMS.

XPS was performed with a Kratos AXIS Ultra DLD spectrometer, using monochromatic AlK_α radiation (hv = 1486.7 eV). The system is equipped with a magnetically confined charge compensation system (low-energy electrons are confined and transported to the sample surface by magnetic field). Spectra were recorded using an acceleration voltage of 15 keV at a power of 225 W. Survey spectra were collected with a pass energy of 160 eV and an analysis area of 300 × 700 μm. High-resolution spectra were obtained using a 20 eV pass energy and an analysis area of ~300 × 700 μm. Data analysis was performed with CasaXPS software (Casa Software Ltd). All binding energies were referenced to the low-energy C 1s peak at 285.0 eV. Core level envelopes were curve fitted with the minimum number of mixed Gaussian–Lorentzian component profiles. The Gaussian–Lorentzian mixing ratio (typically 30% Lorentzian and 70% Gaussian functions); the full width at half maximum, and the positions and intensities of peaks were left unconstrained to result in a best fit.

ToF-SIMS measurements were performed with a PHI TRIFT V nanoTOF instrument (PHI Electronics Ltd, USA). A 30 keV, pulsed primary $^{197}Au^+$ ion beam was used to sputter and ionise species from each sample surface. PHI's patented dual beam charge neutralisation system using a combination of low-energy argon ions (up to 10 eV) and electrons (up to 25 eV) was employed to provide an excellent charge neutralisation performance. Positive mass axis calibration was done with CH_3^+, $C_2H_5^+$ and $C_3H_7^+$. Spectra were acquired in the bunched mode for 60 seconds from an area of 100 μm x 100 μm. The corresponding total primary ion dose was less than 1 x 10^{12} ions cm^{-2}, and thus met the static SIMS regime (Briggs 1998). A mass resolution m/Δm of >7000 at nominal m/z = 27 amu ($C_2H_3^+$) was typically achieved.

Some samples were characterised by multiple positive ion mass spectra, which were collected from sample areas that did not overlap. All recognisable, clear (i.e. unobscured by overlaps) fragment ions from 2 up to 175 amu range were used in calculations. The peaks were normalised to the total intensity of all selected peaks. Multiple mass spectra were processed with the aid of PCA (Jasieniak et al. 2009). PCA was performed using PLS_Toolbox version 3.0 (Eigenvector Research, Inc, Manson, WA) along with MATLAB software v. 6.5 (MathWorks Inc, Natick, MA).

6.2.3 Bacteria

Bacteria (*S. epidermidis* ATCC 35984, *S. aureus* MRSA ATCC 43300 and *E. coli* ATCC 35922) were plated from frozen stock and incubated overnight at 37 ^{o}C. One colony was picked from the plate and grown in 10 ml TSB with glucose (Oxoid) overnight at 37 ^{o}C. Bacteria were diluted 1/100 and grown to log phase and then diluted to 1 x 10^6 bacteria/ml using predetermined spectroscopy measurements as a guide. Depending on the sample size, bacteria solutions were added at 100 ul or 300 ul (actual amounts at approximately 1 x 10^5 or 3 x 10^5; note that growth occurs between diluting and adding to samples, and with some bacteria, even 30 minutes can result in a doubling or more of bacteria) and grown for 5 and 24 hours at 37 ^{o}C. As a control, the same amounts were serial diluted and plated on nutrient agar (Oxoid) and counted to ascertain exact bacteria added to surface. Surfaces were analysed using LIVE/DEAD *Bac*Light Bacterial Viability Assay kits (Invitrogen), and viable bacteria count plating.

Polystyrene slides or ibidi µ-Slide wells were coated for bacterial tests. A FlexiPERM 12-well removable mask was placed on the slide and ibidi µ-Slides were used as is; Nylon polymer solution was added to the wells for grafting overnight. After rinsing, bacteria were added for incubation for various periods of time, followed by rinsing twice to remove loosely attached bacteria. The wells were treated with the LIVE/DEAD *Bac*Light stain and the mask carefully removed before microscopy examination. Viability counts were done by scraping and rinsing the wells carefully with 1 ml of TSB. The wells were visually examined to ascertain that all adherent bacteria were harvested. The 1 ml of TSB with bacteria was then serial diluted and

100 ul was plated onto nutrient agar plates. Plates were incubated for 24 hours and colonies were counted.

6.2.4 Cell Attachment

Two fibroblast cell lines were used—HFF-1 (HFF-1 human fibroblast, ATCC SCRC-1041) and 3T3 (NIH-3T3 mouse fibroblast, ATCC CRL-1658)—primary human fibroblasts harvested from fresh skin (MacNeil, Shepherd & Smith 2011). All cell cultures were maintained according to ATCC instructions or published protocols (MacNeil, Shepherd & Smith 2011). Plasma- and peptide-treated Thermanox coverslips were placed in sterile 24-well culture plates (Nunc, Invitrogen) and prewarmed in a cell culture oven. Primary cells were tested using plasma treatment and attachment of polymers in ibidi micro-chamber 12-well glass slides (ibidi 81201, Germany). Cells were made up to 50,000 transformed cells per ml in medium/serum or 5,000 primary cells per ml in medium/serum and added at 1 ml to each well or 100 μl to ibidi wells. Well plates were placed into the culture oven and left for 48 hours. The coverslips were rinsed to remove non-adherent cells and placed on a glass slide and coverslip for immediate microscopic analysis. ibidi wells were stained using DAPI nucleus stain (Invitrogen) and used as per instructions.

6.2.5 Wound Scratch Assay

The wound scratch assay made use of ibidi μ-dish 35 mm, low-culture insert, sterile uncoated culture dishes (model 80201, ibidi, Australia), the bacteria strain as above, *S. epidermidis* ATCC 35984 and freshly cultured human primary fibroblasts as above. Culture dishes with the insert removed were treated with AGEpp, and Nylon-3 polymers were immobilised as above. The masking insert was placed back onto the sample and the dish was prewarmed in a cell culture incubator. Thirty millilitres of primary fibroblast at 5×10^4 was added to the sample surface areas on each side of the insert and growth medium was placed in the dish surrounding the insert. This was placed in the incubator for overnight growth. Fresh medium was supplied the next day and dishes placed in the oven while the bacteria were prepared. The medium/serum was pipetted off and the insert removed. Thirty millilitres of bacterial solution was carefully

pipetted into the gap between the two confluent cell areas. A drop of warm medium/serum was placed to either side covering the cells and around the cells. This setup was placed back in the oven for 6 hours for the bacteria to attempt to settle on the surface area in the gap. Then, further medium/serum was added and the dish was placed back in the incubator for overnight growth.

6.3 Results

6.3.1 Surface Analysis

XPS analysis of samples with attached antimicrobial polymers showed substantial changes in accord with expectations based on an immobilised layer (Table 6.1). The data show highest surface coverage for nylon 3-1. Nylon 3-1 has multiple amine groups available for attachment, so would naturally have greater capacity for attachment than those with only end groups or a smaller number of amine groups. This is not necessarily a problem because these peptides may need conformational flexibility to maintain activity. Angle-dependent XPS showed an increase by ~33% in the N signal when the take-off angle was varied between 0^o and 75^o relative to the surface normal). This indicates, as expected, that there was minimal in-diffusion of the polymers into the AGEpp layer.

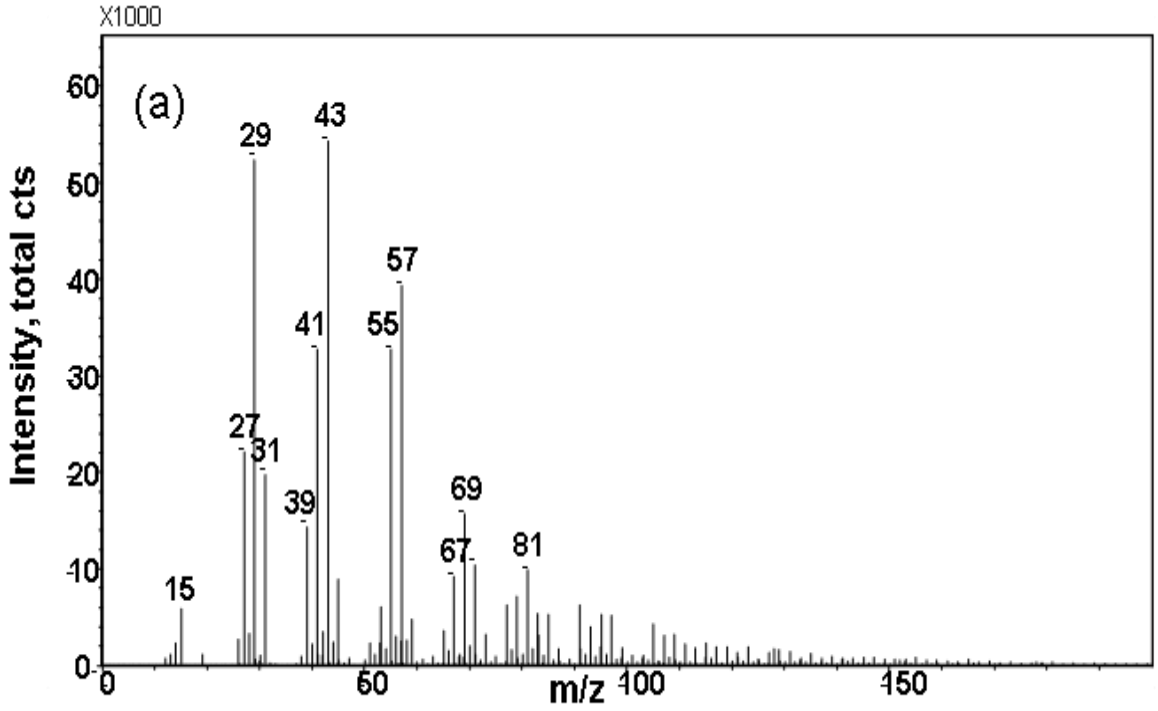
Table 6.1: Compositions determined by XPS of AGE plasma polymer and after grafting of Nylons at 0.1 mg/ml, on a Thermanox (Th) substrate

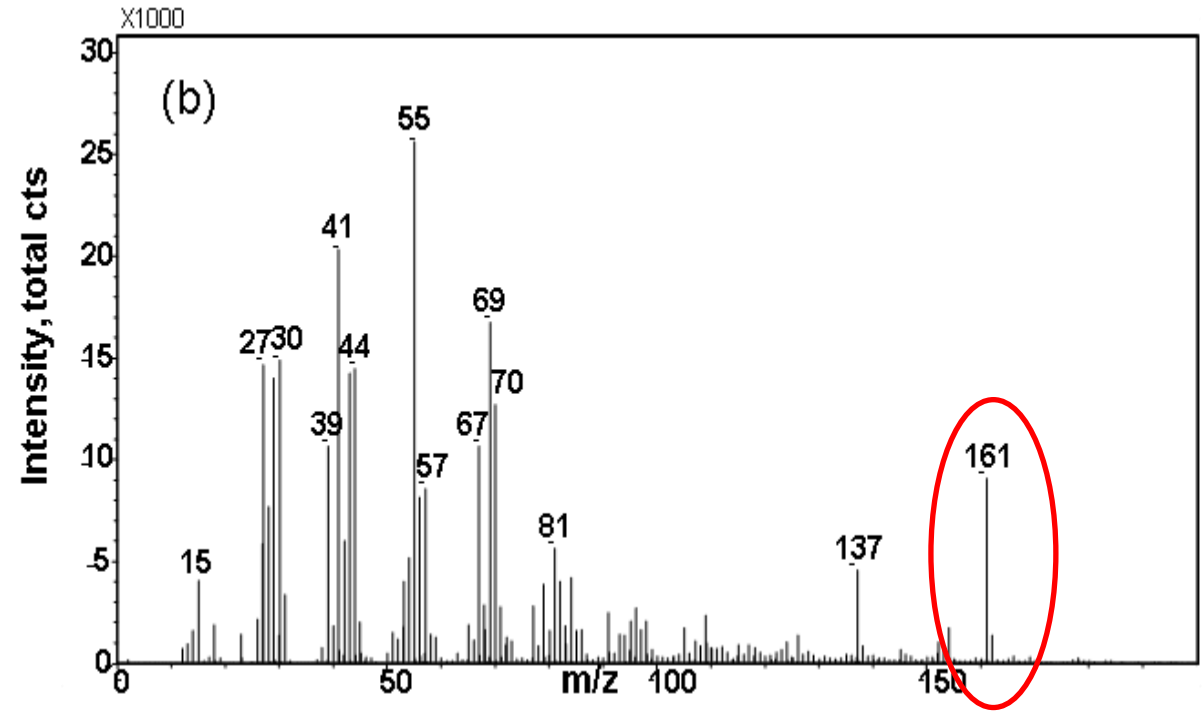
Sample	Concentration, at%		
	O	N	C
Th-AGEpp	20.3	0	79.7
Th-AGEpp-Nyl3-1	14.6	5.3	80.1
Th-AGEpp-Nyl3-2	17.3	5.6	77.1
Th-AGEpp-Nyl3-3	17.0	3.7	79.3

Nylon-3 polymers were also attached at 1 mg per ml solution concentration in a once-off experiment. This gave no measurable increase in the %N, so the experiment was not repeated given the limited amounts of these copolymers, and all further immobilisation experiments and biological testing were done using 0.1 mg per ml solutions of Nylon-3 copolymers.

To test whether some of the compounds might be able to detach from the surface again, samples were stored in PBS for 10 days, them dried and subjected to XPS analysis. This resulted in data within experimental uncertainty of those listed in Table 6.1, indicating that the Nylon-3 copolymers remained immobilised on the surface upon extended soaking.

Samples were also analysed by ToF-SIMS, with the expectation of detecting peaks that would be characteristic of structural elements of the copolymers. Positive ion spectra recorded on AGEpp and after grafting with Nylon-3 polymers showed characteristic, assignable differences, even though peaks from fragment ions originating from the AGEpp still possess significant intensity after copolymer grafting. This is commonly observed when grafting such thin layers of relatively small molecules; the substrate is not totally hidden underneath the grafted molecules. Examples are shown in Figure 6.7. Of particular note in the spectrum of Figure 6.7b is the distinct peak at m/z = 161, which can be unambiguously assigned to the terminal t-butyl-phenyl-carbonyl group of Nylon 3-1. There is no evidence of surface contamination by adventitious silicones or fatty acids.





(c)

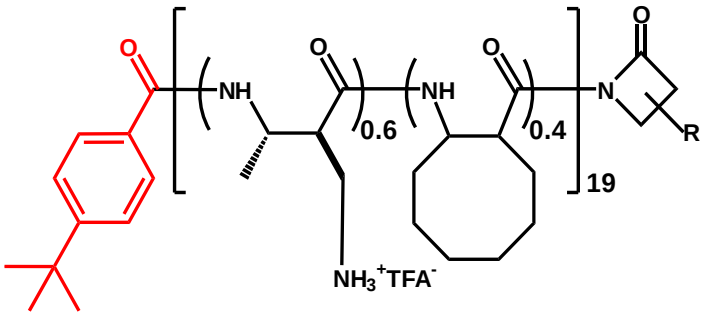


Figure 6.7: Positive static mass spectra of AGEpp (a) and grafted with Nylon 3-1 (b) and Nylon 3-1 with the red end group signifying the circled peak at 161 (c)

To probe for uniformity of the coatings, ToF-SIMS analyses were performed on ten separate spots on each sample and evaluating the results by PCA. As shown in Figure 6.8, the data collected on separate areas of the samples were remarkably uniform, clustering tightly into distinct sets, which indicates that none of the grafted coatings had contained any defect in the coating large enough to show up in these analyses.

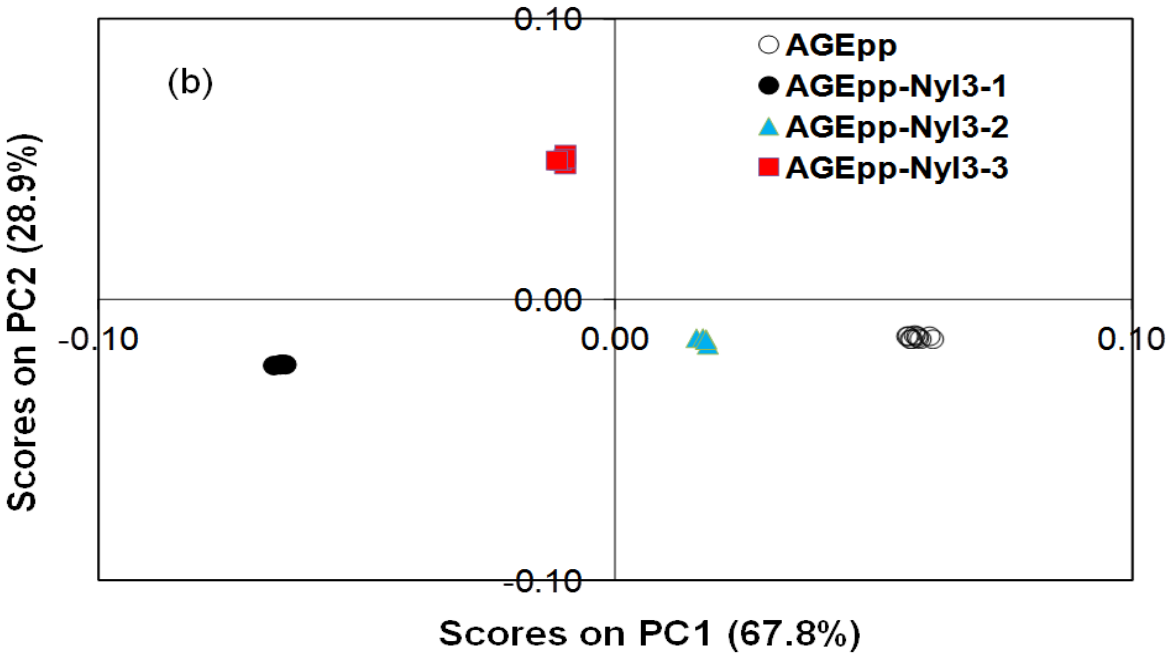


Figure 6.8: Scores plot for positive ion spectra recorded on AGEpp and Nylon-3 copolymer grafted surfaces

The data cluster for Nylon 3-1 lies farthest from that of AGEpp, which indicates that this polymer was grafted with the highest surface density of those three copolymers (noting that while ToF-SIMS quantification can be problematic, with such chemically very similar coatings semi-quantitative interpretation would seem permissible). This conclusion is in accord with the XPS data above.

The accompanying loadings plot is shown in Figure 6.9. As indicated by the scores plot, peaks that *increase* in relative intensity upon grafting of Nylon-3 copolymers will load *negatively* on PC1 in the loadings plot. Indeed the peaks with significant loadings separate very neatly into those that are prominent for the AGEpp (all loading positively) and negatively-loading peaks that can be readily assigned to fragment ions originating from the Nylon-3 copolymer, such as the end group at m/z 161, two fragment ions originating from the cyclo-octane moiety, and the nitrogen-containing fragment at m/z 44, which is absent in the spectrum of the AGEpp.

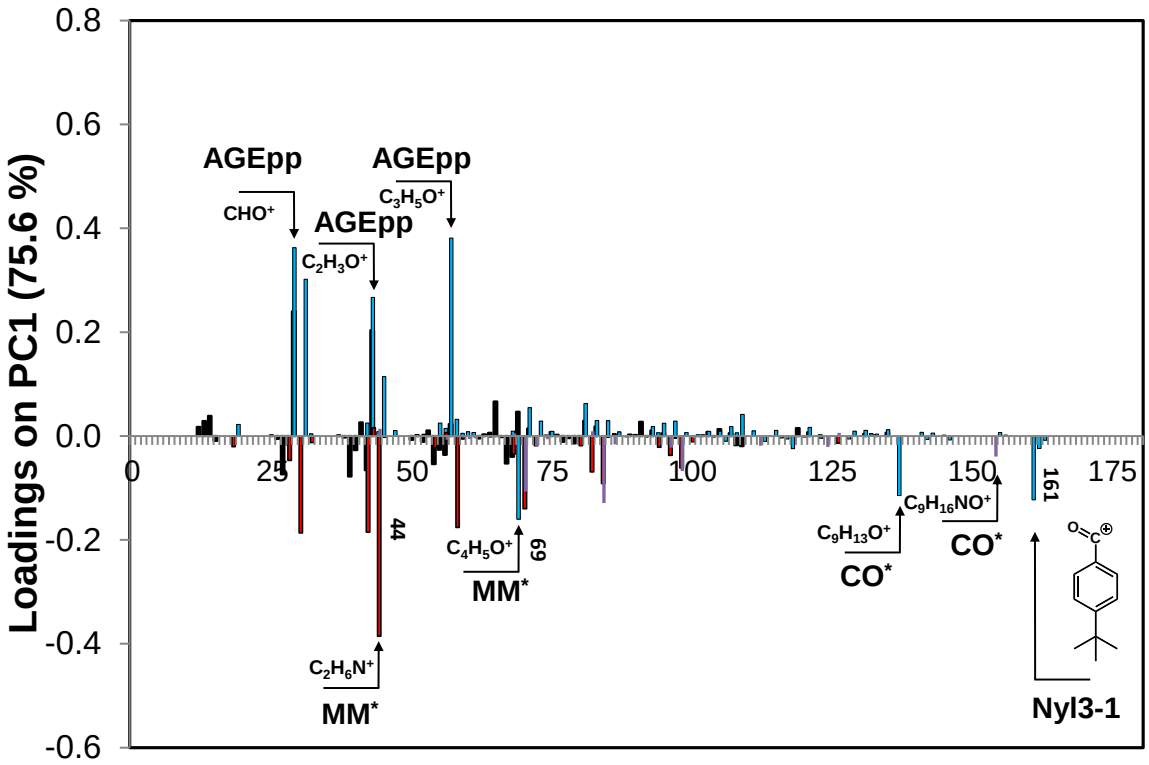


Figure 6.9: Loadings plot on PC1 of positive ions recorded on AGEpp and Nylon-3 copolymer grafted surfaces

6.3.2 Click Chemistry

Figures 6.10 to 6.14 display results from surface analysis after immobilisation of Nylon compounds 3125 and 3127 via Click chemistry.

While for the Nylons discussed above the surface coverage could be related to the %N recorded in XPS survey spectra, this approach was not possible after Click immobilisation because of the N signal arising from the azide groups; interpretation based on differences in %N before and after immobilisation, combined with an overlayer model, would possess a considerable degree of uncertainty. To measure the surface coverage of these Nylons, a different method would be required, for example radiolabelling, but this was not feasible in this project.

Qualitatively, however, the attachment of the copolymers could be confirmed via high-resolution XPS spectra. As shown in Figure 6.10, the C1s signal changes somewhat, consistent

with expectation that upon attaching the Nylon copolymer, the C-O component, which is quite intense in the spectrum recorded on the AGEpp surface, should show reduced intensity, as the copolymer does not contain such a high ratio of C-O bonds as the AGEpp. But the clearest evidence is in the N1s signal, which shows that much of the N is in the form of triazole, as expected upon click coupling. The weaker components at higher binding energy can be assigned to some remaining unreacted azide groups.

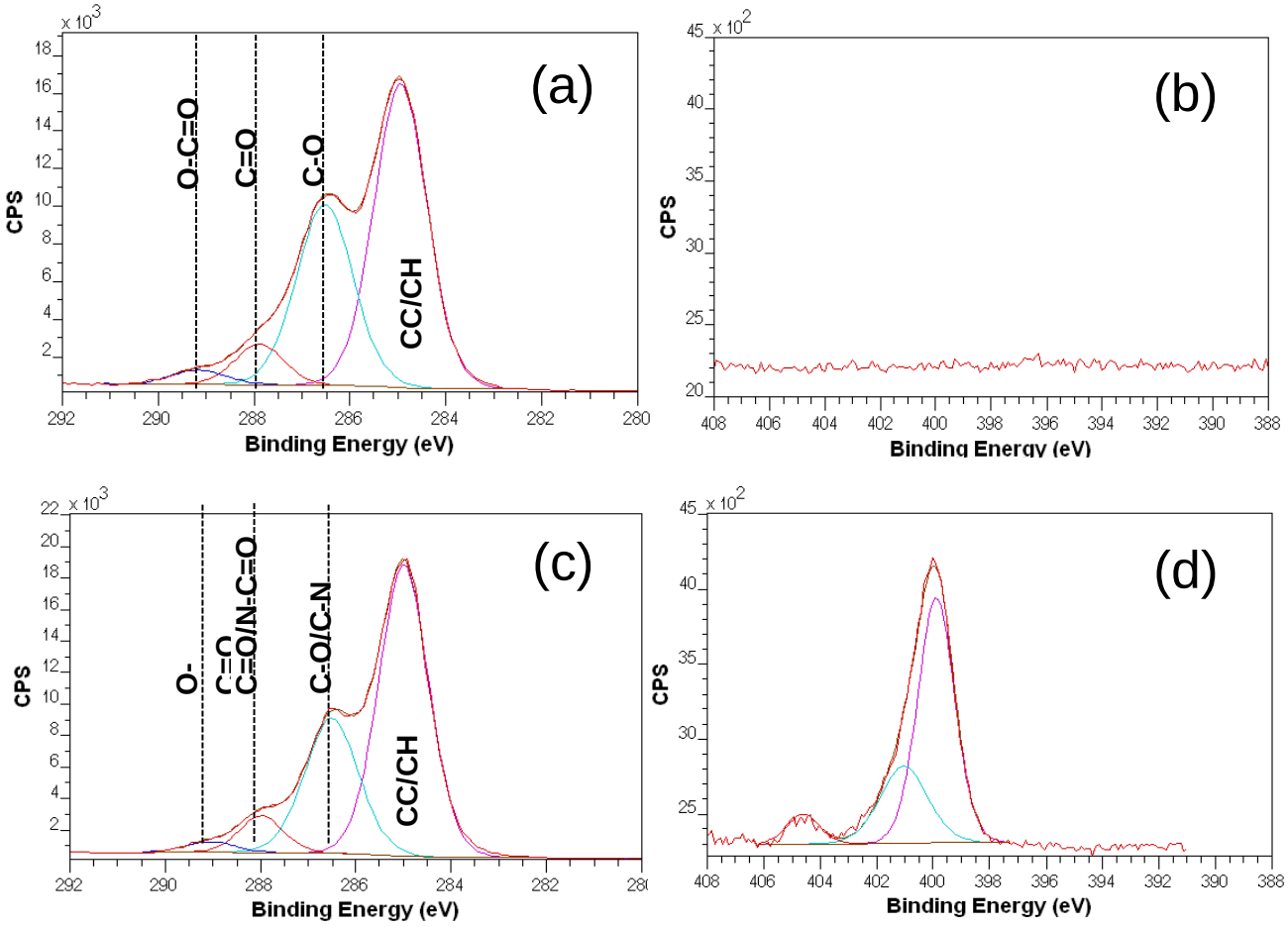


Figure 6.10: High resolution C 1*s* and N 1*s* XPS spectra of the AGEpp substrate [(a) and (b) respectively] and after grafting of Nylon 3127 [(c) and (d) respectively].

Again ToF-SIMS was also used to characterise the coatings because of its molecular information content. ToF-SIMS spectra recorded with an azide-derivatised surface (Th-AGEpp-N_3) and after grafting the Nylon copolymers are shown in Figure 6.11 (the spectrum for the AGEpp is not shown as it was the same as that in Figure 6.7a).

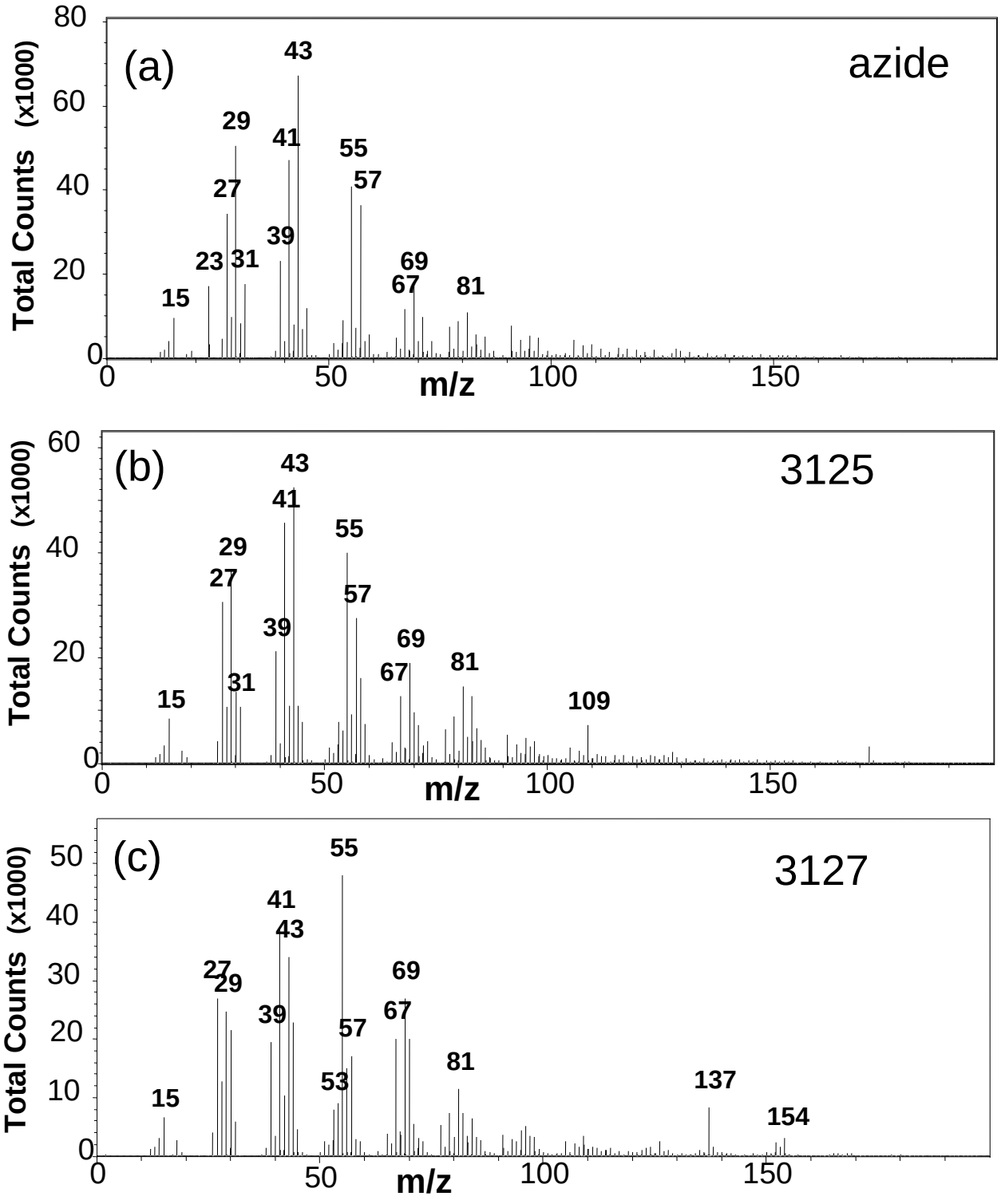
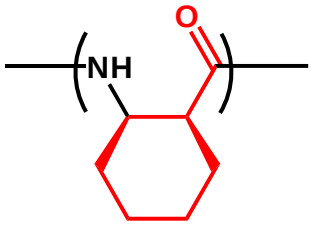
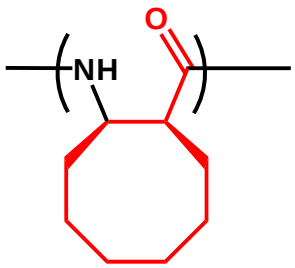


Figure 6.11: Positive mass spectra recorded on (a) Th-AGEpp-N_3; (b) th-AGEpp-N_3-Nyl3215; (c) th-AGEpp-N_3-Nyl3217.

At first glance the spectra look quite similar, which, as for the Nylons discussed above, is not surprising for sub- or near-monolayers of grafted molecules; there is still plenty of scope for emission of ions from the underlying material. There are, however, characteristic fragment ions that are not observed in the spectrum of the azide-derivatised surface, such as m/z 109, which can be assigned to originating from the cyclohexyl structure of Nylon 3125:

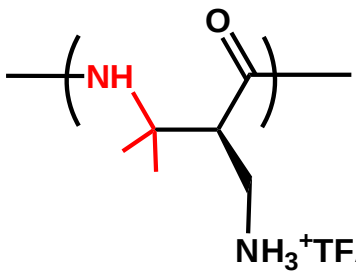


and m/z 137, which can be assigned to originating from the cyclo-octyl ring of Nylon 3127:

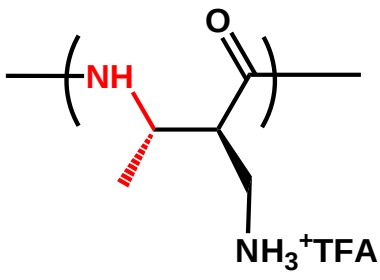


.

Other signals are more intense after grafting of the Nylons, such as m/z 58 and 44, which, on the basis of high-resolution spectra that separate them from close-lying fragment ions possessing C,H, and O, but no N, can be assigned to derive from these structural elements (C-H bonds not shown):



and



.

High resolution spectra were also recorded across specific narrow regions of m/z, so as to gain more information on peaks that may have multiple possible assignments. An example is shown in Figure 6.12, demonstrating that the signal at m/z 42 actually arises from several close-lying fragment ions. Upon adding azide onto the AGEpp, a signal assignable to $C_2H_4N^+$ appears. This

signal is of increased relative intensity after grafting the Nylon copolymers, which is consistent with the expectation that such a fragment ion can be ejected from the copolymer structure.

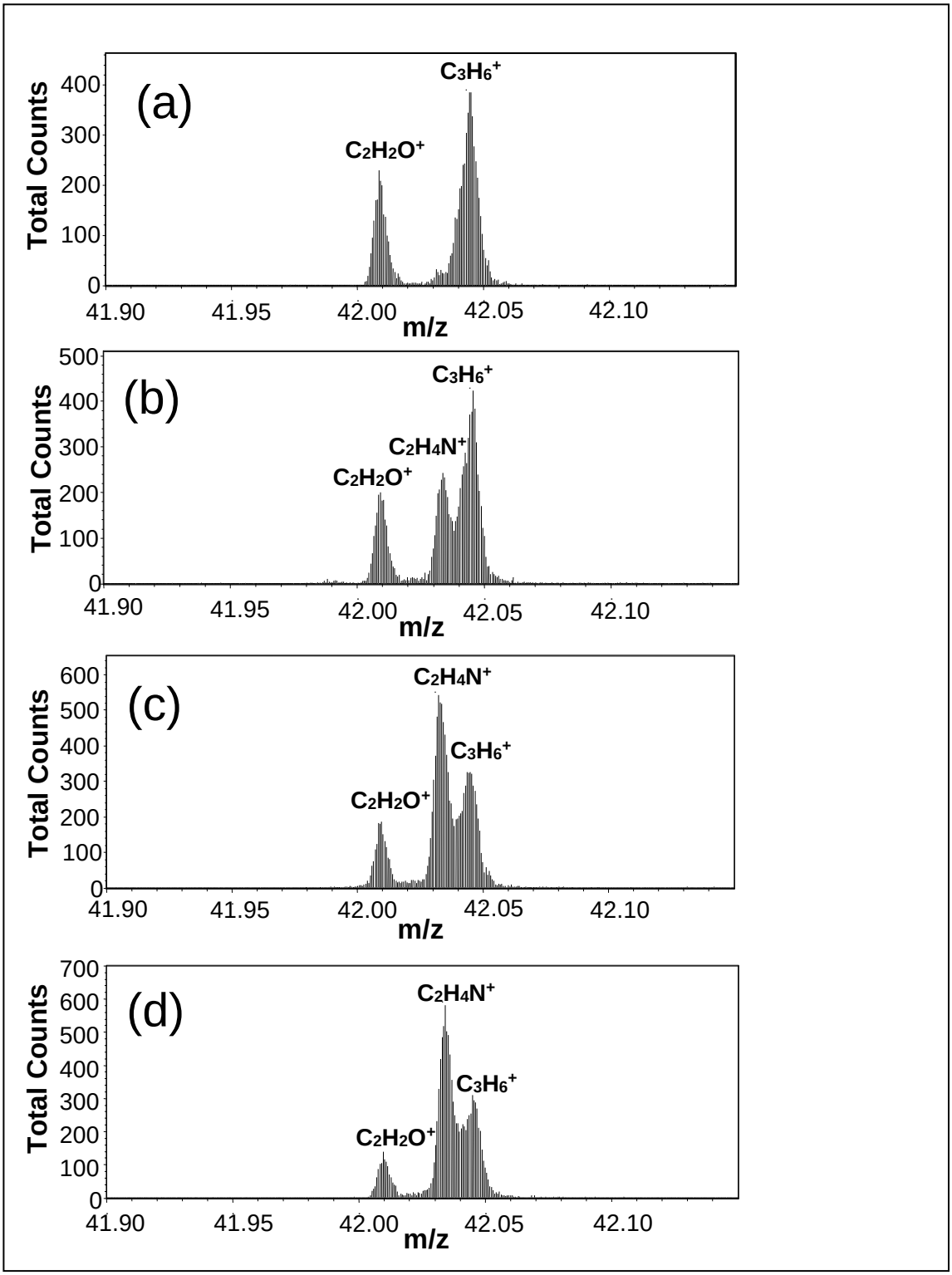


Figure 6.12: High resolution mass spectra of positive ions around m/z 42 for: (a) AGEpp; (b) AGEpp-N_3; (c) AGEpp-N_3-Nyl3125 (d) AGEpp-N_3-Nyl3127

While such visual inspection of the spectra clearly demonstrates successful grafting of the Nylon copolymers via Click chemistry, Principal Component Analysis (PCA) was also used in order to bring out the most distinct differences between spectra. Results from PCA analysis of multiple spectra from each of the four surfaces are shown in Figure 6.13. First, it is evident from the scores plot (Fig. 6.13a) that spectra from separate locations on each sample gave tight clusters, as above for the other Nylon copolymers, again attesting to uniformity of the coatings within the accuracy of ToF-SIMS analysis. In addition, the clusters are well separated, for example between the azide surface and the surfaces after grafting, showing substantial coverage by the Nylon copolymers. The larger separation for Nylon 3127 could be interpreted as it having a greater surface coverage, but quantitative interpretation can be problematic and this conjecture would need to be checked with an independent techniqure for determining surface coverage; this was not possible in this thesis.

The loadings plot (Fig. 6.13b) of peaks on the first Principal Component, which captures over 81% of the information content and thus captures much of the spectral differences, reveals peaks that are in accord with expectations. The positively loading peaks (most distinct for the AGEpp surface) are assignable to $C_xH_yO^+$ fragment ions, which are readily derivable from the AGEpp composition, for example $C_2H_5O^+$ and $C_2H_3O^+$ from the epoxide ring structure. Many of the negatively loading peaks, more intense for the Nylon grafted samples, are assignable to fragment ions that contain N in structures larger than possible with azide. It is also noted that there is no evidence of any adventitious contamination from organosilicones, which could also alter bacterial colonisation and thus give rise to erroneous interpretations.

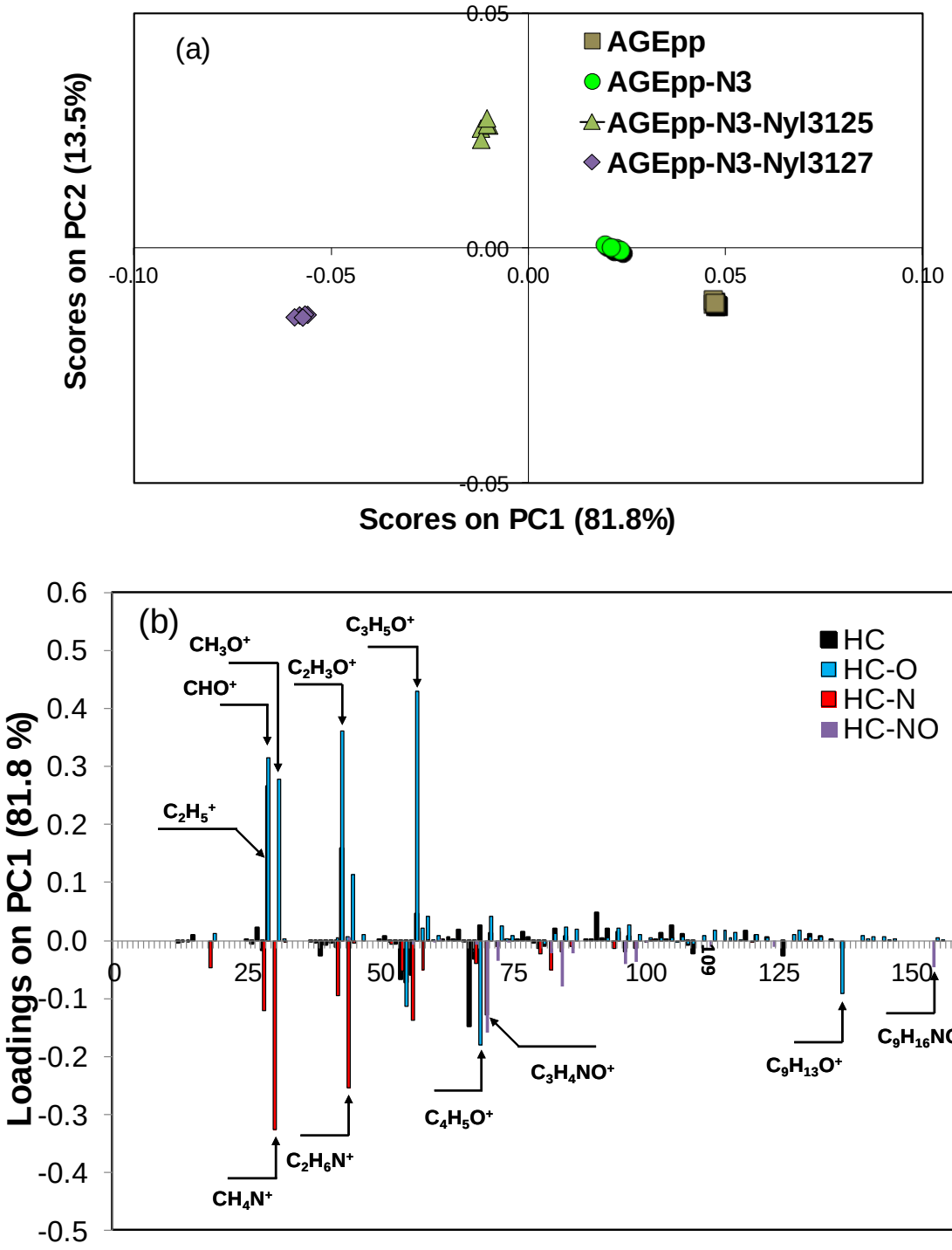


Figure 6.13: PCA analysis of the positive ion spectra recorded on AGEpp, AGEpp with N_3, and after immobilisation of Nylon 3125 and Nylon 3127

When performing a pairwise comparison by PCA of the spectra recorded with the two grafted copolymers, the scores plot (Figure 6.14a) separated the data sets even though the two

compounds differed only in possessing cyclohexyl and cyclo-octyl rings, respectively. On the other hand, the loadings plot (Figure 6.14b) showed not only peaks from those structures, indicating that the two compounds were not immobilised to exactly the same amounts.

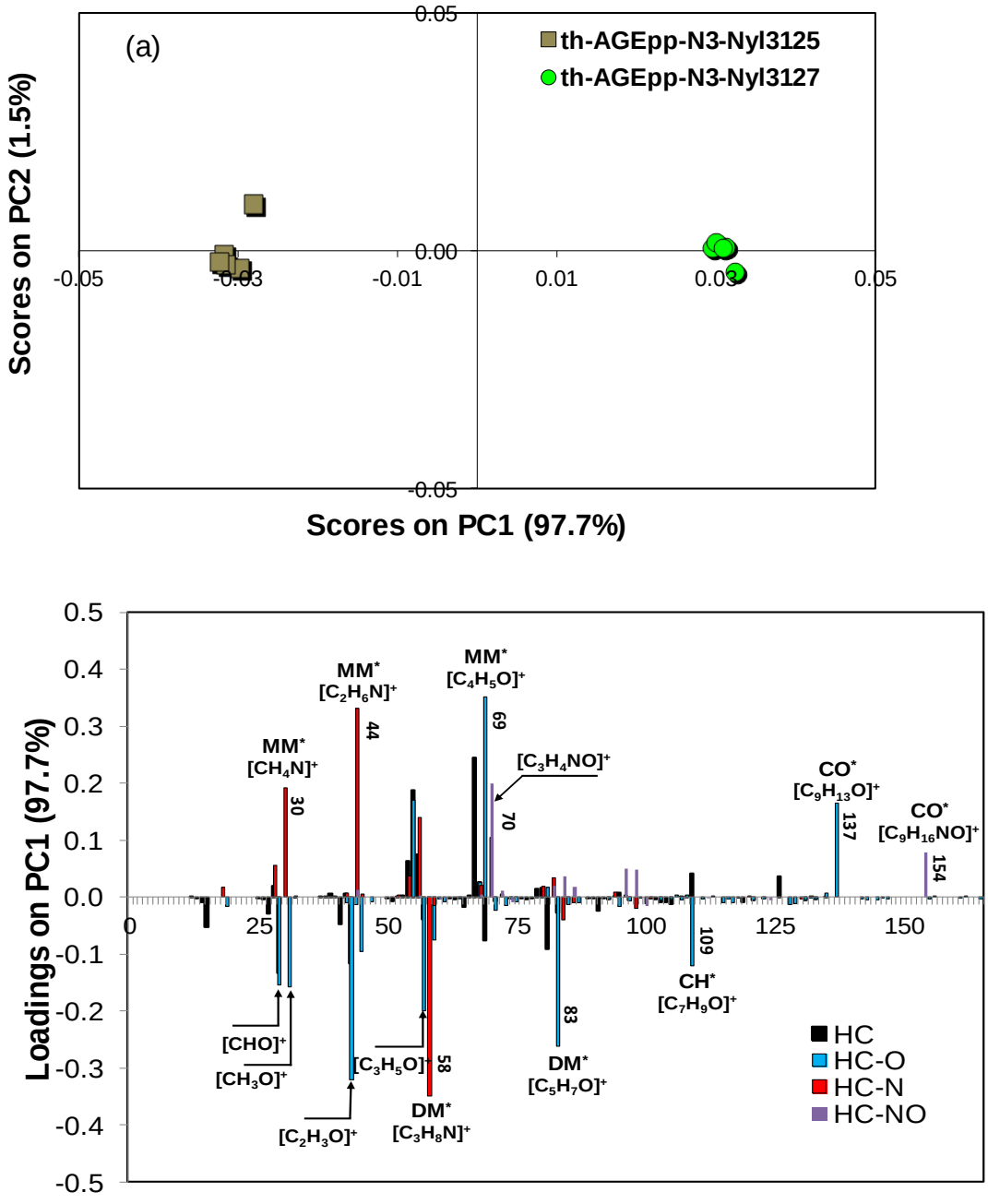


Figure 6.14: Scores (a) and loadings (b) plots of spectra from coatings of Nylon 3125 and Nylon 3127

In summary, for all five Nylon copolymers, surface analysis data clearly confirmed their surface immobilisation and absence of extraneous signals from possible contaminants. These solid surface analytical data provide confidence for going ahead with biological tests, in that the observed biological responses will be interpretable in terms of effects arising from the grafted compounds.

6.3.3 Bacterial Testing

After rinsing, bacteria were visualised using the commercial kit LIVE/DEAD *Bac*Light stain. It is important that the *Bac*Light kit be tested with each system before use to ensure accurate scoring of live and dead cells. This was done in these systems by growing bacteria on solid substrate surfaces with and without plasma treatment and with and without grafted polymers, and negative controls (dead bacteria) were created by treating bacteria in the wells with Virkon for 1–3 minutes. The controls showed good reproducibility. However, biofilm staining by safranin was not reliable as an indicator of biofilm viability because of the combination of dead and live bacteria present.

As shown by the following series of microscopy images, all of the Nylon-3 grafted surfaces produced, relative to control samples, a substantial reduction in bacterial attachment and growth after 6 hours incubation; Nylon 3-1 was the most antibacterially effective. Microscopy images showed a reduction in live bacteria attaching to the surface and also showed dead bacteria that had contacted the surface and then been killed. *S. epidermidis* was the main bacterium used in the following tests because it is the most surface adherent among the bacteria tested. Other bacteria, *E. coli*, *P. aeruginosa*, methicillin-resistant *S. aureus* (MRSA) and methicillin-sensitive *S. aureus* (MSSA), were also tested and similar reductions in attachment were also observed by microscopy, it was difficult to assess them confidently because they stick less well to surfaces and are less surface adherent, and thus more easily washed off when removing the supernatant solution, than the strongly biofilm-forming strain of *S. epidermidis* used. They were only used to gain indicative qualitative results as they were not tested with sufficient numbers of replicates to gain quantitative validity. However, all of those other bacteria had been shown to be killed by the Nylon polymers tested in solution; therefore, even with sparse data with

coatings it can confidently be assumed that the grafted coatings also affect the other bacteria in the same way as they did for *S. epidermidis.*

Figure 6.15 shows a representative image of bacteria attached onto the "control" AGE plasma polymer surface after 6 hours. Clearly, the bacterial cells are able to attach and congregate to form colonies ("clumps" visible in the image) that act as precursors to biofilm formation. There is no evidence of dead bacteria (which would stain red), and the bacteria proliferate, as shown by increasing numbers in images taken at later times (not shown).

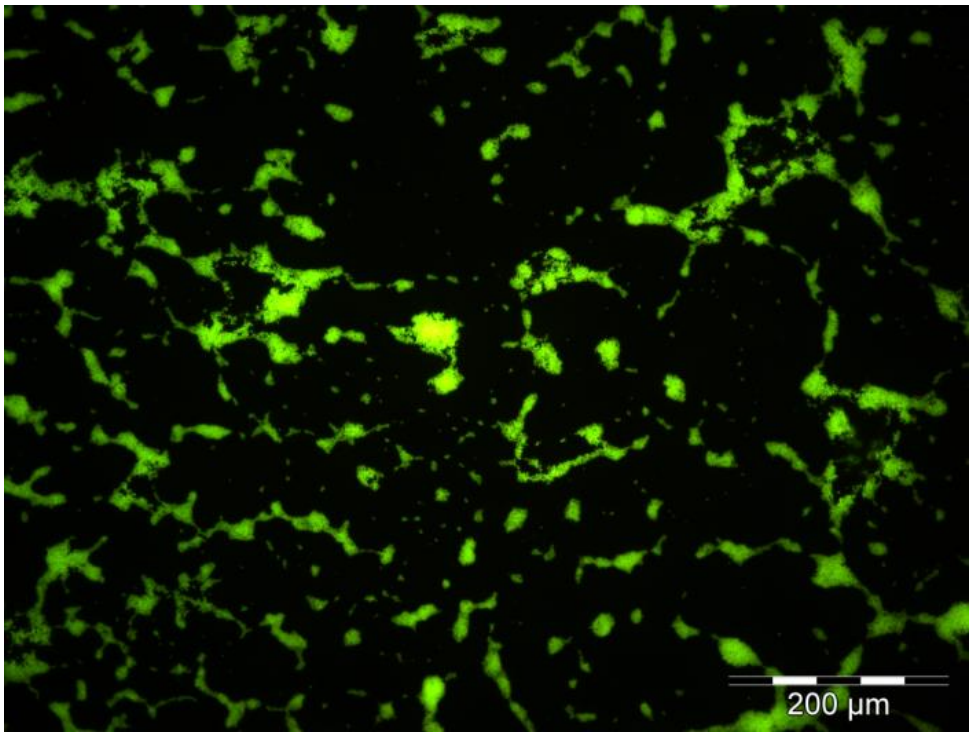


Figure 6.15: Control sample: AGEpp with *S. epidermidis* after 6 hours incubation at 37 ºC and stained with the LIVE/DEAD *Bac*Light stain. Green bacteria are alive; red bacteria are dead. (20x image)

Figure 6.16 shows a representative microscopy image of a sample comprising Nylon 3-1 grafted onto AGEpp. The marked difference to the above image indicates a highly effective grafted layer. Most of the surface-attached bacteria are dead or dying (stained yellow), and there is no evidence of formation of colonies. Thus, some bacteria manage to attach but are then killed

before they congregate into colonies. The smaller total number also suggests that many bacteria are killed before they manage to firmly attach onto the surface.

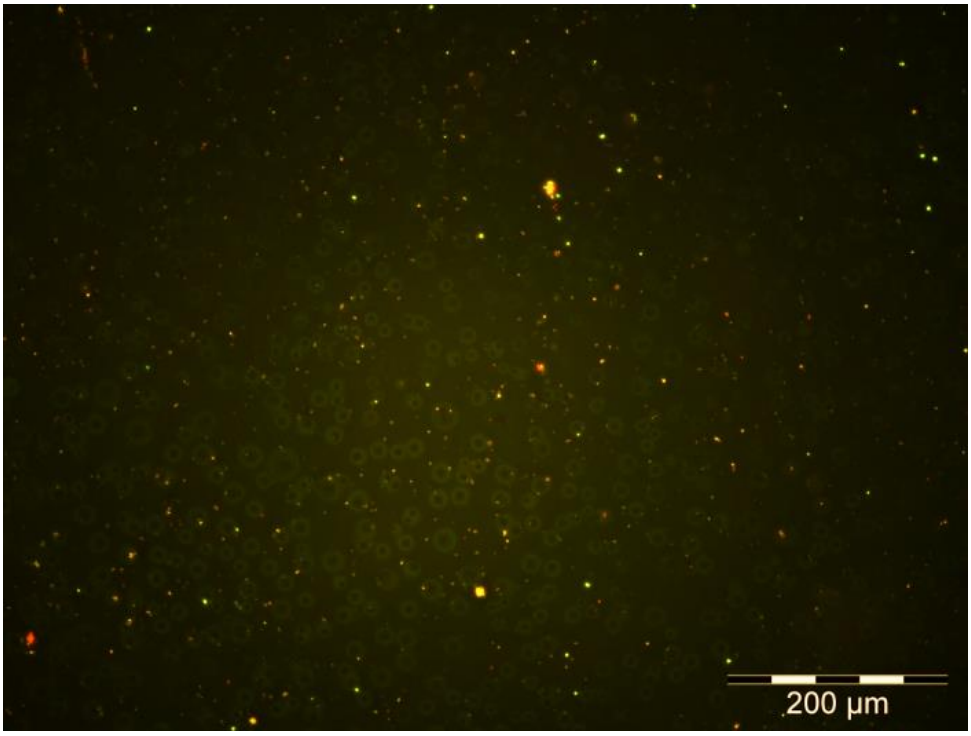


Figure 6.16: AGEpp with Nylon 3-1 immobilised on the surface with *S. epidermidis* after 6 hours incubation at 37 ºC stained with the LIVE/DEAD *Bac*Light stain. There is much less bacterial colonisation of the surface; most are dead as seen by the red staining. There is no biofilm present.

Figure 6.17 shows a somewhat different behaviour for grafted Nylon 3-2. There are both live and dead bacteria present, and while many are surface-attached as isolated individuals, others have aggregated into small colonies. These observations suggest that the Nylon 3-2 grafted layer appears to kill attaching bacteria less rapidly. Yet, there still is a marked difference to the bacterial colonisation on AGEpp, attesting to still strong activity of the surface-grafted molecules.

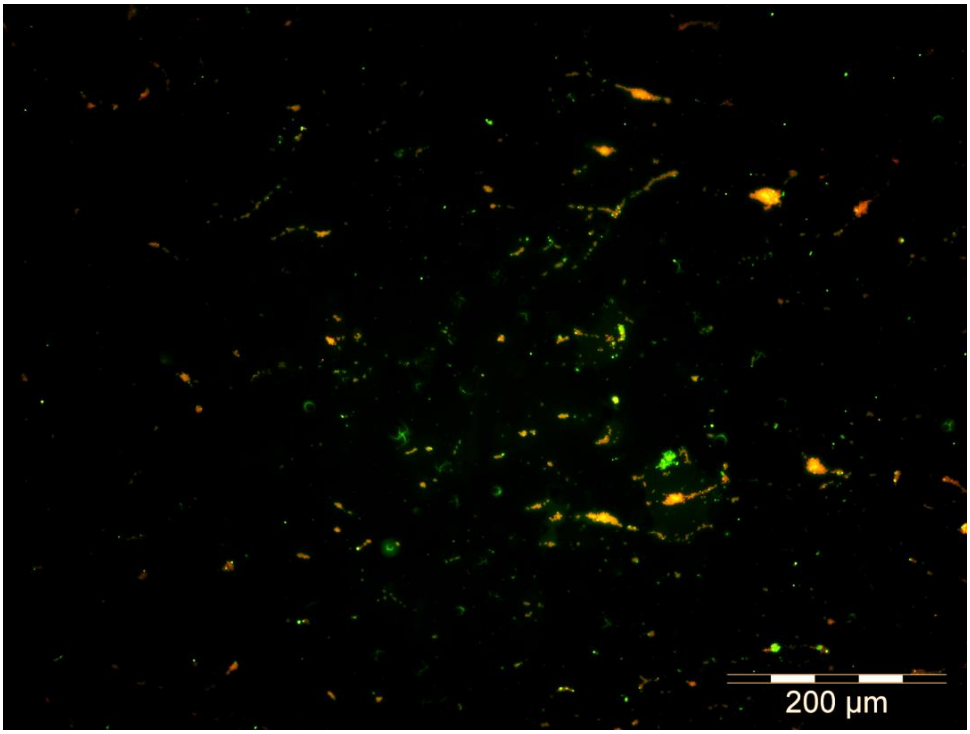


Figure 6.17: AGEpp with Nylon 3-2 immobilised onto the surface with *S. epidermidis* after 6 hours incubation at 37 ºC stained with the LIVE/DEAD *Bac*Light stain. There are patches of dead bacteria on the surface with some live bacteria present.

In contrast, surprisingly, grafted Nylon 3-3 was much less effective. Figure 6.18 shows a representative image. There are again dead bacteria visible by red staining, but there are also significant numbers of live bacteria present. Some are located on top of dead bacteria, which would protect them against the action of a covalently attached antibacterial surface layer. The colonies are smaller than on thye control AGEpp surface (Fig. 6-15), indicating that the grafted layer not only kills attaching bacteria but also slows bacterial attachment and colony formation. It can be hypothesised that the speed of killing is rather slow, thus allowing observation of bacteria that have attached but have not been killed yet. If killing indeed were slow, this would also give bacteria time to engage in some aggregation, and possibly even multiplication on the surface. Perhaps not all cells are arrivals from solution; some may be present due to division of attached cells if the average time for killing is larger than the time of doubling.

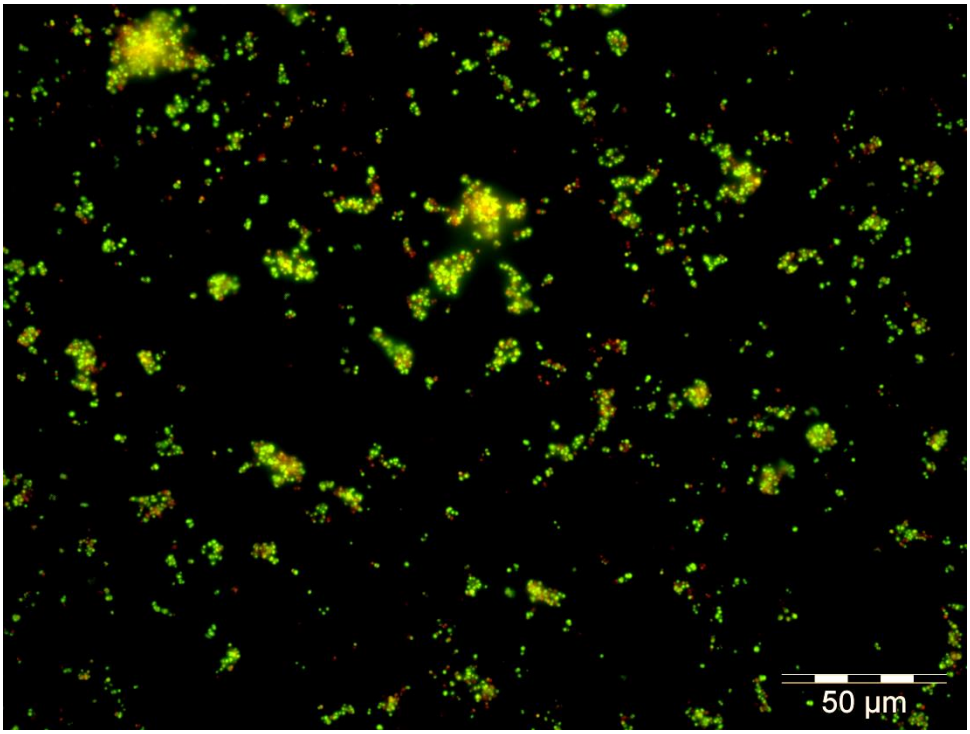


Figure 6.18: AGEpp with Nylon 3-3 immobilised onto the surface with *S. epidermidis* after 6 hours incubation at 37 ºC stained with the LIVE/DEAD *Bac*Light stain. This is shown as a 60x image to show the live bacteria growing on the dead bacteria.

Qnantification of surface amounts of bacteria was achieved by removing all surface-adhered bacteria through scraping and rinsing the surface and checking under a microscope that all bacteria had been removed, then performing serial dilution of bacteria and plating them. The live bacteria removed from the test surfaces grew readily when transferred onto an agar plate and incubated as described in the methodology section. The numbers of colony-forming units (CFUs) determined thus are shown in Figure 6.19. The measured numbers accord well with the qualitative assessment gained from microscopy images.

This quantification was only performed with *S. epidermidis* but not for the other bacteria, for which only microscopy images were collected.

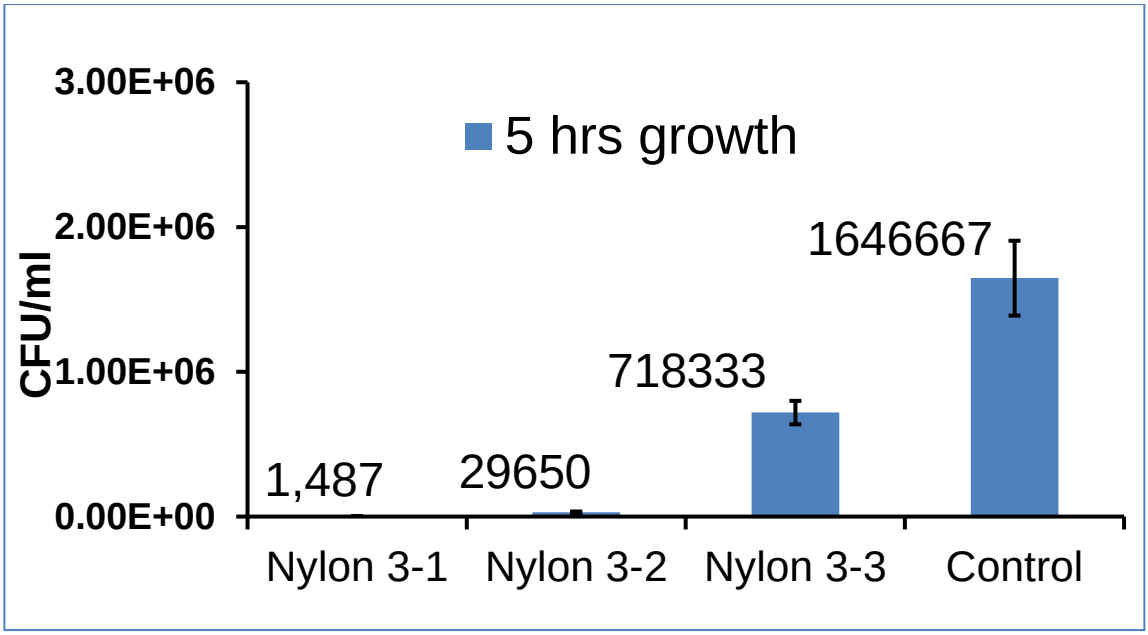


Figure 6.19: Graph showing amounts of bacteria colonising the surfaces with *S. epidermidis* after 6 hours incubation at 37 ºC, after removing adherent bacteria, serial diluting and plating for overnight growth. Averaged numbers are recorded above the bars. Taken over nine samples each, repeated three times.

Analogous experiments were also performed over 24 hours of incubation, in order to test longer-term performance of the grafted coatings. This is an extremely demanding test as the bacteria continue multiplying in solution above the samples and there are ever-increasing numbers of bacteria coming into contact with the surface.

For the sake of brevity, microscopy images are not shown but the numbers of CFUs determined in the same way as above are shown in Figure 6.20. The relative ranking of the samples is the same as for shorter times. On the control surface (AGEpp) the number of CFUs is more than 10^3 times higher than at 6 hours, whereas there are again much smaller numbers present on grafted Nylon 3-1 and Nylon 3-2 layers, with the former again showing the best antibacterial performance.

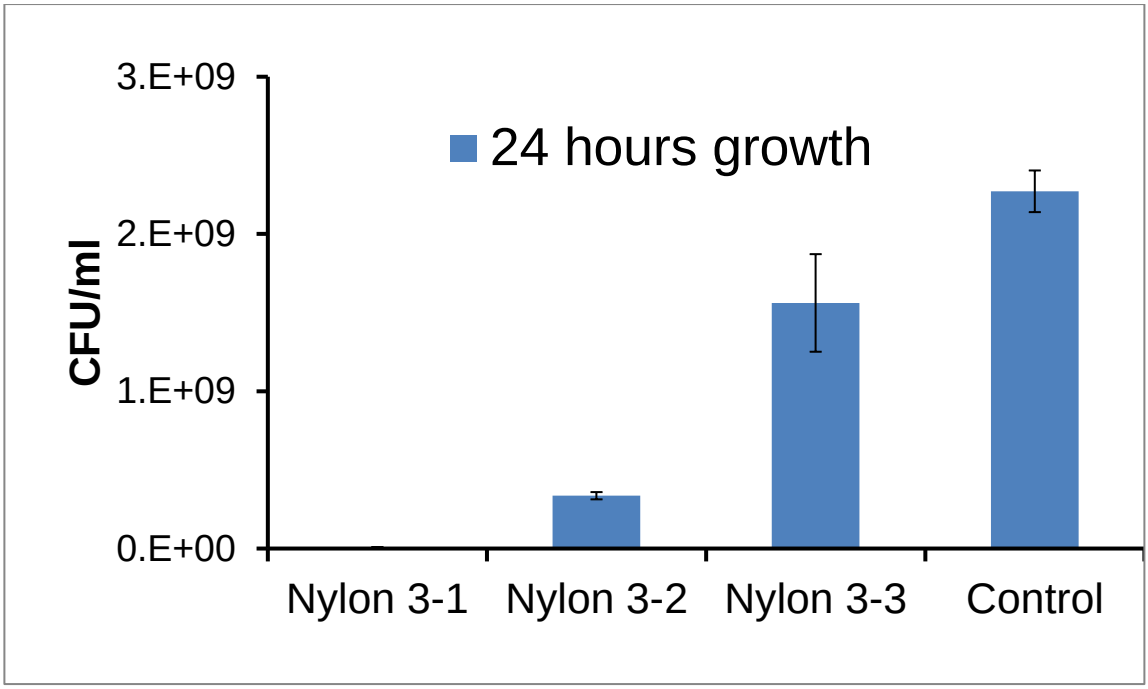


Figure 6.20: Numbers of *S. epidermidis* after 24 hours incubation at 37 ºC, after removing adherent bacteria, serial diluting and plating for overnight growth. Averages over nine samples each, repeated three times.

Results for surfaces modified by click chemistry grafting of the two Nylon copolymers 3125 and 3127 were the same as for the Nylon copolymers grafted onto AGEpp-modified surfaces, again giving excellent antibacterial activity. For these tests, coatings comprising AGEpp derivatized with azide were used, so as to isolate the effect arising from the compounds. Comparing AGEpp with and without azide allowed assessing the effect that surface azide groups might contribute. Figure 6.21 shows an extensive patch of bacterial biofilm formed on the AGEpp + azide surface after 24 hours. Whereas azide in solution is an effective antibacterial compound, evidently surface-attached azide groups do not perform antibacterial action – provided the sample is washed extensively to remove unreacted molecular azide.

After attaching Nylon 3-6 copolymer, a substantial reduction in bacterial biofilm formation was observed (Figure 6.22); while a few patches have formed, they are much smaller and considerably thinner in comparison with the 3-dimensional biofilm formed on the control surface. Dead bacteria are also evident. These low-magnification images both show the rounded edge of the treated area. Some bacterial growth at the edge of the treated sample (left side of

image) may be a result of the mask slipping and exposing some untreated area along the edge, or damaging the treatment when the mask was placed on the surface.

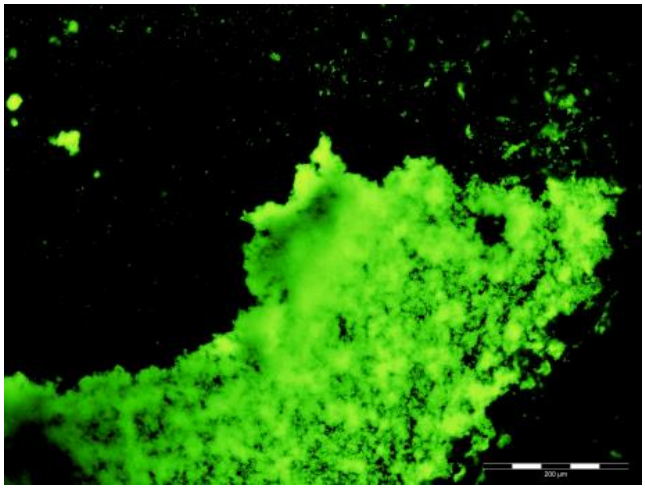


Figure 6.21: Control click pp with 1 x 10^5 cfu/ml *S. epidermidis* after 24 hours growth

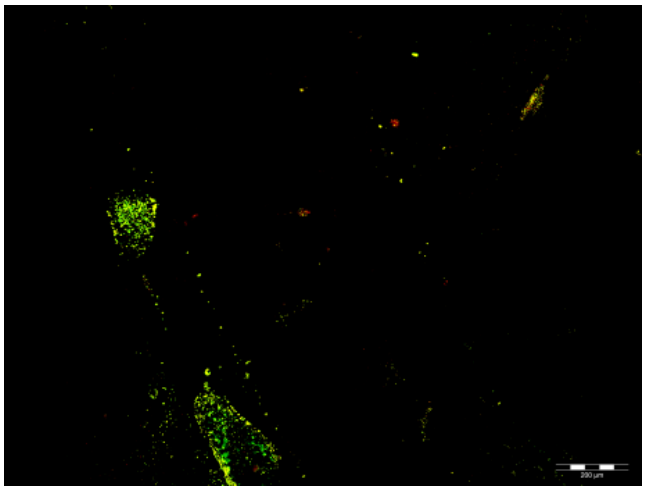


Figure 6.22: Nylon 3-6 immobilised using click reaction to a pp surface with 1 x 10^5 cfu/ml *S. epidermidis* after 24 hours growth

Hence, Nylon 3 copolymers can provide effective antibacterial coatings when grafted onto solid surfaces, extending their solution performance, regardless of how they were grafted. A practical issue, however, arose with the rinsing step in click chemistry grafting; these surfaces need *much* more careful extended washing after grafting because residual azide after brief rinsing was

observed to be highly antibacterial. This meant that there was little gain from using this particular attachment method because grafting onto AGEpp is much quicker and easier, with a brief rinse sufficient. Thus, grafting onto AGEpp via epoxide-amine reaction is advantageous as it avoids the possibility of residual azide interfering with antibacterial testing and also would be easier to scale up as it does not require extended washing.

6.3.4 Cell Studies

It had already been shown by Gellman's group that Nylon-3 copolymers grafted onto solid surfaces provide support for attachment of mammalian cell lines and promote cell growth (Lee et al. 2009). Here, we have extended that study to investigate whether grafted Nylon 3 coatings also promote the attachment and growth of primary human fibroblasts, which serves as a model of wound healing and thus the potential of grafted Nylon-3 copolymers to serve as coatings for antibacterial skin wound care products. Why an antibacterial compound would support and even encourage better growth, as was found in this research, was a key question. It required taking a step backwards and conducting surface analysis to determine what happens when Nylon-3 compounds are exposed to cell growth medium or serum. Because primary cells do not like growing without growth medium/serum and generally die fairly quickly in their absence, it is not particularly worthwhile examining cells without media/serum. Therefore, the obvious experiment is to surface analyse samples with grafted Nylon-3 polymers after exposure to medium/serum, and compare the results with the above analyses of freshly grafted coatings.

XPS analysis after exposure to serum showed evidence of Nylon 3 copolymers adsorbing proteins, as attested by the following data.

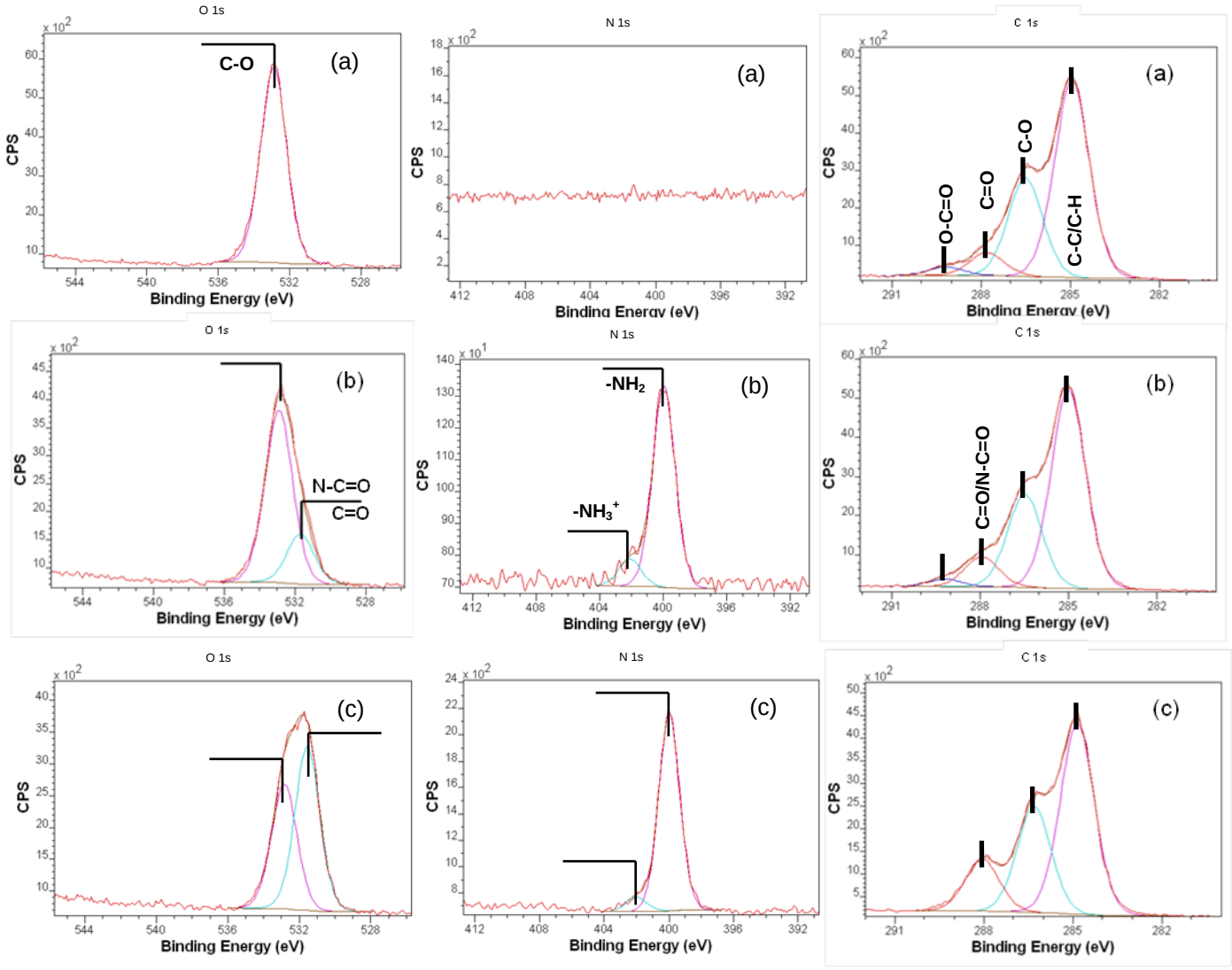


Figure 6.23: O 1s, N 1s and C 1s high-resolution spectra for: (a) AGEpp, (b) AGEpp with nylon 3-1 immobilised, (c) AGEpp with nylon 3-1 immobilised and with medium/serum (cell medium, CM).

Table 6.2: Elemental compositions of samples, with (red) referring to reductive amination. The percentages are calculated from survey spectra.

Sample	Composition, atomic %		
	O	N	C
-AGEpp	20.31	–	79.69
-AGEpp-Nyl3-1	16.47	4.03	79.50
-AGEpp-Nyl3-1+CM	17.75	9.96	72.29
-AGEpp-Nyl3-1(red)	14.63	5.25	80.11
-AGEpp-Nyl3-1(red)+CM	17.21	10.23	72.56
-AGEpp-Nyl3-2	17.34	4.90	77.76
-AGEpp-Nyl3-2+CM	18.33	8.94	72.74
-AGEpp-Nyl3-2(red)	17.36	5.57	77.07
-AGEpp-Nyl3-2(red)+CM	17.54	9.61	72.85
-AGEpp-Nyl3-3	17.23	3.21	79.57
-AGEpp-Nyl3-3+CM	18.05	8.63	73.33
-AGEpp-Nyl3-3(red)	17.04	3.68	79.29
-AGEpp-Nyl3-3(red)+CM	17.24	8.25	74.48

In all cases there is a substantial increase in the N content, as well as a change in the high-resolution spectra (Fig. 6.23). This evidence points to physisorption of serum proteins, which gives nylon 3 coatings their cell-adhesive properties.

It is interesting to note that the amount of increased nitrogen on the surface directly relates to the number of primary cells that grew on the surface. By comparing the number of primary cells on the surface shown in Figure 6.24 and the percentage of nitrogen shown in Table 6.2, it becomes clear how the results work together. Nylon 3-2 has the highest amount of nitrogen and the highest number of cells. Nylon 3-3 has the lowest amount of nitrogen gained and the lowest number of cells. This could be directly related to the number of repeats; however, nylon 3-1 has only 19 in contrast to 22 repeats for nylon 3-3. The monomethyl-cyclohexyl (MM-CH) apparently provides a more efficient interaction with the proteins.

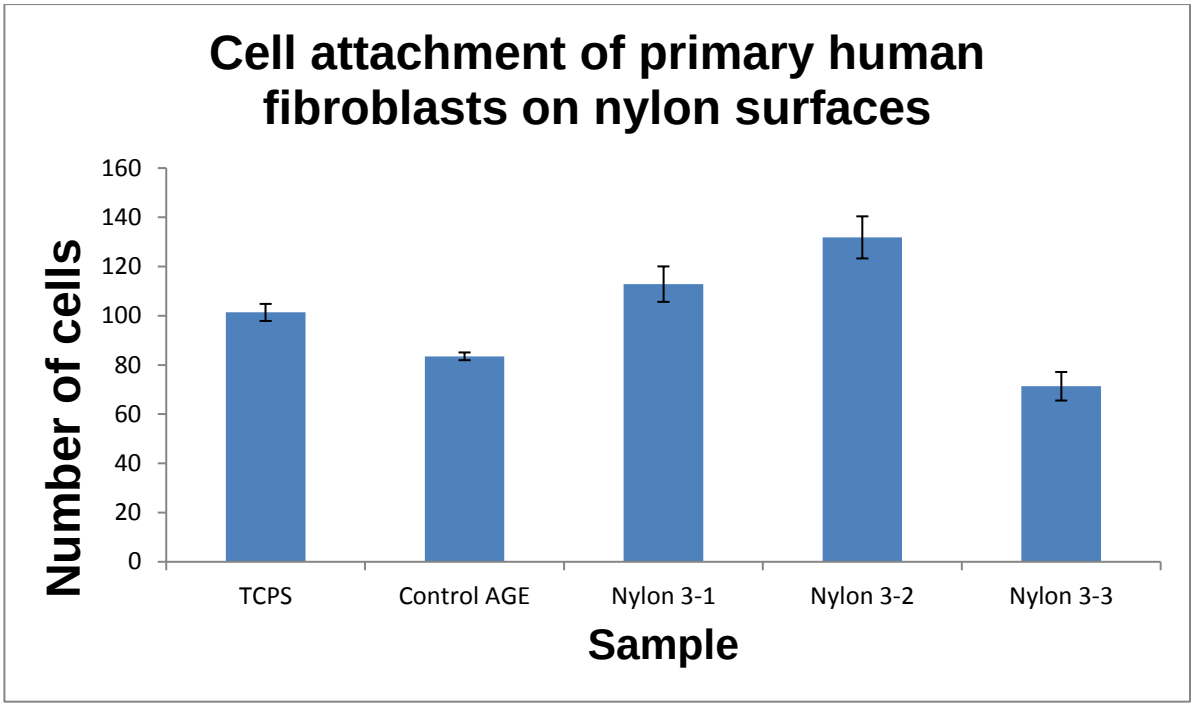


Figure 6.24: Number of human primary fibroblasts on the nylon and control surfaces after 3 days growth, counted per frame

Thus the grafted Nylon-3 coatings support good attachment of fibroblasts while selectively deterring bacterial colonization. This is an extremely interesting and useful outcome, as many antiobacterial coatings also reduce or inhibit human cell attachment. It is, however, also necessary to examine the growth morphology of the attached fibroblasts, to check for possible abnormal cell shapes. Figures 6.25 to 6.29 show that there are no adverse effects.

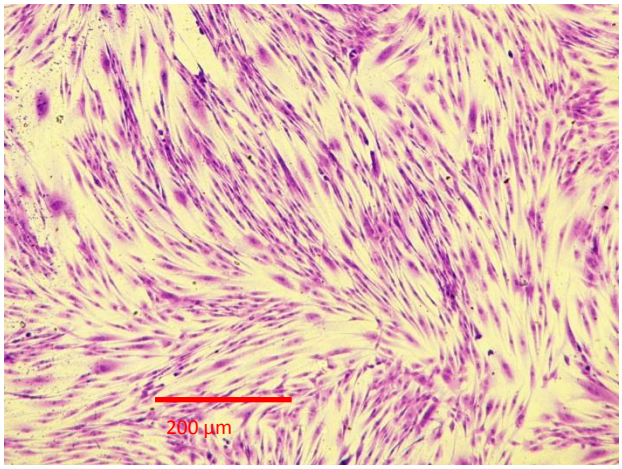


Figure 6.25: Nylon 3-1 immobilised surface with human primary fibroblasts

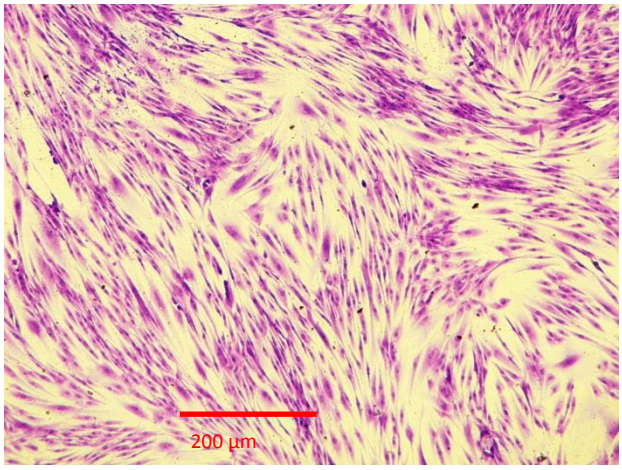


Figure 6.26: Nylon 3-2 immobilised surface with human primary fibroblasts

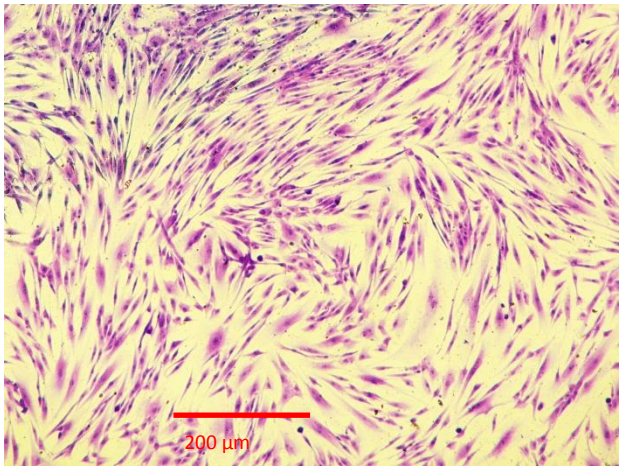


Figure 6.27: Nylon 3-3 immobilised surface with human primary fibroblasts

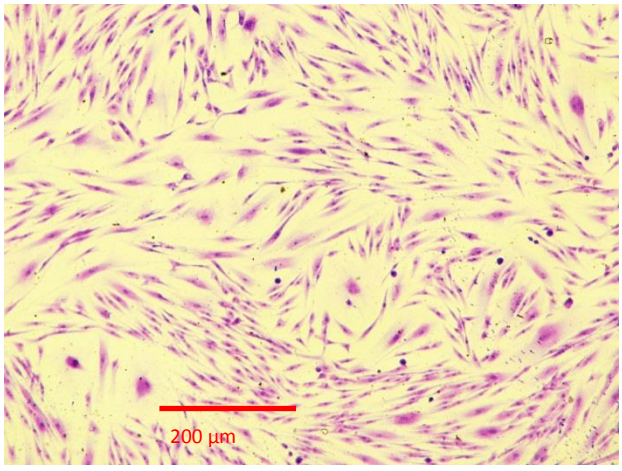


Figure 6.28: Control polystyrene surface with human primary fibroblasts

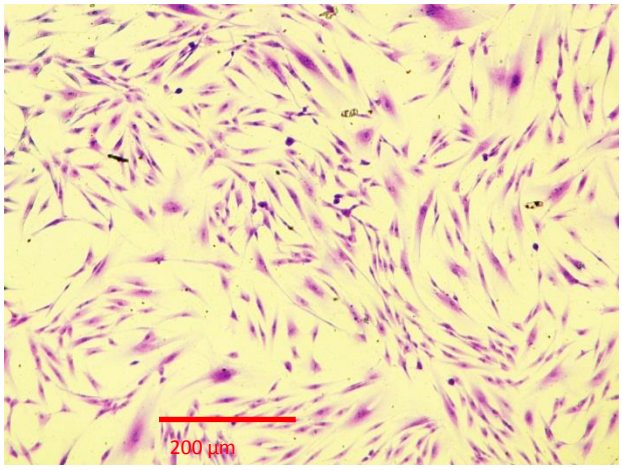
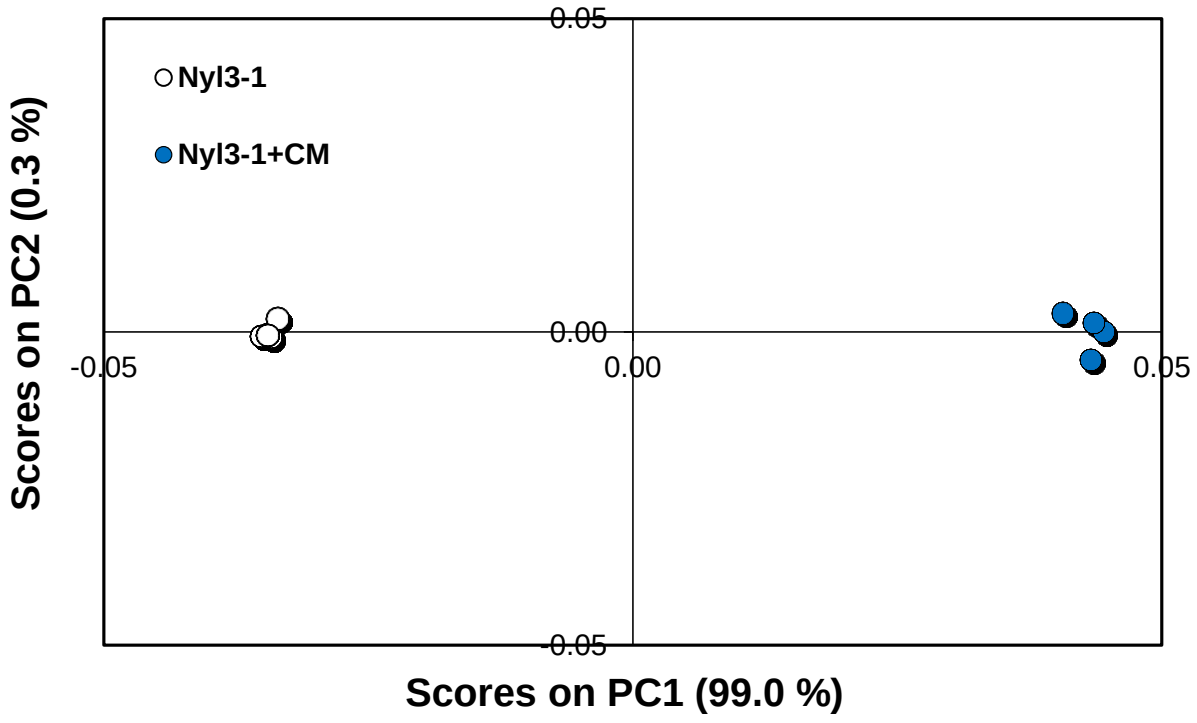


Figure 6.29: Control AGEpp surface with human primary fibroblasts

Returning to surface analyses, ToF-SIMS was used to characterize serum protein adsorption. Figure 6.30 shows that there is a marked difference in the spectra, and the loadings plot shows increased intensity of peaks assignable to various amino acids as well as reduced intensity of fragments characteristic of the Nylon-3 copolymer. This accords with the above interpretation of XPS spectra in terms of substantial amounts of adsorbed cell-adhesive proteins from serum.



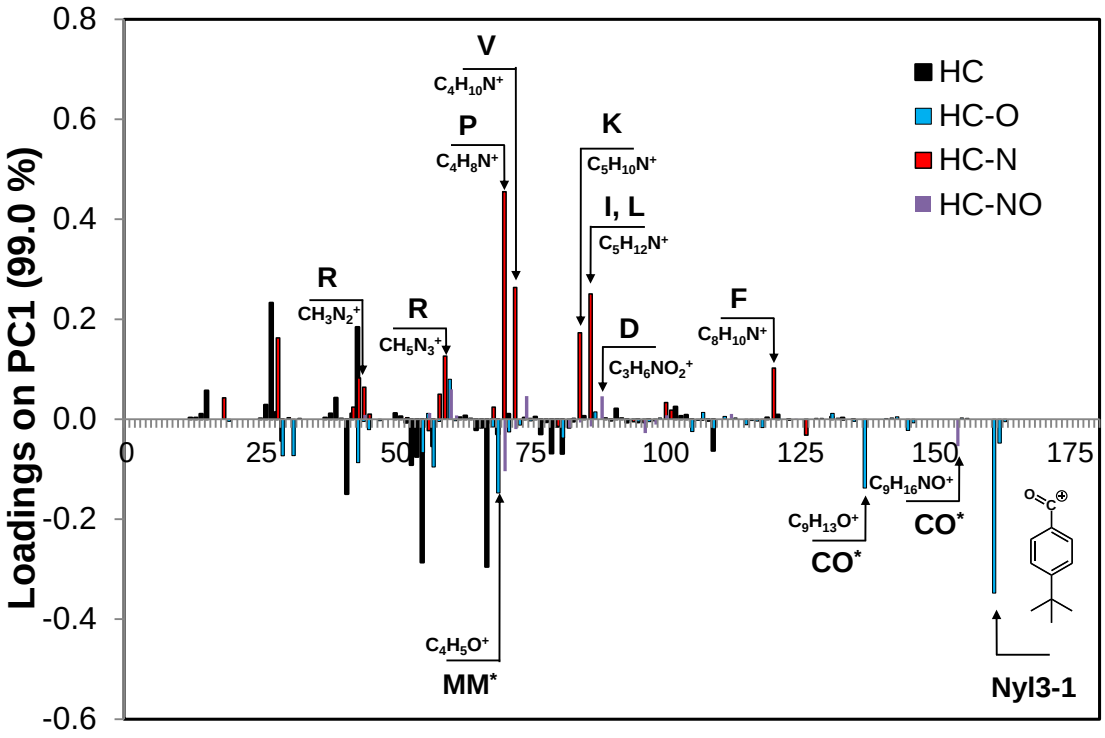
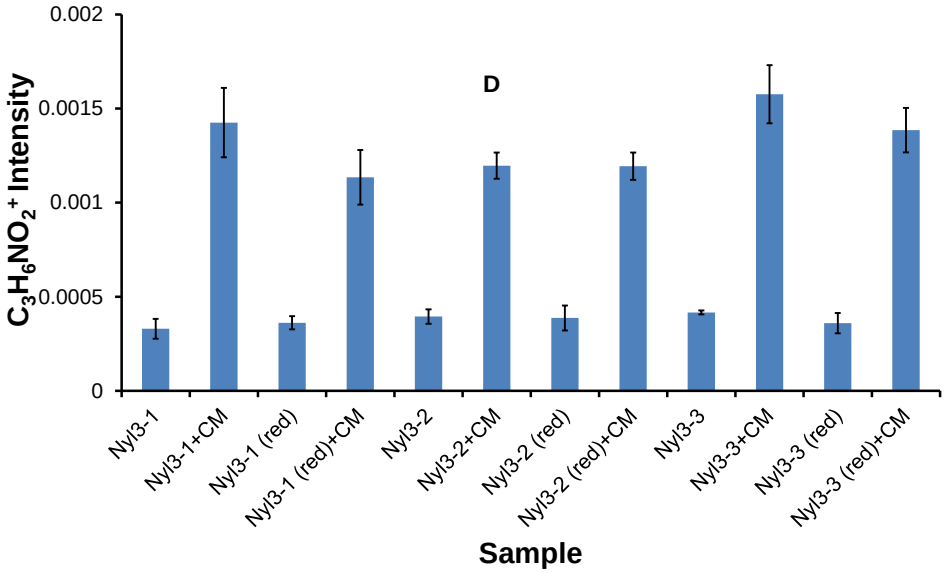


Figure 6.30: Scores on PC1 and PC2 (top) and loadings on PC1 (bottom) of positive mass spectra of nylon 3-1 and nylon 3-1 after contact with medium/serum

The intensities (relative to total intensity of all peaks) of selected peaks is shown below. They reveal clearly which peaks are most useful for characterizing protein adsorption onto the grafted Nylon-3 surfaces.



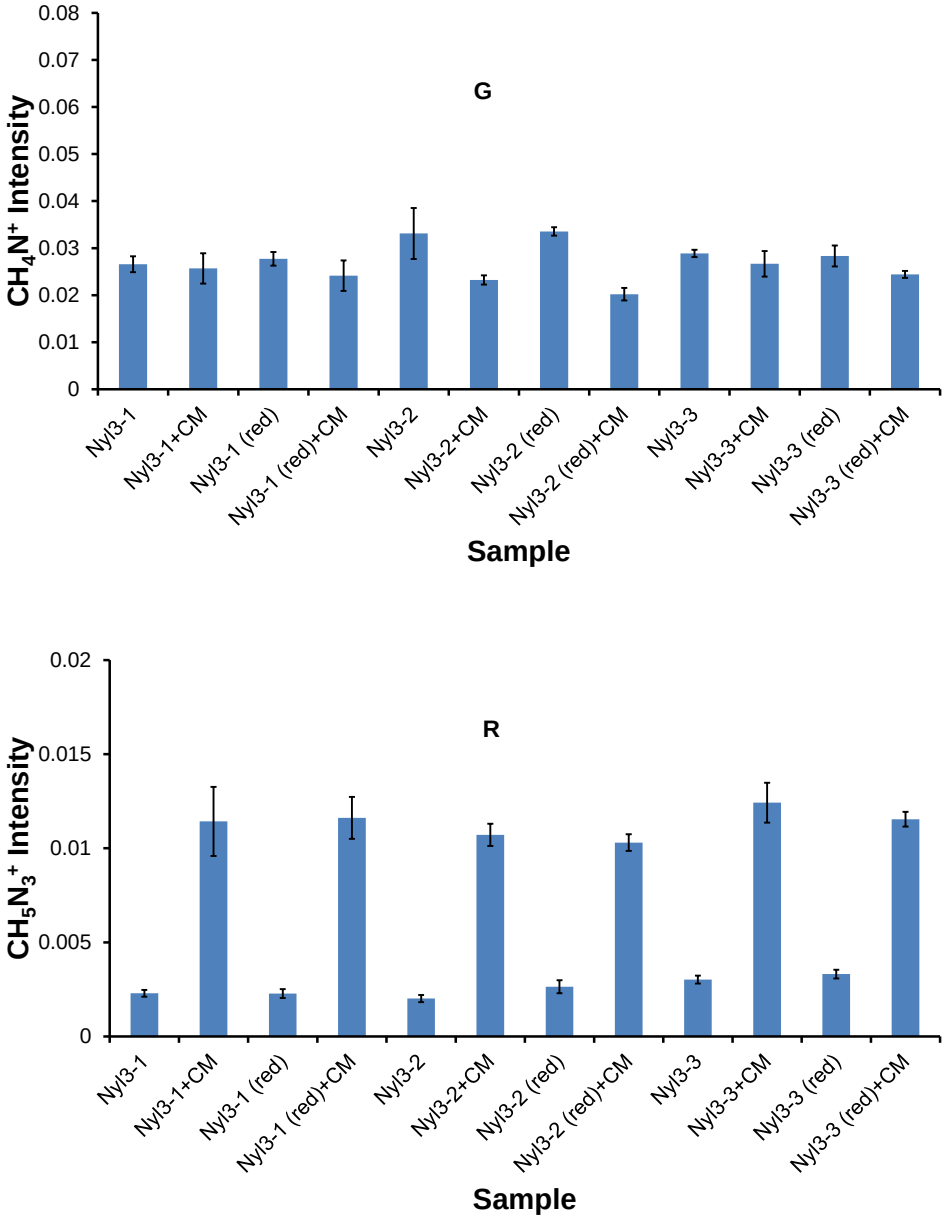


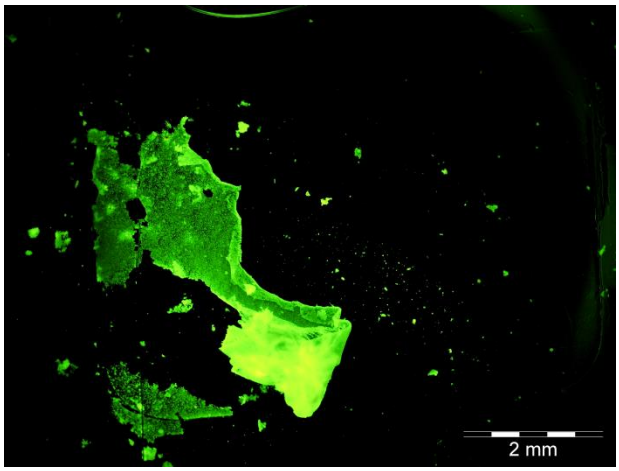
Figure 6.31: Statistically evaluated intensities of signals from aspartic acid (D), glycine (G) and arginine (R) residues across nylon-3 samples (-1, -2 and -3) before and after contact with medium/serum (cell medium, CM)

The signal assignable to the immonium ion from glycine (CH_4N^+) is the least distinct, due to substantial intensity of the same ion emitted from the Nylon-3 copolymer.

6.3.5 Testing for Antibacterial Activity in the Presence of Serum (FBS)

Having shown that serum proteins adsorb onto the Nylon-3 grafted surfaces, the question arises whether the coatings would still be antibacterial in applications where they would be in contact with serum. Adsorbing proteins might bury the grafted Nylon-3 layer and thus mask the antibacterial activity.

Grafted surfaces were tested in the presence of 10% foetal bovine serum (FBS) and albumin. It is well known that serum and, in particular, albumin can block the activity of small molecules. There was no noticeable blocking of surface activity; antimicrobial activity was sustained. However, live bacteria on the control surfaces adsorbed with serum did not stick well, making quantitative assessment difficult. Nylon samples pre-treated with serum prior to bacterial testing seemed to have more dead bacteria on the surface. It can be hypothesised that adsorbed serum proteins encourage bacteria to stick, which accords with literature as all *Staphylococcus* species possess adhesion factors that adhere to albumin and many other proteins found in serum (Cossart 2005). It is these same serum proteins that form the conditioning film on implants after they are implanted in the body (Wilson, Henderson & McNab 2002). However, evidently after the bacteria have attached onto those proteins, the grafted Nylon-3 copolymer still manages to kill them. Repeating these experiments gave a set of samples that showed some reduction of activity. It seems that the results may be affected by different batches of serum. There was insufficient Nylon-3 material available to study this further in detail. Therefore, while available results prevent quantitative analysis and there may be some reduction of antibacterial efficacy upon serum protein adsorption, the positive qualitative conclusion is that there is still activity, the grafted layer does not become completely buried underneath the adsorbed protein layer.



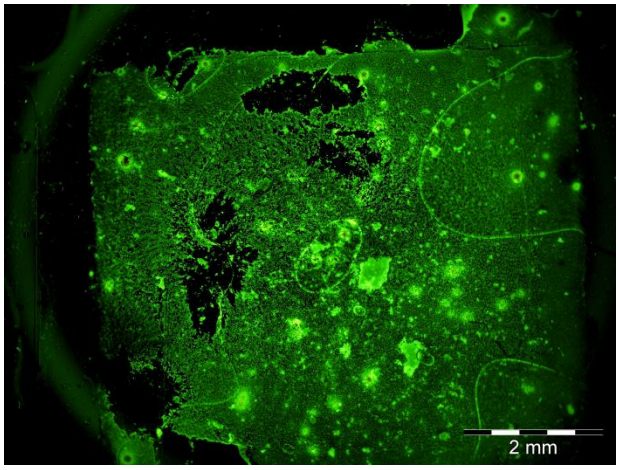


Figure 6.32: A control AGE surface with serum (above) and without serum (below), showing the difficulty of testing any surface with serum added. The serum physiosorbs onto the surface and the bacteria attach to this and are easily removed through rinsing before bacterial assessment.

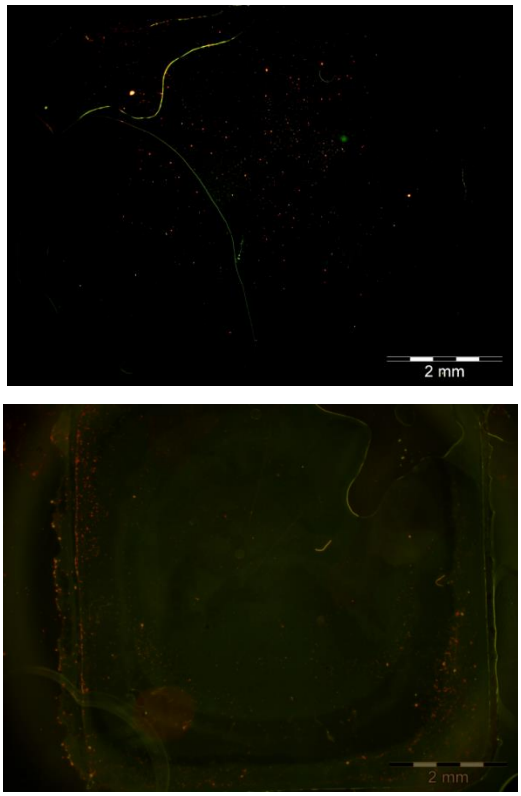


Figure 6.33: AGEpp with nylon-1 immobilised without serum (above) and with serum (below) after 5 hours incubation. There are virtually no bacteria at all on the top image, and there are more dead bacteria on the image with serum added, possibly physisorbed onto the surface.

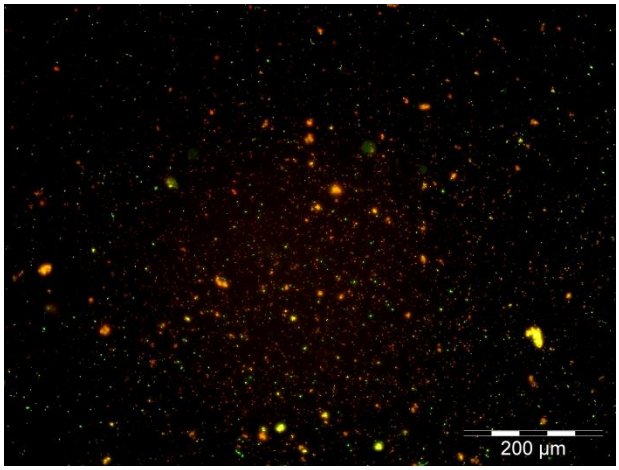


Figure 6.34: AGEpp with nylon 3 immobilised after 5 hours incubation with serum. There are more bacteria, both dead and alive. Normally, it is not useful to look at surfaces after only 5 hours incubation because very few bacteria would be present. Further rinsing may affect this image.

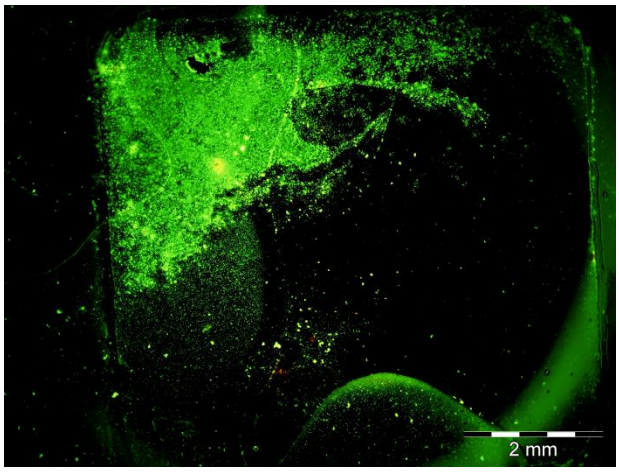


Figure 6.35: AGEpp with nylon-3.1 immobilised after 24 hours incubation with serum. This particular substrate and FBS batch did not show full antibacterial activity with serum added. This may be a result of unusually vigorous bacteria or fresh serum, or it may be a result of a new batch of substrates. The control also showed much heavier biofilm colonisation and adherence, which raises the suspicion that the bacterium may have changed its phenotype.

6.3.6 Testing for Antibacterial Activity after Storage and after Soaking in PBS

Treated surfaces were soaked for 7–10 days or stored in air, and then tested to see if activity remained over time. The samples were found to retain antimicrobial activity after storage and soaking in PBS. However, with limited amounts of Nylon-3 copolymers, a reduced set of evaluations was performed; XPS and *Bac*Light staining were used, and comparison with earlier images of the same kinds of samples was undertaken. XPS showed retention of the grafted compounds on the surface, with the percentage of nitrogen within the range of fresh samples. This shows that the grafted Nylon layer was stable to extended soaking in PBS, as would be expected for covalent grafting.

Table 6.3: XPS results showing percentage of nitrogen on fresh samples and samples soaked for 10 days

XPS %N	Fresh sample	Stored sample	Soaked sample
Nylon 3-1	4.4	4.4	4.4
Nylon 3-2	1.4	1.4	1.4
Nylon 3-3	2.3	2.2	2.3

To complement *Bac*Light staining and acquiring quantitative results on antibacterial activity after storage, manual plate counting would have been useful, but that would have required larger amounts of peptide than were still available by that time.

6.3.7 Wound Scratch Assay

The wound scratch assay is an *in vitro* model used to monitor the migration and new cell growth over an area that had been depleted of cells. This model test can be performed without bacteria present or with bacteria, to model aseptic and septic would healing processes respectively. An infected wound scratch assay has microbes pipetted into the area without cells to observe the interaction of cells and microbes. It is generally done in a time-lapse microscopy set-up, but as such a setup was not available, static images were collected for this study.

The human foetal fibroblast cell line, HFF-1, was grown in an ibidi wound scratch dish. It contains an insert that serves as a mask to generate a central area on which cells cannot attach, but cell layers are formed on both sides of this mask, which is then removed to observe how cells from both sides migrate into the simulated scratch wound to close it. In my experiments, when the cell layers on the areas on both sides of the mask had reached 75%–80% confluence, the insert was removed to reveal the area with no cells, or the 'scratch' area. To simulate septic wound healing, bacteria at 1 x 10^4 cfu/ml were pipetted onto the 'scratch' area. The bacteria were allowed to colonise the area, then medium/serum was added to maintain the cells, and the dish was left overnight. The dish was then observed after 24 hours growth. In this experiment, half the dishes were left as is, as a control or treated with AGEpp, and the other half were plasma treated without the mask insert, immobilised with nylon 3-1 to create an antibacterial surface, and the mask was replaced and the cells added.

To examine septic gap closure without an antibacterial coating present, control samples were tested. The control surface consisted of an AGEpp only. HFF-1 fibroblasts were grown in the two halves besides the mask. Then *S. epidermidis* was added at 1 x 10^4 cfu/ml to the gap in the same way as for the sample with the nylon 3-1. Figure 6.36 shows a typical image showing the cell layer, stained green, on the right-hand side of the image. The gap area that was masked while growing cells is on the left-hand side of this image, and the bacterial suspension was pipetted onto this area. The much smaller green dots in this gap area are bacteria and bacterial colonies. Evidently, bacteria quickly colonised the gap and formed biofilm in the gap and also to some extent around the cells. The LIVE/DEAD *Bac*Light stains showed green, live bacterial cells, and a few red dead cells. Live bacteria were in abundance on the control AGEpp surface. Clearly, bacteria colonise the gap area rapidly and prevent fibroblast cells from moving into the simulated wound gap and closing it.

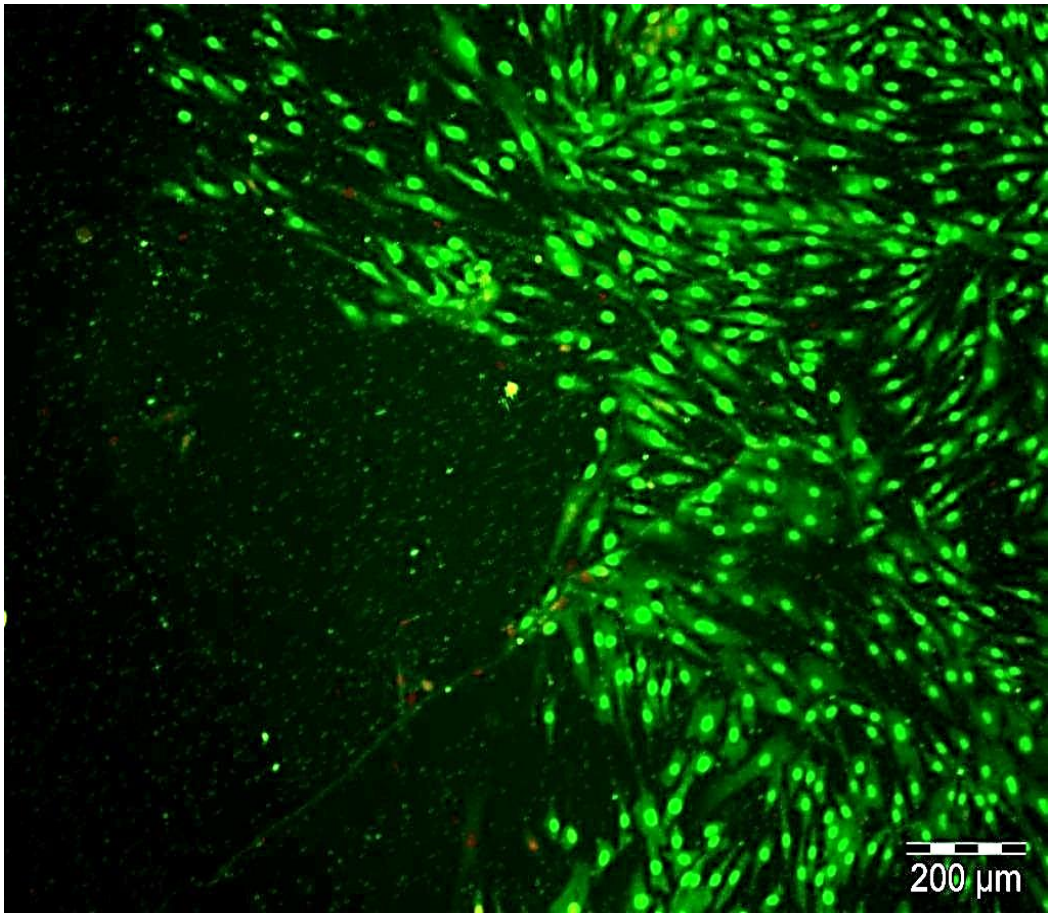


Figure 6.36: Control plasma surface with AGEpp only. LIVE/DEAD *Bac*Light stain shows HFF-1 fibroblasts that are colonised with *S. epidermidis*, the cells have not spread over the wound gap and live bacteria are colonising the wound area and between the cells. Some cells have been affected and are dead.

In contrast, when the gap area had been coated with AGEpp and grafted Nylon 3-1, completely different behaviour was observed. As shown in Figure 6.37, fibroblast cells were able to grow out over the gap area (again the left-hand side of the image) and close the wound gap. There is no visual evidence of any bacteria being present and it can be concluded that the grafted layer prevented their attachment, thus allowing fibroblasts instead to migrate into the area. Also, no cells were affected by bacteria. The bacteria were, however, still alive in suspension, as shown by growth when an aliquot was removed and spread on an agar plate. The LIVE/DEAD *BacLight* stains showed all green or live cells. Thus, the antibacterial coating in the gap area allowed wound closure but did not affect bacteria above, as expected for covalent attachment.

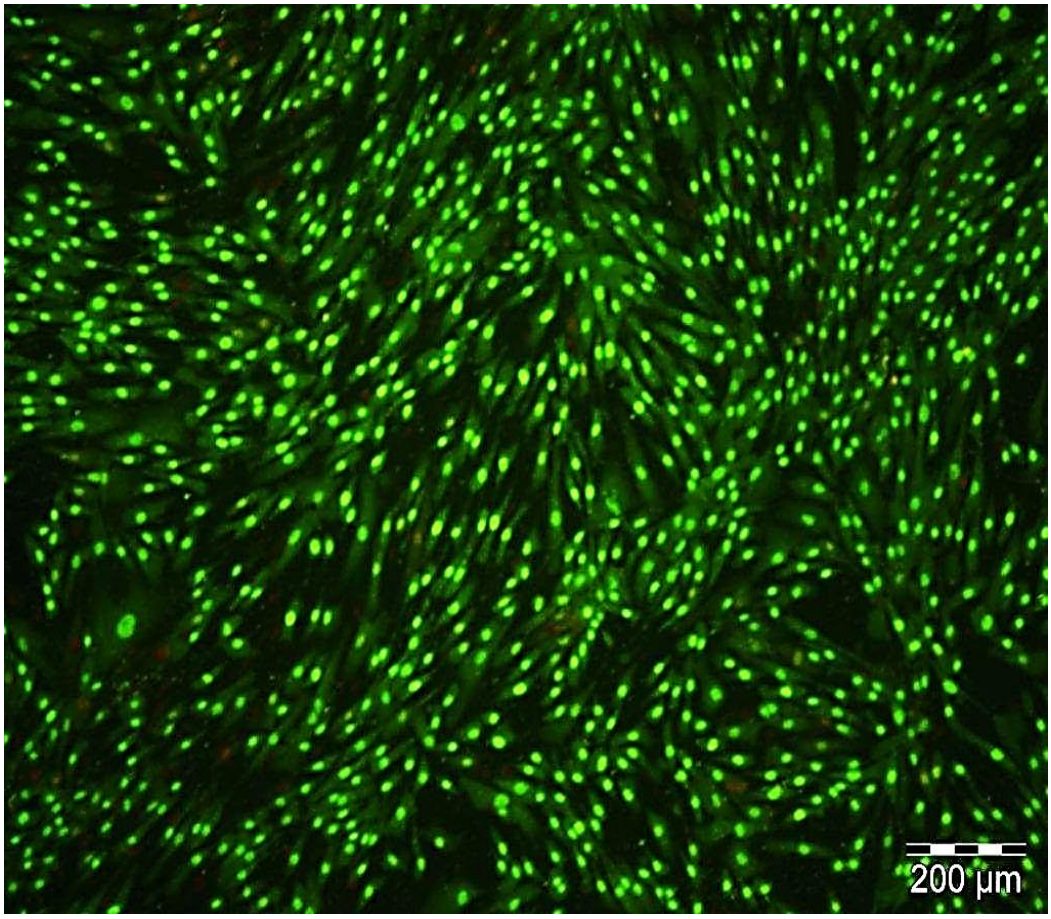


Figure 6.37: The scratch area of the wound scratch assay with HFF-1 cells using the LIVE/DEAD BacLight assay to show green/live cells that have migrated or grown across the wound area, closing it completely. No *S. epidermidis* is visible anywhere on the surface.

This wound scratch assay gives an excellent indication of how the body might react to an implanted biomaterial with nylon 3-1 immobilised onto its surface, and that a surface immobilised with nylon-3 copolymers may provide an antibacterial surface with cell-encouraging features necessary for a successful tissue-integrating biomedical product.

6.4 Discussion

Nylon 3 AMP mimics show powerful antimicrobial activity when attached to surfaces. Commonly used antibiotics require entrance into the bacteria and affect the growing bacteria by inhibiting the nucleic acid synthesis or inhibiting cell wall synthesis. These very important new peptides are bactericidal to bacteria in all states, both growing and persistent. The only other class of antibiotics to show membrane-disrupting properties is atypical tetracyclines; however, they have been found to impart serious toxicity *in vivo* (Chopra & Roberts 2001; Hakenbeck, Brueckner & Henrich 2010; Hurdle et al. 2011). The general theory for the AMP's mechanism of action is that of membrane-pore permeation by the peptides, which involves the formation of membrane-spanning pores. However, other research groups have reported other possibilities, and there is no consensus that this is indeed the mechanism of killing (Wimley & Hristova 2011).

This study also opens questions on the mechanism of action. Nylon 3-1 showed particularly good killing compared with the other two nylon 3 compounds; however, there were fewer dead bacteria on the surface and much fewer live bacteria. One has to ask how much is deterrent and how much is direct killing, and what this method of killing is. It can be ascertained that with nylon 3-1, the bacteria are deterred and any that do contact the surface are killed quickly because of the very small size and lack of biofilm. This was also seen in the wound scratch assay because the bacteria were floating on the surface of the media/broth solution rather than attaching onto the sample surface. *S. epidermidis* are surface-loving bacteria: they want to be surface bound and will always try to contact a surface. That they are not observed on the Nylon-grafted surfaces shows clearly that they do not find it acceptable and will stay in a planktonic state rather than compete with fibroblasts for space on a surface inhospitable to them.

Yet, why is this so? The nylon 3-1 is based on an amphiphilic AMP with a less ridged backbone, allowing more conformational movement, in less rigid ways, than for the usual interpretation of a rigid, membrane-pore-forming peptide (Mowery et al. 2009). The nylon 3-1 in particular is relatively hydrophobic and has a positive charge, whereas a comparable natural AMP, LL37, is less hydrophobic and has irregular charges. The repeat units of the nylon 3s also allow them to extend from the surface. The surface analysis data show that there is much scope for absorption of proteins among the many repeats and it makes a highly suitable surface for cell

adhesion. The highly charged, hydrophobic nature, on the other hand, would make it inhospitable to bacteria, and even when interspersed with proteins, Nylon 3-1 appears capable of membrane disruption. Nylon 3-1 provides a preferential surface for cells, yet an inhospitable surface for bacteria. Nylon 3-3 has a slightly different subunit group: DM, versus CH. This may render the surface less hydrophobic and changes the charge. A few more bacteria attempt to colonise and manage to adhere to it —possibly via proteins absorbing from the TSB, and the slower killing allows some bacteria to attach. More studies will need to be done considering surface charge, which may give an indication of why bacteria are deterred and killed.

Why is this subtle mechanism enough to deter and kill bacteria in very large numbers adjacent to the surface? Highly hydrophobic surfaces, such as Teflons, prevent cell attachment and are known as deterrents of bacteria, yet bacteria manage to eventually overcome them. Studies have investigated surface charge in relation to bacteria (Wilson, Henderson & McNab 2002) and many theories surmise about their interactions, yet bacteria are evolving, living things and it is difficult to say whether their surface interactions are sufficiently well understood. Antibacterial peptides have a definite membrane-destabilising activity—albeit one that is still being defined. Therefore, it could be said that it is the combination of all of these interactions that makes the nylon-3 compounds a successful antibacterial surface layer.

6.5 Conclusion

Nylon 3 antimicrobial mimics can be covalently immobilised using plasma polymerisation onto biomaterial surfaces and have excellent antimicrobial activity, creating a true antimicrobial surface. The differences in effectiveness between the Nylon copolymers can be interpreted, in the same way as for the AMPs of the previous chapter, in terms of the speed of killing bacteria attempting to attach to the surface. If membrane-permeabilising ability kills bacteria before they can firmly attach, very few dead bacteria are observed. Nylon 3 surfaces are also highly hospitable to fibroblast cell attachment, growth and migration, in that they absorb the proteins necessary for cells to attach, grow, and encourage migration. It is also likely they could be involved in immune signalling, which may promote healing, as has been found in natural AMPs, but this was beyond the scope of this thesis.

Chapter 7: Daptomycin Covalently Attached to a Biomedical Surface Using a Plasma Polymer

Abstract

The diversity of Gram-positive pathogens continues to rise steadily, yet very few new antibiotics targeting these important pathogens are entering the market. Daptomycin is a cyclic anionic lipopeptide that is thought to exert its rapid bactericidal effect by perturbing the bacterial cell membrane, a mode of action different from that of most of the traditionally used antibiotics. Hypothetically, this makes it a good target pharmaceutical for attaching covalently to surfaces to produce an antibacterial coating for biomaterial implants and medical products. Daptomycin was covalently coupled to Thermanox surfaces using an ALDpp interlayer to provide active tethering groups. The surfaces were analysed using XPS and ToF-SIMS to assess the amount of bound daptomycin and surface coverage. The surfaces were also tested against *S. epidermidis* for antibacterial activity. The daptomycin coatings were found to show no discernible activity. This raises questions about the hypothesised main mode of action because attachment should have allowed the perturbing mechanism to remain active.

This chapter is an expanded version of a publication intended for submission to a journal that had not yet been chosen at the time of writing this thesis.

The surface analyses were performed by Marek Jasieniak because of the extensive training required to become proficient in running the XPS and ToF-SIMS instrumentation. Marek also provided valuable assistance in the interpretation of the data.

7.1 Introduction

Prosthetic joints such as hips and knees are increasingly used to maintain an active and pain-free life in patients with damaged joints. They generally give good long-term results; however,

there is still a risk of bacterial infection, particularly with the common Gram-positive *Staphylococcus* strains. These can lead to serious infections involving the removal of the implant and even death. *S. epidermidis* has been found to be responsible for 30%–43% of hip and knee implant infections, and *S. aureus* is responsible for 12%–23% of infections (Zimmerli, Trampuz & Ochsner 2004). *S. aureus* can produce toxins and has strains that are highly resistant to antibiotics, which makes it a more virulent pathogen that can lead to death. After an implant is surgically fitted, the surface is covered with extracellular plasma proteins, which is often referred to as a 'conditioning film' (Wilson, Henderson & McNab 2002). *Staphylococci* adhere to these proteins through their microbial surface components recognising adhesive matrix molecules (MSCRAMM). As the bacteria multiply, they aggregate to form biofilm, which consists of polysaccharide intercellular adhesion (PIA), extracellular DNA, or proteins such as fibronectin binding proteins (Cossart 2005). This biofilm matures into a complex three-dimensional structure that protects bacteria from the immune responses by preventing bacterial complement binding and reducing phagocytosis. The biofilm also makes it difficult for antibiotics to permeate this complex structure and kill multiplying bacteria. Growth of the biofilm is maintained by the PIA, which controls gene expression of virulence factors (Cossart 2005; John et al. 2011); other gene changes stabilise *Staphylococci*, some enter the persister or dormant phase, and others are released to colonise further areas and form new biofilm (Lewis 2010).

To prevent device-related infection, it would be highly advantageous to have drugs with bactericidal effects on surface-adhering, slow-growing and biofilm-producing microorganisms that could then be used as coatings for implantable devices. It would also be beneficial if those drugs could act independently of the bacterial physiological state and prevent adherence and biofilm formation of the bacteria at the surface.

Daptomycin (Figure 7.1) is a cyclic lipopeptide produced by *Streptomyces roseosporus*, which exhibits a concentration-dependent bactericidal activity against Gram-positive organisms, including MRSA (Steenbergen et al. 2005). Daptomycin has a very low MIC of <1 ug/ml even against MRSA (Carpenter & Chambers 2004).

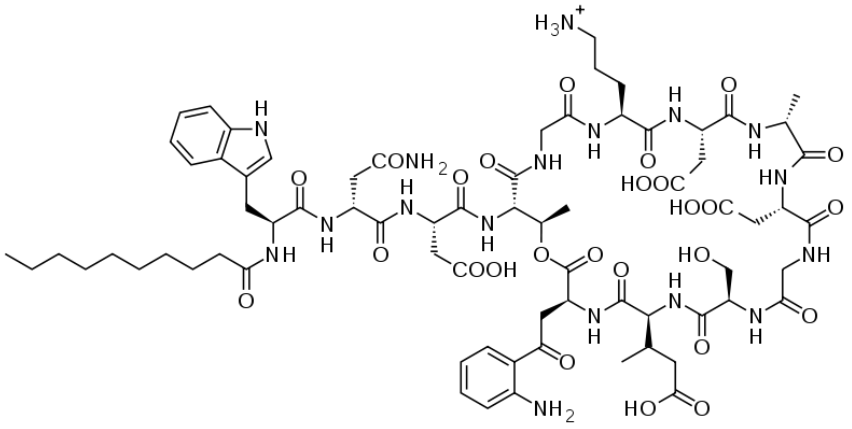


Figure 7.1: Daptomycin, $C_{72}H_{101}N_{17}O_{25}$ (1619.7086 MW)

It is believed that the bacterial membrane is the only target, and that lipophilic peptides target and bind to the bacterial cytoplasmic membrane directly, leading to leakage of potassium and possibly other ions, and ultimately to loss of membrane potential and cell death (Silverman, Perlmutter & Shapiro 2003; Straus & Hancock, 2006). Daptomycin adopts a structure that is reasonably well defined but not highly amphiphilic. Three different structures have been reported in the literature (Ball et al. 2004; Jung et al. 2004; Rotondi & Gierasch 2005). Hancock et al. have proposed, however, that in the presence of calcium ions, daptomycin adopts an amphiphilic structure similar to cationic AMPs. Once a 1:1 calcium to daptomycin molar ratio is reached, the lipopeptide oligomerises to form a 14–16-mer and most likely arranges itself into a micelle (Ho et al. 2008), and according to them, this process is not accompanied by a change in conformation, as originally proposed. Once the daptomycin micelle comes into close proximity with the bacterial membrane, the multimer dissociates, and daptomycin inserts into the bacterial membrane bilayer. Insertion of daptomycin into the membrane is accompanied by the induction of positive membrane curvature (Jung et al. 2008). Oligomerisation and/or conformational changes of daptomycin in the membrane may occur and the membrane ends up being perforated (Scott et al. 2007; Straus & Hancock 2006). Finally, bacterial cells are killed by membrane perforation (assessed as depolarisation) or some other membrane-associated event (Scott et al. 2007).

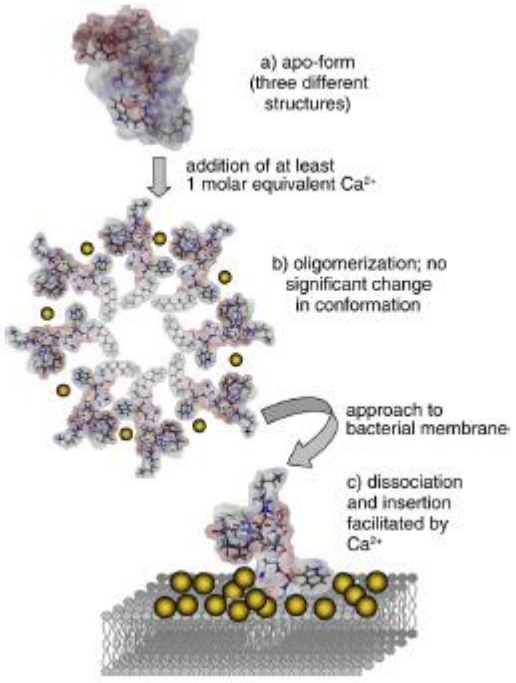


Figure 7.2: Possible mechanism of action of daptomycin: (a) without calcium, (b) with calcium in a 1:1 ratio, (c) upon contact with the bacterial membrane

Research by Pogliano, Pogliano and Silverman (2012) provides further insight into the possible mechanism. In that study, they stained the bacterial membrane, tagged the daptomycin with a BODIPY label and observed the interaction in real time. Bacteria grown in sublethal concentrations showed a striking change in bacteria membrane morphology. The cells became severely bent and occasionally swollen with patches of extra membrane. In Gram-positive bacteria, the essential cell division protein DivIVA relies upon changes in membrane geometry to regulate its localisation and activity (Eswaramoorthy et al. 2011; Lenarcic et al. 2009; Pogliano, Pogliano & Silverman 2012; Ramamurthi & Losick 2009). DivIVA is an essential cell division protein that regulates cell division assembly for the specific type of bacteria used in this study, and is thought to be associated with membrane curvature (part of cell division). The daptomycin BODIPY conjugate gave clear insights into the mechanism of action and showed that the first effect of daptomycin on the cell is the generation of randomly positioned membrane patches at both lethal and sublethal doses. The second effect is that these membrane patches recruit proteins thought to be capable of recognising negative membrane curvature, specifically the protein DivIVA. Thirdly, the dramatic effect on the cell wall physiology was

observed with altered growth shapes and changes in cell wall physiology. This hypothesis is summed up in Figure 7.3.

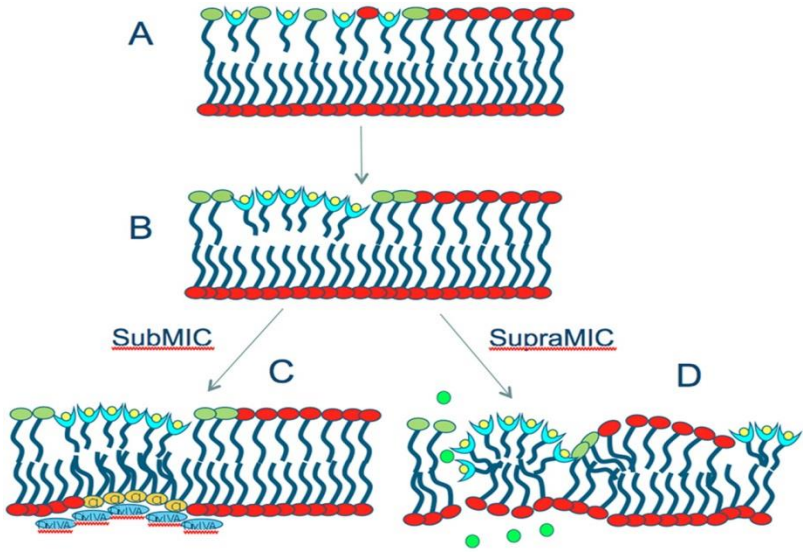


Figure 7.3: A refined model for the mechanism of action of daptomycin (light-blue 'cups' with yellow circles). Also shown is phosphatidylglycerol (green lipids), cardiolipin (yellow lipids), potassium ions (green circles), and DivIVA (blue ovals). (Pogliano, Pogliano & Silverman 2012)

Daptomycin does not inhibit any of the enzymatic steps in cell wall biosynthesis that have been tested so far (Dugourd et al. 2011; Hashizume et al. 2011; Rubinchik et al. 2011), further supporting the theory that membrane geometry is the essential target. Because daptomycin is sourced from *S. roseosporus*, it has been suggested that it normally serves as a diffusible morphogen—an ecological role in bacterial evolution because it could stimulate the formation of DivIVA patches and encourage branching in its own species, yet kill other species such as *Bacillus*.

Thus, despite nearly 25 years of study and 8 years of clinical use, aspects of the mechanism of action are still unclear. Daptomycin has definitely membrane-destabilising functions, which makes it a good candidate for covalent surface attachment onto biomaterials in an attempt to create antibacterial coatings. But will it function if, by being surface-tethered, it can't form micelles? A model that shows the possible integration of daptomycin into the bacteria

membrane (Figure 7.4) raises the possibility that by tethering daptomycin via the amine groups, located mainly along the top edge, it may still function when surface attached. Considering the lack of definite information on the specific mechanism of activity, it is an extremely interesting target for surface attachment.

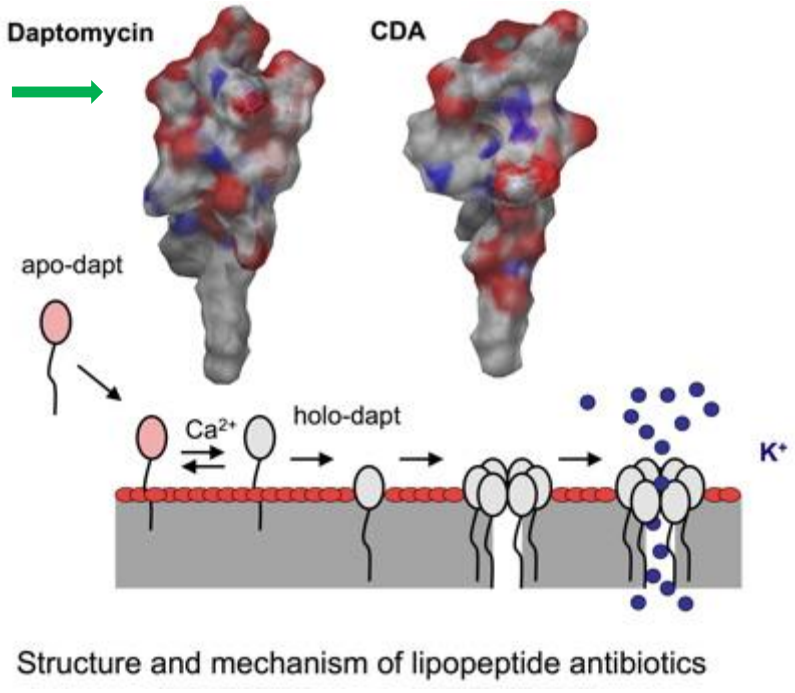


Figure 7.4: A proposed mechanism of antibacterial activity if surface attached via the upper cluster of amine group indicated by the green arrow (Powell, Al Nakeeb et al. 2007; Powell, Borg et al. 2007). There are other amine groups in this area and the opposite side that would also attach.

In this study, daptomycin was covalently tethered to aldehyde functional groups producing using plasma polymerisation (Griesser & Chatelier 1990; Thierry et al. 2008). This might lead to tethering that is too rigid for the peptide to function, or might not allow it to form the micelles necessary as hypothesised by Hancock (Jung et al. 2008). Studying daptomycin covalently attached to a surface might shed further light on its activity and requirements for mobility and micelle formation.

The studies supporting resistance of bacteria also lead to questions about the mechanism of action, because it has been believed that antibiotics that do not enter the bacteria will be less susceptible to resistance. Resistance to daptomycin has come from mutations in the genes responsible for the cell membrane formation, such as MprF, a membrane protein responsible for synthesising a positively charged phospholipid. The cell wall has also been shown to be affected: studies have shown that daptomycin induces the cell wall stress response typically induced by cell wall–active antibiotics. Thus, the question is whether tethered daptomycin can affect the bacterial cell wall to a sufficient extent.

7.2 Methods

7.2.1 Samples

Daptomycin (Sigma, USA) was covalently immobilised onto intermediate thin coatings, (approximately 18–20 nm thick as determined by ellipsometry) prepared by the plasma polymerisation (pp) of propanal (99% Aldrich, USA) or AGE (99% Aldrich, USA) as described in previous chapters. Immobilisation onto AGEpp requires no further stabilisation (Thierry et al. 2008); however, ALDpp requires reductive amination using $NaBH_3CN$. As substrates, silicon wafers (Micro Materials and Research Consumables, Australia), Thermanox coverslips (ProSciTech, Australia), polystyrene slides (ProSciTech, Australia) with FlexiPERM removable 12-well masks (Sarstedt, Australia), and ibidi 1 u-Slide 18-well uncoated microscopy chambers (no. 81821, ibidi, Australia) were used. All work was undertaken in a biohazard cupboard, except plasma coating, which is a sterilising procedure anyway. Daptomycin arrived in a 1 mg vial; 10 ul DMSO was added and vortexed thoroughly to remove powder from the entire flask; when in solution, 990 ul of sterile PBS was added and vortexed further. The daptomycin solution was diluted 1/10 and aloquated into tubes for later use; 100 ul was added per sample to cover the surface. Aldhyde plasma polymer samples had 100 ul of 1 mg/ml NaBH3CN added after 1 hour contact with daptomycin. Samples were left overnight at 18 ^{o}C. Before testing, samples were soaked and rinsed a minimum of 12 times over 2 hours. The final rinse occurred after covalent attachment was collected and tested against bacteria to prove that no peptide remained in solution; results were indeed from covalently attached peptides only.

7.2.2 Surface Analysis

Surface characterisation was performed by XPS and ToF-SIMS. For XPS, a Kratos AXIS Ultra DLD spectrometer was used, with monochromatic AlK_α radiation ($h\nu$ = 1486.7 eV). The system is equipped with a magnetically confined charge compensation system (low-energy electrons are confined and transported to the sample surface by magnetic field). Spectra were recorded using an acceleration voltage of 15 keV at a power of 225 W. Survey spectra were collected with a pass energy of 160 eV and an analysis area of 300 × 700 μm. High-resolution spectra were obtained using a 20 eV pass energy and an analysis area of ~300 × 700 μm. Data analysis was performed with CasaXPS software (Casa Software Ltd). All binding energies were referenced to the low-energy C 1s peak at 285.0 eV. Core level envelopes were curve fitted with the minimum number of mixed Gaussian–Lorentzian component profiles. The Gaussian–Lorentzian mixing ratio (typically 30% Lorentzian and 70% Gaussian functions); the full width at half maximum, and the positions and intensities of peaks were left unconstrained to result in a best fit.

ToF-SIMS measurements were performed with a PHI TRIFT V nanoTOF instrument (PHI Electronics Ltd, USA). A 30 keV, pulsed primary $^{197}Au^+$ ion beam was used to sputter and ionise species from each sample surface. PHI's patented dual beam charge neutralisation system using a combination of low-energy argon ions (up to 10 eV) and electrons (up to 25 eV) was employed to provide an excellent charge neutralisation performance. Positive mass axis calibration was done with CH_3^+, $C_2H_5^+$ and $C_3H_7^+$. Spectra were acquired in the bunched mode for 60 seconds from an area of 100 μm x 100 μm. The corresponding total primary ion dose was less than 1 x 10^{12} ions cm^{-2}, and thus met the static SIMS regime (Briggs 1998). A mass resolution m/Δm of >7000 at nominal m/z = 27 amu ($C_2H_3^+$) was typically achieved.

Some samples were characterised by multiple positive ion mass spectra, which were collected from sample areas that did not overlap. All recognisable, clear (i.e. unobscured by overlaps) fragment ions from 2 up to 175 amu range were used in calculations. The peaks were normalised to the total intensity of all selected peaks. Multiple mass spectra were processed with the aid of

PCA (Jasieniak et al. 2009). PCA was performed using PLS_Toolbox version 3.0 (Eigenvector Research, Inc, Manson, WA) along with MATLAB software v. 6.5 (MathWorks Inc, Natick, MA).

7.2.3 Bacteria

Bacteria (*S. epidermidis* ATCC 35984, *S. aureus* MRSA ATCC 43300 and *E. coli* ATCC 35922) were plated from frozen stock and incubated overnight at 37 ^{o}C. One colony was picked from the plate and grown in 10 ml TSB with glucose (Oxoid) overnight at 37 ^{o}C. Bacteria were diluted 1/100 and grown to log phase and then diluted to 1 x 10^6 bacteria/ml using predetermined spectroscopy measurements as a guide. Depending on the substrate, bacteria solutions were added at 100 ul or 300 ul (actual amounts at approximately 1 x 10^5 or 3 x 10^5; note that growth occurs between diluting and adding to samples and with some bacteria even 30 minutes can result in a doubling or more of bacteria) and grown for 5 and 24 hours at 37 ^{o}C. As a control, the same amounts were serial diluted and plated on nutrient agar (Oxoid) and counted to ascertain exact bacteria added to surface. Surfaces were analysed using LIVE/DEAD *Bac*Light Bacterial Viability assay kits (Invitrogen), and viable bacteria count plating.

Polystyrene slides or ibidi u-Slide wells were plasma treated. A FlexiPERM 12-well removable mask was placed on the slide and ibidi u-Slides were used as is; antimicrobial polymers were added to the wells for grafting overnight. After rinsing, bacteria were added for incubation for various periods, followed by rinsing twice to remove loosely attached bacteria. The wells were treated with the LIVE/DEAD *Bac*Light stain and the mask carefully removed before microscopy examination. Viability counts were done by scraping and rinsing the wells carefully with 1 ml of TSB. The wells were visually examined to ascertain that all adherent bacteria were harvested. The 1 ml of TSB with bacteria was then serial diluted and 100 ul was plated onto nutrient agar plates. Plates were incubated for 24 hours and colonies were counted. Daptomycin was also tested in the presence of 100 mg/L Ca^{2+} and without calcium (John et al. 2011), because it is has been found to improve killing and promote micelle formation (Straus & Hancock 2006).

7.2.4 Cell Attachment

To test whether surface-grafted daptomycin would manifest cytotoxicity, two fibroblast cell lines were used—HFF-1 (HFF-1 human fibroblast, ATCC SCRC-1041) and 3T3 (NIH-3T3 mouse fibroblast, ATCC CRL-1658)—primary human fibroblasts harvested from fresh skin (MacNeil, Shepherd & Smith 2011). All cell cultures were maintained according to ATCC instructions or published protocols (MacNeil, Shepherd & Smith 2011). Plasma- and-peptide-treated Thermanox coverslips were place in sterile 24-well culture plates (Nunc, Invitrogen) and prewarmed in a cell culture oven. Primary cells were tested using plasma treatment and attachment of polymers in ibidi micro-chamber 12-well glass slides (ibidi 81201, Germany). Cells were made up to 50,000 transformed cells per ml in medium/serum or 10,000 primary cells per ml in medium/serum and added at 1 ml to each well or 100 ul to ibidi wells. Well plates were placed into the culture oven and left for 48 hours. The coverslips were rinsed to remove non-adherent cells and placed on a glass slide and coverslip for immediate microscopic analysis. ibidi wells were stained using DAPI nucleus stain (Invitrogen) and used as per instructions.

7.3 Results and Discussion

7.3.1 Surface Immobilisation and Characterisation

Daptomycin has a molecular weight of 1619.71 Da and the formula is $C_{72}H_{101}N_{17}O_{25}$. Because of the small size of the molecule (compared with other proteins) and the small number of nitrogen-containing functionalities, surface analysis was not as informative as it is with larger molecules. In initial grafting experiments, Daptomycin was trialled on both the AGE plasma polymer and the ALD plasma polymer, in the latter case with the addition of reductive amination to stabilise the imine bonds. AGEpp was preferred because reductive amination is toxic and less amenable to handling. Attachment was found to be similar in both cases as shown by %N in XPS; therefore, AGE was chosen for all the following experiments. The AGEpp surface did not have any measurable amount of nitrogen present; therefore, the N intensity can be assigned solely to daptomycin.

Table 7.1: Surface composition using XPS

Sample	Composition, atomic %		
	O	N	C
-AGEpp	22.18	–	77.82
-AGEpp-Dapt (1)	22.33	1.13	76.54
-AGEpp-Dapt (2)	22.01	0.72	77.27

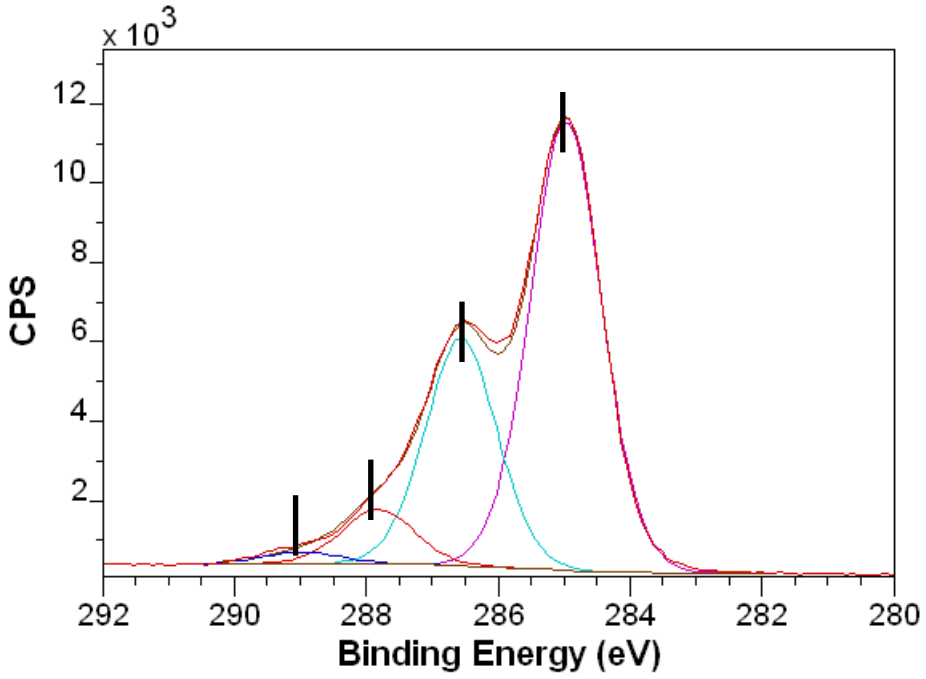


Figure 7.5: High-resolution C 1s spectrum of AGEpp

The XPS C1s signal accords with spectra recorded previously. The peak assignments (from right to left) are:

1. C-H/C-C (BE = 285.0 eV)
2. C-O (BE = 286.5 eV)
3. C=O (288.0 eV)
4. O-C=O (289.0 eV)

7.3.2 Bacterial Testing

Surfaces were tested with *S. epidermidis* ATCC 35084, which give an excellent biofilm that remains attached to the surface in controls. The LIVE/DEAD *Bac*Light stain was used to give an indication of activity and followed up with plating of the bacteria on the surface to give approximate colony counts.

The *Bac*Light stain shows the live bacteria as green and the dead bacteria as red. When a biofilm has formed, there is a yellow/green colour that indicates live bacteria. This test was repeated four times and at 6 hours and 24 hours for each set of samples, and at 12 samples per set or 24 samples for each period (see Figures 7.6 to 7.11).

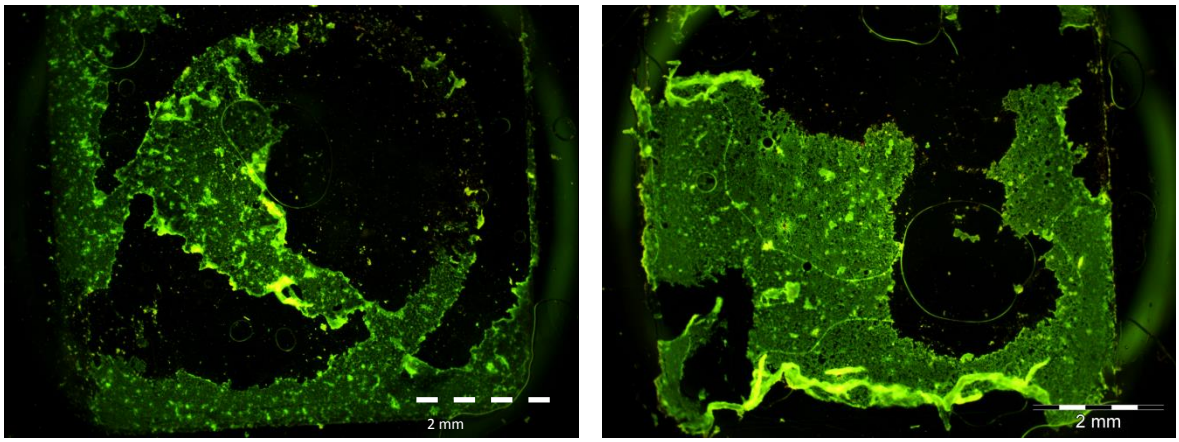


Figure 7.6: *S. epidermidis* after 24 hours incubation at 37 ºC on an AGEpp control surface, and ALDpp control surface with $NaBH_3CN$. Both surfaces showed full biofilm over the entire surface, which detached with rinsing.

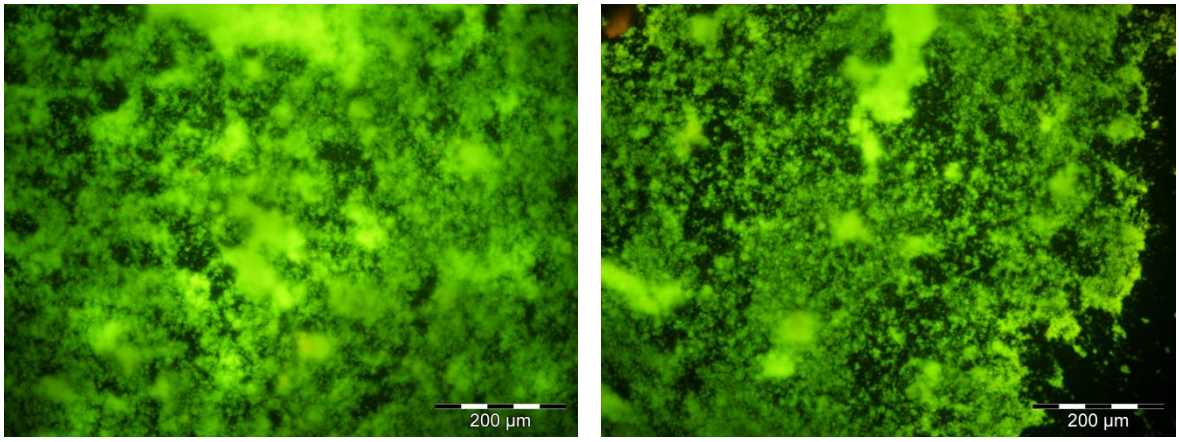


Figure 7.7: The same samples as the ones above shown at 20x magnification. No dead bacteria are visible.

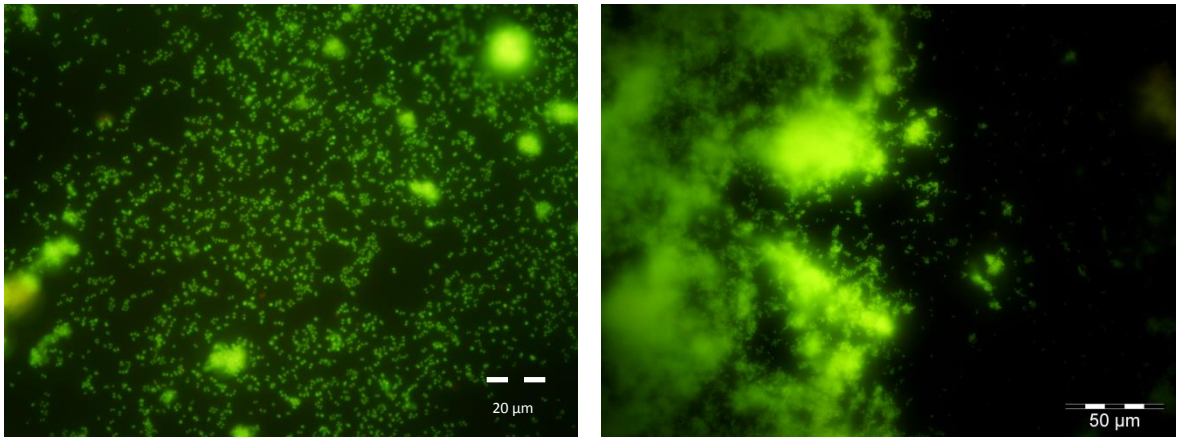


Figure 7.8: The same samples again at 100x and 60x magnification and very few dead bacteria are seen

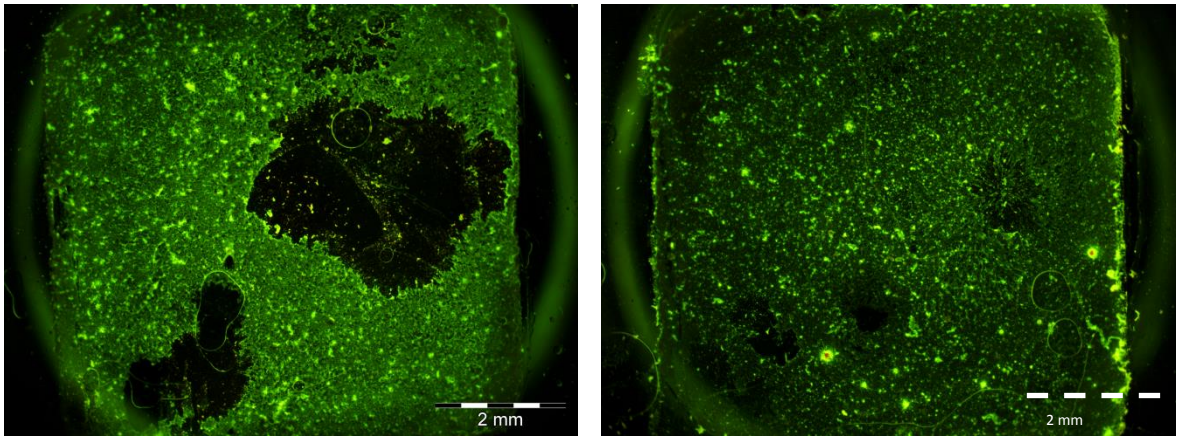


Figure 7.9: *S. epidermidis* after 24 hours incubation at 37 ºC on an AGEpp daptomycin surface, and ALDpp daptomycin surface with $NaBH_3CN$. Both surfaces showed full biofilm over the entire surface, which seemed to be more firmly adhered and detached less with rinsing.

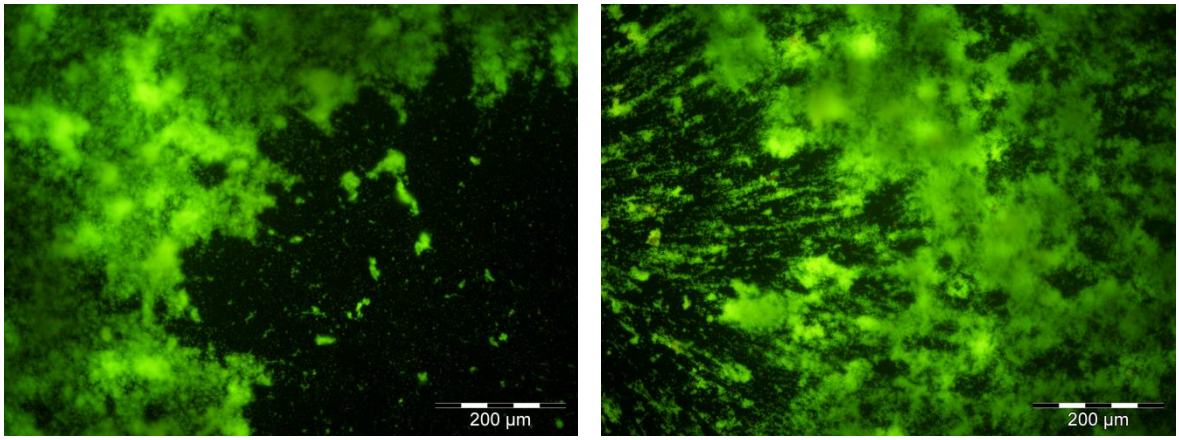


Figure 7.10: The same samples as the ones in Figure 7.9 shown at 20x magnification. No dead bacteria are visible.

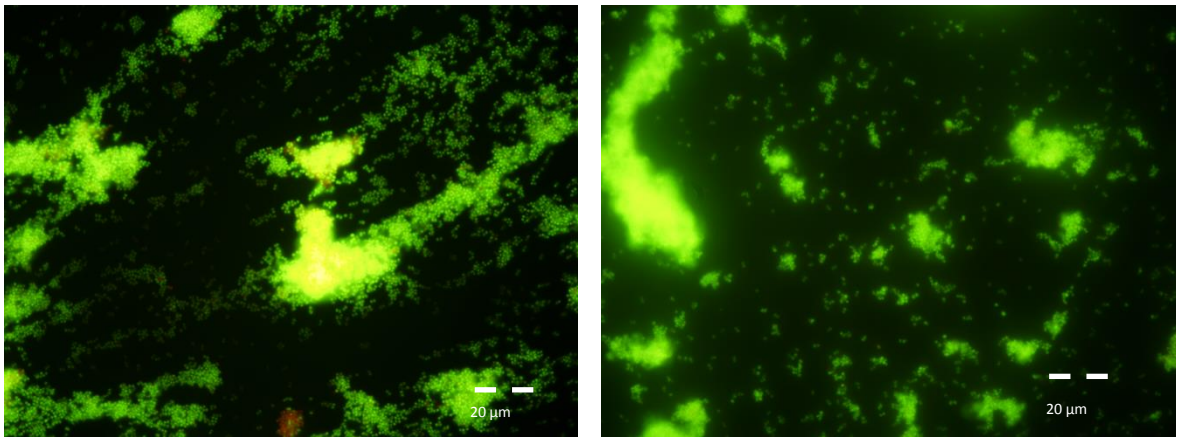


Figure 7.11: The same samples again at 100x magnification and very few dead bacteria are seen.

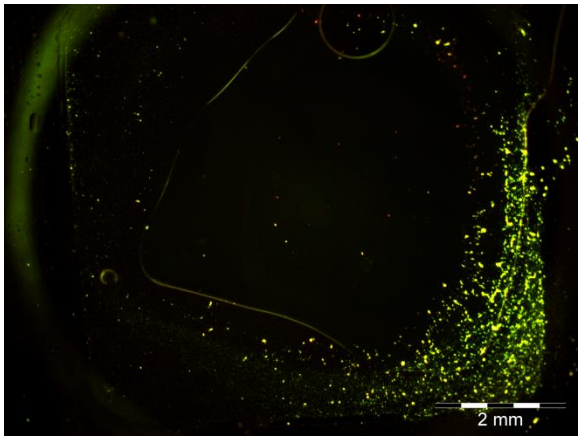
To verify the results of the *Bac*Light images, bacterial biofilms from three samples from the four sets of 24 samples used to record the images in Figures 7.6 to 7.11 were manually scraped off using a microscope to make sure that all the bacteria were removed. These bacteria from the samples were collected, serially diluted, plated onto nutrient agar plates, and incubated overnight; colonies were counted the next day. The results are shown in Table 7.2.

Table 7.2 Bacterial counts obtained by manual scraping and plating of bacteria from control AGEpp and Daptomycin-coated surfaces

Dilutions	Samples			
	Control AGEpp	Control ALDpp with $NaBHC^3N$	Daptomycin AGEpp	Daptomycin ALDpp with $NaBHC^3N$
1	>300 smear	>300 biofilm smear	> 300biofilm smear	>300 biofilm smear
2	>300 smear	>300 biofilm smear	>300 biofilm smear	>300 biofilm smear
3	>300	>300	>300 biofilm smear	>300
4	>300	>300	>300	>300
5	>300	>300	>300	>300
6	>300	457	470	606
7	215	417	463	195
8	80	196	187	45
9	39	141	128	34
10	21	225	41	21
11	3	>300	28	7
12	0	210	22	15

These tests were repeated three times and all results were the same within experimental variability. They clearly indicate that surface-grafted Daptomycin is not active against *S. epidermidis* biofilm formnation. It was ascertained that this was not caused by a non-viable batch of bacteria (cultured up from frozen suspension) by using the same batch with samples of surface-grafted Nylon-3 synthetic peptide mimics; they were tested at the same time and as reported in the previous chapter, they showed effcient killing as shown by *Bac*Light assessment and plating. Thus, it appears that Daptomycin loses activity when surface-coupled.

A further set of samples was examined after only 6 hours of incubation (Figures 7.12 and 7.13).



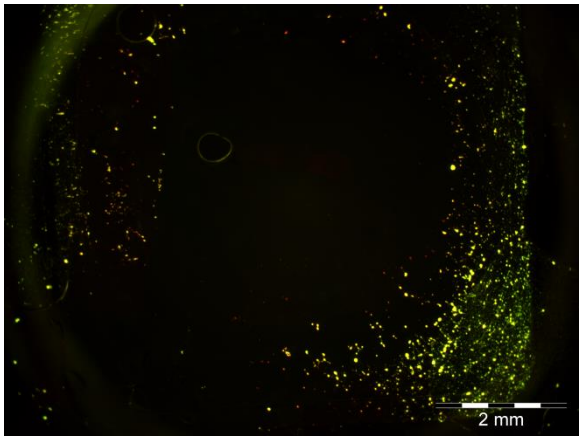


Figure 7.12: *S. epidermidis* after 6 hours incubation at 37 ºC on an AGEpp surface, and ALDpp surface with $NaBH_3CN$. Both surfaces show some bacteria colonising the surface with a few dead bacteria towards the centre; this could be a result of damage during staining.

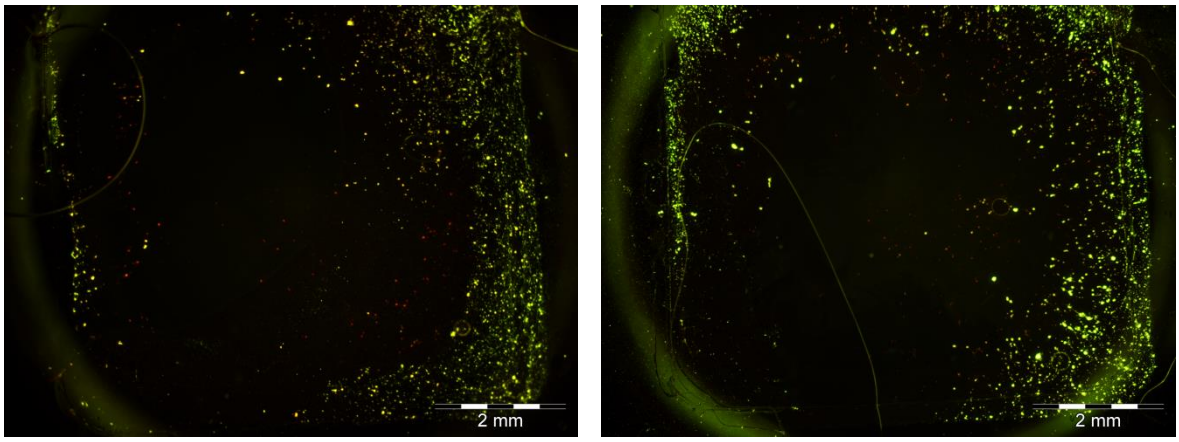


Figure 7.13: *S. epidermidis* after 24 hours incubation at 37 ºC on an AGEpp + Daptomycin surface, and ALDpp + Daptomycin surface with $NaBH_3CN$

In both cases the images show mostly live bacteria on the surface with a few dead bacteria; as above, this may be a result of damage during staining. As the results in Figures 7.12 and 7.13 show, this was not evident after 24 hours. Although there might have been some killing after 6 hours, any such effect is rather minor and was not statistically significant. Accordingly, there is no stastistically significant evidence for killing when daptomycin is covalently tethered to a biomaterial.

It has also been reported that addition of Ca2+ enhances the bactericidal activity of daptomycin in solution and on adherent bacteria (John et al. 2011). It was found that an addition of 100 mg/litre Ca^{2+} to a 30 ug/ml daptomycin solution significantly reduced adherence of MRSA, whereas Ca^{2+} alone has no effect on bacterial survival. I added 5 mMol/l Ca^{2+} to one aliquot of the 0.1 mg/ml daptomycin solution, and to the bacterial solution of a second set (Figure 7.14). Neither set showed any significant reduction in the amount of biofilm formed on the solid surface.

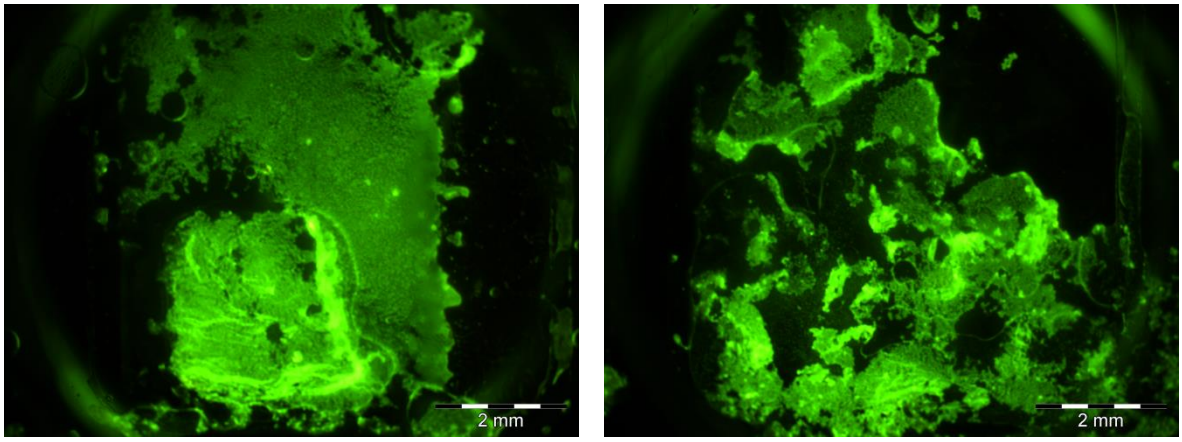


Figure 7.14: *S. epidermidis* after 24 hours incubation at 37 ºC on a control pp with 5 mM/l Ca^{2+} added to the bacteria solution, and daptomycin surface with 5 mM/l Ca^{2+}. Both surfaces showed biofilm over the surface, which seemed to be more easily detached with rinsing. The daptomycin surface showed much more loosely attached biofilm.

The results were similar for both sets of Ca^{2+} additions. It seems that the Ca^{2+} absorbed onto the surface, causing a looser attachment of the biofilm. The literature on daptomycin and Ca^{2+} is incongruent, because Scott et al. (Barraud et al. 2006) claim it is necessary for micelle formation, which is in turn necessary for activity. Yet the research by Pogliano, Pogliano and Silverman (2012) does not mention any use of Ca^{2+} in their visualisation of activity experiments. Investigations on adherent bacteria have found that it enhances bactericidal activity (John et al. 2011), yet they also had reasonable activity without the Ca^{2+} addition. This raises questions about the true importance of oligomerisation and micelles on the activity of daptomycin. The research from Pogliano, Pogliano and Silverman does indicate that daptomycin must lodge itself through the cell wall quite deeply into the cell membrane to induce the membrane patches and attract the cell division proteins and the resulting curvature and leakage. It leads one to question how only a single molecule of daptomycin could cause such devastation; it does seem as though some sort of oligomerisation is necessary but still questions the role Ca^{2+} has to play.

7.3.3 Cell Testing

Daptomycin surfaces were also tested with primary human fibroblast and no difference was noted between the control surfaces and the daptomycin surfaces. No toxicity was observed during visualisation and there was no difference in the number of cells on the surface; numbers were between 400 and 500 cells per view, with an average for both the control and daptomycin surfaces at around 460 cells per view.

7.4 Conclusion

This study clearly demonstrates that daptomycin exhibits no significant antibacterial activity when it is grafted onto a solid carrier surface; hence, it is not suitable as a covalently grafted layer for antibacterial protection of implants and biomedical devices. The literature contains a number of examples of surface-grafted antimicrobials, as reviewed in Chapter 2, but these results for daptomycin show that not all antimicrobials are suitable for covalent attachment. It makes sense that antibacterial drugs that interact with cytoplasmic targets, such as isomerase enzymes, cannot be active when covalently surface-grafted. As daptomycin is reported to act via a mechanism involving the bacterial cell wall membrane, however, it seemed a reasonable hypothesis that it might be active when immobilized. Clearly, this is not the case.

It would seem reasonable to postulate that covalent surface immobilization does not allow the bound molecules to have sufficient conformational flexibility to insert into the membrane, or that to be effective, insertion has to be deeper than is feasible when covalently anchored. Daptomycin may have to insert fully into the membrane to exert its effect and surface tethering simply confines it too closely to allow it to contact the lipid bilayer beyond the outermost glycocalyx.

A further complication arises from reports stating that daptomycin needs to oligomerise and to form micelles to be active. When bound to the surface, they may not function because they cannot form micelles to insert into the membrane and cause the membrane to collapse.

This study can certainly dismiss the earlier hypothesis that daptomycin functions in a similar manner to amphipathic AMPs.

Chapter 8: Antifungal Compounds Covalently Immobilised onto Plasma Polymers

Abstract

Hospital-acquired infections remain one of the greatest threats to patient safety. *Candida* species, particularly *C. albicans*, are a widely underappreciated cause of these infections. It is most often associated with biofilms formed on medical devices associated with non-sterile sites. *C. albicans* can also co-exist with bacteria (Kojic & Darouiche 2004; Peleg, Hogan & Mylonakis 2010) and is not killed by antibacterial drugs.

Thus, there is a desire to develop antifungal coatings that prevent the attachment and biofilm formation of fungal pathogens on biomedical devices. While the majority of antifungal compounds target intracellular processes, others target the fungal cell wall. By immobilising such antifungal chemicals on biomaterials, it may be possible to prevent fungal attachment and avoid infections. In this study, plasma polymerisation was used to immobilise two antifungal agents—amphotericin B and Caspofungin— on model biomaterial surfaces. Surface analysis and antifungal testing were used to assess attachment and activity. Caspofungin retains activity when covalently bound and microscopy images indicate that caspofungin disrupts the cell wall integrity of colonising *Candida* cells.

This chapter is an expanded version of a publication being prepared for submission:

Stefani S. Griesser, Marek Jasieniak, Bryan R. Coad, Hans J. Griesser, 'Antifungal coatings by caspofungin immobilization onto biomaterials surfaces via a plasma polymer interlayer', *Biointerphases*, **10**, 04A307 (2015).

I performed all the experiments in this chapter except for operating the surface analysis instruments and interpretation beyond sample loading and XPS curve fitting. The surface analyses were performed by Marek Jasieniak because of the extensive training required to become proficient in running the XPS and ToF-SIMS instrumentation. The extra training and

time in surface analysis instrumentation would have made it impossible to finish the experimental work within the required time if I had done it myself. Marek also performed PCA.

8.1 Introduction

While bacterial infections have long been the subject of much research, the past decade has seen the emergence of a different class of life-threatening pathogens. Advancements in the treatment of cancer and transplant medicine, as well as the progression of AIDS, have paved the way for fungal infections to establish themselves in these new groups of immunocompromised patients. The wider implications are more hospital-acquired infections involving fungal pathogens. Invasive biomaterials such as catheters, intravenous lines and implants are a major risk factor in transferring these opportunistic pathogens into the patient. These foreign medical devices are associated with non-sterile sites such as the skin or upper respiratory tract and provide opportune surroundings where the opportunistic and pathogenic bacteria and fungi are an abundant microbial mix, and mixed microbial biofilms are readily formed (Chim, Tan & Song 2007; Kojic & Darouiche 2004; Peleg, Hogan & Mylonakis 2010; Rosenthal et al. 2006). The most common hospital-acquired infections are urinary tract infections, ventilator-associated pneumonia and bloodstream infections (Peleg & Hooper 2010), all of which can lead to septic shock and death. The impact of fungal *Candida* species in hospital-associated infections is widely underappreciated. It causes over 400,000 life-threatening infections globally per year and is the third most common cause of catheter-associated bloodstream infection, with a mortality reaching 45% (Brown et al. 2012; Hidron et al. 2008).

While fungal microbes and bacteria both produce biofilm, it must be remembered that bacteria are prokaryotes and fungi are eukaryotes. Fungi have many elements in their cell biology structures and functions that are similar to our own cells, and it is important to explore these differences in order to seek selective antifungal strategies (avoiding cytotoxicity to human cells and tissue). The most prevalent human fungal pathogen, *Candida albicans* is a dimorphic fungus that normally colonises mucosal tissues, forming part of the microflora in an

opportunistic manner. Its population is normally controlled by the mucosal microenvironment, the bacterial flora, and through a healthy, innate immune system (Wilson, Henderson & McNab 2002). *Candida albicans* is by far the most prevalent species; it colonises humans from birth and can persist as a lifelong commensal in the gastrointestinal tract. It is dimorphic in that it can undergo a reversible transition between yeast and hyphae growth forms; invasive infection usually occurs in the hyphal form. It quite likely confers some benefit to the host in the yeast form in terms of maintaining immune homeostasis and balancing the intestinal flora (Cassone 2013). When the fungus infects the blood stream (referred to as candidaemia), and when hyphae spread to internal organs, it becomes a deep-seated, invasive infection with high lethality.

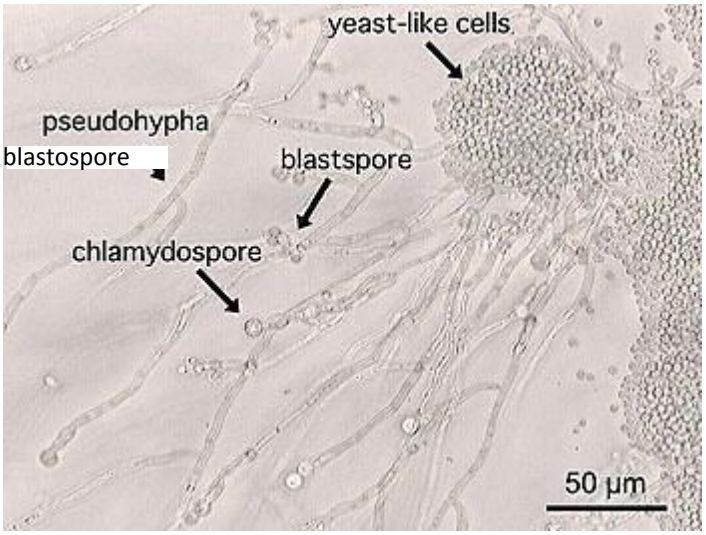
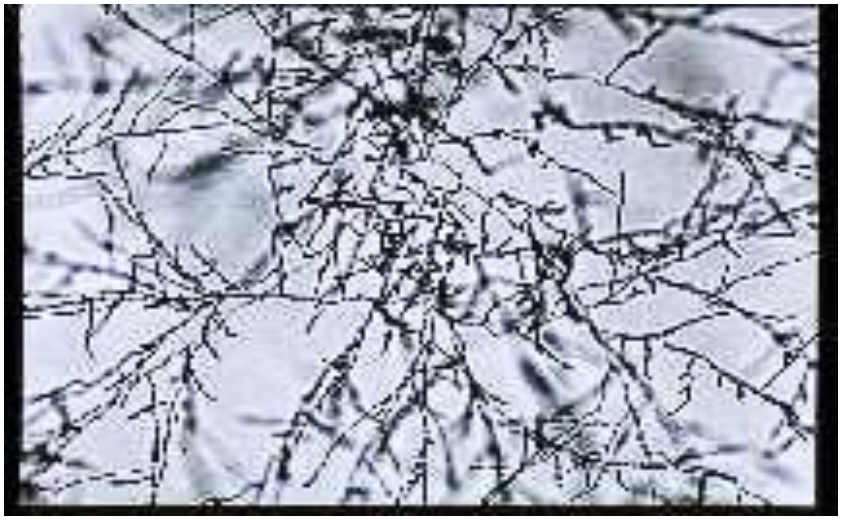
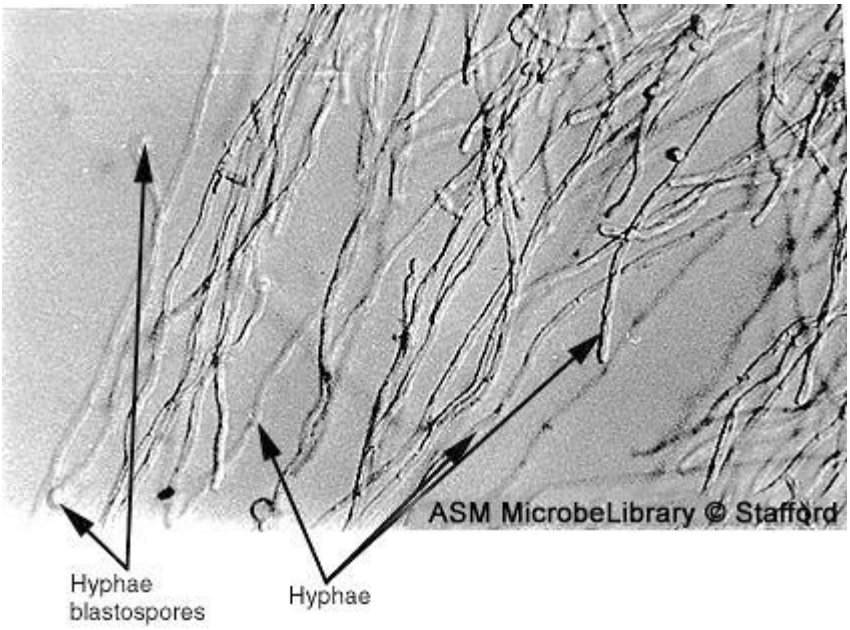


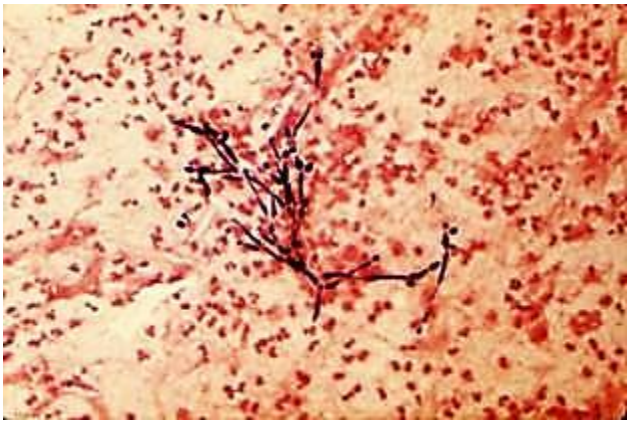
Figure 8.1: *Candida albicans* ATCC 10231. The yeast cells reproduce from buds on the blastospores. The pseudohyphae are elongated chains of yeast cells. Pseudohyphae grow from a bud that remains attached to the mother cell. Chlamydospores are attached to a blastospore via a suspension cell and may represent a dormant phase of yeast. True hyphae grow at the tip and can have branches. (Deacon & Deacon 2006) Sourced from http://commons.wikimedia.org/wiki/File:C_albicans_en.jpg.



a



b



c

Figure 8.2: Images of *Candida albicans* showing the hyphal form: (a) an image of mature hyphae to give an indication of the invasiveness of the hyphae as it branches and invades tissue (http://en.wikipedia.org/wiki/File:C_albicans_en.jpg); (b) the hyphae forming from the blastospores and the beginning of branching—the growth changes in that it grows from the tips of the hyphae and has a much higher amount of chitin in the cell wall (http://lib.jiangnan.edu.cn/ASM/317-3.jpg; Lee, Campbell & Buckley 1975); c) *Candida albicans* hyphae (Gram stain) in a section of lung confirming *Candidal* pneumonia (http://www.life-worldwide.org/fungal-diseases/histopathology/)

The cell wall of *Candida albicans* contains carbohydrates and cell wall proteins that are not present in the human body. The cell wall consists of two main layers: an outer layer that is composed of glycoproteins and an inner layer that contains skeletal polysaccharides. The cell wall contains 80%–90% carbohydrate, and the outer layer consists mainly of *O*- and *N*-linked mannose polymers or mannans that are covalently associated with proteins to form glycoproteins (Gow et al. 2012). These protrude from the cell wall, creating a protective layer (Figure 8.3).

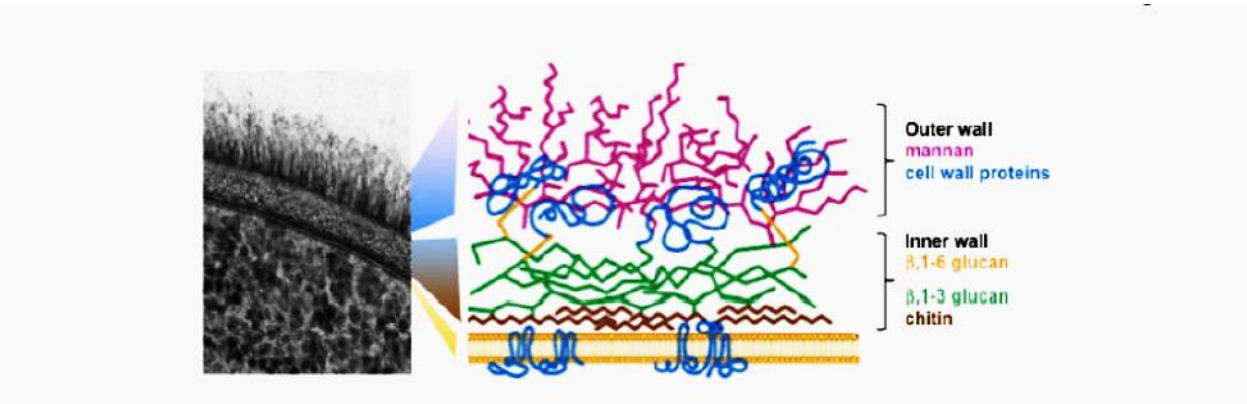


Figure 8.3: Structure of the *Candida albicans* cell wall. The two layers are seen in the first photo; the outer layer is highly enriched with *O*- and *N*-linked glycoproteins, whereas the inner layer contains the skeletal polysaccharides chitin and β-1,3 glucan that confer strength and cell shape. The outer cell wall proteins are attached to this framework predominantly by glycosylphosphatidylinositol (GPI) remnants that are linked to the skeleton through a more flexible β-1,6 glucan (Gow et al. 2012). Chitin connects this to the plasma membrane.

The extent to which the structure of the mannans in the cell wall differs between the yeast form and the hyphae is not certain; however, the cell wall proteins do differ in function in that the hyphae-specific cell wall proteins are major antigens and function as adhesins and invasins that can modulate an immune response (Shibata et al. 2007). It is quite likely that there are other differences between the yeast and hyphal forms.

The inner layer of the cell wall contains the skeletal polysaccharides chitin and β-1, 3 glucan, which gives strength and shape to the cell wall. The proteins from the outer layer are attached to this framework. Chitin is unique to fungi and plays a stabilising role in the network of glucans around the fungal cell membrane and is involved in hypha production and sporogenesis. Chitin normally comprises only ~2% of the cell wall in the yeast form and three to five times more in the hyphae form. Another distinguishing feature is the presence of ergosterol as a stabilising sterol in the fungal phospholipid bilayer. In general, the structure and composition of the cell wall varies greatly during the life cycle of *Candida* species, which in turn affects how the immune system will respond.

The yeast form of *Candida albicans* colonises the surface of the mucosal epithelium, invades the cells and disseminates into the blood to colonise other areas of the body (Romani, Bistoni & Puccetti 2003). How this occurs is still debated, because the body seems tolerant of this initial colonisation, in contrast with the inductions of powerful defence mechanisms following tissue invasion (Gow et al. 2012). Without proper immune recognition and control at the initial stages of colonisation, *Candida* colonisation at mucosal surfaces can lead to severe and long-term infection (chronic mucocutaneous candidiasis) (Kirkpatrick 2001).

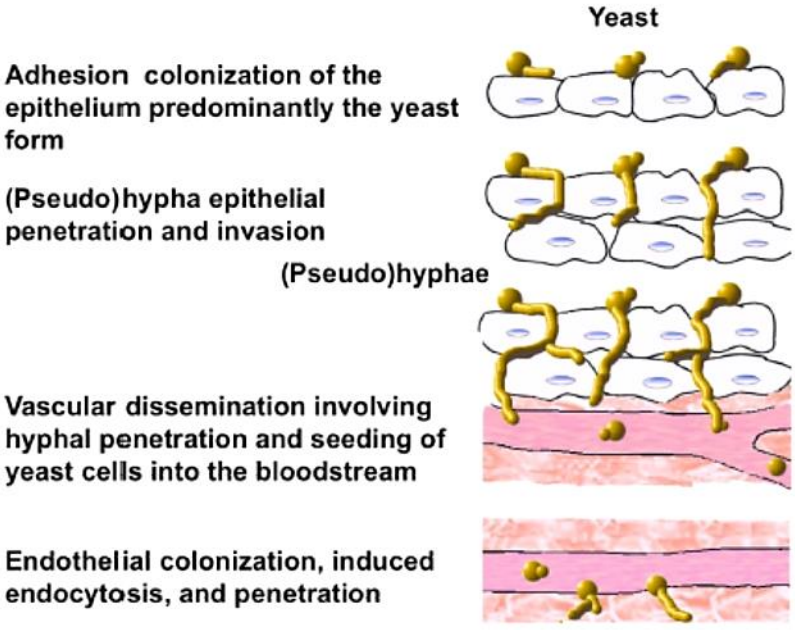


Figure 8.4: *Candida albicans* invading the epithelium and its subsequent seeding into the bloodstream (Gow et al. 2012)

Disturbances in the composition of the competitive commensal bacteria can also cause a distorted immunological response and contribute to pathological autoinflammation, which can occur in patients with Crohn's disease (Gerard et al. 2013; Sendid et al. 2009).

Antifungal chemotherapy has been slow to develop because there are very limited targets owing to the close eukaryotic relationships between fungi and human cells. Treatment of invasive

fungal infection requires long courses of systemic antifungal drugs, which can be associated with serious side effects.

Ergosterol is one feature of fungi that is absent in humans cells and has been the target for the polyene drug class (Coad 2014). A number of topical antifungals were developed; however, amphotericin B remained the standard treatment for serious fungal infections for over 40 years until the azole –class drug fluconazole was finally introduced in the 1990s (Lewis 2011; Moore, Robson & Trinci 2011). Amphotericin B and nystatin are polyene antibiotics that bind to ergosterol in the fungal cell membrane and form channels through which essential fungal cell constituents are lost.

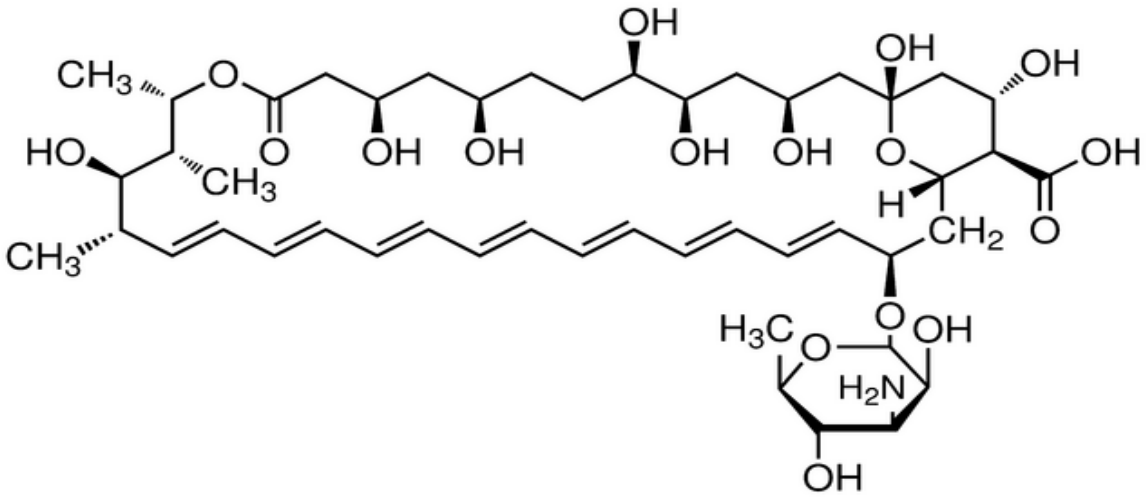


Figure 8.5: Chemical structure of amphotericin B. MW 924.08 $C_{47}H_{73}NO_{17}$

Amphotericin B consists of a macrolide ring of carbon atoms (a macrolide is a large macrocyclic structure) that is closed into a ring by formation of a lactone (a lactone is a cyclic ester resulting from condensation of an alcohol group and a carboxylic acid group in the same molecule) to which a six-carbon deoxyamine sugar is characteristically attached. With one exception, the hexosamine carbohydrate is the deoxyamino sugar, mycosamine. Amphotericin B has nine hydroxyls on the macrocyclic ring system and the mycosamine sugar on one side of the macrolide ring (which is hydrophilic as a result) and the polyene (-ene meaning double bonded) on the other side of the ring (and this side is hydrophobic as a result) (Moore, Robson & Trinci 2011). Amphotericin B is amphoteric, capable of behaving chemically as an acid or a base.

These features are thought to govern the biological activity of the molecule and the much higher affinity for fungal sterols than for the cholesterol in mammalian cell wall membranes. Polyenes have limited solubility in water but readily interact with the sterol molecule or allyl side chains of phospholipids in biological membranes. This is the basis of their biological activity because, as a result of their interaction with membrane sterol complexes, they can produce pores (partial or complete) through the cell membrane leading to leakage and cell death (Golan 2008). Amphotericin B is an extremely important drug in that it is the last line of defence in the treatment of life-threatening fungal infections. However, it is highly toxic and can also form ion channels in living eukaryotic cells (Lewis 2011). It is remarkable in that, in stark contrast to most antimicrobial agents, resistance to amphotericin B has remained exceptionally rare, despite over 40 years of use (Gray et al. 2012).

The azole drugs inhibit cytochrome lanosterol-α-demethylase, an enzyme that converts lanosterol to ergosterol. This causes lanosterol to accumulate and leads to perturbation of the fungal cell membrane and fungistasis (Golan 2008).

The echinocandins are a newer class of antifungal drugs comprising large lipopeptide molecules. Caspofungin is one of two key drugs in this class and is a semi-synthetic derivative of Pneumocandin B_0, a fermentation product of *Glarea lozoyensis* (Moore, Robson & Trinci 2011). It has a fatty acid side chain that is thought to intercalate with the phospholipid bilayer of the cell membrane. Caspofungin acts by non-competitive inhibition of the synthetic cell wall enzyme complex β-1,3-d-glucan synthase. This prevents the synthesis of β-1,3 glucan, an essential polysaccharide component of the rigid cell wall, and causes osmotic lysis of the fungal cells, producing both fungistatic and fungicidal effects (Foye, Lemke & Williams 2008; Neal 2012).

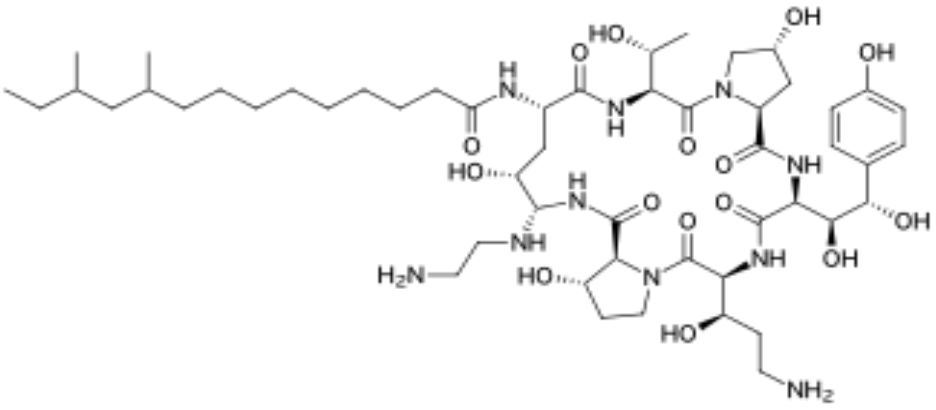


Figure 8.6: Chemical structure of caspofungin MW 1093.31 $C_{52}H_{88}N_{10}O_{15}$

Fungi easily colonise surfaces of a wide variety of synthetic biomaterials, polymeric, ceramic and metallic in composition. This eventually leads to the formation and establishment of proliferating fungal biofilms that can harbour polymicrobial biofilms of both fungi and bacteria. To stop biofilms from reaching this point, it would be highly advantageous to treat medical devices with an antifungal coating that encourages the opportunistic pathogens to remain away from the device and stops the initial colonisation of the device. Although much research has been undertaken on antibacterial and antimicrobial surfaces, very little work has focused on antifungal surfaces specifically. This may be because fungal infections are far more difficult to diagnose, and the importance and severity of fungal infections has only recently started to be recognised. Because of the differences between bacteria and fungi that were listed above, it is not appropriate to expect that antibacterial surfaces will also be antifungal.

Most antibacterial surface coatings target cell wall disturbance. Fungi have a much thicker cell wall, with a thickness of around 100 nm (Dupres, Dufrene & Heinisch 2010), in contrast to bacteria, which is nearly half as thick (Alberts 2008). Many surfaces have been produced that can be labelled ‘antiseptic’ and are coated with compounds such as QACs, which disrupt cell membranes of bacteria, fungi and viruses, but they also tend to be cytotoxic and give rise to adverse immune responses in humans (Lachapelle 2014; Vasilev, Cook & Griesser 2009). It has been suggested that surface tethering of these compounds can limit the toxicity. However, the toxic mechanism requires the insertion of the hydrophobic domain into the cell membrane, leading to disturbances of the phospholipid head groups and membrane disruption, which makes it difficult to understand how it could affect fungi in a manner that would not affect human cells.

Some AMPs (or HDPs) and synthetic antimicrobial mimics have also been found to show good antifungal activity (Del Gaudio et al. 2013; Liu et al. 2013); however, none of these have been tested when tethered to surfaces. A number of synthetic cationic peptides with linkers were covalently surface tethered and tested against *P. aeruginosa*, *S. aureus* and *Candida albicans* using luminescence measurements after 4 and 6 hours of incubation and complete killing of all microbes was reported (Hilpert et al. 2009). However, they were not plated and counted to verify killing; moreover, *Candida albicans* does not proliferate at a similar rate to bacteria (Chandra et al. 2001), which raises questions as to how reliable the testing method was. The mechanism of action for AMPs is also still questionable, particularly against fungi because their structure is so dissimilar to bacteria (Estivill et al. 2011). It is difficult to believe that any AMP would affect both bacteria and fungi without showing cytotoxic effects.

Established antifungal drugs offer potential advantages when tethered to surfaces. Many antifungal drugs have well-known modes of action and proven clinical effectiveness. In addition, the mode of action in both the polyenes and the echinocandins is direct interference with the cell wall and membrane. This makes them likely to be successful unless their action becomes sterically hindered upon immobilisation on a solid material surface (Coad 2014).

This research study investigated the potential utility of covalently tethering amphotericin B and caspofungin to ALDpp biomaterial surfaces using reductive amination. The mode of action of these two antifungal agents renders them excellent candidates for surface attachment because they target the fungal plasma membrane (amphotericin B) and the fungal cell wall (caspofungin). Other antifungal drugs target DNA and ergosterol synthesis or the mitotic spindle and require entrance into the fungus cell; therefore, they would not be able to function when tethered to a surface coating. Amphotericin B disrupts the fungal membrane by binding to ergosterol, which would require it to penetrate some distance into the cell membrane. Whether this could be achieved while still tethered to a surface coating was a major question that needed to be answered. Caspofungin is thought to disrupt the cell wall by inhibiting the synthesis of β-(1, 3)-D-glucans; however, this theory is still in question and the ability of caspofungin to disrupt membrane function successfully makes it a good candidate for surface attachment and testing.

Surfaces of samples were analysed to assess attachment, and tests using *Candida albicans* were used to assess effectiveness. Coatings were also tested with primary fibroblast cells to assess cytotoxicity.

8.2 Methods

8.2.1 Samples

Caspofungin and amphotericin B (research only, kindly donated by SA Pathology's Mycology Unit, Adelaide, SA), as well as caspofungin and amphotericin B purchased from Sigma-Aldrich, were covalently immobilised onto thin coatings (approximately 18–20 nm thick as determined by ellipsometry) prepared by the plasma polymerisation (pp) of propanal (99% Aldrich, USA) as described in previous chapters. Grafting onto ALDpp requires reductive amination using $NaBH_3CN$ for stabilisation of the covalent attachment by reduction of the initially formed imine bond. As substrates, I used silicon wafer (Micro Materials and Research Consumables, Australia), Thermanox coverslips (ProSciTech, Australia), and ibidi 15 µ-Slide 12-well uncoated microscopy chambers (no. 81201, ibidi, Australia).

All materials arrived sterile from the manufacturer and all work was undertaken in a biohazard cupboard, except plasma, which is a sterilising procedure. Caspofungin was used in two forms—in 1.6 mg/ml solution (Research only, SA Pathology) and in a powder (Sigma-Aldrich)—and was diluted to a 1 mg/ml solution in PBS. Amphotericin B was also tested in a 1.6 mg/ml solution (Research only, SA Pathology) which was diluted to 1 mg/ml, and as a powder (Sigma-Aldrich), which required dissolving in a 10% DMSO before it could be made up into a 1 mg/ml solution in PBS. Both solutions ware diluted 1/10 to a 0.1 mg/ml solution and aliquoted into 1 ml tubes and frozen for later use; 100 µl was added per sample to cover the surface. ADLpp samples had 100µl of 1 mg/ml $NaBH_3CN$ added after 1–2 hour/s contact. Samples were left overnight at 18 ^{o}C. Before testing, samples were soaked and rinsed with PBS a minimum of 12 times over 2 hours; other samples were soaked and rinsed with PBS for 2 weeks before testing. The final rinse after covalent attachment was collected and tested against fungi to prove that no antifungal compounds remained in solution and results were indeed from covalently attached antifungals only.

Amphotericin B is highly insoluble in water and requires addition of DMSO to solubilise it. After grafting, samples were rinsed extensively in order to ensure removal of any remaining DMSO (which is an antiseptic and could give misleading results in biofilm tests). The absence of a S signal in XPS indicates complete removal.

8.2.2 Surface Analysis

Surface analysis was done using XPS and ToF-SIMS. As for previous chapters, I acknowledge Marek Jasieniak for performing the measurements on these instruments and assisting me with data interpretations.

XPS was performed with a Kratos AXIS Ultra DLD spectrometer, using monochromatic AlK_α radiation (hv = 1486.7 eV). The system is equipped with a magnetically confined charge compensation system (low-energy electrons are confined and transported to the sample surface by magnetic field). Spectra were recorded using an acceleration voltage of 15 keV at a power of 225 W. Survey spectra were collected with a pass energy of 160 eV and an analysis area of 300 × 700 μm. High-resolution spectra were obtained using a 20 eV pass energy and an analysis area of ~300 × 700 μm. Data analysis was performed with CasaXPS software (Casa Software Ltd). All binding energies were referenced to the low-energy C 1s peak at 285.0 eV. Core level envelopes were curve fitted with the minimum number of mixed Gaussian–Lorentzian component profiles. The Gaussian–Lorentzian mixing ratio (typically 30% Lorentzian and 70% Gaussian functions); the full width at half maximum, and the positions and intensities of peaks were left unconstrained to result in a best fit.

ToF-SIMS measurements were performed with a PHI TRIFT V nanoTOF instrument (PHI Electronics Ltd, USA). A 30 keV, pulsed primary $^{197}Au^+$ ion beam was used to sputter and ionise species from each sample surface. PHI's patented dual beam charge neutralisation system using a combination of low-energy argon ions (up to 10 eV) and electrons (up to 25 eV) was employed to provide an excellent charge neutralisation performance. Positive mass axis calibration was done with CH_3^+, $C_2H_5^+$ and $C_3H_7^+$. Spectra were acquired in the bunched mode for 60 seconds from an area of 100 μm x 100 μm. The corresponding total primary ion dose

was less than 1 x 10^{12} ions cm^{-2}, and thus met the static SIMS regime (Briggs 1998). A mass resolution m/Δm of >7000 at nominal m/z = 27 amu ($C_2H_3^+$) was typically achieved.
Some samples were characterised by multiple positive ion mass spectra, which were collected from sample areas that did not overlap. All recognisable, clear (i.e. unobscured by overlaps) fragment ions from 2 up to 175 amu range were used in calculations. The peaks were normalised to the total intensity of all selected peaks. Multiple mass spectra were processed with the aid of PCA (Jasieniak et al. 2009). PCA was performed using PLS_Toolbox version 3.0 (Eigenvector Research, Inc, Manson, WA) along with MATLAB software v. 6.5 (MathWorks Inc,).

8.2.3 Fungal Testing

Fungi (*Candida albicans* ATCC 90028) was plated on SAB+ANTI (Oxoid) plates from –80ºC frozen stock and incubated overnight at 37 ºC. One colony was picked from the plate and spread on a fresh plate and incubated at 35 ºC overnight as a stock plate; the other colonies were collected and frozen for future experiments. One colony was selected from the stock plate and grown in 10 ml YPD Broth (20 g glucose, 20 g peptone, 10 g yeast in 500 mL reverse osmosis water, Ausubel 2002, Oxoid) overnight at 35 ºC. The following day this was measured for McFarland units using a VITEK colorimeter (no longer available for purchase) and made up to 0.5 McFarland, then diluted 1/100 giving approximately 1–3 x 10^6 CFU/ml^{-1}. Depending on the substrate, bacteria solutions were added at 100 ul or 300 ul (actual amounts at approximately 1 x 10^5 or 3 x 10^5 CFU/ml^{-1}, and incubated for 3 days at 35º C. Surfaces were analysed using LIVE/DEAD *Bac*Light Bacterial Viability assay kits (Invitrogen), which is the same as the LIVE/DEAD fungus imaging kit, and the FUN 1 kit (Invitrogen). Polystyrene slides or ibidi µ-Slide wells were plasma treated. A FlexiPERM 12-well removable mask was placed on the slide and ibidi µ-Slides were used as is; antimicrobial polymers were added to the wells for grafting overnight. After rinsing, fungi were added for incubation for 3 days, followed by rinsing twice to remove loosely attached and yeast from fungi. The wells were treated with the LIVE/DEAD *Bac*Light stain or FUN 1 and the mask carefully removed before microscopy examination.

8.2.4 Cell Attachment

Primary human fibroblasts were harvested from fresh skin (MacNeil, Shepherd & Smith 2011). All cell cultures were maintained according to published protocols (MacNeil, Shepherd & Smith 2011). Plasma- and antifungal-treated Thermanox coverslips were placed in sterile 24-well culture plates (Nunc, Invitrogen) and prewarmed in a cell culture oven. Primary cells were tested using plasma treatment and attachment of polymers in ibidi micro-chamber 12-well glass slides (ibidi 81201, Germany). Cells were made up to 50,000 transformed cells per ml in medium/serum or 10,000 primary cells per ml in medium/serum and added at 1 ml to each well or 100 µl to ibidi wells. Well plates were placed into the culture oven and left for 48 hours. The coverslips were rinsed to remove non-adherent cells and placed on a glass slide and coverslip for immediate microscopic analysis. ibidi wells were stained using DAPI nucleus stain (Invitrogen) and used as per instructions.

8.4 Results

8.4.1 Surface Analysis

8.4.1.1 XPS Results

XPS provides an indication of the surface coverage of the two antifungal compounds via the %N in survey spectra, and high-resolution C1s and N1s spectra can be used to confirm the intended coating composition.

8.4.1.2 Amphotericin B Coatings Surface Analysis

Amphotericin B contains only one N atom in its molecular structure, which leads to the expectation that a grafted layer would show a low at% N, even when grafted at close to monolayer coverage. The molecule is rich in oxygen, more so than the ALDpp, and thus changes in the O/C ratio can also be used to detect immobilisation of amphotericin B. The XPS data in Table 8.1 indicate that attachment was successful, but it is desirable to perform further analysis.

Table 8.1. Composition of ALDpp and its amphotericin B modification by XPS

Sample	Composition, atomic %		
	O	N	C

-ALDpp	10.7	–	88.5
-ALDpp-AmphB	12.9	0.6	86.4

Further analysis with ToF-SIMS was deemed necessary. Positive ion spectra (Figure 8.7) showed only minor differences, which is not too surprising given that the molecule is rich in structures containing both C and O and thus presumably giving rise to similar or the same fragment ions.

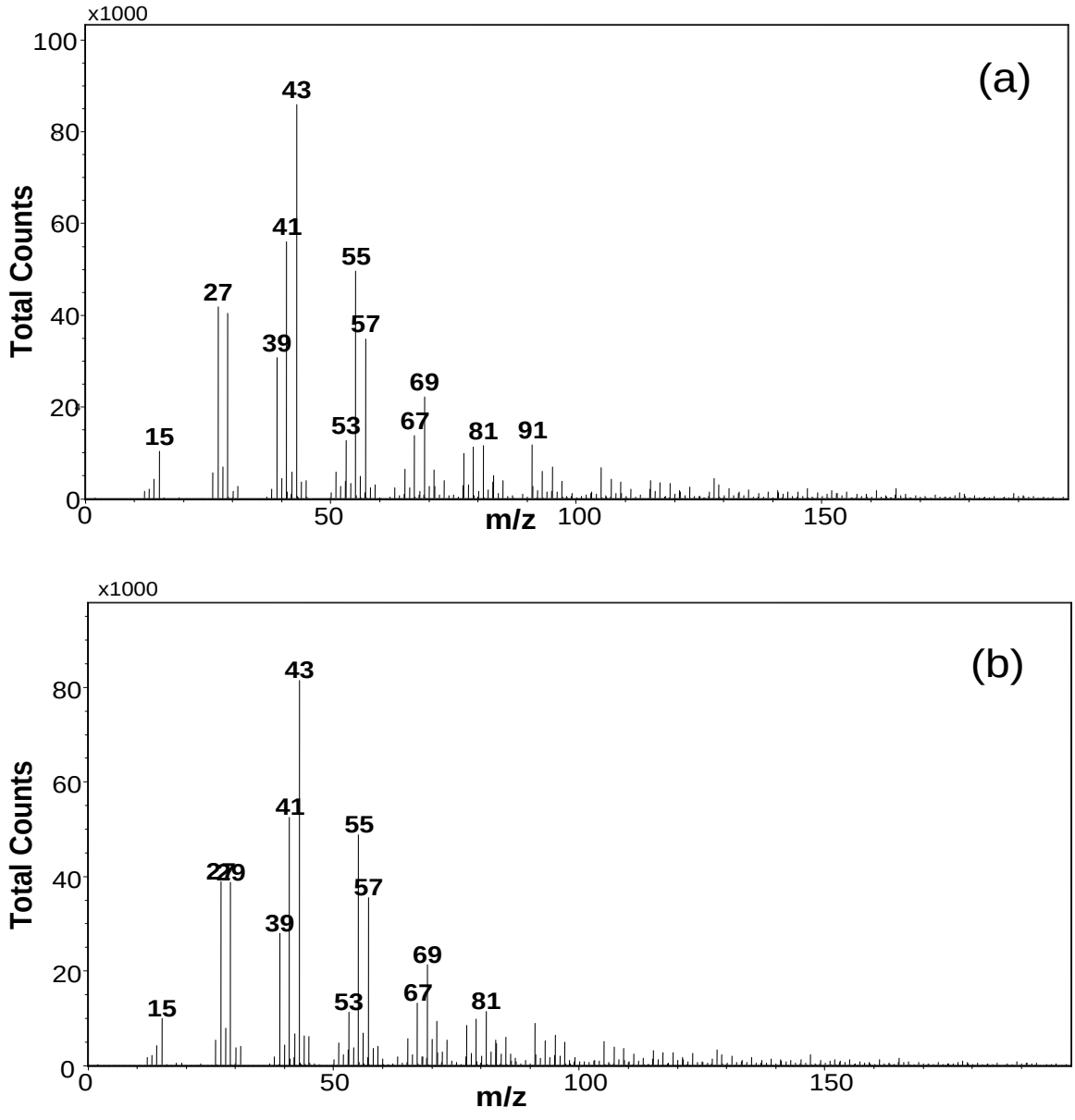


Figure 8.7: Positive mass spectra for: (a) ALDpp, (b) ALDpp-AmphB

To determine whether amphotericin B is indeed coupled, PCA is needed because it brings out spectral differences not readily detected visually. Results are shown in Figure 8.8.

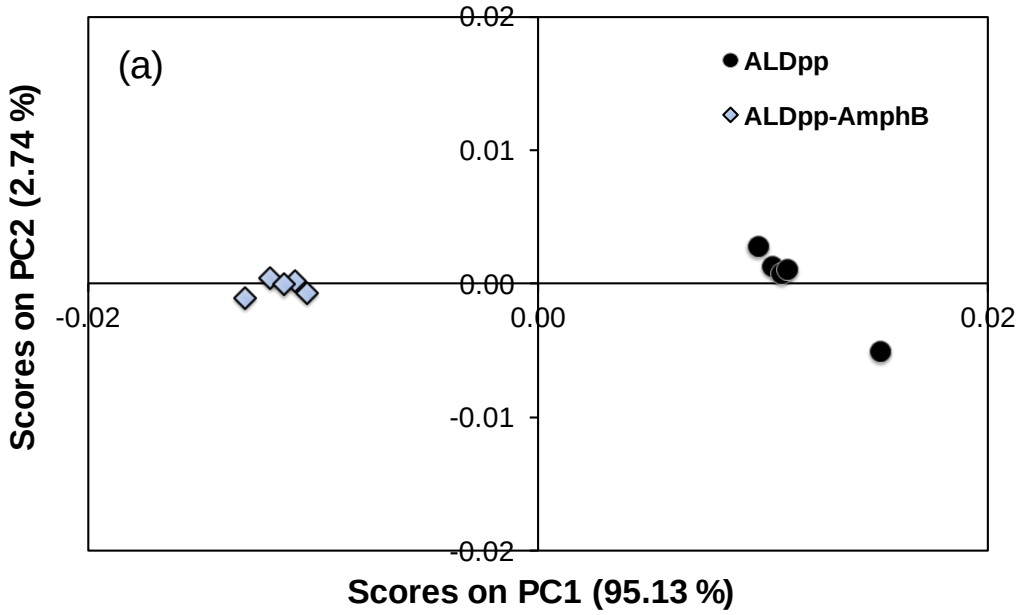


Figure 8.8: PCA Scores plot on PC1 and PC2

The scores plot shown in Figure 8.8 reveals clear differences in surface chemistry. The tight clustering of data points shows high uniformity of the coating; some data points are not visible in this plot because the points are layered on top of each other.

Loadings plots against principal components reveal the fragment ions whose intensities vary most strongly between samples when measured against that principal component. With a weight of > 95% for PC1 (Figure 8.8) in the present case it is necessary to process only the loadings plot for PC1 to extract the main fragment ions that give rise to the differences in the spectra.

The loadings plot in Figure 8.9 clearly shows information in agreement with expectations. The ALDpp gives rise to relatively higher intensities of hydrocarbon fragment ions, whereas the Amphotericin B grafted surface shows signals from ions that would be expected to arise in its fragmentation. Particularly informative are fragment ions arising from the aminated sugar ring (circled in red). These analyses clearly confirm that the molecule has been tethered to the plasma polymer surface.

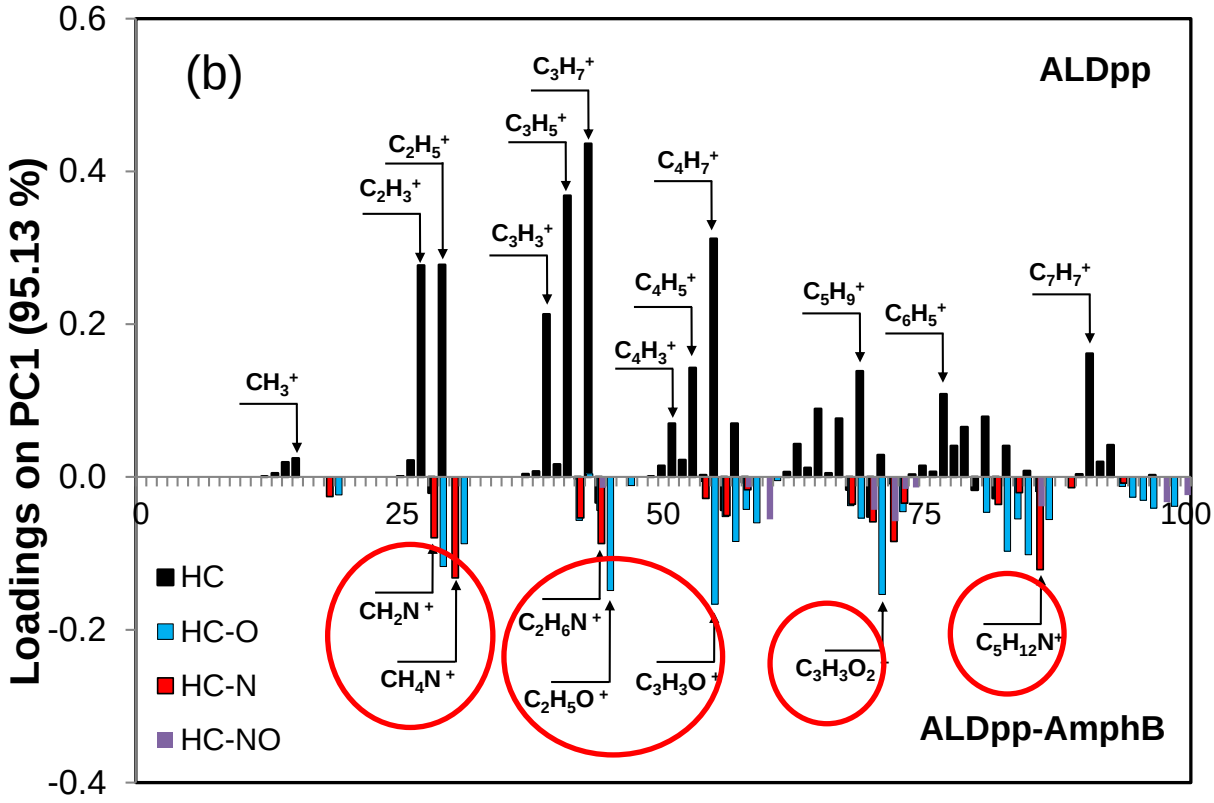
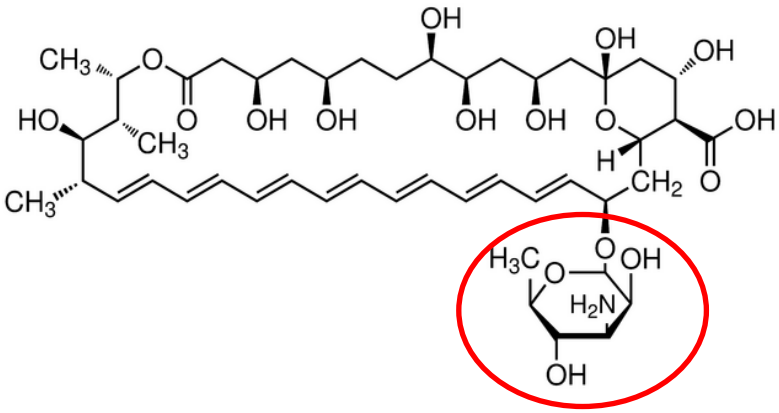


Figure 8.9: Loading comparison of the positive mass spectra across ALDpp and its modification with amphotericin B (ALDpp-AmphB). The red circled groups indicate identifiable fragments from the amnosugar ring of amphotericin B.



The loadings plot also shows that there are no surface contaminants such as fatty esters, hydrocarbons or silicones that might affect biological testing.

8.4.1.2 Caspofungin Coatings Surface Analysis

Table 8.2 presents XPS data for an ADLpp control surface and an ADLpp surface with caspofungin covalently attached to the surface. The N content of the latter confirms grafting and indicates excellent coverage with caspofungin.

Table 8.2: Composition of ALDpp and ALDpp + caspofungin, by XPS

Sample	Composition, atomic %		
	O	N	C
-ALDpp	12.5	–	87.5
-ALDpp-Casp	13.2	2.6	84.2

ToF-SIMS analysis was again also used to verify attachment and confirm surface uniformity of the caspofungin grafted surface. The structural elements shown in red were expected to give rise to identifiable distinct fragment ions.

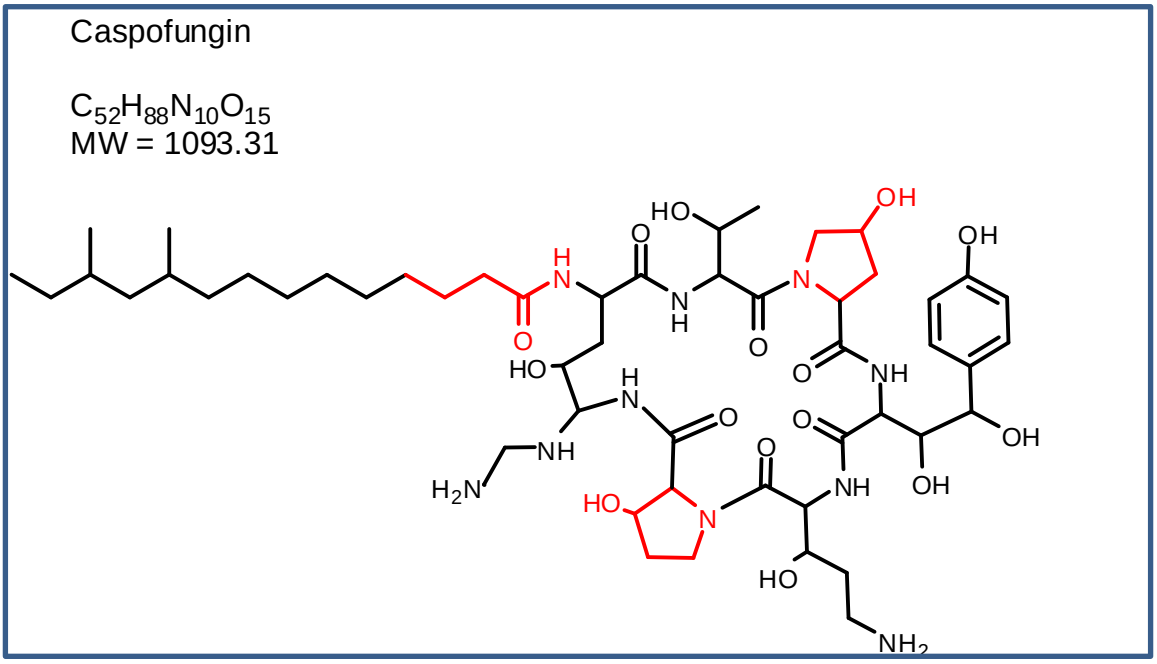


Figure 8.10: Structure and molecular weight of caspofungin (red-marked structural components contribute to the $C_4H_8NO^+$ fragment ion highlighted in the positive mass spectrum for ALDpp-caspofungin)

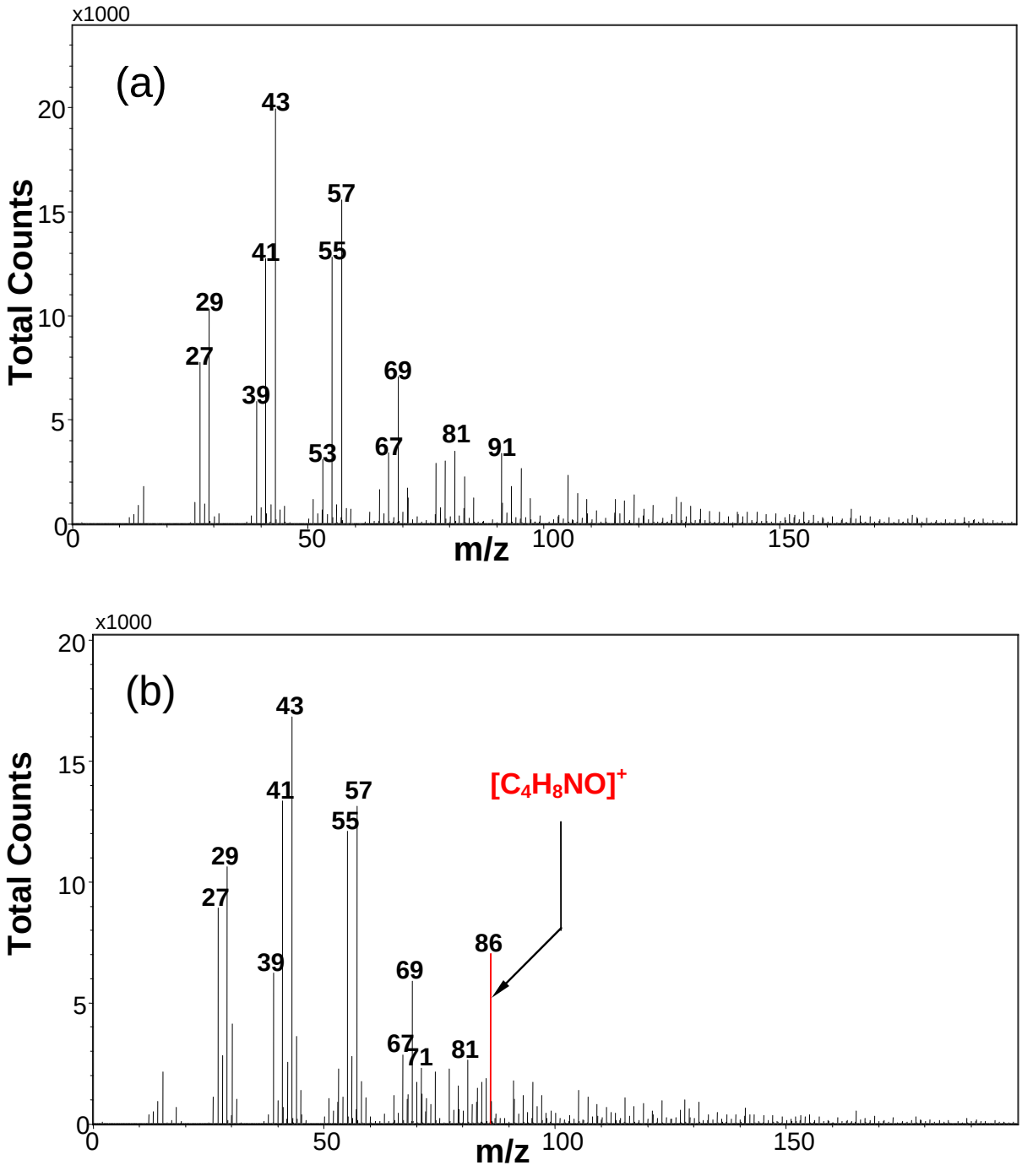


Figure 8.11: ToF-SIMS analysis of surface immobilisation of caspofungin to the surface: (a) the control aldehyde surface, (b) the caspofungin-modified surface, with the distinct fragment ion highlighted

In contrast to the amphotericin immobilisation, in this case the spectra clearly reveal at first glance the immobilisation of caspofungin, via the presence of a peak that can be assigned to a distinct fragment ion.

PCA ws also performed to gain further information. The scores plot is shown in Figure 8.12.

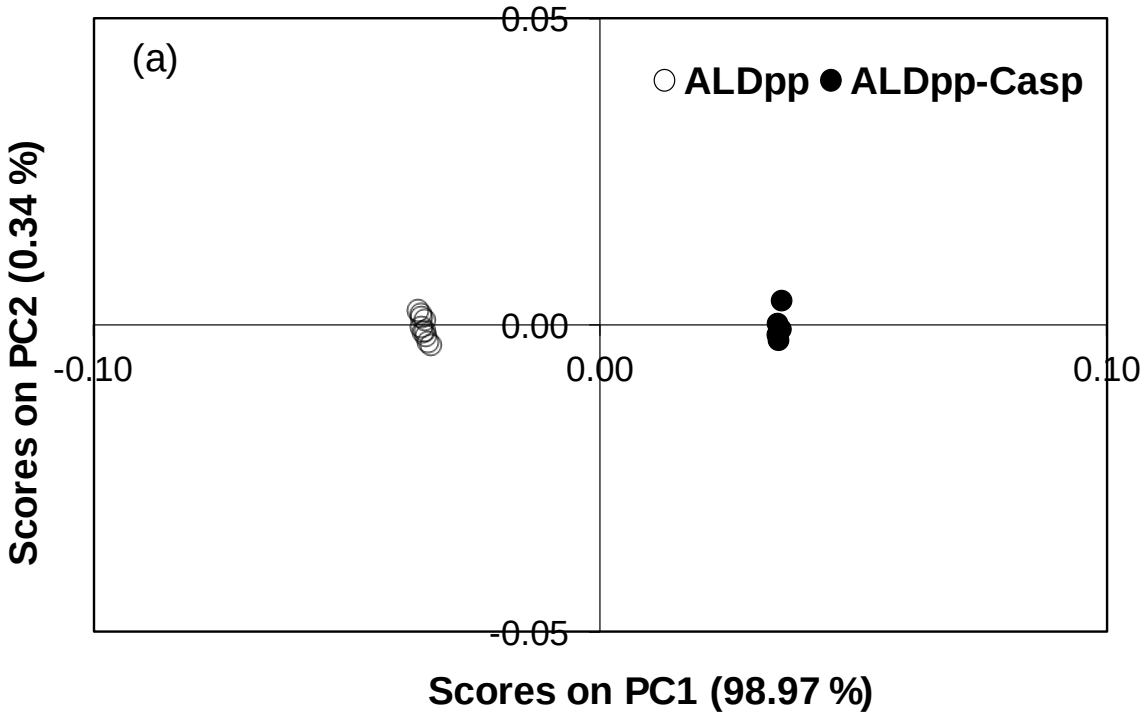


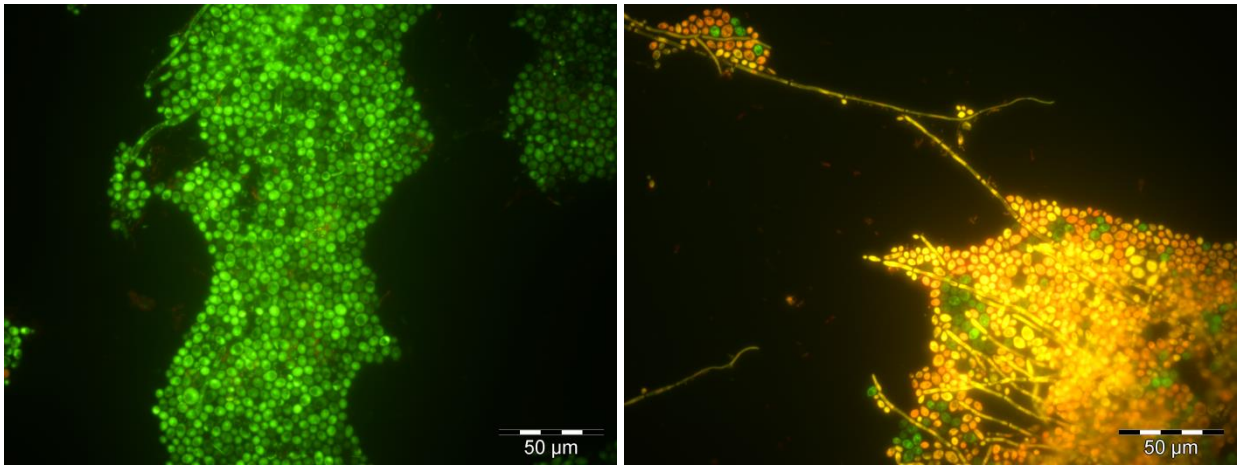
Figure 8.12: Scores plot on PC1 and PC2: (a) loadings on PC1 (b) positive mass spectra for ALDpp and ALDpp-Casp

Again there is good uniformity within samples and also no surface contaminants.

8.4.2 Fungal Testing

As stated above, *Candida albicans* is dimorphic; it grows as rounded yeast cells and hyphae. This depends on the specific colonisation area, growth conditions, temperature and strain. Little information is available about its growth and morphology on solid polymer surfaces; accordingly, preliminary control experiments had to be performed.

The images in Figure 8.13 show *Candida albicans* grown on a polystyrene slide with no treatment after 48 hours, which gives a positive control with live green-stained fungi (a), and a negative control (b), which after 48 hrs of growth was treated with Virkon antiseptic solution for 10 minutes, to prduce a biofilm with dead cells. Normally the LIVE/DEAD stain would stain the dead cells red; however, there are still a number of green rounded yeast cells. Repeated studies found that 10 minutes of Virkon did not fully kill the fungi and has probably only damaged the cell wall and left many undamaged and alive, thus giving rise to yellow and orange staining. A full negative control required 20 minutes of exposure to Virkon to kill all the *Candida albicans* yeast and hyphae cells. However, this exposure of Virkon starts to destroy the coating as well. Therefore, the negative control was kept at 10 minutes, which means the stain could not be fully scored and the LIVE/DEAD stain can only be used as indicative of a result, as is generally the case for this particular stain. Note the rounded yeast cells, with hyphae stringing their way across the surface. The green/live biofilm shows pseudohyphae and some of the 'strings' show the mother cell still attached.



a b

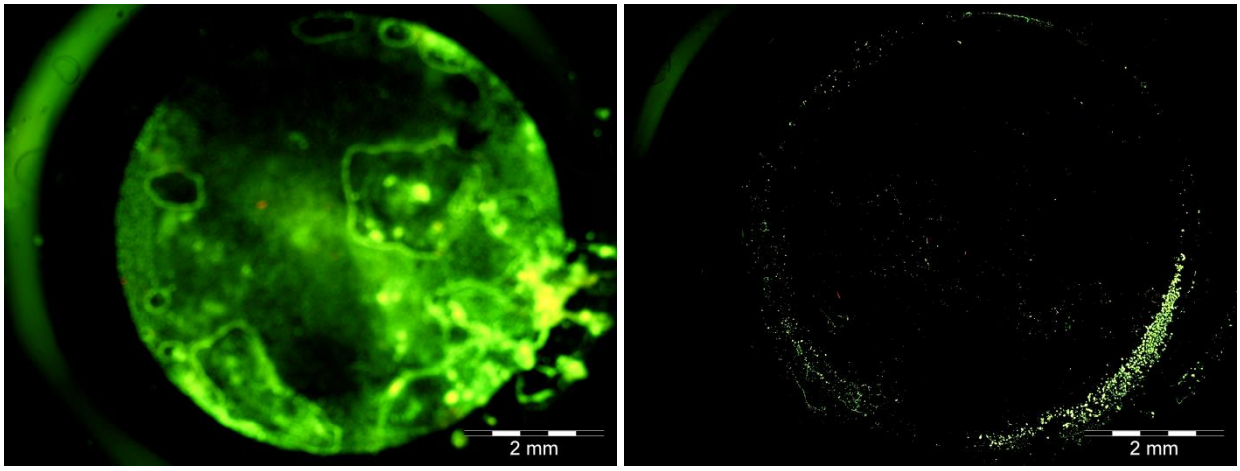
Figure 8.13: *Candida albicans* grown after 48 hours: (b) positive control with green live stained fungi; (b) negative control, fungi treated with Virkon for 10 minutes

As was stated in the methods section, we were given samples of drugs labelled for 'research only' from SA Pathology to conduct our initial tests. The amphotericin B was in a liquid form. This was used in our initial tests and then I switched to a pure powder form because I could not

identify how much DMSO was in the liquid form of amphotericin B, and DMSO has known antibacterial abilities and some cytotoxic abilities.

8.4.2.1 Amphotericin B

The results from the surfaces treated with amphotericin B were difficult to interpret. The initial results showed excellent killing (Figure 8.14), which was somewhat unexpected because amphotericin B requires insertion and interaction of the mycosamine sugar with the ergosterol and then the alignment of the macrolide ring that forms the pore in fungal membranes (Lewis 2011; Moore, Robson & Trinci 2011). The orientation of the sugar moiety also affects the affinity of amphotericin B for ergosterol over cholesterol (Neumann, Baginski & Czub 2010). It is possible that the interaction of the macrolide ring alone may be enough to destabilise the cell wall enough to cause death or at least perturb the fungus enough not to colonise the surface and kill the yeast form and smaller hyphae. Paulo, Vidal and Ferreira (2010) claim to have made antifungal nanoparticles with amphotericin B attached and that this aligns with 'current knowledge' on the activity of amphotericin B on fungal membranes. However, the references used in that study were from 1991, 1991 and 1994 and thus not representative of newer research that specifically investigates the orientation of amphotericin B in the fungal cell membrane.



a b

Figure 8.14: *Candida albicans* after 48 hours growth on (a) Control surface, (b) surface-grafted amphotericin B (liquid form at 0.6 mg/ml), which shows good killing

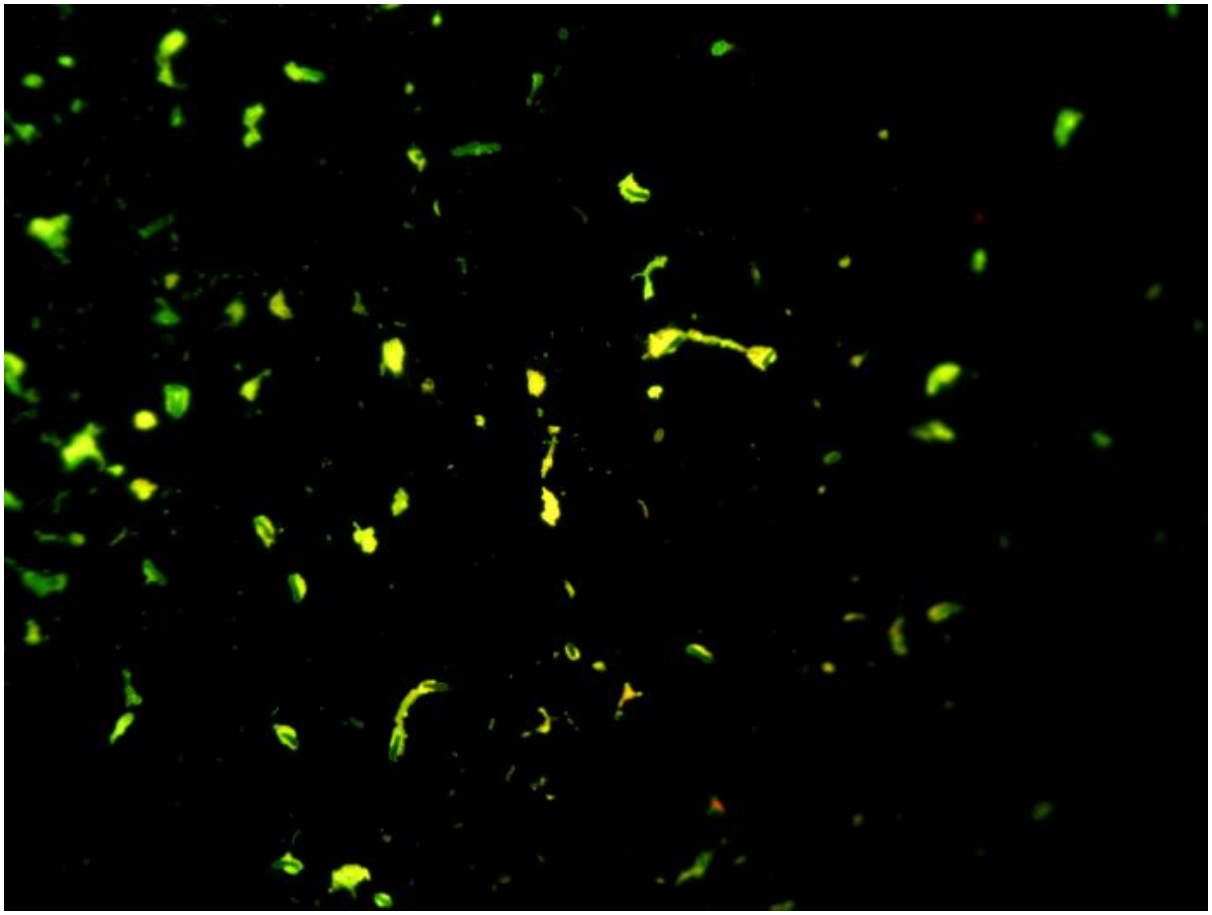


Figure 8.15: Image at 100x magnification: *Candida albicans* after 48 hours incubation. Amphotericin B liquid form treated surface with larger pseudohypae; membranes seem to be compromised and evidence of leakage is seen.

On the amphotericin grafted surface there seems to be a higher percentage of microbial cells in the hyphal form over the yeast form. Perhaps the yeast cells may have been killed faster; mostly pseudohypae and hyphae remain. Yeast cells seem to be more easily affected by antifungal compounds in the yeast form than in the hyphal stage. While this microbiological detail would need further investigation, clearly the results show antifungal activity of the coating.

Amphotericin B is highly insoluble in water and PBS, so it may be possible that the liquid form requires a further compound to assist with solubility, which may show some toxicity that could also be absorbed into our plasma polymer and diffuse out. Although the amphotericin B in solution obviously has something to render it soluble, we do not know exactly what it is, so it must be kept in mind that it may have affected the results, even though the surface analyses did not reveal any extraneous signals. Therefore, it was decided to also investigate the drug in powder form. The powder form of amphotericin B required addition of 10% DMSO to PBS, to keep it in solution, due to its highly insoluble properties.

Figure 8.16 shows a higher-resolution microscopy image of *C. albicans* cells attached on a control polystyrene surface, while Figure 8.17 shows colonisation on polystyrene coated with ALDpp and amphotericin B.

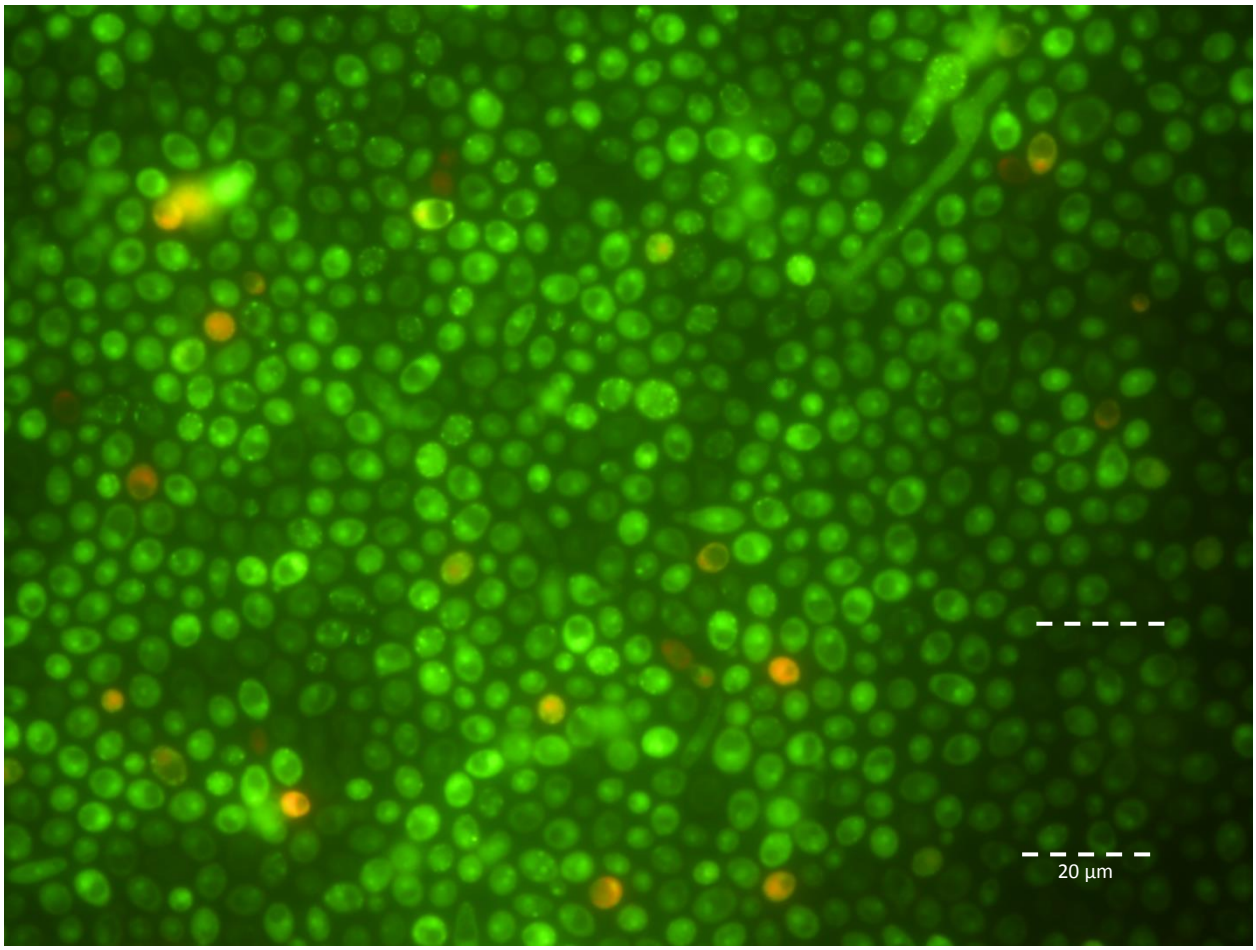


Figure 8.16: Control surface with *Candida albicans*

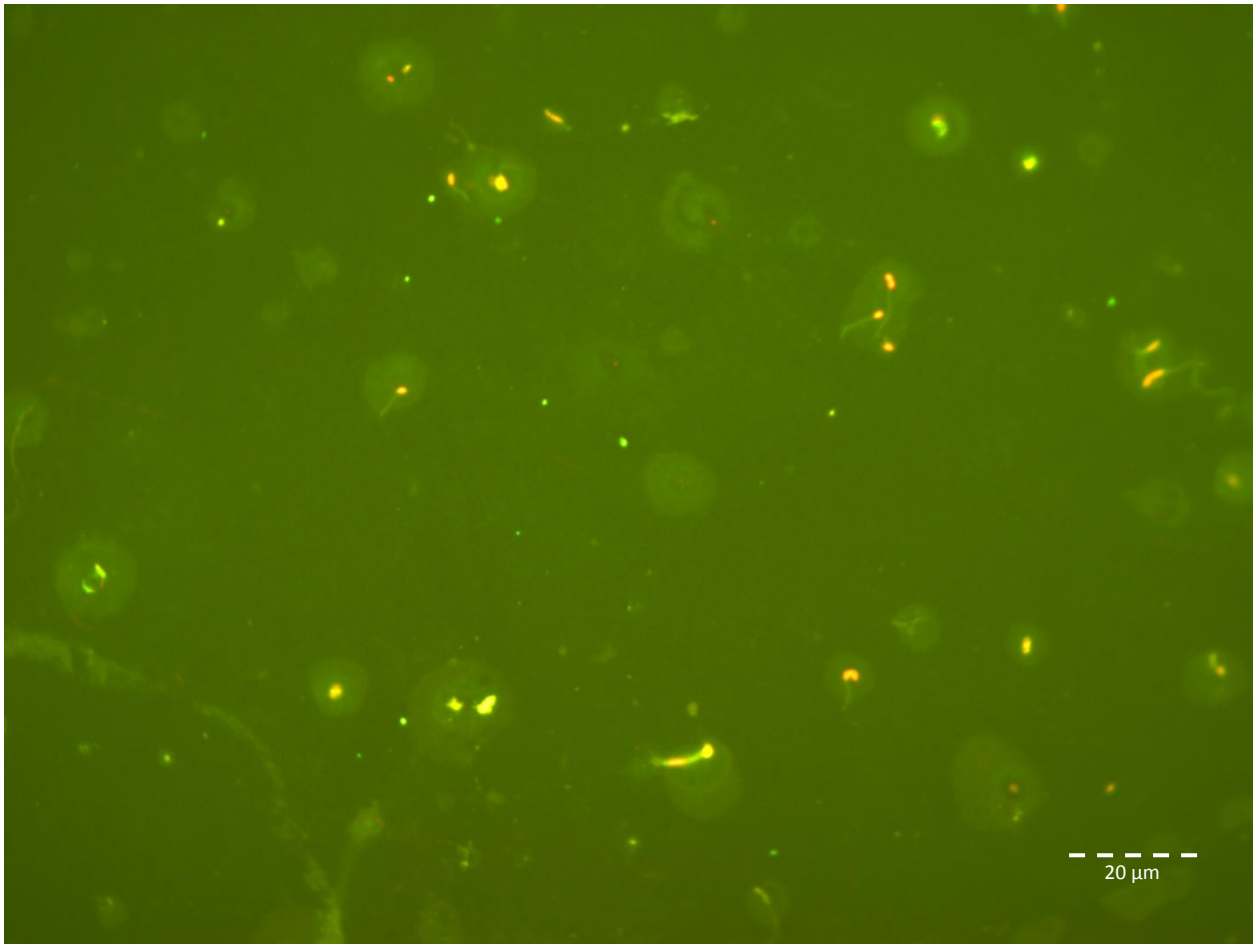


Figure 8.17: Amphotericin B on polystyrene + ALDpp surface. Few live *Candida albicans* are noted.

Clearly, the amphotericin has a marked effect. The control surface allowed attachment of healthy-looking fungal cells, mostly in the yeast form, whereas the treated surface shows cells with only extremely small pseudohyphae and no yeast cells. Most cells seem to be dead or dying.

In an attempt to determine whether amphotericin B was only covalently bound on the surface rather than adsorbed as a multilayer, perhaps crystallised precipitates on the surface, a set of samples were left soaking for 2 weeks, then exposed to intense rinsing. They then underwent thorough surface analysis and were re-tested with *Candida.* Surface analysis proved that there still was Amphotericin B on the surface; however, there were areas that were delaminated. Surface analysis also showed that there was no contamination.

After such extensive washing, amphotericin B grafted surfaces did no longer produce a fully antifungal surface, as shown by increased amounts of *Candida albicans* on treated samples (Figure 8.18).

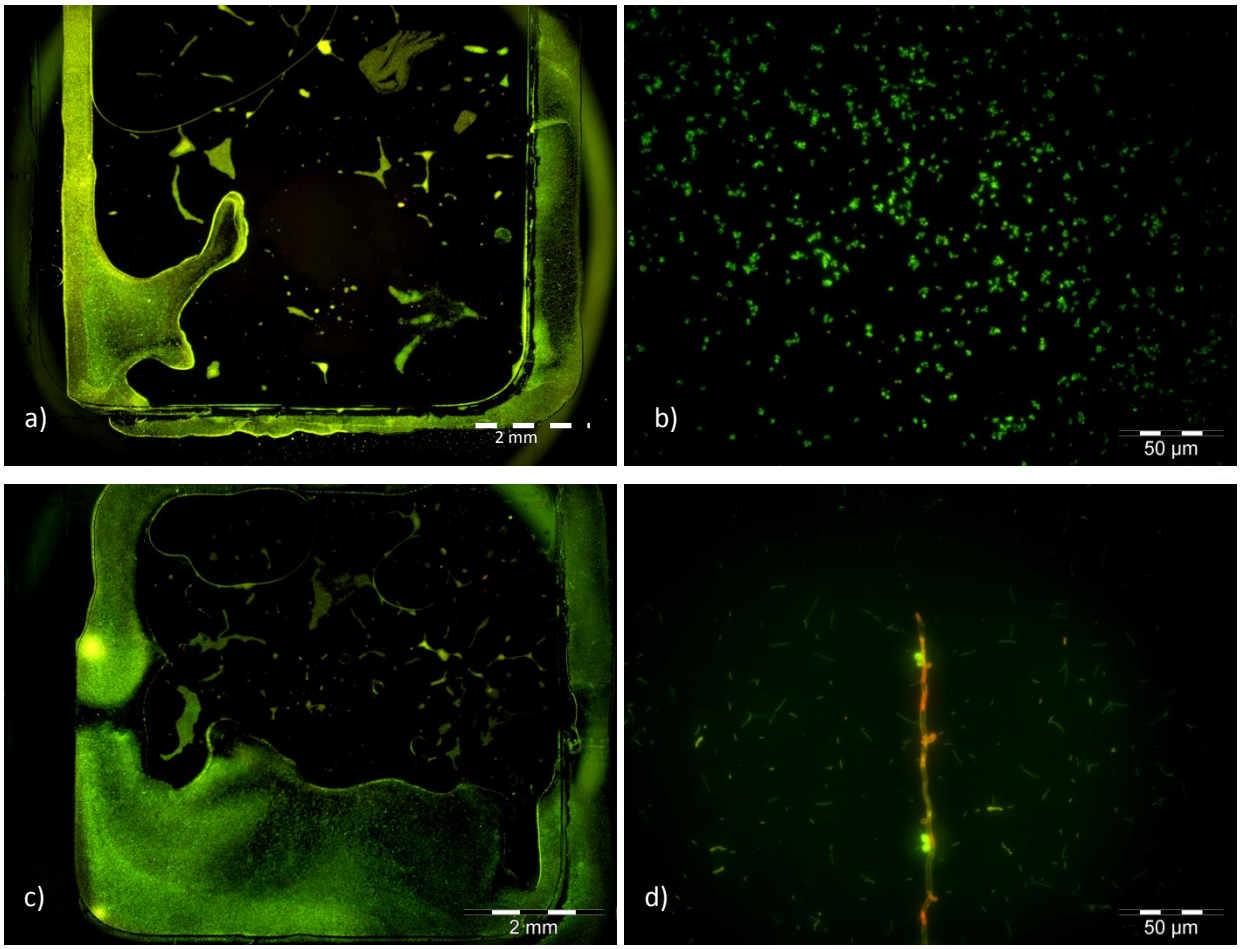


Figure 8.18: Surfaces with amphotericin B immobilised were soaked for 2 weeks: (a) and b) are the control surfaces showing biofilm and mostly yeast cells; (c) and (d) are the amphotericin-treated surface, showing an increase in hyphae and pseudohyphae formation

Amphotericin B coated samples showed many broken-up pieces of fungi; these pieces were unusually small. Some were pseudohyphae because they were still attached to the mother cell, but most were small, segmented hypae, some with branches. This indicates that there was some effect of the treated surface on the *Candida albicans* cells, but there was definitely more

colonisation and biofilm formation than on the earlier coatings described above. The control surfaces show a proliferation of yeast-form cells with many budding from the surface and some elongation of pseudohyphae from the mother cells. The amphotericin B surfaces show some large psuedohyphae with yeast mother buds and very small, segmented hypae with septa, some with branches.

Thus, there is still an adverse effect on *C. albicans* attachment arising from surface-grafted Amphotericin B, but the effect is weaker than when a less-washed sample with presumed adsorbed molecules is used.

These data show that one has to be extremely careful when assigning observed antimicrobial activity to drugs that are presumed to be tethered covalently to surfaces. It is easy to ignore, or fail to detect, evidence of molecules that are not covalently bound, but, instead, appear to be adsorbed and resistant to a brief wash but able to desorb upon extended washing. While coatings with adsorbed drug molecules may still be useful, activity is not retained longer term.

From a scientific point of view, the danger is mis-interpretation. There are many publications claiming biological activity from covalently immobilised bioactive molecules. In the large majority of cases, no extended washing was performed to check for potentially desorbable molecules. How many of those studies might have been marred by failure to detect and take into account effects arising from adsorbed, desorbable molecules?

Despite extensive investigation for over 50 years, the mechanism of action of amphotericin B remains unclear. New research has found that amphotericin B kills yeast primarily by binding ergosterol, and then forming ion channel–mediated membrane permeabilisation. However, it is this simple binding of a functionally vital lipid as an antimicrobial mode of action that makes it most interesting, because several antibacterial peptides exert their effects via specific lipid binding as well (Gray et al. 2012). It is the selective binding of ergosterol, rather than the cholesterol found in human cells, that gives it selectivity. Less clear is the effect this binding has on the hyphal and pseudohyphal forms because they contain far less ergosterol. Perhaps the ion channel membrane permeabilisation is required for killing of the hyphae. In this research,

it is clear that our surfaces with amphotericin B immobilisation have some effect on the fungi; the possible mechanism of action could be a disturbance of the ergosterol that triggers it to move from the yeast to the hyphae form rapidly. The macrolide tail may be tethered too tightly or in a way so that it cannot penetrate the ergosterol/lipid membrane enough to kill but to trigger the yeast to change forms, or kill only the yeast form and struggle with the hyphae form. Alternatively, perhaps it is the simple perturbation of the membrane that encourages the dimorphic change. At present, there is insufficient understanding of the mechanisms that cause *Candida* to transition between forms, and researchers are only beginning to understand the phenotypal changes that fungi undergo.

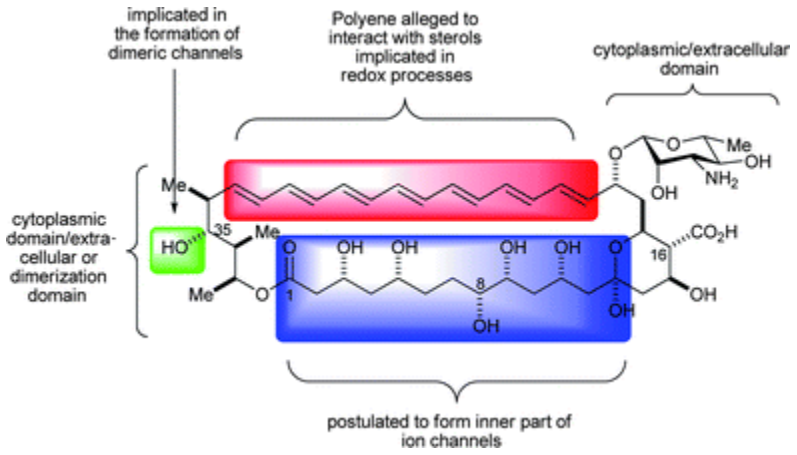


Figure 8.19: Proposed mechanism of action of amphotericin B (Volmer, Szpilman & Carreira 2010) (From http://www.rsc.org/ej/NP/2010/b820743g/b820743g-f6.gif)

Figure 8.19 is another proposed mechanism of action that does not require an effect of the sugar moiety in the orientation of the amphotericin B into the cell membrane. This mechanism suggests that the sugar residue may be less important in the activity of amphotericin B against the yeast form. This could also help explain why we saw some activity when amphotericin B was attached to a surface via this amino-sugar group; however, as mentioned earlier, the *Candida albicans* wall is approximately 100 nm thick, and it is still hard to understand how it could be affected by tethered amphotericin B.

Further investigation will be needed to determine the exact mechanisms on the surface, including live cell imaging, which may pick up the dimorphic changes that may be affected by the surface. At present, results from this study are inconclusive about whether amphotericin B would be able to produce a viable antifungal surface when tethered to a plasma polymer coating.

8.4.2.2 Caspofungin

Surface-attached caspofungin achieved excellent killing, even after 2 weeks soaking. XPS and ToF-SIMS verified covalent attachment. The surfaces of controls were colonised by good yeast-form cells and biofilm-producing *Candida albicans*, whereas Caspofungin-coated surfaces showed little to no viable fungi, and some microscopy images revealed complete disruption of hyphae-form cell walls and leakage. The following images show representative examples of the attachment and growth of *C. albicans* on control and caspofungin-grafted surfaces, showing large-area images of biofilms and magnified smaller areas showing fungal colonies.

The images in Figure 8.20 show that attachment and formation of colonies and biofilm is similar on tissue culture polystyrene and ALDpp surfaces; both are able to serve as good controls for effects arising from caspofungin grafting. On caspofungin-grafted surfaces, on the other hand, no analogous formation of large patches of well-formed biofilm were observed (Figure 8.21). Colonies of fungal cells are visible as clumps, but many cells are dead, as are most of the individual fungal cells. Thus, it appears that fungal cells are not killed rapidly upon contact with the surface; it seems that many cells are able to attach and are killed afterwards. This is reasonable given that caspofungin interferes with cell wall synthesis, a mechanism that would set in after fungal cells have established close contact with the surface.

It should be noted that the staining is not as clearcut as the simple rule of green = alive and red = dead. The green dye diffuses into the ALDpp and thus gives some background staining. Also, cells that have not disintegrated seem to stain yellow/orange. Nevertheless the images in Figure 8.21 provide clear evidence that caspofungin grafted onto ALDpp interferes in major ways with fungal attachment and prevents biofilm formation.

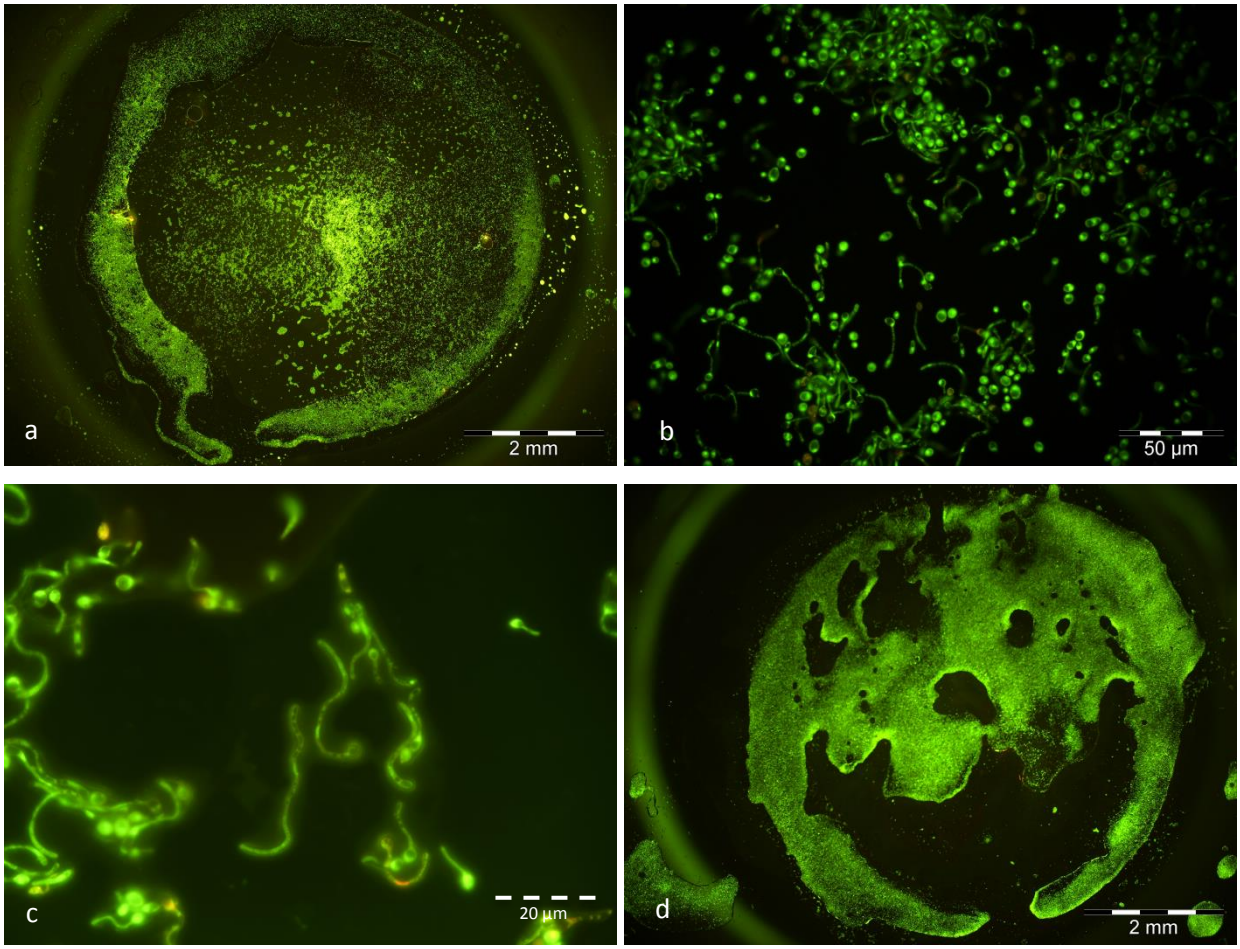


Figure 8.20: Control ALDpp surfaces after 48–56 hours with *Candida albicans* on the surface of: (a) ALDpp showing full sample size, (b) 60x image, (c) 100x image, (d) TCPS control surface, full sample size.

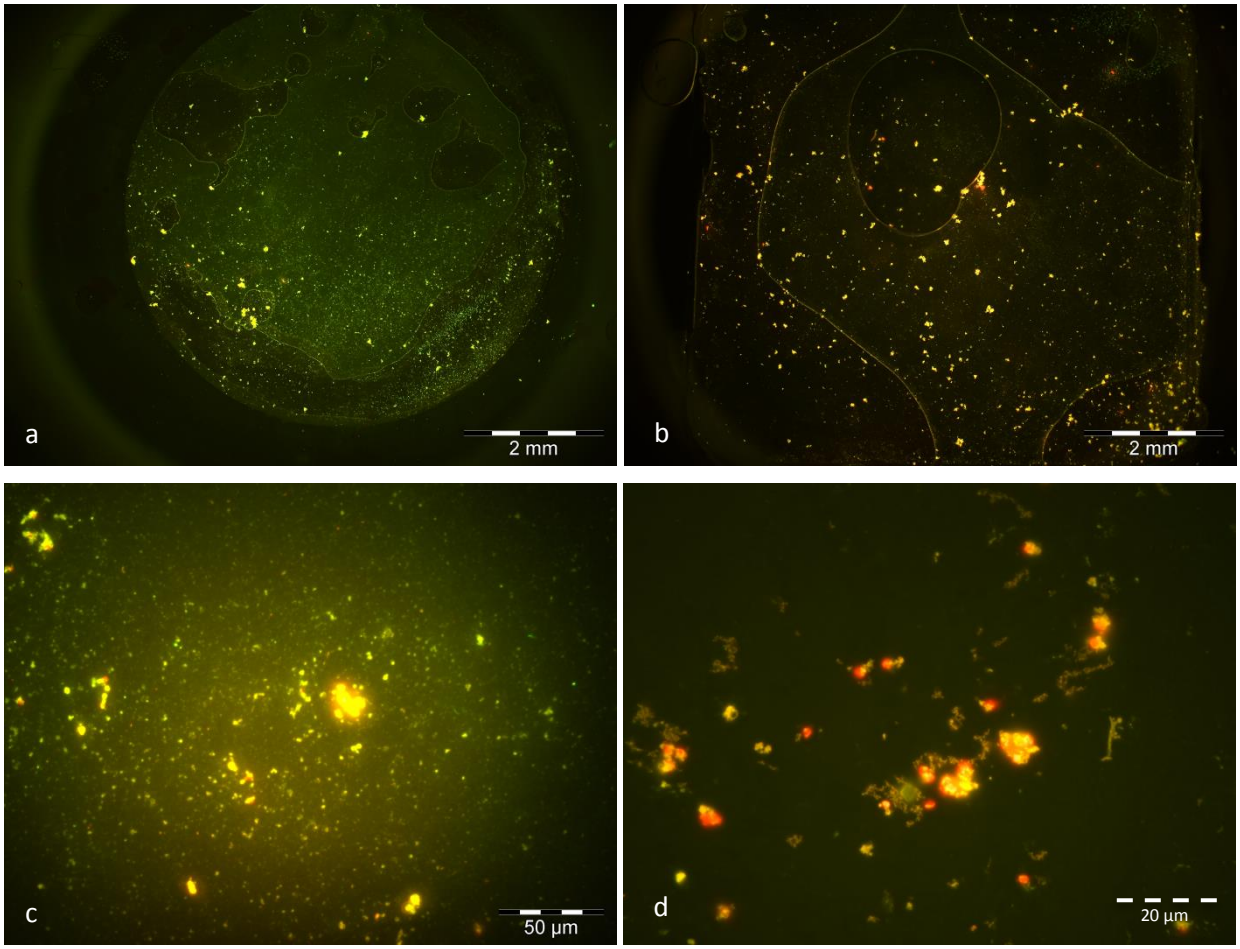


Figure 8.21: Caspofungin-treated plasma polymer surfaces with *Candida albicans* after 48 hours incubation—no intact yeast cells or hyphae were found on the surface: (a) appears greenish due to background fluorescence; (b) full frame of dead fungi; (c) 60x image of dead fungi—backgroup fluorescence makes them appear greenish, but they are misshapen and leaking; (d) 100x image of dead fungi, showing possible leaking and broken hyphae

To investigate whether there might be any effects arising from adsorbed rather than covalently grafted drug molecules, samples were soaked for 2 weeks in PBS. In contrast to amphotericin B, caspofungin is well soluble in water and thus it was expected that such soaking would remove any adsorbed molecules. XPS data recorded on samples washed for 2 weeks were identical to those recorded above, suggesting that even the initial washing had removed all adsorbed molecules and the further 2-week soaking had not led to any further detachment.

Interestingly, these thoroughly washed samples gave even better antifungal performance, as shown in Figure 8.22. In the right-hand image the automatic camera setting compensated for the low intensity and enhanced markedly the weak delocalised background staining within the ALDpp. Only a few colonies are observed, and they have not formed a biofilm matrix.

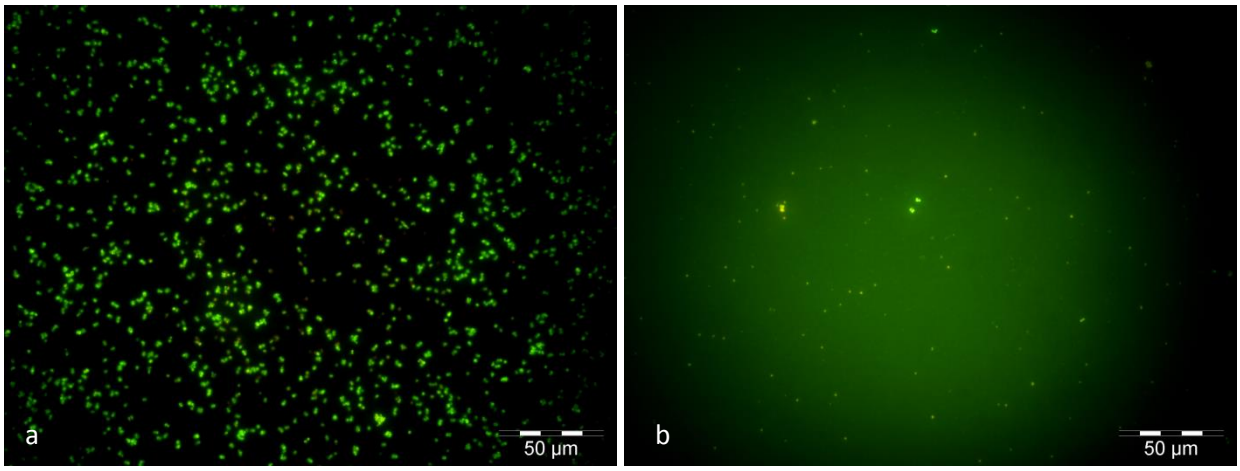


Figure 8.22: Aldehyde plasma polymer surfaces: (a) control surface with multiple yeast cell colonies and some pseudohypae, (b) caspofungin surface soaked and stored for 2 weeks before testing, with *Candida albicans* after 48 hours incubation, showing some contamination from removal of the mask but no viable cells.

Thus, these images clearly show that caspofungin-grafted surfaces showed excellent antifungal capability. Surface analysis showed that it is indeed attached covalently, with good uniformity. The antifungal tests were quite definite in showing killing of fungal cells on the surface.

The mechanism of action of caspofungin is to target the enzyme controlling the synthesis of cell wall β-1,3-D-glucans. However, treatment of *Candida albicans* with caspofungin also alters cell morphology (Bizerra et al. 2011; Dunyach et al. 2011; Formosa et al. 2013), lowers cell wall mechanical strength, increases sensitivity of osmotic pressure and eventually leads to cell lysis and death (El-Kirat-Chatel et al. 2013; Letscher-Bru & Herbrecht 2003). The structure of caspofungin is such that it would have to penetrate into the fungal cell wall and membrane to affect the β-1, 3-glucan synthase enzyme, which is embedded in the lipid bilayer. While it is obvious that caspofungin causes damage to the cell structure, how this happens exactly is still not well established and other mechanisms may be found.

8.4.3 Cell Toxicity Studies

For implant applications and wound healing products, coatings should selectively deter microbial colonisation but not cause adverse effects on apposite human cells and tissue. The same surfaces as mentioned above were tested with primary human fibroblast, harvested from human skin. They were added in suspension to well plates containing control and coated samples and grown for 3 days. As shown in Figure 8.23, no toxicity was observed.

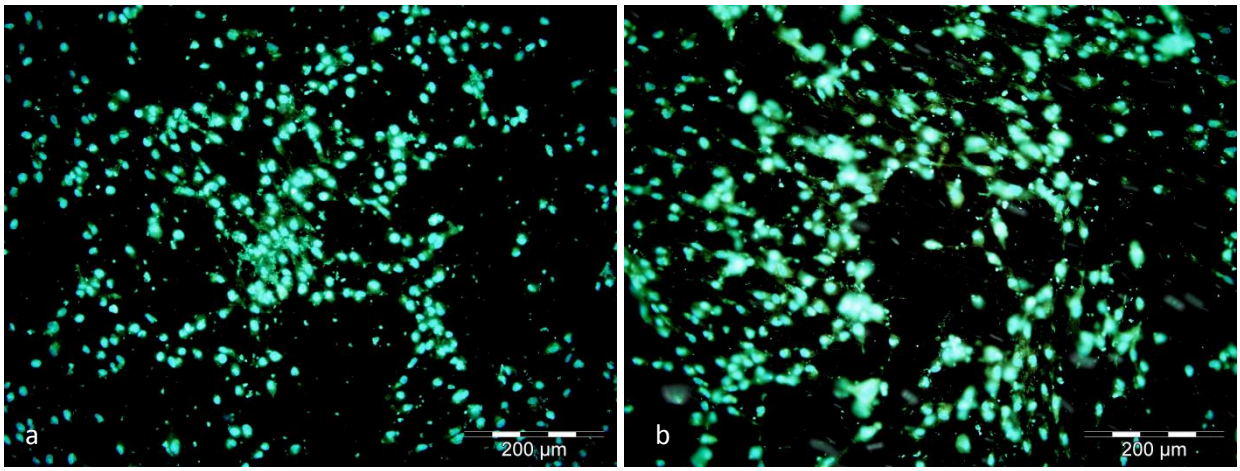


Figure 8.23: Control and Caspofungin-treated surfaces with primary fibroblasts after 3 days growth: (a) control surface, (b) caspofungin-treated surface

For quantitiative analysis, cells were counted within nine images and the average numbers determined; they are shown in Figure 8.24. To further study the effect of surface density, caspofungin was also grafted from a 10x diluted solution. Clearly, there is no difference between samples within experimental uncertainty.

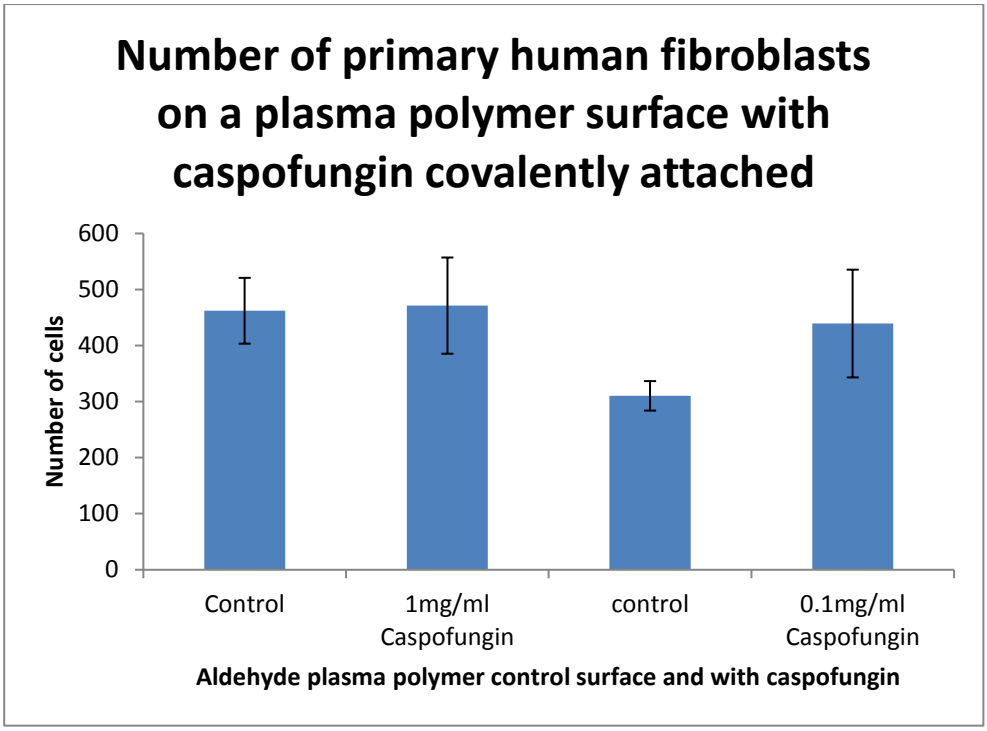


Figure 8.24: Primary human fibroblast cells per view area. Caspofungin was not toxic to cells.

The lack of toxicity to finroblasts can be explained either by the tethering effect, which prevents the caspofungin from penetrating into the fibroblast cells, or because it does not affect the human membranes owing to their differing structures and not possessing a similar glucan synthase enzyme. Human cells tend to have a cell membrane of approximately 10 nm (Mitra et al. 2004), as opposed to fungi, which have complicated membranes of more than 100 nm thickness (Chaffin 2008).

8.5 Conclusions

In this chapter it was explored whether two commercially available antifungal compounds, amphotericin B and caspofungin, would retain activity when covalently grafted onto propanal plasma polymer surfaces. Both compounds are believed to target membrane-associated processes, which might confer activity to these drugs as a coating unless the covalent attachment process causes too much steric hindrance and restricts (partial) insertion into the fingal lipid bilayer membrane.

Caspofungin attached to plasma polymer surfaces created an excellent antifungal surface coating without showing toxicity to primary fibroblasts. Further investigation will be needed to define the mechanism and steric aspects by which this drug is still capable of acting even when covalently tethered. With Amphotericin B, results were less clearcut; it also had antifungal activity when attached to a plasma surface; however, the results did show some variation and will also need to be investigated further. The poor solubility of amphotericin B in aqueous media makes it much harder than for caspofungin to ensure that all adsorbed or precipitated molecules are washed off prior to testing and observed antifungal effects can be assigned unambiguously only to covalently tethered molecules.

Chapter 9: Conclusion and Future Outlook

9.1 Conclusion

This thesis describes the careful preparation, characterisation and assessment of several antimicrobial biomaterials coatings. The research was conducted to understand better the underlying mechanisms and criteria that are necessary to produce an antimicrobial surface. The production of antimicrobial surfaces requires a suitable substrate, a surface chemistry modified to provide an appropriate chemical group for bonding the antimicrobial substance, and an antimicrobial substance that will function when covalently tethered to a biomaterial surface. Although many groups have expertise in the different areas, this project utilised the authors' in-depth understanding of biomaterials, surface modification and chemistry, antimicrobial pharmacology, microbiology and immunology.

This research project started off with basic experiments investigating silver nanoparticles in order to assess the cytotoxicity of silver on simple cell lines. Silver nanoparticles are well known and heavily used in everything from wound dressings to toys. The results showed that silver has a greater toxic effect on the fibroblasts and precursor cells than on cells that form tight junctions and layers. These results were understated because cells were not counted and graphed but simply displayed to show simple effects of silver on the individual cells.

The study then examined the developing field of AMPs used as coatings and the possibility that the surface-permeable mechanism of action on bacteria, when tethered to a biomaterial surface, may still be functional and thereby create an antibacterial surface. The results were promising and are certainly worthy of further studies on their use in pharmacology and as an antimicrobial surface.

The next series of experiments used synthetic antimicrobial nylon-3 polymers, modelled on the research on AMPs that was discussed in the preceding chapter. The results were extremely exciting and show that a highly effective antimicrobial surface can be successfully produced

with the best synthetic polymer. Synthetic antimicrobial mimics are highly useful; they use the antibacterial structures found naturally and enhance them, giving them a lower MIC and the ability to penetrate the bacteria cell, further causing a higher rate of destruction and the benefit of killing bacteria in each state rather than only in the multiplying state. Moreover, coatings of synthetic AMP analogues do not possess the potential disadvantage of susceptibility to degradation by proteolytic enzymes.

The next chapter examined daptomycin, a new drug whose method of action has yet to be clearly elucidated. Earlier microbiological research had deduced that it was also permeabilising to the bacterial membrane, causing destabilisation and death. However, if it were simply a surface-permeabilising drug, it should have been active when covalently grafted on a solid substrate. The results indicate that it does indeed have further actions other than just cell permeabilisation by lipid layer destabilisation because it did not show activity when immobilised.

The final experimental chapter included experiments towards an antifungal surface coating using two antifungal pharmaceuticals that research has indicated are membrane active; thus it was hypothesised that they might still retain activity when surface immobilised. Caspofungin was indeed found to be active when surface tethered, providing a successful antifungal surface coating. With amphotericin B, there was also some activity, but its poor solubility made it difficult to fully exclude effects arising from molecules possibly present without covalent bonding to the surface and thus able to diffuse into fungal cells.

Many published studies claim to have created antimicrobial surfaces; however, very few have used surface analysis and accepted testing methods to prove both exclusively covalent attachment and activity. This thesis intended to remedy this problem by creating a set of well-proven testing methods to assess coatings accurately for proof of attachment of the antimicrobials, to estimate amounts of the antimicrobial compound on the surface, and a number of techniques that enable assessing antimicrobial activity and reveal the mechanism of action.

One issue that could not be covered in this thesis was the reactions of the immune system to antibacterial coatings and assessment of whether their presence would assist healing. The scratch test indicated that the nylon-3 surfaces encourage cell growth and migration into the wound area by filling the wound area, as opposed to the control where bacterial colonisation prevented closure of the gap by fibroblasts. Preliminary enzyme-linked immunosorbent assay (ELISA) tests, which would show what signalling processes are stimulated, were inconclusive, as were other experiments that attempted to examine signalling from cells, and time did not permit to progress this aspect. It would be interesting to conduct an *in vitro* experiment to examine exactly how cells respond and signal in response to the coatings. However, that was beyond the scope of this thesis.

The research also needs to extend into animal and human testing to give a full picture of how the whole body system will react to the foreign biomaterial and its modified surface. The methods for undertaking this type of research are still in the beginning stages and leave much room for improvement. Animals are not humans, and mice are capable of healing and recovering from far more serious bacterial infections than humans. In addition, the human immune system is much more reactive in very individual ways. There is also the issue of ethics in that wounding animals is not pleasant, and in humans, the ethos of 'do no harm' makes it difficult to proceed with the unknown consequences of trialling a new product.

While this study has found that biomaterials can be equipped with antimicrobial coatings, it is only the beginning of a long journey towards the actual production of an antimicrobial hip or knee implant. Many questions have yet to be studied. How the microbial world responds to an antimicrobial surface also needs to be considered. Once the bacteria are controlled, will fungi colonise? Once we have one fungal biofilm formation under control, will yet another one take over and cause even worse infection? These are questions that can only be answered once the risk is taken and an antimicrobial coating is selected and produced for progress to clinical testing.

References

Al-Badri, ZM, Som, A, Lyon, S, Nelson, CF, Nusslein, K & Tew, GN 2008, 'Investigating the effect of increasing charge density on the hemolytic activity of synthetic antimicrobial polymers', *Biomacromolecules*, vol. 9, 2805–2810.

Albers, CE, Hofstetter, W, Siebenrock, KA, Landmann, R & Klenke, FM 2013, 'In vitro cytotoxicity of silver nanoparticles on osteoblasts and osteoclasts at antibacterial concentrations', *Nanotoxicology*, vol. 7, 30–36.

Alberts, B 2008, *Molecular biology of the cell*, Garland Science, New York.

Albrich, WC, Angstwurm, M, Bader, L & Gartner, R 1999, 'Drug resistance in intensive care units', *Infection*, vol. 27**,** S19–S23.

Almeida, PF & Pokorny, A 2009, 'Mechanisms of antimicrobial, cytolytic, and cell-penetrating peptides: from kinetics to thermodynamics', *Biochemistry*, vol. 48, 8083–8093.

Amberg, M, Grieder, K, Barbadoro, P, Heuberger, M & Hegemann, D 2008, 'Electromechanical behavior of nanoscale silver coatings on PET fibers', *Plasma Processes and Polymers*, vol. 5, 874–880.

Andersson, J, Ekdahl, KN, Lambris, JD & Nilsson, B 2005, 'Binding of C3 fragments on top of adsorbed plasma proteins during complement activation on a model biomaterial surface', *Biomaterials*, vol. 26, 1477–1485.

Andersson, J, Ekdahl, KN, Larsson, R, Nilsson, UR & Nilsson, B 2002, 'C3 adsorbed to a polymer surface can form an initiating alternative pathway convertase', *The Journal of Immunology*, vol. 168**,** 5786.

Andrade, JD & Chen, WY 1986, 'Probing polymer surface and interface dynamics', *Surface and Interface Analysis*, vol. 8, 253–256.

Aoki, W, Kuroda, K & Ueda, M 2012, 'Next generation of antimicrobial peptides as molecular targeted medicines', *Journal of Bioscience and Bioengineering*, vol. 114**,** 365–370.

Arvidsson, PI, Frackenpohl, J, Ryder, NS, Liechty, B, Petersen, F, Zimmermann, H, Camenisch, GP, Woessner, R & Seebach, D 2001, 'On the antimicrobial and hemolytic activities of amphiphilic beta-peptides', *Chembiochem*, vol. 2**,** 771–+.

Aspnes, DE 2013, 'Spectroscopic ellipsometry: a perspective', *Journal of Vacuum Science & Technology A*, vol. 31.

Atiyeh, BS, Costagliola, M, Hayek, SN & Dibo, SA 2007, 'Effect of silver on burn wound infection control and healing: review of the literature', *Burns*, vol. 33**,** 139–148.

Ausubel, FM 2002, *Short protocols in molecular biology: a compendium of methods from current protocols in molecular biology*, Wiley, New York.

Aziz, Z, Abu, SF & Chong, NJ 2012, 'A systematic review of silver-containing dressings and topical silver agents (used with dressings) for burn wounds', *Burns*, vol. 38, 307–318.

Azzam, RMA 1976, 'Perspective on ellipsometry', *Surface Science*, vol. 56, 6–18.

Ball, LJ, Goult, CM, Donarski, JA, Micklefield, J & Ramesh, V 2004, 'NMR structure determination and calcium binding effects of lipopeptide antibiotic daptomycin', *Organic & Biomolecular Chemistry*, vol. 2, 1872–1878.

Barbey, R, Lavanant, L, Paripovic, D, Schuewer, N, Sugnaux, C, Tugulu, S & Klok, H-A 2009, 'Polymer brushes via surface-initiated controlled radical polymerization: synthesis, characterization, properties, and applications', *Chemical Reviews*, vol. 109, 5437–5527.

Barns, KJ & Weisshaar, JC 2013, 'Real-time attack of LL-37 on single *Bacillus subtilis* cells', *Biochimica et Biophysica Acta-Biomembranes*, vol. 1828, 1511–1520.

Barraud, N, Hassett, DJ, Hwang, SH, Rice, SA, Kjelleberg, S & Webb, JS 2006, 'Involvement of nitric oxide in biofilm dispersal of *Pseudomonas aeruginosa*', *Journal of Bacteriology*, vol. 188, 7344–7353.

Bechinger, B 1999, 'The structure, dynamics and orientation of antimicrobial peptides in membranes by multidimensional solid-state NMR spectroscopy', *Biochimica et Biophysica Acta—Biomembranes*, vol. 1462, 157–183.

Bechinger, B & Lohner, K 2006, 'Detergent-like actions of linear amphipathic cationic antimicrobial peptides', *Biochimica et Biophysica Acta—Biomembranes*, vol. 1758, 1529–1539.

Belu, AM, Graham, DJ & Castner, DG 2003, 'Time-of-secondary ion mass spectroscopy: techniques and applications for the characterization of biomaterial surfaces', *Biomaterials*, vol. 24, 3635–3653.

Benbow, M 2010, 'Wound swabs and chronic wounds', *Practice Nurse*, vol. 39, 27.

Biederman, H 1987, 'British Vacuum Council Annual Address 1986—Polymer-films prepared by plasma polymerization and their potential application', *Vacuum*, vol. 37, 367–373.

Biesinger, MC, Corcoran, PL & Walzak, AJ 2011, 'Developing ToF-SIMS methods for investigating the degradation of plastic debris on beaches', *Surface and Interface Analysis*, vol. 43, 443–445.

Bizerra, FC, Melo, ASA, Katchburian, E, Freymueller, E, Straus, AH, Takahashi, HK & Colombo, AL 2011, 'Changes in cell wall synthesis and ultrastructure during paradoxical growth effect of caspofungin on four different *Candida* species', *Antimicrobial Agents and Chemotherapy*, vol. 55, 302–310.

Blattler, TM, Pasche, S, Textor, M & Griesser, HJ 2006, 'High salt stability and protein resistance of poly(L-lysine)-g-poly(ethylene glycol) copolymers covalently immobilized via aldehyde plasma polymer interlayers on inorganic and polymeric substrates', *Langmuir*, vol. 22, 5760–5769.

Boyes, SG, Granville, AM, Baum, M, Akgun, B, Mirous, BK & Brittain, WJ 2004, 'Polymer brushes—surface immobilized polymers', *Surface Science*, vol. 570, 1–12.

Brett, DW 2013, 'The in-vitro antibacterial activity of nanocrystalline silver dressings against bacteria with NDM-1 carbapenemase', *American Journal of Infection Control*, vol. 41, S46–S47.

Briggs, D 1986, 'SIMS for the study of polymer surfaces: a review', *Surface and Interface Analysis*, vol. 9, 391–404.

Briggs, D 1998, *Surface analysis of polymers by XPS and static SIMS*, Cambridge University Press.

Briggs, D, Fletcher, IW & Goncalves, NM 2002, 'High-mass-resolution ToF-SIMS study of chlorine-containing polymers', *Surface and Interface Analysis*, vol. 33, 178–184.

Broekhuizen, CAN, De Boer, L, Schipper, K, Jones, CD, Quadir, S, Vandenbroucke-Grauls, CMJE & Zaat, SAJ 2008, '*Staphylococcus epidermidis* is cleared from biomaterial implants but persists in peri-implant tissue in mice despite rifampicin/vancomycin treatment', *Journal of Biomedical Materials Research Part A*, vol. 85A, 498–505.

Brogden, KA 2005, 'Antimicrobial peptides: pore formers or metabolic inhibitors in bacteria?', *Nature ReviewsMicrobiology*, vol. 3, 238–250.

Brooks, BD, Brooks, AE & Grainger, DW (eds) 2013, *Antimicrobial medical devices in preclinical development and clinical use*, Springer, New York.

Brown, GD, Denning, DW, Gow, NAR, Levitz, SM, Netea, MG & White, TC 2012, 'Hidden killers: human fungal infections', *Science Translational Medicine*, vol4.

Brown, KL, Poon, GFT, Birkenhead, D, Pena, OM, Falsafi, R, Dahlgren, C, Karlsson, A, Bylund, J, Hancock, REW & Johnson, P 2011, 'Host defense peptide LL-37 selectively reduces proinflammatory macrophage responses', *Journal of Immunology*, vol. 186, 5497–5505.

Browne, MM, Lubarsky, GV, Davidson, MR & Bradley, RH 2004, 'Protein adsorption onto polystyrene surfaces studies by XPS and AFM', *Surface Science*, vol. 553, 155–167.

Burd, A, Chiu, T & Huang, L 2008, 'Acticoat™: a critique of application', *Burns*, vol. 34, 575–577.

Campoccia, D, Montanaro, L & Arciola, CR 2006, 'The significance of infection related to orthopedic devices and issues of antibiotic resistance', *Biomaterials*, vol. 27, 2331–2339.

Campoccia, D, Montanaro, L, Arciola CR, 2013, 'A review of the biomaterials technologies for infection-resistant surfaces', *Biomaterials*, vol. 34, 8533-8554.

Carpenter, CF & Chambers, HF 2004, 'Daptomycin: another novel agent for treating infections due to drug-resistant Gram-positive pathogens', *Clinical Infectious Diseases*, vol. 38, 994–1000.

Carville, K 2005, *Wound care manual*, Silver Chain Nursing Association, Osborne Park, WA.

Cassone, A 2013, 'Development of vaccines for *Candida albicans*: fighting a skilled transformer', *Nature Reviews Microbiology*, vol. 11, 884–891.

Castner, DG & Ratner, BD 2002, 'Biomedical surface science: foundations to frontiers', *Surface Science*, vol. 500, 28–60.

Chaffin, WL 2008, '*Candida albicans* cell wall proteins', *Microbiology and Molecular Biology Reviews*, vol. 72, 495–+.

Chandra, J, Kuhn, DM, Mukherjee, PK, Hoyer, LL, McCormick, T & Ghannoum, MA 2001, 'Biofilm formation by the fungal pathogen *Candida albicans*: development, architecture, and drug resistance', *Journal of Bacteriology*, vol. 183, 5385–5394.

Charnley, M, Textor, M & Acikgoz, C 2011, 'Designed polymer structures with antifouling-antimicrobial properties', *Reactive & Functional Polymers*, vol. 71, 329–334.

Chatelier, RC, Xie, X, Gengenbach, TR & Griesser, H 1995a, 'Quantitative analysis of polymer surface restructuring', *Langmuir*, vol. 11, 2574–2584.

Chatelier, RC, Xie, X, Gengenbach, TR & Griesser, HJ 1995b, 'Effect of plasma modification conditions on surface restructuring', *Langmuir*, vol. 11, 2585–2591.

Chen, R, Willcox, MDP, Cole, N, Ho, KKK, Rasul, R, Denman, JA & Kumar, N 2012, 'Characterization of chemoselective surface attachment of the cationic peptide melimine and its effects on antimicrobial activity', *Acta Biomaterialia*, vol. 8, 4371–4379.

Cheng, X, Canavan, HE, Stein, MJ, Hull, JR, Kweskin, SJ, Wagner, MS, Somorjai, GA, Castner, DG & Ratner, BD 2005, 'Surface chemical and mechanical properties of plasma-polymerized N-isopropylacrylamide', *Langmuir*, vol. 21, 7833–7841.

Chim, H, Tan, BH & Song, C 2007, 'Five-year review of infections in a burn intensive care unit: high incidence of *Acinetobacter baumannii* in a tropical climate', *Burns*, vol. 33, 1008–1014.

Cho, JH, Park, IY, Kim, MS & Kim, SC 2002, 'Matrix metalloproteinase 2 is involved in the regulation of the antimicrobial peptide parasin I production in catfish skin mucosa', vol. 531**,** 459–463.

Chopra, I 2007, 'The increasing use of silver-based products as antimicrobial agents: a useful development or a cause for concern?', *Journal of Antimicrobial Chemotherapy*, vol. 59, 587–590.

Chopra, I & Roberts, M 2001, 'Tetracycline antibiotics: mode of action, applications, molecular biology, and epidemiology of bacterial resistance', *Microbiology and Molecular Biology Reviews*, vol. 65, 232–+.

Chua, KYL, Seemann, T, Harrison, PF, Monagle, S, Korman, TM, Johnson, PDR, Coombs, GW, Howden, BO, Davies, JK, Howden, BP & Stinear, TP 2011, 'The dominant Australian community-acquired methicillin-resistant *Staphylococcus aureus* clone ST93-IV 2B is highly virulent and genetically distinct', *PloS ONE*, vol. 6.

Coad, BR, Jasieniak, M, Griesser, SS & Griesser, HJ 2013, 'Controlled covalent surface immobilisation of proteins and peptides using plasma methods', *Surface & Coatings Technology*, vol. 233, 169–177.

Coad, R, Kidd, SE, Ellis, DH, Griesser, HJ 2014, 'Biomaterials surfaces capable of resisting fungal attachment and biofilm formation', *Biotechnology Advances*, vol. 32, no. 2, 296–307.

Coombs, GW, Monecke, S, Pearson, JC, Tan, H-L, Chew, Y-K, Wilson, L, Ehricht, R, O'Brien, FG & Christiansen, KJ 2011, 'Evolution and diversity of community-associated methicillin-resistant *Staphylococcus aureus* in a geographical region', *BMC Microbiology*, vol. 11.

Cossart, P 2005, *Cellular microbiology*, ASM Press, Washington, DC.

Costa, F, Carvalho, IF, Montelaro, RC, Gomes, P & Martins, MCL 2011, 'Covalent immobilization of antimicrobial peptides (AMPs) onto biomaterial surfaces', *Acta Biomaterialia*, vol. 7, 1431–1440.

Costerton, JW, Stewart, PS & Greenberg, EP 1999, 'Bacterial biofilms: a common cause of persistent infections', *Science*, vol. 284, 1318–1322.

Craft, JE 2011, 'Dissecting the immune cell mayhem that drives lupus pathogenesis', *Science Translational Medicine*, vol. 3.

Daghighi, S, Sjollema, J, Jaspers, V, De Boer, L, Zaat, SAJ, Dijkstra, RJB, Van Dam, GM, van der Mei, HC & Busscher, HJ 2012, 'Persistence of a bioluminescent *Staphylococcus aureus* strain on and around degradable and non-degradable surgical meshes in a murine model', *Acta Biomaterialia*, vol. 8, 3991–3996.

Dai, L, StJohn, HAW, Bi, J, Zientek, P, Chatelier, RC & Griesser, HJ 2000, 'Biomedical coatings by the covalent immobilization of polysaccharides onto gas-plasma-activated polymer surfaces', *Surface and Interface Analysis*, vol. 29, 46–55.

De Santa Maria, LC, Souza, JDC, Aguiar, M, Wang, SH, Mazzei, JL, Felzenszwalb, I & Amico, SC 2008, 'Synthesis, characterization, and bactericidal properties of composites based on crosslinked resins containing silver', *Journal of Applied Polymer Science*, vol. 107, 1879–1886.

Deacon, JW & Deacon, JW 2006, *Fungal biology*, Blackwell, Malden, MA.

Del Gaudio, G, Lombardi, L, Maisetta, G, Esin, S, Batoni, G, Sanguinetti, M, Senesi, S & Tavanti, A 2013, 'Antifungal activity of the noncytotoxic human peptide hepcidin 20 against fluconazole-resistant *Candida glabrata* in human vaginal fluid', *Antimicrobial Agents and Chemotherapy*, vol. 57, 4314–4321.

Delcorte, A, Bertrand, P, Arys, X, Jonas, A, Wischerhoff, E, Mayer, B & Laschewsky, A 1996, 'ToF-SIMS study of alternate polyelectrolyte thin films: chemical surface characterization and molecular secondary ions sampling depth', *Surface Science*, vol. 366, 149.

Despax, B & Raynaud, P 2007, 'Deposition of "polysiloxane" thin films containing silver particles by an RF asymmetrical discharge', *Plasma Processes and Polymers*, vol. 4, 127–134.

Duday, D, Vreuls, C, Moreno, M, Frache, G, Boscher, ND, Zocchi, G, Archambeau, C, Van De Weerdt, C, Martial, J & Choquet, P 2013, 'Atmospheric pressure plasma modified surfaces for immobilization of antimicrobial nisin peptides', *Surface and Coatings Technology*, vol. 218, 152–161.

Dugourd, D, Yang, H, Elliott, M, Siu, R, Clement, JJ, Straus, SK, Hancock, REW & Rubinchik, E 2011, 'Antimicrobial properties of MX-2401, an expanded-spectrum lipopeptide active in the presence of lung surfactant', *Antimicrobial Agents and Chemotherapy*, vol. 55, 3720–3728.

Dunyach, C, Drakulovski, P, Bertout, S, Jouvert, S, Reynes, J & Mallie, M 2011, 'Fungicidal activity and morphological alterations of *Candida albicans* induced by echinocandins: study of strains with reduced caspofungin susceptibility', *Mycoses*, vol. 54, E62–E68.

Dupres, V, Dufrene, YF & Heinisch, JJ 2010, 'Measuring cell wall thickness in living yeast cells using single molecular rulers', *ACS Nano*, vol. 4, 5498–5504.

Durr, UHN, Sudheendra, US & Ramamoorthy, A 2006, 'LL-37, the only human member of the cathelicidin family of antimicrobial peptides', *Biochimica et Biophysica Acta-Biomembranes*, vol. 1758, 1408–1425.

Edmondson, S, Osborne, VL & Huck, WTS 2004, 'Polymer brushes via surface-initiated polymerizations', *Chemical Society Reviews*, vol. 33, 14.

Eksik, O, Erciyes, AT & Yagci, Y 2008, 'In situ synthesis of oil based polymer composites containing silver nanoparticles', *Journal of Macromolecular Science Part A—Pure and Applied Chemistry*, vol. 45, 698–704.

El-Kirat-Chatel, S, Beaussart, A, Alsteens, D, Jackson, DN, Lipke, PN & Dufrene, YF 2013, 'Nanoscale analysis of caspofungin-induced cell surface remodelling in *Candida albicans*', *Nanoscale*, vol. 5, 1105–1115.

Engler, AC, Shukla, A, Puranam, S, Buss, HG, Jreige, N & Hammond, PT 2011, 'Effects of side group functionality and molecular weight on the activity of synthetic antimicrobial polypeptides', *Biomacromolecules*, vol. 12, 1666–1674.

Estivill, D, Arias, A, Torres-Lana, A, Carrillo-Muñoz, AJ & Arévalo, MP 2011, 'Biofilm formation by five species of *Candida* on three clinical materials', *Journal of Microbiological Methods*, vol. 86, 238–242.

Eswaramoorthy, P, Erb, ML, Gregory, JA, Silverman, J, Pogliano, K, Pogliano, J & Ramamurthi, KS 2011, 'Cellular architecture mediates DivIVA ultrastructure and regulates min activity in *Bacillus subtilis*', *mBio*, vol. 2.

Fites, JS, Ramsey, JP, Holden, WM, Collier, SP, Sutherland, DM, Reinert, LK, Gayek, AS, Dermody, TS, Aune, TM, Oswald-Richter, K & Rollins-Smith, LA 2013, 'The invasive chytrid fungus of amphibians paralyzes lymphocyte responses', *Science*, vol. 342, 366–369.

Formosa, C, Schiavone, M, Martin-Yken, H, Francois, JM, Duval, RE & Dague, E 2013, 'Nanoscale effects of caspofungin against two yeast species, *Saccharomyces cerevisiae* and *Candida albicans*', *Antimicrobial Agents and Chemotherapy*, vol. 57, 3498–3506.

Fox, JL 2013, 'Antimicrobial peptides stage a comeback', *Nature Biotechnology*, vol. 31, 379–382.

Fox, MA, Thwaite, JE, Ulaeto, DO, Atkins, TP & Atkins, HS 2012, 'Design and characterization of novel hybrid antimicrobial peptides based on cecropin A, LL-37 and magainin II', vol. 33, 197–205.

Foye, WO, Lemke, TL & Williams, DA 2008, *Foye's principles of medicinal chemistry*, Lippincott Williams & Wilkins, Philadelphia.

Franklin, MJ & Stewart, PS 2008, 'Physiological heterogeneity in biofilms', *Nature Reviews Microbiology*, vol. 6, 199–210.

Fraunholz, M & Sinha, B 2012, 'Intracellular *Staphylococcus aureus*: live-in and let die', *Frontiers in Cellular and Infection Microbiology*, vol. 2, 43.

Furno, F, Morley, KS, Wong, B, Sharp, BL, Arnold, PL, Howdle, SM, Bayston, R, Brown, PD, Winship, PD & Reid, HJ 2004, 'Silver nanoparticles and polymeric medical devices: a new approach to prevention of infection?', *Journal of Antimicrobial Chemotherapy*, vol. 54, 1019–1024.

Gabriel, GJ, Madkour, AE, Dabkowski, JM, Nelson, CF, Nusslein, K & Tew, GN 2008, 'Synthetic mimic of antimicrobial peptide with nonmembrane-disrupting antibacterial properties', *Biomacromolecules*, vol. 9, 2980–2983.

Galya, T, Sedlarik, V, Kuritka, I, Novotny, R, Sedlarikova, J & Saha, P 2008, 'Antibacterial poly(vinyl alcohol) film containing silver nanoparticles: preparation and characterization', *Journal of Applied Polymer Science*, vol. 110, 3178–3185.

Gazit, E, Miller, IR, Biggin, PC, Sansom, MSP & Shai, Y 1996, 'Structure and orientation of the mammalian antibacterial peptide cecropin P1 within phospholipid membranes', *Journal of Molecular Biology*, vol. 258, 860–870.

Gengenbach, TR, Chatelier, RC & Griesser, HJ 1996, 'Characterization of the aging of plasma-deposited polymer films: global analysis of X-ray photoelectron spectroscopy data', *Surface and Interface Analysis*, vol. 24, 271–281.

Gengenbach, TR & Griesser, HJ 1998, 'Compositional changes in plasma-deposited fluorocarbon films during ageing', *Surface and Interface Analysis*, vol. 26, 498–511.

Gengenbach, TR & Griesser, HJ 1999, 'Aging of 1,3-Diaminopropane plasma-deposited polymer films: mechanisms and reaction pathways', *Journal of Polymer Science; Part A: Polymer Chemistry*, vol. 37, 2191–2206.

Gengenbach, TR, Vasic, ZR, Chatelier, RC & Griesser, HJ 1994, 'A multi-technique study of the spontaneous oxidation of n-hexane plasma polymers', *Journal of Polymer Science; Part A: Polymer Chemistry*, vol. 32, 1399–1414.

Gengenbach, TR, Xie, X, Chatelier, RC & Griesser, HJ 1994, 'Evolution of the surface composition and topography of perflourinated polymers following ammonia-plasma treatment', *Journal of Adhesion Science and Technology*, vol. 8, 305–328.

Gerard, R, Sendid, B, Techy, AG, Vernier-Massouille, G, Jouault, T, Francois, N, Colombel, J-F & Poulain, D 2013, '*Candida albicans* colonization and anti-glycan antibodies in active and quiescent Crohn's disease', *Gastroenterology*, vol. 144, S829–S829.

Glinel, K, Jonas, AM, Jouenne, T, Leprince, J, Galas, L & Huck, WTS 2009, 'Antibacterial and antifouling polymer brushes incorporating antimicrobial peptide', *Bioconjugate Chemistry*, vol. 20, 71–77.

Glinel, K, Thebault, P, Humblot, V, Pradier, CM & Jouenne, T 2012, 'Antibacterial surfaces developed from bio-inspired approaches', *Acta Biomaterialia*, vol. 8, 1670–1684.

Golan, DE 2008, *Principles of pharmacology: the pathophysiologic basis of drug therapy*, Lippincott Williams & Wilkins, Philadelphia.

Gong, X, Dai, L, Griesser, HJ & Mau, AWH 2000, 'Surface immobilization of poly(ethylene oxide): structure and properties', *Journal of Polymer Science; Part B: Polymer Physics*, vol. 38, 2323–2332.

Gordon, O, Slenters, TV, Brunetto, PS, Villaruz, AE, Sturdevant, DE, Otto, M, Landmann, R & Fromm, KM 2010, 'Silver coordination polymers for prevention of implant infection: thiol interaction, impact on respiratory chain enzymes, and hydroxyl radical induction', *Antimicrobial Agents and Chemotherapy*, vol. 54, 4208–4218.

Gow, NAR, Van De Veerdonk, FL, Brown, AJP & Netea, MG 2012, '*Candida albicans* morphogenesis and host defence: discriminating invasion from colonization', *Nature Reviews Microbiology*, vol. 10, 112–122.

Graham, DJ & Ratner, BD 2002, 'Multivariate analysis of TOF-SIMS spectra from dodecanethiol SAM assembly on gold: spectral interpretation and TOF-SIMS fragmentation processes', *Langmuir*, vol. 18, 5861–5868.

Grainger, DW, van der Mei, HC, Jutte, PC, Van Den Dungen, JJAM, Schultz, MJ, Van Der Laan, BFAM, Zaat, SAJ & Busscher, HJ 2013, 'Critical factors in the translation of improved antimicrobial strategies for medical implants and devices', *Biomaterials*, vol. 34, 9237–9243.

Gray, JE, Norton, PR & Griffiths, K 2005, 'Mechanism of adhesion of electroless-deposited silver on poly(ether urethane)', *Thin Solid Films*, vol. 484, 196–207.

Gray, KC, Palacios, DS, Dailey, I, Endo, MM, Uno, BE, Wilcock, BC & Burke, MD 2012, 'Amphotericin primarily kills yeast by simply binding ergosterol', *Proceedings of the National Academy of Sciences*, vol. 109, 2234–2239.

Griesser, HJ 1989, 'Small scale reactor for plasma processing of moving substrate web', *Vacuum*, vol. 39, 485–488.

Griesser, HJ & Chatelier, RC 1990, 'Surface characterization of plasma polymers from amine, amide and alcohol monomers'.

Griesser, HJ, Hall, H, Jenkins, T, Griesser, S, Vasilev, K & Grandin, HM 2012, *Antimicrobial and anti-inflammatory intelligent surfaces*, Wiley.

Griesser, HJ, Hartley, PG, McArthur, SL, McLean, KM, Meagher, L & Thissen, H 2001, 'Fabrication and characterization of nanoscale biological coatings on synthetic carriers', *BioMEMS and Smart Nanostructures*, vol. 4590, 45–56.

Griesser, HJ, Wagner, MS, Catner, DG, Kingshott, P & McLean, KM 2003, 'XPS, ToF-SIMS, and MALDI-MS for characterizing adsorbed protein films', *Surfactant Science Series*, vol. 110, 641–669.

Griesser, HJ, Youxian, D, Hughes, AE, Gengenbach, TR & Mau, AWH 1991, 'Shallow reorientation in the surface dynamics of plasma-treated flourinated ethylene propylene polymer', *Langmuir*, vol. 7, 2484–2491.

Gristina, AG, Naylor, P, Myrvik, Q, 1989, 'Infections from Biomaterials and Implants: a race for the surface', *Medical Progress through Technology*, vol. 14, 205-224.

Grönberg, A, Zettergren, L & Agren, MS 2011, 'Stability of the cathelicidin peptide LL-37 in a non-healing wound environment', *Acta Dermato-Venereologica*, vol. 91, 511.

Gudlaugsson, O, Gillespie, S, Lee, K, Berg, JV, Hu, JF, Messer, S, Herwaldt, L, Pfaller, M & Diekema, D 2003, 'Attributable mortality of nosocomial candidemia, revisited', *Clinical Infectious Diseases*, vol. 37, 1172–1177.

Guerraromero, L, Telenti, A, Thompson, RL & Roberts, GD 1989, 'Polymicrobial fungemia: microbiology, clinical-features, and significance', *Reviews of Infectious Diseases*, vol. 11, 208–212.

Gurtner, GC, Werner, S, Barrandon, Y & Longaker, MT 2008, 'Wound repair and regeneration', *Nature*, vol. 453, 314–321.

Hakenbeck, R, Brueckner, R & Henrich, B 2010, 'Cell wall targeted antibiotics'.

Halevy, R, Rozek, A, Kolusheva, S, Hancock, REW & Jelinek, R 2003, 'Membrane binding and permeation by indolicidin analogs studied by a biomimetic lipid/polydiacetylene vesicle assay', *Peptides*, vol. 24, 1753–1761.

Hamuro, Y, Schneider, JP & Degrado, WF 1999, 'De novo design of antibacterial beta-peptides', *Journal of the American Chemical Society*, vol. 121, 12200–12201.

Harriott, MM & Noverr, MC 2009, '*Candida albicans* and *Staphylococcus aureus* form polymicrobial biofilms: effects on antimicrobial resistance', *Antimicrobial Agents and Chemotherapy*, vol. 53, 3914–3922.

Hartley, PG, McArthur, SL, McLean, KM & Grisser, HJ 2002, 'Physicochemical properties of polysacharide coatings based on grafted multilayer assemblies', *Langmuir*, vol. 18, 2483–2494.

Hashizume, H, Sawa, R, Harada, S, Igarashi, M, Adachi, H, Nishimura, Y & Nomoto, A 2011, 'Tripropeptin C blocks the lipid cycle of cell wall biosynthesis by complex formation with undecaprenyl pyrophosphate', *Antimicrobial Agents and Chemotherapy*, vol55, 3821–3828.

Hell, E., Giske, CG, Nelson, A, Römling, U & Marchini, G 2010, 'Human cathelicidin peptide LL37 inhibits both attachment capability and biofilm formation of *Staphylococcus epidermidis*', *Letters in Applied Microbiology*, vol. 50, 211.

Henzler Wildman, KA, Lee, D-K & Ramamoorthy, A 2003, 'Mechanism of lipid bilayer disruption by the human antimicrobial peptide, LL-37', *Biochemistry*, vol. 42, 6545–6458.

Herrera, JR, Cabo, ML, Gonzalez, A, Pazos, I & Pastoriza, L 2007, 'Adhesion and detachment kinetics of several strains of *Staphylococcus aureus* subsp *aureus* under three different experimental conditions', *Food Microbiology*, vol. 24, 585–591.

Hidron, AI, Edwards, JR, Patel, J, Horan, TC, Sievert, DM, Pollock, DA, Fridkin, SK, National Healthcare Safety Network Team & Participating National Healthcare Safety Network Facilities 2008, 'Antimicrobial-resistant pathogens associated with healthcare-associated infections: annual summary of data reported to the National Healthcare Safety Network at the Centers for Disease Control and Prevention, 2006–2007', *Infection Control and Hospital Epidemiology*, vol. 29, 996–1011.

Hilpert, K, Elliott, M, Jenssen, H, Kindrachuk, J, Fjell, CD, Koerner, J, Winkler, DFH, Weaver, LL, Henklein, P, Ulrich, AS, Chiang, SHY, Farmer, SW, Pante, N, Volkmer, R & Hancock, REW 2009, 'Screening and characterization of surface-tethered cationic peptides for antimicrobial activity', *Chemistry & Biology*, vol. 16, 58–69.

Ho, CH, Tobis, J, Sprich, C, Thomann, R & Tiller, JC 2004, 'Nanoseparated polymeric networks with multiple antimicrobial properties', *Advanced Materials*, vol. 16**,** 957–+.

Ho, SW, Jung, D, Calhoun, JR, Lear, JD, Okon, M, Scott, WRP, Hancock, REW & Straus, SK 2008, 'Effect of divalent cations on the structure of the antibiotic daptomycin', *European Biophysics Journal with Biophysics Letters*, vol. 37, 421–433.

Hoffman, LR, D'Argenio, DA, Maccoss, MJ, Zhang, ZY, Jones, RA & Miller, SI 2005, 'Aminoglycoside antibiotics induce bacterial biofilm formation', *Nature*, vol. 436, 1171–1175.

Horne, WS & Gellman, SH 2008, 'Foldamers with heterogeneous backbones', *Accounts of Chemical Research*, vol. 41, 1399–1408.

Hurdle, JG, O'Neill, AJ, Chopra, I & Lee, RE 2011, 'Targeting bacterial membrane function: an underexploited mechanism for treating persistent infections', *Nature Reviews Microbiology*, vol. 9**,** 62–75.

Inácio, ÂS, Costa, GN, Domingues, NS, Santos, MS, Moreno, AJM, Vaz, WLC & Vieira, OV 2013, 'Mitochondrial dysfunction is the focus of quaternary ammonium surfactant toxicity to mammalian epithelial cells', *Antimicrobial Agents and Chemotherapy*, vol. 57, 2631.

Jang, SA, Kim, H, Lee, JY, Shin, JR, Kim, DJ, Cho, JH & Kim, SC 2012, 'Mechanism of action and specificity of antimicrobial peptides designed based on buforin IIb', *Peptides*, vol. 34, 283–289.

Jasieniak, M, Graham, D, Kingshott, P, Gamble, L & Griesser, HJ 2009, *Surface Analysis of Biomaterials*, CRC Press.

John, A.-K, Schmaler, M, Khanna, N & Landmann, R 2011, 'Reversible daptomycin tolerance of adherent staphylococci in an implant infection model', *Antimicrobial Agents and Chemotherapy*, vol. 55, 3510–3516.

Jung, D, Powers, JP, Straus, SK & Hancock, REW 2008, 'Lipid-specific binding of the calcium-dependent antibiotic daptomycin leads to changes in lipid polymorphism of model membranes', *Chemistry and Physics of Lipids*, vol. 154, 120–128.

Jung, D, Rozek, A, Okon, M & Hancock, REW 2004, 'Structural transitions as determinants of the action of the calcium-dependent antibiotic daptomycin', *Chemistry & Biology*, vol. 11, 949–957.

Kahlenberg, JM & Kaplan, MJ 2013, 'Little peptide, big effects: the role of LL-37 in inflammation and autoimmune disease', *Journal of Immunology*, vol. 191, 4895–4901.

Kelly, FM, Johnston, JH, Borrmann, T & Richardson, MJ 2007, 'Functionalised hybrid materials of conducting polymers with individual fibres of cellulose', *European Journal of Inorganic Chemistry*, 5571–5577.

Kim, JS, Kuk, E, Yu, KN, Kim, J.-H, Park, SJ, Lee, HJ, Kim, SH, Park, YK, Park, YH, Hwang, C.-Y, Kim, Y.-K, Lee, Y.-S, Jeong, DH & Cho, M-H 2007, 'Antimicrobial effects of silver nanoparticles', *Nanomedicine-Nanotechnology Biology and Medicine*, vol. 3, 95–101.

Kim, YS, Kim, JS, Cho, HS, Rha, DS, Kim, JM, Park, JD, Choi, BS, Lim, R, Chang, HK, Chung, YH, Kwon, IH, Jeong, J, Han, BS & Yu, IJ 2008, 'Twenty-eight-day oral toxicity, genotoxicity, and gender-related tissue distribution of silver nanoparticles in Sprague-Dawley rats', *Inhalation Toxicology*, vol. 20, 575–575.

Kingshott, P 1998, 'Interfacial aspects of protein and lipid adsorption to contact lens surfaces', PhD Thesis, University of New South Wales, Adelaide.

Kingshott, P, Helmut, T & Griesser, HJ 2002, 'Effects of cloud-point grafting, chain length, and density of PEG layers on competitive adsorption of ocular proteins', *Biomaterials*, vol. 23, 2043–2056.

Kingshott, P, McArthur, S, Thissen, H, Castner, DG & Griesser, HJ 2002, 'Ultrasensitive probing of the protein resistance of PEG surfaces by secondary ion mass spectrometry', *Biomaterials*, vol. 23, 4775–4785.

Kingshott, P, Wei, J, Bagge-Ravn, D, Gadegaard, N & Gram, L 2003, 'Covalent attachment of poly(ethylene glycol) to surfaces, critical for reducing bacterial adhesion', *Langmuir*, vol. 19, 6912–6921.

Kinmond, EJ, Coulson, SR, Badyal, JPS, Brewer, SA & Willis, C 2005, 'High structural retention during pulsed plasma polymerization of 1H,1H,2H-perfluorododecene: an NMR and TOF-SIMS study', *Polymer*, vol. 46, 6829–6835.

Kirkpatrick, CH 2001, 'Chronic mucocutaneous candidiasis', *Pediatric Infectious Disease Journal*, vol. 20**,** 197–206.

Klasen, HJ 2000a, 'Historical review of the use of silver in the treatment of burns I Early uses', *Burns*, vol. 26**,** 117–130.

Klasen, HJ 2000b, 'A historical review of the use of silver in the treatment of burns II Renewed interest for silver', *Burns*, vol. 26, 131–138.

Klatte, JM, Newland, JG & Jackson, MA 2013, 'Incidence, classification, and risk stratification for *Candida* central line-associated bloodstream infections in pediatric patients at a

tertiary care children's hospital, 2000–2010', *Infection Control and Hospital Epidemiology*, vol. 34, 1266–1271.

Klevens, RM, Edwards, JR, Richards, J, Chesley L, Horan, TC, Gaynes, RP, Pollock, DA & Cardo, DM 2007, 'Estimating health care-associated infections and deaths in U.S hospitals, 2002', *Public health reports (Washington, D.C: 1974)*, vol. 122**,** 160–166.

Klotz, SA, Chasin, BS, Powell, B, Gaur, NK & Lipke, PN 2007, 'Polymicrobial bloodstream infections involving *Candida* species: analysis of patients and review of the literature', *Diagnostic Microbiology and Infectious Disease*, vol. 59, 401–406.

Koerner, E, Aguirre, MH, Fortunato, G, Ritter, A, Ruehe, J & Hegemann, D 2010, 'Formation and distribution of silver nanoparticles in a functional plasma polymer matrix and related Ag+ release properties', *Plasma Processes And Polymers*, vol. 7, 619–625.

Kojic, EM & Darouiche, RO 2004, '*Candida* infections of medical devices', *Clinical Microbiology Reviews*, vol. 17, 255–+.

Kong, H & Jang, J 2008a, 'Antibacterial properties of novel poly(methyl methacrylate) nanofiber containing silver nanoparticles', *Langmuir*, vol. 24, 2051–2056.

Kong, H & Jang, J 2008b, 'Synthesis and antimicrobial properties of novel silver/polyrhodanine nanofibers', *Biomacromolecules*, vol. 9, 2677–2681.

Koo, YS, Kim, JM, Park, IY, Yu, BJ, Jang, SA, Kim, K-S, Park, CB, Cho, JH & Kim, SC 2008, 'Structure-activity relations of parasin I, a histone H2A-derived antimicrobial peptide', *Peptides*, vol. 29, 1102–1108.

Krauson, AJ, He, J & Wimley, WC 2012, 'Determining the mechanism of membrane permeabilizing peptides: identification of potent, equilibrium pore-formers', *Biochimica et Biophysica Acta—Biomembranes*, vol. 1818, 1625–1632.

Kügler, R, Bouloussa, O & Rondelez, F 2005, 'Evidence of a charge-density threshold for optimum efficiency of biocidal cationic surfaces', *Microbiology*, vol. 151, 1341–1348.

Kumar, A, Vemula, PK, Ajayan, PM & John, G 2008, 'Silver-nanoparticle-embedded antimicrobial paints based on vegetable oil', *Nature Materials*, vol. 7, 236–241.

Kumar, V & Robbins, SL 2007 *Robbins basic pathology*, Saunders/Elsevier, Philadelphia, PA.

Lachapelle, JM 2014, 'A comparison of the irritant and allergenic properties of antiseptics', *European Journal of Dermatology*, vol. 24, 3–9.

Larsen, ST, Verder, H & Nielsen, GD 2012, 'Airway effects of inhaled quaternary ammonium compounds in mice', *Basic & Clinical Pharmacology & Toxicology*, vol. 110, 537–543.

Lee, H, Lee, Y, Statz, AR, Rho, J, Park, TG & Messersmith, PB 2008, 'Substrate-independent layer-by-layer assembly by using mussel-adhesive-inspired polymers', *Advanced Materials*, vol. 20, 1619–+.

Lee, KL, Campbell, CC & Buckley, HR 1975, 'Amino-acid liquid synthetic medium for development of mycelial and yeast forms of *Candida-albicans*', *Sabouraudia—Journal of Medical and Veterinary Mycology*, vol. 13, 148–153.

Lee, M-R, Stahl, SS, Gellman, SH & Masters, KS 2009, 'Nylon-3 copolymers that generate cell-adhesive surfaces identified by library screening', *Journal of the American Chemical Society*, vol. 131, 16779–16789.

Leeson, AM, Alexander, MR, Short, RD, Briggs, D & Hearn, MJ 1997, 'Secondary ion mass spectroscopy of polymers: a ToF-SIMS study of monodispersed PMMA standards', *Surface and Interface Analysis*, vol. 25, 261–274.

Lenarcic, R, Halbedel, S, Visser, L, Shaw, M, Wu, LJ, Errington, J, Marenduzzo, D & Hamoen, LW 2009, 'Localisation of DivIVA by targeting to negatively curved membranes', *Embo Journal*, vol. 28, 2272–2282.

Leonard, D & Mathieu, HJ 1999, 'Characterisation of biomaterials using ToF-SIMS', *Fresenius' Journal of Analytical Chemistry*, vol. 365, 3–11.

Leroy, O, Gangneux, J-P, Montravers, P, Mira, J-P, Gouin, F, Sollet, J-P, Carlet, J, Reynes, J, Rosenheim, M, Regnier, B, Lortholary, O & AmarC and Study Group 2009, 'Epidemiology, management, and risk factors for death of invasive *Candida* infections in critical care: a multicenter, prospective, observational study in France (2005–2006)', *Critical Care Medicine*, vol. 37, 1612–1618.

Letscher-Bru, V & Herbrecht, R 2003, 'Caspofungin: the first representative of a new antifungal class', *Journal of Antimicrobial Chemotherapy*, vol. 51, 513–521.

Lewis, K 2010, 'Persister cells', *Annual Review of Microbiology*, vol. 64, 357–372.

Lewis, KB & Ratner, BD 1993, 'Observation of surface rearrangement of polymers using ESCA', *Journal of Colloid and Interface Science*, vol. 159, 77–85.

Lewis, REP 2011, 'Current concepts in antifungal pharmacology', *Mayo Clinic Proceedings*, vol. 86, 805–817.

Lhoest, JB, Detrait, E & van den Bosch de Aguilar, P 1998, 'Fibronectin adsorption, conformation, and orientation on polystyrene substrates studied by radiolabeling, XPS, and ToF-SIMS', *Journal of Biomedical Materials Research*, vol. 41, 95–103.

Lhoest, JB, Wagner, MS, Tidwell, CD & Castner, DG 2001, 'Characterization of adsorbed protein films by time of flight secondary ion mass spectroscopy', *Journal of Biomedical Materials research*, vol. 57, 432–440.

Li, L, Ng, K-M, Chan, C-M, Feng, J-Y & Zeng, X-M, Weng, L-T 2000, 'Surface studies of the rearrangement of end groups of a polymer by ToF-SIMS and AFM', *Macromolecules*, vol. 33, 5588–5592.

Li, Y, Kumar, KN, Dabkowski, JM, Corrigan, M, Scott, RW, Nuesslein, K & Tew, GN 2012, 'New bactericidal surgical suture coating', *Langmuir*, vol. 28, 12134–12139.

Lin, YS, Chang, CH & Huang, TJ 2006, 'Enhanced corrosion protection of cold rolled steel by low-temperature plasma cleaning and plasma polymerization', *Surface & Coatings Technology*, vol. 200, 4929–4938.

Liu, DH & Degrado, WF 2001, 'De novo design, synthesis, and characterization of antimicrobial beta-peptides', *Journal of the American Chemical Society*, vol. 123, 7553–7559.

Liu, J, Sonshine, DA, Shervani, S & Hurt, RH 2010, 'Controlled release of biologically active silver from nanosilver surfaces', *ACS Nano*, vol. 4, 6903–6913.

Liu, R, Chen, X, Gellman, SH & Masters, KS 2013, 'Nylon-3 polymers that enable selective culture of endothelial cells', *Journal of the American Chemical Society*, vol. 135, 16296–16299.

Liu, R, Chen, X, Hayouka, Z, Chakraborty, S, Falk, SP, Weisblum, B, Masters, KS & Gellman, SH 2013, 'Nylon-3 polymers with selective antifungal activity', *Journal of the American Chemical Society*, vol. 135, 5270–5273.

Liu, R, Vang, KZ, Kreeger, PK, Gellman, SH & Masters, KS 2012, 'Experimental and computational analysis of cellular interactions with nylon-3-bearing substrates', *Journal of Biomedical Materials Research Part A*, vol. 100A, 2750–2759.

Liu, SX, He, JH, Xue, JF & Ding, WJ 2009, 'Efficient fabrication of transparent antimicrobial poly(vinyl alcohol) thin films', *Journal of Nanoparticle Research*, vol. 11, 553–560.

Loeffler, JM, Garbino, J, Lew, D, Harbarth, S & Rohner, P 2003, 'Antibiotic consumption, bacterial resistance and their correlation in a Swiss university hospital and its adult intensive care units', *Scandinavian Journal of Infectious Diseases*, vol. 35, 843–850.

Lopez-Donaire, ML, Sussman, EM, Fernandez-Gutierrez, M, Mendez-Vilas, A, Ratner, BD, Vazquez-Lasa, B & San Roman, J 2012, 'Amphiphilic self-assembled "polymeric drugs": morphology, properties, and biological behavior of nanoparticles', *Biomacromolecules*, vol. 13, 624-635.

Lorenz, C, Windler, L, Von Goetz, N, Lehmann, RP, Schuppler, M, Hungerbuehler, K, Heuberger, M & Nowack, B 2012, 'Characterization of silver release from commercially available functional (nano)textiles', *Chemosphere*, vol. 89, 817–824.

Losina, E, Walensky, RP, Reichmann, WM, Holt, HL, Gerlovin, H, Solomon, DH, Jordan, JM, Hunter, DJ, Suter, LG, Weinstein, AM, Paltiel, AD & Katz, JN 2011, 'Impact of obesity and knee osteoarthritis on morbidity and mortality in older Americans', *Annals of Internal Medicine*, vol. 154, 217–226.

Lu, J, Moon, KS & Wong, CP 2008, 'Silver/polymer nanocomposite as a high-k polymer matrix for dielectric composites with improved dielectric performance', *Journal of Materials Chemistry*, vol. 18, 4821–4826.

Ludtke, SJ, He, K, Heller, WT, Harroun, TA, Yang, L & Huang, HW 1996, 'Membrane pores induced by magainin', *Biochemistry*, vol. 35, 13723.

MacNeil, S, Shepherd, J & Smith, L 2011, 'Production of tissue-engineered skin and oral mucosa for clinical and experimental use', in JW Haycock (ed.), *3d cell culture: methods and protocols*, Humana Press, Totowa.

Mah, TF, Pitts, B, Pellock, B, Walker, GC, Stewart, PS & O'Toole, GA 2003, 'A genetic basis for *Pseudomonas aeruginosa* biofilm antibiotic resistance', *Nature*, vol. 426, 306–310.

Maillard, J.-Y & Hartemann, P 2013, 'Silver as an antimicrobial: facts and gaps in knowledge', *Critical Reviews in Microbiology*, vol. 39, 373–383.

Mallick, K, Witcomb, MJ & Scurrell, MS 2006, 'Self-assembly of silver nanoparticles: formation of a thin silver film in a polymer matrix', *Materials Science & Engineering C-Biomimetic and Supramolecular Systems*, vol. 26, 87–91.

Mantus, DS, Ratner, BD, Carlson, BA & Moulder, JF 1993, 'Static secondary ion mass spectrometry of adsorbed proteins', *Analytical Biochemistry*, vol. 65, 1431–1438.

Mao, G, Castner, DG & Grainger, DW 1997, 'Polymer immobilization to alkylchlorosilane organic monolayer films using sequential derivatization reactions', *Chemistry of Materials*, vol. 9, 1741–1750.

Marambio-Jones, C & Hoek, EMV 2010, 'A review of the antibacterial effects of silver nanomaterials and potential implications for human health and the environment', *Journal of Nanoparticle Research*, vol. 12, 1531–1551.

Marr, AK, Gooderham, WJ & Hancock, REW 2006, 'Antibacterial peptides for therapeutic use: obstacles and realistic outlook', *Current Opinion in Pharmacology*, vol. 6, 468–472.

McArthur, SL, Wagner, MS, Hartley, PG, McLean, KM, Griesser, HJ & Castner, DG 2002, 'Characterization of sequentially grafted polysaccharide coatings using time-of-flight secondary ion mass spectroscopy (ToF-SIMS) and principal component analysis (PCA)', *Surface and Interface Analysis*, vol. 33, 924–931.

Medard, N, Aouinti, M, Poncin-Epaillard, F & Bertrand, P 2001, 'ToF-SIMS ability to quantify surface chemical groups: correlation with XPS analysis and spectrochemical titration', *Surface and Interface Analysis*, vol. 31, 1042–1047.

Mihajlovic, M & Lazaridis, T 2012, 'Charge distribution and imperfect amphipathicity affect pore formation by antimicrobial peptides', *BBA—Biomembranes*, vol. 1818, 1274–1283.

Mijnendonckx, K, Leys, N, Mahillon, J, Silver, S & Van Houdt, R 2013, 'Antimicrobial silver: uses, toxicity and potential for resistance', *Biometals: An International Journal on the Role of Metal Ions in Biology, Biochemistry, and Medicine*, vol. 26, 609–621.

Miller, LG, Hajjeh, RA & Edwards, JE 2001, 'Estimating the cost of nosocomial candidemia in the United States', *Clinical Infectious Diseases*, vol. 32, 1110–1110.

Minko, S, Patil, S, Datsyuk, V, Simon, F, Eichhorn, KJ, Motornov, M, Usov, D, Tokarev, I & Stamm, M 2002, 'Synthesis of adaptive polymer brushes via "grafting to" approach from melt', *Langmuir*, vol. 18, 289–296.

Mitra, K, Ubarretxena-Belandia, T, Taguchi, T, Warren, G & Engelman, DM 2004, 'Modulation of the bilayer thickness of exocytic pathway membranes by membrane proteins rather than cholesterol', *Proceedings of the National Academy of Sciences of the United States of America*, vol. 101, 4083–4088.

Moiset, G, Cirac, AD, Stuart, MCA, Marrink, S-J, Sengupta, D & Poolman, B 2013, 'Dual action of BPC194: a membrane active peptide killing bacterial cells', *PloS ONE*, vol. 8, e61541.

Moore, D, Robson, GS & Trinci, APJ 2011, *21st century guidebook to fungi*.

Mowery, BP, Lee, SE, Kissounko, DA, Epand, RF, Epand, RM, Weisblum, B, Stahl, SS & Gellman, SH 2007, 'Mimicry of antimicrobial host-defense peptides by random copolymers', *Journal of the American Chemical Society*, vol. 129, 15474–15476.

Mowery, BP, Lindner, AH, Weisblum, B, Stahl, SS & Gellman, SH 2009, 'Structure-activity relationships among random nylon-3 copolymers that mimic antibacterial host-defense peptides', *Journal of the American Chemical Society*, vol. 131, 9735–9745.

Munoz-Bonilla, A & Fernandez-Garcia, M 2012, 'Polymeric materials with antimicrobial activity', *Progress in Polymer Science*, vol. 37, 281–339.

Nascimento, JM, Franco, OL, Oliveira, MDL & Andrade, CAS 2012, 'Evaluation of magainin I interactions with lipid membranes: an optical and electrochemical study', *Chemistry and Physics of Lipids*, vol. 165, 537–544.

Nast, S, Fassbender, M, Bormann, N, Beck, S, Montali, A, Lucke, M, Schmidmaier, M, Wildermann, B, 2016, 'In vivo quantifivation of gentamicin released from an implant coating', *Journal of Biomaterials Applications*, vol. 31, 45-54.

Neal, MJ 2012, *Medical pharmacology at a glance*, Wiley-Blackwell, Chichester, UK.

Neumann, A, Baginski, M & Czub, J 2010, 'How do sterols determine the antifungal activity of amphotericin B? Free energy of binding between the drug and its membrane targets', *Journal of the American Chemical Society*, vol. 132, 18266–18272.

Nguyen, LT, Chau, JK, Perry, NA, De Boer, L, Zaat, SAJ & Vogel, HJ 2010, 'Serum stabilities of short tryptophan-and arginine-rich antimicrobial peptide analogs', *PloS ONE*, vol. 5.

Oda, Y, Kanaoka, S, Sato, T, Aoshima, S & Kuroda, K 2011, 'Block versus random amphiphilic copolymers as antibacterial agents', *Biomacromolecules*, vol. 12, 3581–3591.

Onaizi, SA & Leong, SSJ 2011, 'Tethering antimicrobial peptides: current status and potential challenges', *Biotechnology Advances*, vol. 29, 67–74.

Oran, U, Swaraj, S, Friedrich, JF & Unger, WES 2005, 'Surface analysis of plasma-deposited polymer films by time of flight static secondary ion mass spectrometry (ToF-SSIMS)

before and after exposure to ambient air', *Surface and Coatings Technology*, vol. 200, 463–467.

Palavecino, EL 2014, 'Clinical, epidemiologic, and laboratory aspects of methicillin-resistant *Staphylococcus aureus* infections', *Methods in Molecular Biology*, vol. 1085, 1–24.

Palermo, EF, Vemparala, S & Kuroda, K 2012, 'Cationic spacer arm design strategy for control of antimicrobial activity and conformation of amphiphilic methacrylate random copolymers', *Biomacromolecules*, vol. 13, 1632–1641.

Pandey, BK, Ahmad, A, Asthana, N, Azmi, S, Srivastava, RM, Srivastava, S, Verma, R, Vishwakarma, AL & Ghosh, JK 2010, 'Cell-selective lysis by novel analogues of melittin against human red blood cells and *Escherichia coli*', *Biochemistry*, vol. 49, 7920–7929.

Pasche, S, Depaul, SM, Voros, J, Spencer, ND & Textor, M 2003, 'Poly(L-lysine)-graft-poly(ethylene glycol) assembled monolayers on niobium oxide surfaces: a quantitative study of the influence of polymer interfacial architecture on resistance to protein adsorption by ToF-SIMS and in situ OWLS', *Langmuir*, vol. 19, 9216–9225.

Paulo, CSO, Vidal, M & Ferreira, LS 2010, 'Antifungal nanoparticles and surfaces', *Biomacromolecules*, vol. 11, 2810–2817.

Peleg, AY, Hogan, DA & Mylonakis, E 2010, 'Medically important bacterial-fungal interactions', *Nature Reviews Microbiology*, vol. 8, 340–349.

Peleg, AY & Hooper, DC 2010, 'Hospital-acquired infections due to Gram-negative bacteria: current concepts', *The New England Journal of Medicine*, vol. 362, 1804.

Percival, SL, Bowler, PG & Russell, D 2005, 'Bacterial resistance to silver in wound care', *Journal of Hospital Infection*, vol. 60, 1–7.

Peschel, A & Sahl, H-G 2006, 'The co-evolution of host cationic antimicrobial peptides and microbial resistance', *Nature Reviews Microbiology*, vol. 4, 529–536.

Pieta, P, Mirza, J & Lipkowski, J 2012, 'Direct visualization of the alamethicin pore formed in a planar phospholipid matrix', *Proceedings of the National Academy of Sciences of the United States of America*, vol. 109, 21223–21227.

Pogliano, J, Pogliano, N & Silverman, JA 2012, 'Daptomycin-mediated reorganization of membrane architecture causes mislocalization of essential cell division proteins', *Journal of Bacteriology*, vol. 194, 4494–4504.

Poon, VKM & Burd, A 2004, 'In vitro cytotoxity of silver: implication for clinical wound care', *Burns*, vol. 30, 140–147.

Porter, EA, Weisblum, B & Gellman, SH 2002, 'Mimicry of host-defense peptides by unnatural oligomers: antimicrobial β-peptides', *Journal of the American Chemical Society*, vol. 124, 7324–7330.

Poulter, N, Munoz-Berbel, X, Johnson, AL, Dowling, AJ, Waterfield, N & Jenkins, ATA 2009, 'An organo-silver compound that shows antimicrobial activity against *Pseudomonas aeruginosa* as a monomer and plasma deposited film', *Chemical Communications*, 7312–7314.

Poulter, N, Vasilev, K, Griesser, S & Griesser, H 2013, 'Silver containing biomaterials', in TF Moriarty, SAJ Zaat & HJ Busscher (eds), *Biomaterials associated infection*, Springer, New York.

Powell, A, Al Nakeeb, M, Wilkinson, B & Micklefield, J 2007, 'Precursor-directed biosynthesis of nonribosomal lipopeptides with modified glutamate residues', *Chemical Communications*, 2683–2685.

Powell, A, Borg, M, Amir-Heidari, B, Neary, JM, Thirlway, J, Wilkinson, B, Smith, CP & Micklefield, J 2007, 'Engineered biosynthesis of nonribosomal lipopeptides with modified fatty acid side chains', *Journal of the American Chemical Society*, vol. 129, 15182-15191.

Powers, CM, Slotkin, TA, Seidler, FJ, Badireddy, AR & Padilla, S 2011, 'Silver nanoparticles alter zebrafish development and larval behavior: distinct roles for particle size, coating and composition', *Neurotoxicology and teratology*, vol. 33, 708–714.

Pulimood, S, Ganesan, L, Alangaden, G & Chandrasekar, P 2002, 'Polymicrobial candidemia', *Diagnostic Microbiology and Infectious Disease*, vol. 44, 353–357.

Ramamurthi, KS & Losick, R 2009, 'Negative membrane curvature as a cue for subcellular localization of a bacterial protein', *Proceedings of the National Academy of Sciences of the United States of America*, vol. 106, 13541–13545.

Ramanathan, B, Davis, EG, Ross, CR & Blecha, F 2002, 'Cathelicidins: microbicidal activity, mechanisms of action, and roles in innate immunity', *Microbes and Infection*, vol. 4, 361–372.

Ramos, R, Silva, JP, Rodrigues, AC, Costa, R, Guardao, L, Schmitt, F, Soares, R, Vilanova, M, Domingues, L & Gama, M 2011, 'Wound healing activity of the human antimicrobial peptide LL37', *Peptides*, vol. 32, 1469–1476.

Ramstedt, M, Cheng, N, Azzaroni, O, Mossialos, D, Mathieu, HJ & Huck, WTS 2007, 'Synthesis and characterization of poly(3-sulfopropylmethacrylate) brushes for potential antibacterial applications', *Langmuir*, vol. 23, 3314–3321.

Ramstedt, M, Ekstrand-Hammarstrom, B, Shchukarev, AV, Bucht, A, Osterlund, L, Welch, M & Huck, WTS 2009, 'Bacterial and mammalian cell response to poly(3-sulfopropyl methacrylate) brushes loaded with silver halide salts', *Biomaterials*, vol. 30, 1524–1531.

Rapaport, D & Shai, Y 1991, 'Interaction of fluorescently labeled pardaxin and its analogs with lipid bilayers', *Journal of Biological Chemistry*, vol. 266, 23769–23775.

Ratner, BD 1995, 'Advances in the analysis of surfaces of biomedical interest', *Surface and Interface Analysis*, vol. 23, 521–528.

Ratner, BD 1996, 'The engineering of biomaterials exhibiting recognition and specificity', *Journal of Molecular Recognition*, vol. 9, 617–625.

Ratner, BD 2013, *Biomaterials science: an introduction to materials in medicine*, Elsevier/Academic, Oxford.

Ratner, BD, Horbett, TA, Shuttleworth, D & Thomas, HR 1981, 'Analysis of the organization of protein films on solid surface by ESCA', *Journal of Colloid and Interface Science*, vol. 83, 630–642.

Read, R, Kumar, N, Willcox, M, Zhu, H, Griesser, HJ, Muir, B, Thissen, H & Hughes, T 2003, *Antimicrobial coatings*, Australia patent application.

Romani, L, Bistoni, F & Puccetti, P 2003, 'Adaptation of *Candida albicans* to the host environment: the role of morphogenesis in virulence and survival in mammalian hosts', *Current Opinion in Microbiology*, vol. 6, 338–343.

Rosenthal, VD, Maki, DG, Salomao, R, Alvarez-Moreno, C, Mehta, Y, Higuera, F, Cuellar, LE, Arikan, OA, Abouqal, R, Leblebicioglu, H & International Nosocomial Infection Control Consortium 2006, 'Device-associated nosocomial infections in 55 intensive care units of 8 developing countries', *Annals of Internal Medicine*, vol. 145, 582–591.

Rotondi, KS & Gierasch, LM 2005, 'A well-defined amphipathic conformation for the calcium-free cyclic lipopeptide antibiotic, daptomycin, in aqueous solution', *Biopolymers*, vol. 80, 374–385.

Rubinchik, E, Schneider, T, Elliott, M, Scott, WRP, Pan, J, Anklin, C, Yang, H, Dugourd, D, Mueller, A, Gries, K, Straus, SK, Sahl, HG & Hancock, REW 2011, 'Mechanism of action and limited cross-resistance of new lipopeptide MX-2401', *Antimicrobial Agents and Chemotherapy*, vol. 55, 2743–2754.

Sabbatini, L & Zambonin, PG 1996, 'XPS and SIMS surface chemical analysis of some important classes of polymeric biomaterials', *Journal of Electron Spectroscopy and Related Phenomena*, vol. 81, 285–301.

Safdar, N, O'Horo, JC & Maki, DG 2013, 'Arterial catheter-related bloodstream infection: incidence, pathogenesis, risk factors and prevention', *Journal of Hospital Infection*, vol. 85, 189–195.

Sambhy, V, MacBride, MM, Peterson, BR & Sen, A 2006, 'Silver bromide nanoparticle/polymer composites: dual action tunable antimicrobial materials', *Journal of the American Chemical Society*, vol. 128, 9798–9808.

Sambhy, V, Peterson, BR & Sen, A 2008, 'Multifunctional silane polymers for persistent surface derivatization and their antimicrobial properties', *Langmuir*, vol. 24, 7549–7558.

Sanchez-Valdes, S, Ortega-Ortiz, H, Valle, L, Medellin-Rodriguez, FJ & Guedea-Miranda, R 2009, 'Mechanical and antimicrobial properties of multilayer films with a polyethylene/silver nanocomposite layer', *Journal of Applied Polymer Science*, vol. 111, 953–962.

Schmidtchen, A, Frick, IM, Andersson, E, Tapper, H & Bjorck, L 2002, 'Proteinases of common pathogenic bacteria degrade and inactivate the antibacterial peptide LL-37', *Molecular Microbiology*, vol. 46, 157–168.

Schneider, OD, Loher, S, Brunner, TJ, Schmidlin, P & Stark, WJ 2008, 'Flexible, silver containing nanocomposites for the repair of bone defects: antimicrobial effect against *E. coli* infection and comparison to tetracycline containing scaffolds', *Journal of Materials Chemistry*, vol. 18, 2679–2684.

Schwarz, F, Thorwarth, G, Wehlus, T & Stritzker, B 2008, 'Silver nanocluster containing diamond like carbon', *Physica Status Solidi (a)—Applications and Materials Science*, vol. 205, 976–979.

Scott, WRP, Baek, S.-B, Jung, D, Hancock, REW & Straus, SK 2007, 'NMR structural studies of the antibiotic lipopeptide daptomycin in DHPC micelles', *Biochimica et Biophysica Acta—Biomembranes*, vol. 1768, 3116–3126.

Sendid, B, Jouault, T, Vitse, A, Fradin, C, Colombel, JF & Poulain, D 2009, 'Anti glycans antibodies establish an unexpected link between *C. albicans* and Crohn disease', *M S-Medecine Sciences*, vol. 25, 473–481.

Shestakov, A, Jenssen, H, Hancock, REW, Nordstrom, I & Eriksson, K 2013, 'Synthetic analogues of bovine bactenecin dodecapeptide reduce herpes simplex virus type 2 infectivity in mice', *Antiviral Research*, vol. 100, 455–459.

Shibata, N, Suzuki, A, Kobayashi, H & Okawa, Y 2007, 'Chemical structure of the cell-wall mannan of *Candida albicans* serotype A and its difference in yeast and hyphal forms', *Biochemical Journal*, vol. 404, 365–372.

Silverman, JA, Perlmutter, NG & Shapiro, HM 2003, 'Correlation of daptomycin bactericidal activity and membrane depolarization in *Staphylococcus aureus*', *Antimicrobial Agents and Chemotherapy*, vol. 47, 2538–2544.

Siow, KS, Britcher, L, Kumar, S & Griesser, HJ 2006, 'Plasma methods for the generation of chemically reactive surfaces for biomolecule immobilization and cell colonization—A review', *Plasma Processes and Polymers*, vol. 3, 392–418.

Skarnes, RC & Watson, DW 1957, 'Antimicrobial factors of normal tissues and fluids', *Bacteriological Reviews*, vol. 21, 273–294.

Som, A, Choi, Y & Tew, GN 2009, 'Monovalent salt effects on the membrane activity of antimicrobial polymers', *Macromolecular Symposia*, vol. 283–84, 319–325.

Som, A, Navasa, N, Percher, A, Scott, RW, Tew, GN & Anguita, J 2012, 'Identification of synthetic host defense peptide mimics that exert dual antimicrobial and anti-inflammatory activities', *Clinical and Vaccine Immunology*, vol. 19, 1784–1791.

Som, A, Vemparala, S, Ivanov, I & Tew, GN 2008, 'Synthetic mimics of antimicrobial peptides', *Peptide Science*, vol. 90, 83–93.

Sorensen, OE, Follin, P, Johnsen, AH, Calafat, J, Tjabringa, GS, Hiemstra, PS & Borregaard, N 2001, 'Human cathelicidin, hCAP-18, is processed to the antimicrobial peptide LL-37 by extracellular cleavage with proteinase 3', *Blood*, vol. 97, 3951–3959.

Spindler, EC, Hale, JDF, Giddings, TH, Jr, Hancock, REW & Gill, RT 2011, 'Deciphering the mode of action of the synthetic antimicrobial peptide Bac8c', *Antimicrobial Agents and Chemotherapy*, vol. 55, 1706–1716.

Steenbergen, JN, Alder, J, Thorne, GM & Tally, FP 2005, 'Daptomycin: a lipopeptide antibiotic for the treatment of serious Gram-positive infections', *Journal of Antimicrobial Chemotherapy*, vol. 55, 283–288.

Steinstraesser, L, Hirsch, T, Schulte, M, Kueckelhaus, M, Jacobsen, F, Mersch, EA, Stricker, I, Afacan, N, Jenssen, H, Hancock, REW & Kindrachuk, J 2012, 'Innate defense regulator peptide 1018 in wound healing and wound infection', *PloS ONE*, vol. 7.

Stewart, PS & Costerton, JW 2001, 'Antibiotic resistance of bacteria in biofilms', *Lancet*, vol. 358, 135–138.

StJohn, HAW, Gengenbach, TR, Hartley, PG & Griesser, H 2000, 'Surface analysis of polymers', in DJ O'Connor & CA Smart (eds), *Surface analysis methods in material science*, Springer-Verlag Berlin, Hiedelberg.

Stone, PW, Hedblom, EC, Murphy, DM & Miller, SB 2005, 'The economic impact of infection control: making the business case for increased infection control resources', *AJIC: American Journal of Infection Control*, vol. 33, 542–547.

Straus, SK & Hancock, REW 2006, 'Mode of action of the new antibiotic for Gram-positive pathogens daptomycin: comparison with cationic antimicrobial peptides and lipopeptides', *Biochimica et Biophysica Acta (BBA)—Biomembranes*, vol. 1758, 1215–1223.

Tachi, T, Epand, RF, Epand, RM & Matsuzaki, K 2002, 'Position-dependent hydrophobicity of the antimicrobial magainin peptide affects the mode of peptide-lipid interactions and selective toxicity', vol. 41, 10723.

Tamaki, M, Imazeki, Y, Shirane, A, Fujinuma, K, Shindo, M, Kimura, M & Uchida, Y 2011, 'Novel gratisin derivatives with high antimicrobial activity and low hemolytic activity', *Bioorganic & Medicinal Chemistry Letters*, vol. 21, 440–443.

Ter Boo, G.-J.A…Grijpma,D.W., Moriarty\ T.F., Richards R.G., Eglin E., 2015, ‘Antimicrobial delivery systems for local infection prophylaxis in orthopedic- and trauma surgery‘, *Biomaterials*, vol. 52, 113-125.

Thaker, HD, Cankaya, A, Scott, RW & Tew, GN 2013, ‘Role of amphiphilicity in the design of synthetic mimics of antimicrobial peptides with Gram-negative activity’, *ACS Medicinal Chemistry Letters*, vol. 4, 481–485.

Thaker, HD, Sgolastra, F, Som, A, Scott, RW, Anguita, J & Tew, GN 2012, ‘Synthetic mimics of antimicrobial peptides from aryl scaffolds’, *Abstracts of Papers of the American Chemical Society*, vol. 244.

Thaker, HD, Som, A, Ayaz, F, Lui, D, Pan, W, Scott, RW, Anguita, J & Tew, GN 2012, ‘Synthetic mimics of antimicrobial peptides with immunomodulatory responses’, *Journal of the American Chemical Society*, vol. 134, 11088–11091.

Thierry, B, Jasieniak, M, De Smet, L, Vasilev, K & Griesser, HJ 2008, ‘Reactive epoxy-functionalized thin films by a pulsed plasma polymerization process’, *Langmuir*, vol. 24, 10187–10195.

Thissen, H, Hayes, JP, Kingshott, P, Johnson, G, Harvey, EC & Griesser, HJ 2002, ‘Nanometer thickness laser ablation for spatial control of cell attachment’, *Smart Materials & Structures*, vol. 11, 792–799.

Tidwell, CD, Castner, DG, Golledge, SL, Ratner, BD, Meyer, K, Hangenhoff, B & Benninghoven, A 2001, ‘Static time-of-flight secondary ion mass spectrometry and x-ray photoelectron spectroscopy characterization of adsorbed albumin and fibronectin films’, *Surface and Interface Analysis*, vol. 31, 724–733.

Tiller, JC, Bieser, AM, Fuchs, A, Waschinski, C & Fik, CP 2012, ‘Antimicrobial surfaces derived by surface-grafted biocidal groups: designs and mechanisms’, *Abstracts of Papers of the American Chemical Society*, vol. 243.

Tiller, JC, Lee, SB, Lewis, K & Klibanov, AM 2002, ‘Polymer surfaces derivatized with poly(vinyl-N-hexylpyridinium) kill airborne and waterborne bacteria’, *Biotechnology and Bioengineering*, vol. 79, 465–471.

Tiller, JC, Liao, CJ, Lewis, K & Klibanov, AM 2001, ‘Designing surfaces that kill bacteria on contact’, *Proceedings of the National Academy of Sciences of the United States of America*, vol. 98, 5981–5985.

Trop, M, Novak, M, Rodl, S, Hellbom, B, Kroell, W & Goessler, W 2006, 'Silver coated dressing Acticoat caused raised liver enzymes and argyria-like symptoms in burn patient', *Journal of Trauma-Injury Infection and Critical Care*, vol. 60, 648–652.

Tyler, BJ 1997, 'XPS and SIMS studies of surfaces important in biofilm formation: three case studies', *Annals of the New York Academy of Sciences*, vol. 831, 114–126.

Uyterhoeven, ET, Butler, CH, Ko, D & Elmore, DE 2008, 'Investigating the nucleic acid interactions and antimicrobial mechanism of buforin II', vol. 582, 1715–1718.

Vachon, DJ & Yager, DR 2006, 'Novel sulfonated hydrogel composite with the ability to inhibit proteases and bacterial growth', *Journal of Biomedical Materials Research Part A*, vol. 76A, 35–43.

van der Mei, HC & Busscher, HJ 2012, 'Bacterial cell surface heterogeneity: a pathogen's disguise', *PLOS Pathogens*, vol. 8.

Vanden Eynde, X & Bertrand, P 1997, 'ToF-SIMS quantification of polystyrene spectra based on principal component analysis (PCA)?', *Surface and Interface Analysis*, vol. 25, 878–888.

Vanden Eynde, X & Bertrand, P 1999, 'Quantification of polystyrene blend surfaces based on end group ToF-SIMS analysis', *Applied Surface Science*, vol. 141, 1–20.

Vasilev, K, Britcher, L, Casanal, A & Griesser, HJ 2008, 'Solvent-induced porosity in ultrathin amine plasma polymer coatings', *Journal of Physical Chemistry B*, vol. 112, 10915–10921.

Vasilev, K, Casanal, A, Challougui, H & Griesser, HJ 2009, 'Template-assisted generation of nanocavities within plasma polymer films', *Journal of Physical Chemistry B*, vol. 113, 7059–7063.

Vasilev, K, Cook, J & Griesser, HJ 2009, 'Antibacterial surfaces for biomedical devices', *Expert Review of Medical Devices*, vol. 6, 553–567.

Vasilev, K, Griesser, SS & Griesser, HJ 2011, 'Antibacterial surfaces and coatings produced by plasma techniques', *Plasma Processes and Polymers*, vol. 8, 1010–1023.

Vasilev, K, Sah, V, Anselme, K, Ndi, C, Mateescu, M, Dollmann, B, Martinek, P, Ys, H, Ploux, L & Griesser, HJ 2010, 'Tunable antibacterial coatings that support mammalian cell growth', *Nano Letters*, vol. 10, 202–207.

Vermette, P & Meagher, L 2002, 'Immobilization and characterization of Poly(acrylic acid) graft layers', *Langmuir*, vol. 18, 10137–10145.

Vila-Farres, X, de la Maria, CG, Lopez-Rojas, R, Pachon, J, Giralt, E & Vila, J 2012, 'In vitro activity of several antimicrobial peptides against colistin-susceptible and colistin-resistant *Acinetobacter baumannii*', *Clinical Microbiology and Infection*, vol. 18, 383–387.

Vimala, K, Sivudu, KS, Mohan, YM, Sreedhar, B & Raju, KM 2009, 'Controlled silver nanoparticles synthesis in semi-hydrogel networks of poly(acrylamide) and carbohydrates: a rational methodology for antibacterial application', *Carbohydrate Polymers*, vol. 75, 463–471.

Vincent, JL, Bihari, DJ, Suter, PM, Bruining, HA, White, J, Nicolaschanoin, MH, Wolff, M, Spencer, RC & Hemmer, M 1995, 'The prevalence of nosocomial infection in intensive-care units in Europe: results of the European Prevalence of Infection in Intensive-Care (Epic) Study', *JAMA—Journal of the American Medical Association*, vol. 274, 639–644.

Voccia, S, Ignatova, M, Jerome, R & Jerome, C 2006, 'Design of antibacterial surfaces by a combination of electrochemistry and controlled radical polymerization', *Langmuir*, vol. 22, 8607–8613.

Volmer, AA, Szpilman, AM & Carreira, EM 2010, 'Synthesis and biological evaluation of amphotericin B derivatives', *Natural Product Reports*, vol. 27, 1329–1349.

Von Gradowski, M, Jacoby, B, Hilgers, H, Barz, J, Wahl, M & Kopnarski, M 2005, 'ToF-SIMS characterisation of ultra-thin fluorinated carbon plasma polymer films', *Surface and Coatings Technology*, vol. 200, 334–340.

Wadhwani, P, Reichert, J, Buerck, J & Ulrich, AS 2012, 'Antimicrobial and cell-penetrating peptides induce lipid vesicle fusion by folding and aggregation', *European Biophysics Journal with Biophysics Letters*, vol. 41, 177–187.

Wagner, MS & Castner, DG 2001, 'Characterization of adsorbed protein films by time-of-flight secondary ion mass spectrometry with principal component analysis', *Langmuir*, vol. 17, 4649–4660.

Wagner, MS & Castner, DG 2003, 'Characterization of adsorbed protein films by time-of-flight secondary ion mass spectroscopy and multivariate analysis', *Applied Surface Science*, vol. 203–204, 698–703.

Wagner, MS, Horbett, TA & Castner, DG 2003, 'Characterisation of the structure of binary and ternary adsorbed protein films using electron spectroscopy for chemical analysis, time-of-flight secondary ion mass spectroscopy and radiolabeling', *Langmuir*, vol. 19, 1708–1715.

Ward, AJ & Short, RD 1995, 'A ToF-SIMS and XPS investigation of the structure of plasma polymers prepared from the methacrylate series of monomers: 2. The influence of the W/F parameter on structural and functional group retention', *Polymer*, vol. 36, 3439–3450.

Waschinski, CJ, Herdes, V, Schueler, F & Tiller, JC 2004, 'Influence of satellite groups on telechelic antimicrobial functions of polyoxazolines', *Macromolecular Bioscience*, vol. 5, 149–156.

Weinstein, AM, Rome, BN, Reichmann, WM, Collins, JE, Burbine, SA, Thornhill, TS, Wright, J, Katz, JN & Losina, E 2013, 'Estimating the burden of total knee replacement in the United States', *The Journal of Bone & Joint Surgery*, vol. 95, 385–392.

Wilson, M, Henderson, B & McNab, R 2002, *Bacterial disease mechanisms*, Cambridge University Press, Cambridge.

Wimley, WC 2010, 'Describing the mechanism of antimicrobial peptide action with the interfacial activity model', *ACS Chemical Biology*, vol. 5, 905–917.

Wimley, WC & Hristova, K 2011, 'Antimicrobial peptides: successes, challenges and unanswered questions', *Journal of Membrane Biology*, vol. 239, 27–34.

Woo, H-J & Wallqvist, A 2011, 'Spontaneous buckling of lipid bilayer and vesicle budding induced by antimicrobial peptide magainin 2: a coarse-grained simulation study', *The Journal of Physical Chemistry B*, vol. 115, 8122.

Wright, JB, Hansen, DL & Burrell, RE 1998a, 'The comparative efficacy of two antimicrobial barrier dressings: in-vitro examination of two controlled release of silver dressings', *Wounds—A Compendium of Clinical Research and Practice*, vol. 10, 179–188.

Wright, JB, Lam, K & Burrell, RE 1998b, 'Wound management in an era of increasing bacterial antibiotic resistance: a role for topical silver treatment', *American Journal of Infection Control*, vol. 26, 572–577.

Wu, P & Grainger, DW 2006, 'Drug/device combinations for local drug therapies and infection prophylaxis', *Biomaterials*, vol. 27, 2450–2467.

Yang, D, Biragyn, A, Hoover, DM, Lubkowski, J & Oppenheim, JJ 2004, 'Multiple roles of antimicrobial defensins, cathelicidins, and eosinophil-derived neurotoxin in host defense', *Annual Review of Immunology*, vol. 22, 181–215.

Yoneyama, H & Katsumata, R 2006, 'Antibiotic resistance in bacteria and its future for novel antibiotic development', *Bioscience, Biotechnology, and Biochemistry*, vol. 70, 1060–1075.

Zaat, SAJ & Hiemstra, PS 2013, *Antimicrobial peptides and innate immunity*, Springer, Basel.

Zaporojtchenko, V, Podschun, R, Schurmann, U, Kulkarni, A & Faupel, F 2006, 'Physico-chemical and antimicrobial properties of co-sputtered Ag-Au/PTFE nanocomposite coatings', *Nanotechnology*, vol. 17, 4904–4908.

Zhang, J, Markiewicz, MJ, Mowery, BP, Weisblum, B, Stahl, SS & Gellman, SH 2011, 'C-terminal functionalization of nylon-3 polymers: effects of C-terminal groups on antibacterial and hemolytic activities', *Biomacromolecules*, vol. 13, 323–331.

Zimmerli, W, Trampuz, A & Ochsner, PE 2004, 'Current concepts: prosthetic-joint infections', *New England Journal of Medicine*, vol. 351, 1645–1654.